

**Development and application of nanopore sequencing based methods
for rapid, culture-free diagnosis of tuberculosis**

Michael John Strinden

Submitted in partial fulfilment of the requirements of the degree of Doctor of Philosophy

University of East Anglia, Norwich, UK

Faculty of Medicine and Health Sciences

March 2022

This copy of the thesis has been supplied on condition that anyone who consults it is understood to recognise that its copyright rests with the author and that use of any information derived therefrom must be in accordance with current UK Copyright Law. In addition, any quotation or extract must include full attribution.

Abstract

Tuberculosis (TB) is a condition of global health concern with an estimated 1/3 of the human population infected. A growing percentage of these infections also demonstrate resistance to antibiotics, increasing morbidity and mortality in affected populations. The gold standard for drug susceptibility testing (DST), microbial culture, is very slow (weeks-months) and can't provide the necessary information within a clinically useful timeframe. Culture DST also requires specialist equipment that is not broadly available, therefore drug-resistant TB (DR-TB) is underdiagnosed globally. These limitations mean there is an urgent need for the development and uptake of new, rapid, DST technologies. Existing molecular technologies such as Xpert MTB/RIF offer rapid TB diagnosis but are only capable of detecting Rifampicin resistance due to limitations in PCR multiplexing technology. Comparatively, the GenoType MTBDRplus and MTBDRsl assays provide broader DST testing capability but are far from comprehensive for detecting all important drug-resistance associated mutations.

Targeted next-generation sequencing (tNGS) has the potential to rapidly diagnose TB and determine drug-resistance by amplification of known mutation loci. We developed a tNGS assay for DST covering 13 anti-tuberculous drugs using known SNPs (~200) in 16 *Mycobacterium tuberculosis* genes. Genotypic and phenotypic test performance were assessed during a blinded study of 392 contrived samples provided by the Foundation for Innovative New Diagnostics (FIND). This tNGS assay was found to have an overall genotypic sensitivity of 95% and specificity of 99% when compared to Illumina. The phenotypic sensitivity was 95%-97% and specificity was 96%-100% across all targeted drugs.

Clinical metagenomics has the potential to diagnose TB, perform DST, and provide epidemiological information directly from sputum in a single assay. We developed a metagenomic sequencing based TB test and evaluated it on spiked sputum samples from collaborators at the Norfolk and Norwich University Hospital (NNUH). Analysis showed commensal bacteria were present in high numbers, accounting for the majority of reads, thereby reducing analytical sensitivity. Attempts to design a commensal depletion protocol proved unsuccessful and metagenomic development was halted.

In conclusion, two approaches for rapid DST and TB diagnosis were designed and tested using contrived clinical samples. The tNGS method showed excellent potential for clinical use and is undergoing continued evaluation by FIND and the WHO under their Seq&Treat program. Continued development of the method has led to reductions in assay complexity, cost and turnaround time and use of the new WHO mutation list and simplified analysis tool will aid implementation of the test in the future.

Access Condition and Agreement

Each deposit in UEA Digital Repository is protected by copyright and other intellectual property rights, and duplication or sale of all or part of any of the Data Collections is not permitted, except that material may be duplicated by you for your research use or for educational purposes in electronic or print form. You must obtain permission from the copyright holder, usually the author, for any other use. Exceptions only apply where a deposit may be explicitly provided under a stated licence, such as a Creative Commons licence or Open Government licence.

Electronic or print copies may not be offered, whether for sale or otherwise to anyone, unless explicitly stated under a Creative Commons or Open Government license. Unauthorised reproduction, editing or reformatting for resale purposes is explicitly prohibited (except where approved by the copyright holder themselves) and UEA reserves the right to take immediate 'take down' action on behalf of the copyright and/or rights holder if this Access condition of the UEA Digital Repository is breached. Any material in this database has been supplied on the understanding that it is copyright material and that no quotation from the material may be published without proper acknowledgement.

Table of Contents

Abstract.....	1
Table of Contents.....	2
List of Figures.....	7
List of Tables.....	10
Acknowledgements.....	16
Chapter 1 – Introduction.....	17
1.1: Mycobacterial Biology.....	17
1.2: Tuberculosis Epidemiology.....	20
1.2.1: What is TB?.....	20
1.2.2: TB Demographics.....	21
1.2.3: Global TB Trends.....	23
1.2.4: COVID and TB.....	24
1.3: Drug Resistance in TB.....	25
1.3.1: RR/MDR TB.....	27
1.3.2: XDR/TDR TB.....	28
1.3.3: Factors in the Emergence of Drug Resistance.....	29
1.4: TB Treatment.....	31
1.4.1: First-Line Medications.....	31
1.4.2: Drug Resistant TB Treatment.....	32
1.5: Tuberculous Disease by Non- <i>M. tuberculosis</i> Agents.....	35
1.5.1: Zoonotic TB.....	35
1.5.2: Non-Tuberculous Mycobacteria.....	36
1.5.3: <i>M. tuberculosis</i> -Like Pathogens.....	37
1.6: A Brief Overview of Molecular Epidemiology.....	38
1.6.1: IS6110 Typing.....	38
1.6.2: MIRU-VNTR.....	38
1.6.3: Spoligotyping.....	39
1.6.4: Whole Genome Sequencing.....	39
1.7: Economics of TB.....	40
1.8: Diagnosing TB and DR-TB.....	43
1.8.1: Drug-Susceptible TB Diagnosis.....	43
1.8.1.1: Gold Standard.....	43
1.8.1.2: PCR.....	43

1.8.2: Drug-Resistant TB Diagnosis.....	44
1.8.2.1: Gold Standard.....	44
1.8.2.2: PCR.....	44
1.8.3: Strength and Weakness Summary.....	46
1.8.3.1: Culture/Microscopy.....	46
1.8.3.2: PCR.....	47
1.9: Whole Genome Sequencing (WGS) in TB.....	47
1.9.1: WGS DST.....	48
1.9.2: Strengths and Weaknesses of WGS.....	48
1.10: The Future of TB Diagnostics.....	49
1.10.1: Metagenomic Diagnostics.....	50
1.10.2: Targeted Next-Generation Sequencing.....	51
1.11: Study Aims.....	52
Chapter 2 – Methods.....	53
2.1: Bacterial Culture Conditions for Method Development.....	53
2.2: Clinical Sample Ethics.....	54
2.3: DNA Extraction.....	55
2.3.1: MagNA Pure Extraction.....	55
2.3.2: Promega Maxwell Extraction.....	56
2.4: DNA Quantification.....	57
2.4.1: Qubit.....	57
2.4.2: Promega.....	57
2.4.3: Bacterial Cell Equivalent Calculation.....	58
2.5: DNA Quantification by qPCR.....	58
2.5.1: SYBR Green qPCR.....	59
2.5.2: TaqMan Probe-Based qPCR.....	60
2.5.3: Nested qPCR Amplification.....	62
2.5.4: qPCR Amplification Analysis.....	62
2.5.5: Melt Curve Analysis.....	62
2.6: Fragment Size Analysis.....	64
2.7: Contrived Clinical Samples.....	64
2.8: Design of tNGS PCR Primers.....	64
2.9: Nucleic Acid Host Depletion.....	65
2.10: Sputum NaOH/NALC-Na Decontamination and Sedimentation.....	66

2.11: Determining Analytical Limit-of-Detection.....	67
2.11.1: qPCR Determination of the Metagenomic LoD.....	68
2.11.2: MinION Sequencing for Determination of the tNGS DST Assay LoD.....	68
2.12: Multiplex PCR Using Qiagen Kit.....	68
2.13: DNA Purification and Concentration with AMPure XP Beads.....	69
2.14: MinION Library Preparation.....	70
2.14.1: Rapid PCR Barcoding Kit Library Preparation for Metagenomics.....	71
2.14.2: LSK109 Ligation with PCR Barcoding Expansion.....	72
2.14.3: Native Barcoding 96 Expansion Kit Library Preparation.....	75
2.15: MinION Loading.....	76
2.16: Sequencing Analysis.....	76
Chapter 3 – Results and Discussion.....	79
3.1: Comparison of Extraction and Purification Methods for Optimization of Mycobacterial DNA Yields.....	79
3.1.1: DNA Purification Method Comparison.....	80
3.1.2: Importance of Automated Extraction.....	82
3.1.3: Comparison of Bead Beating Matrices for DNA Extraction.....	83
3.1.4: Mechanical Disruption Optimisation Summary.....	85
3.2: Targeted Next-Generation Sequencing.....	86
3.2.1: Selection of Resistance Associated Mutations for Development of a tNGS Test for Drug-Resistant TB.....	87
3.2.1.1: Assay Target Selection Sources.....	89
3.2.1.2: Target SNP Selection.....	90
3.2.2: Design and Optimization of PCR Primers for Target Resistance Genes.....	92
3.2.2.1: Design of PCR Primers.....	92
3.2.2.2: Gene Target Primer Pair Redesign.....	94
3.2.2.3: Redesign of <i>inhA</i> Primer Pair.....	95
3.2.2.4: Redesign of <i>pncA</i> Primer Pair.....	96
3.2.2.5: Redesign of <i>rpoB</i> Primer Pair.....	96
3.2.2.6: Redesign of <i>rrl</i> Primer Pair.....	96
3.2.2.7: Redesign of <i>rplC</i> Primer Pair.....	97
3.2.2.8: Redesign of <i>tlyA</i> Primer Pair.....	98
3.2.2.9: Redesign of <i>rv0678</i> Primer Pair.....	99
3.2.2.10: Redesign of <i>fabG1</i> Primer Pair.....	101

3.2.2.11: Redesign of <i>ethA</i> Primer Pair.....	102
3.2.2.12: Redesign of <i>rrs</i> (16S rRNA gene) Primer Pair.....	103
3.2.2.13: Redesign of <i>rpsL</i> Primer Pair.....	104
3.2.2.14: Redesign of <i>embB</i> Primer Pair.....	106
3.2.2.15: Redesign of <i>katG</i> Primer Pair.....	109
3.2.2.16: Redesign of <i>eis</i> Primer Pair.....	110
3.2.2.17: Final Targets and Primers.....	113
3.2.3: Optimisation of Multiplex Groups for tNGS Based DR-TB Detection.....	114
3.2.3.1: <i>in silico</i> Multiplex Grouping.....	114
3.2.3.2: <i>in vitro</i> Multiplex Optimisation.....	116
3.2.3.3: Multiplex Optimisation Summary.....	133
3.2.4: Optimisation of Sample Extraction for Amplification of Drug Resistance	
Gene Targets in Multiplex.....	134
3.2.4.1: Comparison of Nucleic Acid Extraction Methods for Sedimented Samples.....	134
3.2.4.2: Comparison of Maxwell Extraction Kits for Mycobacterial Extraction.....	135
3.2.4.3: Optimisation of NaOH/NALC-Na Decontamination protocol for Use with	
Low Sample Volumes.....	136
3.2.4.3.1: Why Optimise Sputum Decontamination?.....	138
3.2.5: Optimisation of PCR Conditions.....	138
3.2.5.1: Why PCR Reagent Optimisation Matters.....	146
3.2.6: Development of External Assay Controls.....	147
3.2.7: Inclusivity and Specificity Testing.....	149
3.2.7.1: Specificity and Inclusivity Summary.....	155
3.2.8: Limit of Detection.....	156
3.2.9: Clinical Validation of the tNGS Drug Resistance Assay.....	158
3.2.9.1: Sequencing and Analysis of FIND Samples.....	159
3.2.9.2: Genotypic Sensitivity and Specificity.....	160
3.2.9.3: Phenotypic Sensitivity and Specificity.....	162
3.2.9.4: Indeterminate Rates and Reproducibility.....	165
3.2.9.5: Mixed Clinical Samples to Measure Heteroresistance Detection.....	166
3.2.9.6: Dynamic Range.....	168
3.2.10: Assay Performance Summary.....	169
3.2.11: Post-Validation Optimisation.....	170
3.2.12: Continuing Research.....	173

3.3: Metagenomic Sequencing.....	174
3.3.1: Assessment of a Host DNA Depletion Method for Diagnosis of TB and Drug Resistance by Metagenomic Sequencing.....	174
3.3.2: Development of a Commensal Bacteria DNA Depletion Method for Mycobacterial Samples.....	178
3.3.2.1: Assessment of Lysis Buffers for the Depletion of Commensal Bacterial DNA in Sputum Samples.....	178
3.3.2.2: Assessment of Reagents for the Depletion of Commensal Bacterial DNA in Sputum Samples.....	181
3.3.2.3: Effectiveness of Depletion Methodologies.....	185
3.3.2.4: Future Depletion Research.....	187
3.3.3: Preliminary Limit of Detection Experiment.....	187
3.3.4: Metagenomic Assay Performance Summary.....	189
Chapter 4 – Implementation and Conclusion.....	190
4.1: Implementation of the tNGS Assay.....	190
4.1.1: Current tNGS Assay Landscape.....	190
4.1.2: TB Diagnostic Time Requirements.....	190
4.1.3: Cost of TB Diagnosis.....	193
4.2: Benefits of Nanopore Sequencing for TB Diagnosis.....	194
4.3: Conservation and Ecology Applications.....	195
4.4: Conclusions.....	195
Appendices.....	197
Appendix I.....	197
Appendix II.....	208
Appendix III.....	225
Appendix IV.....	232
Appendix V.....	251
Appendix VI.....	261
References.....	271

List of Figures

Figure 1.1: 15,549x magnification colourised scanning electron microscope image of <i>Mycobacterium tuberculosis</i>	17
Figure 1.2: Phylogenetic tree of slow-growing mycobacteria anchored by two rapid-growing mycobacteria.....	19
Figure 1.3: Causes of death globally in 2019.....	21
Figure 1.4: Global incidence rates of WHO reporting countries, 2021.....	23
Figure 1.5: Global trends in the estimated number of TB deaths and the mortality rate 2000-2020.....	24
Figure 1.6: Trends in case notifications of individuals newly diagnosed with TB by WHO region, 2016-2020.....	25
Figure 1.7: Global MDR/RR-TB rate in new and previously treated TB cases.....	26
Figure 1.8: Visual representation of the relationship between the three most common types of drug-resistant TB.....	27
Figure 1.9: Global map showing the proportion of TB infections due to the Beijing strain of <i>M. tuberculosis</i> in select geographic regions in 2002.....	31
Figure 1.10: MRI of a disseminated central nervous system TB infection.....	36
Figure 1.11: Colourised 1,600x magnification scanning electron microscope image of <i>Nocardia asteroides</i> structure.....	37
Figure 1.12: Countries in the three high-burden country lists for TB, TB/HIV, and MDR-TB between 2016 and 2020, with overlaps.....	41
Figure 1.13: Percentage of the general population facing catastrophic health expenditure.....	42
Figure 2.1: Example of qPCR melt curve analysis from two experiments.....	63
Figure 2.2: Flowchart illustrating the usage of three nanopore sequencing library barcoding methods depending on the sequencing purpose.....	71
Figure 2.3: Example Epi2Me TB Resistance pipeline output for resistant samples.....	77
Figure 2.4: Example output of sequencing reads mapped to a concatenated assay reference for visualisation of coverage in samples.....	78
Figure 3.1: Line chart showing the increase in mean DNA yield by MagNA Pure extraction as a function of mechanical lysis time using triplicate samples.....	81
Figure 3.2: A flowchart illustrating the general progression and timeline of development for the tNGS assay.....	87
Figure 3.3: Example of a gene map showing the locations of known high-confidence resistance mutations in the <i>pncA</i> gene.....	92

Figure 3.4: Example output from the Epi2Me TB Resistance Profile pipeline for the mutation in <i>rv0678</i> associated with resistance to bedaquiline and clofazimine compared to that for <i>katG</i> associated with resistance to isoniazid.....	100
Figure 3.5: Qualimap coverage map of genes targeted by primers within multiplex group 1 after tNGS amplification and sequencing with <i>embB</i> primer iteration 1.....	106
Figure 3.6: Qualimap coverage map of genes targeted by primers in the group 1 multiplex after tNGS amplification and sequencing with <i>embB</i> redesign iteration 2 primers.....	107
Figure 3.7: Qualimap coverage map of group 1 gene targets using <i>eis</i> redesign 8 primers from Pooled triplicate samples for improved resolution.....	112
Figure 3.8: TapeStation gel image of 5-plex configuration 1 indicating non-specific amplification identified as secondary and tertiary banding as well as indicating no target amplicons in 5-plex 2 or the 15-plex reaction.....	118
Figure 3.9: 5-plex configuration 2 TapeStation gel image showing no evidence of non-specific amplification identified as dual banding or loss of target amplicon in pooled triplicate samples for improved resolution.....	121
Figure 3.10: Multiplex configuration 3 TapeStation gel image showing no evidence of non-specific amplification identified as dual banding or loss of target amplicon in pooled triplicate samples for improved resolution.....	123
Figure 3.11: Multiplex configuration 4 TapeStation gel image showing no evidence of non-specific amplification identified as dual banding or loss of target amplicon in pooled triplicate samples for improved resolution.....	125
Figure 3.12: Qualimap visualization of multiplex configuration 5 sequenced reads mapped to a concatenated reference of assay gene targets using pooled triplicate samples for improved resolution.....	126
Figure 3.13: One of a triplicate set of qPCR amplification curves for simplex assay primers using Takara amplification.....	139
Figure 3.14: TapeStation analysis of PCR products indicating non-specific amplification in <i>embB</i> , <i>rpoB</i> , <i>fabG1/inhA</i> , <i>rv0678</i> , <i>rplC</i> , and <i>katG</i> reactions using pooled triplicate samples for improved resolution.....	140
Figure 3.15: TapeStation analysis of PCR for <i>embB</i> , <i>rplC</i> , <i>gidB</i> , and <i>ethA</i> using SYBR Green Mastermix using pooled triplicate samples for improved resolution.....	141

Figure 3.16: qPCR amplification curves for triplex reactions amplified using NEB cycling conditions with SYBR Green master mix.....	142
Figure 3.17: qPCR melt curves for triplex reactions amplified using NEB cycling conditions with SYBR Green master mix.....	142
Figure 3.18: TapeStation analysis of five triplex PCRs amplified using the SYBR Green kit Using pooled triplicate samples for improved resolution.....	143
Figure 3.19: qPCR amplification curves for one of a triplicate set of 5-plex reactions.....	144
Figure 3.20: TapeStation fragment size analysis of three 5-plex reactions using pooled triplicate samples for improved resolution.....	144
Figure 3.21: TapeStation analysis of the 3 5-plex reactions using Qiagen and NEB mastermixes using pooled triplicate samples for improved resolution.....	145
Figure 3.22: Screenshot of Epi2Me TB Resistance Profile pipeline output for external controls showing expected fully susceptible profile as designed.....	148
Figure 3.23: Qualimap visualization of <i>Pseudomans aeruginosa</i> reads mapped onto the TB tNGS assay gene target reference to identify areas of cross-reactivity.....	150
Figure 3.24: Qualimap visualization of <i>M. africanum</i> reads mapped onto the TB tNGS assay gene target reference.....	152
Figure 3.25: Qualimap visualization of 5 NTM genomes and <i>M. leprae</i> mapped onto the TB tNGS assay gene target reference to identify areas of potential non-specific assay reactivity.....	153
Figure 3.26: Qualimap visualization of 6 MTBC species genomes mapped onto the TB tNGS assay gene target reference.....	154
Figure 3.27: Initial FIND analysis of mixed infection detection.....	167
Figure 3.28: Analysis of mixed infection detection following adjustment of the phenotypic resistance threshold and correction of errors in <i>katG</i> and <i>pncA</i> calling.....	167
Figure 3.29: One of a triplicate set of nested qPCR C ₇ s for configuration 9 multiplex group 2 gene targets with original and reformulated <i>katG</i> primer pairs	171
Figure 3.30: Qualimap visualization sequencing of a mixed infection sample showing equivalent coverage of all targets when using multiplex configuration 9 using one of a set of triplicate samples.....	171
Figure 4.1: Flow and time requirements for each step of the tNGS multiplex assay following receipt of a sample excluding 6 hour recommended sequencing time.....	192

List of Tables

Table 1.1: A summary of the primary strengths and weaknesses inherent with culture and microscopy for TB.....	46
Table 1.2: A summary of the primary strengths and weaknesses inherent with PCR for TB.....	47
Table 1.3: A summary of the primary strengths and weaknesses inherent with WGS for TB.....	48
Table 1.4: A summary of the primary strengths and weaknesses inherent with metagenomics.....	51
Table 2.1: SYBR Green qPCR working solution formula per sample.....	59
Table 2.2: SYBR Green PCR amplification primers for amplification of three targets of interest.....	60
Table 2.3: Cycling conditions for SYBR Green qPCR amplification.....	60
Table 2.4: Probe-based qPCR working solution formula per sample.....	61
Table 2.5: Primer/Probe sets selected for qPCR amplification of three DNA targets.....	61
Table 2.6: Probe-based qPCR cycling conditions.....	62
Table 2.7: Preparation of NaOH/NALC-Na Citrate Digestant Solution.....	67
Table 2.8: Multiplex group amplification reaction formula per sample.....	69
Table 2.9: Multiplex group amplification cycling conditions.....	69
Table 2.10: Example table of AMPure XP beads used for different bead wash concentrations.....	70
Table 2.11: Cycling conditions for ONT PCR barcoding.....	72
Table 2.12: PCR barcoding 96-Expansion reaction reagent concentrations.....	73
Table 2.13: PCR Barcoding 96-Expansion cycling conditions.....	74
Table 3.1: Qubit quantification comparing nucleic acid extraction methods using duplicate sample sets.....	80
Table 3.2: Qubit quantification comparing nucleic acid extraction methods for triplicate samples.....	81
Table 3.3: Post-extraction DNA concentrations after using two mechanical cell disruption protocols.....	82
Table 3.4: Bead-beating matrices chosen for comparison of mycobacterial cell lysis efficiency and their material compositions.....	83
Table 3.5: DNA quantifications by Qubit and qPCR from various bead-beating matrices on two homogenizers.....	84
Table 3.6: DNA quantifications by Qubit and qPCR of two MP Biomedicals bead-beating matrices on two homogenizers.....	84
Table 3.7: DNA quantifications by Qubit and qPCR of spiked NRF sputum lysed in three MP Biomedicals bead-beating matrices using triplicate samples.....	85

Table 3.8: Anti-tuberculosis drugs and the genes which are known to harbour resistance mutations as informed by two international studies.....	88
Table 3.9: Anti-tuberculosis drugs and the genes which are known to harbour resistance mutations as informed by existing literature.....	89
Table 3.10: Primer design parameters for use in designing target gene primer pairs in Primer-BLAST.....	93
Table 3.11: tNGS target gene primer simplex QC test for original primers using triplicate samples.....	94
Table 3.12: Redesign history for <i>inhA</i> primers.....	96
Table 3.13: Redesign history for <i>pncA</i> primers.....	96
Table 3.14: Redesign history for <i>rpoB</i> primers.....	96
Table 3.15: Redesign history for <i>rrl</i> primers.....	97
Table 3.16: Redesign history for <i>rplC</i> primers.....	98
Table 3.17: Nested qPCR C _T results for comparison of multiplex amplification efficiency in multiplex with various <i>tlyA</i> concentrations.....	99
Table 3.18: Redesign history for <i>tlyA</i> primers.....	99
Table 3.19: Redesign history for <i>rv0678</i> primers.....	101
Table 3.20: Redesign history for <i>fabG1</i> primers.....	102
Table 3.21: Nested qPCR C _T s for five multiplexes testing redesigned <i>ethA</i> primer pairs using triplicate samples.....	102
Table 3.22: Redesign history for <i>ethA</i> primers.....	103
Table 3.23: Nested mean qPCR C _T s for four multiplexes testing redesigned <i>rrs</i> primer pairs.....	104
Table 3.24: Redesign history for <i>rrs</i> primers.....	104
Table 3.25: Nested mean qPCR C _T s for five multiplexes testing redesigned <i>rpsL</i> primer pairs using triplicate samples.....	105
Table 3.26: Redesign history for <i>rpsL</i> primers.....	106
Table 3.27: Mean nested qPCR C _T s for four multiplexes testing redesigned <i>embB</i> primer pairs using triplicate samples.....	108
Table 3.28: Redesign history for <i>embB</i> primers.....	108
Table 3.29: Mean nested qPCR C _T s for five multiplexes testing redesigned <i>katG</i> primer pairs using triplicate samples.....	109
Table 3.30: Mean nested qPCR C _T s for five multiplexes testing redesigned <i>katG</i> primer pairs with the removal of <i>hsp65</i> primers using triplicate samples.....	110

Table 3.31: Mean nested qPCR C _T s testing redesigned <i>eis</i> primer pairs using triplicate samples.....	111
Table 3.32: Mean nested qPCR C _T s testing redesigned <i>eis</i> primer pairs using triplicate samples.....	111
Table 3.33: Redesign history for <i>eis</i> primer pairs.....	113
Table 3.34: Final optimised gene target primer sets for tNGS multiplex assay.....	114
Table 3.35: Triplex groups as designed by use of MultiPLX 2.1 software.....	116
Table 3.36: Configuration 1 of the 5-plex primer mixes for the tNGS assay.....	117
Table 3.37: SYBR Green qPCR results for evaluation of 5-plex configuration 1 amplification on <i>M. bovis</i> BCG DNA using dual sets of triplicate samples.....	117
Table 3.38: Nested primer sequences for tNGS amplification analysis with design parameters.....	119
Table 3.39: Configuration 2 of 5-plex primer mixes for tNGS amplification.....	120
Table 3.40: Mean results of nested SYBR Green qPCR analysis on amplification of assay targets using multiplex primer group configuration 2 using triplicate samples.....	120
Table 3.41: Configuration 3 of multiplex primer mixes for tNGS amplification.....	121
Table 3.42: Mean results of nested SYBR Green qPCR analysis on amplification of assay targets using multiplex primer group configuration 3 using triplicate samples.....	122
Table 3.43: Configuration 4 of multiplex primer mixes for tNGS amplification.....	123
Table 3.44: Mean results of nested SYBR Green qPCR analysis on amplification of assay targets using multiplex primer group configuration 3 using triplicate samples.....	124
Table 3.45: Configuration 5 of multiplex primer mixes for tNGS amplification.....	125
Table 3.46: Configuration 6 of multiplex primer mixes for tNGS amplification.....	127
Table 3.47: Mean results of nested SYBR Green qPCR analysis on amplification of assay targets using multiplex primer group configuration 6 using triplicate samples.....	127
Table 3.48: Configuration 7 of multiplex primer mixes for tNGS amplification.....	128
Table 3.49: Mean results of nested SYBR Green qPCR analysis on amplification of assay targets using multiplex primer group configuration 7 using triplicate samples.....	129
Table 3.50: Mean results of nested SYBR Green qPCR analysis on amplification of multiplex configuration 7 with doubled <i>eis</i> and <i>embB</i> primer concentrations using triplicate samples.....	130
Table 3.51: Configuration 8 of multiplex primer mixes for tNGS amplification.....	130
Table 3.52: Mean results of nested SYBR Green qPCR analysis on amplification of assay targets using multiplex primer group configuration 8 using triplicate samples.....	131

Table 3.53: Mean results of nested SYBR Green qPCR analysis on amplification of multiplex group 1 targets using multiplex primer configuration 7 with increased MgCl ₂ using triplicate samples.....	132
Table 3.54: Configuration 7 qPCR results for relative amplification of multiplex group 1 targets using three redesigned <i>eis</i> primer pair options using triplicate samples.....	133
Table 3.55: Comparison of two automated extraction methods for extraction of nucleic acids from sedimented spiked NRF sputum samples using triplicate samples.....	134
Table 3.56: Mean qPCR quantification C _T results for comparison of two automated nucleic acid extraction kits using two different buffers during bead-beating using triplicate samples.....	135
Table 3.57: Mean qubit quantification of paired samples for comparison of decanting and pipetting supernatant in a head-to-head trial using two sets of triplicate samples.....	136
Table 3.58: Mean qPCR C _T results of two <i>M.bovis</i> BCG gene targets for comparison of nucleic acid yields in decontaminated versus non-decontaminated samples using triplicate samples.....	137
Table 3.59: Cycling conditions for Takara simplex amplification of tNGS assay primers.....	139
Table 3.60: Cycling conditions for SYBR Green simplex amplification with Takara temperatures....	140
Table 3.61: NEB cycling conditions used for triplex amplification with SYBR Green mastermix.....	141
Table 3.62: Qiagen Multiplex kit PCR cycling conditions.....	145
Table 3.63: NEB Multiplex master mix PCR cycling conditions.....	145
Table 3.64: Post-amplification DNA concentrations for Qiagen and NEB mastermixes.....	146
Table 3.65: Total identified reads across all samples for mixed samples analysed using the Epi2Me WIMP pipeline.....	150
Table 3.66: Identified reads in 3 samples spiked with <i>M. africanum</i> analysed using the Epi2Me WIMP pipeline.....	151
Table 3.67: A list of NTM and <i>M. leprae</i> genomes used for <i>in silico</i> specificity testing.....	152
Table 3.68: Testing assay specificity in a sample containing equal concentrations of three Mycobacteria.....	154
Table 3.69: Metagenomic sequencing LoD culture dilution series and spiking with Tween grown <i>M. bovis</i> BCG culture.....	156
Table 3.70: Mean DNA concentration quantifications for LoD determination of tNGS assay multiplex amplifications from two triplicate sets of 5 contrived clinical sample dilutions.....	157

Table 3.71: Example results for phenotypic resistance prediction based on 15% read threshold....	159
Table 3.72: Overall genotypic sensitivity and specificity results for XDR+PZA resistance SNPs.....	160
Table 3.73: Overall genotypic sensitivity and specificity results for each tNGS assay gene target calculated from reported SNP findings.....	161
Table 3.74: Optimum and minimum acceptable sensitivity and specificity for phenotypic resistance calling as determined by FIND for the analysis of the tNGS assay.....	163
Table 3.75: Overall calculated phenotypic sensitivity and specificity of tNGS assay resistance calls as compared to a phenotypic DST reference.....	163
Table 3.76: Comparison of tNGS DST assay to LPA DST as performed by FIND.....	164
Table 3.77: Results for comparison of dynamic detection range performed by FIND in pan- susceptible samples.....	169
Table 3.78: Results for comparison of dynamic detection range performed by FIND in XDR samples.....	169
Table 3.79: Configuration 9 of multiplex primer mixes for tNGS amplification.....	170
Table 3.80: Redesign primers to mitigate and avoid the non-resistance conferring mutation.....	172
Table 3.81: Detection of heteroresistant reads using a forward primer shifted to mitigate the non-resistance conferring SNP site in 50/50 mixed samples.....	172
Table 3.82: Redesign history for <i>katG</i> primers.....	173
Table 3.83: Mean human DNA qPCR results and calculated host depletion levels using triplicate samples.....	175
Table 3.84: Mean <i>M. bovis</i> BCG DNA qPCR results and calculated target loss using triplicate samples.....	175
Table 3.85: Mean 16S rRNA gene qPCR results and calculated bacterial loss using triplicate samples.....	176
Table 3.86: Mean human DNA qPCR results and calculated host depletion levels using triplicate samples.....	176
Table 3.87: Mean <i>M. bovis</i> BCG DNA qPCR results and calculated bacterial loss using triplicate samples.....	177
Table 3.88: Mean 16S rRNA gene qPCR results and calculated bacterial loss using triplicate samples.....	177
Table 3.89: Lysis buffer solutions designed for testing in the optimisation of commensal bacterial DNA depletion.....	178
Table 3.90: Mean 16S rRNA gene qPCR results and calculated bacterial reduction using two sets of triplicate samples.....	179

Table 3.91: Mean human RNA polymerase A gene qPCR results and calculated host depletion levels using four sets of triplicate samples.....	180
Table 3.92: Mean <i>M. bovis</i> BCG qPCR results and calculated bacterial loss using two sets of triplicate samples.....	180
Table 3.93: Tukey HSD Post-Hoc test results for commensal bacterial DNA depletion using two bacterial lysis buffer incubations.....	181
Table 3.94: Mean 16S rRNA gene qPCR results and calculated bacterial reduction using three sets of triplicate samples.....	182
Table 3.95: Mean human RNA polymerase A qPCR for assessing DNA depletion using four pre-host depletion detergent incubations using three sets of triplicate samples.....	184
Table 3.96: Mean <i>M. bovis</i> BCG qPCR for assessing DNA loss using four pre-host depletion detergent incubations using three sets of triplicate samples.....	185
Table 3.97: Mean Roche probe-based qPCR results for <i>M. bovis</i> BCG testing the concentration of DNA available for metagenomic sequencing following depletion protocols using triplicate samples.....	188
Table 3.98: Epi2Me WIMP pipeline results of three 10-fold serially diluted <i>M. bovis</i> BCG samples in NRF sputum.....	189

Acknowledgments

Firstly, I'd like to thank my incredible wife Leah who supported me through the highest and lowest points of my studies. I am eternally grateful for your continued support and understanding while this journey consumed me.

I'd also like to thank my supervisory team, Prof. Justin O'Grady and Prof. John Wain. This work would not have been possible without their help, guidance, and support. I feel together we made something truly incredible.

To Dr. Gemma Kay, who unfailingly had time and energy to assist me through every phase of my PhD. I wish everyone could have a mentor as patient and knowledgeable as you.

Finally, to my family who gave me the encouragement to pursue my passions and continue my studies. It has been a long bumpy road but we made it!

Chapter 1 - Introduction

1.1: Mycobacterial Biology

Mycobacterium tuberculosis was discovered by Dr. Robert Koch in 1882. *M. tuberculosis* is a gram-positive, acid-fast bacilli approximately 2-4 μm long, and is transmitted primarily via aerosols (Figure 1.1). *M. tuberculosis* is strictly intracellular and lacks a known environmental reservoir outside of endemic hosts¹⁻⁴. Lipid-rich cellular walls and layers of peptidoglycan, lipoglycan, mycolic acids, and waxes create an extremely hardy microbe^{2,3}. The Genus Mycobacteria are extremely fastidious organisms and can be divided into slow-growing and rapid-growing groups^{3,5-19}. The doubling time for slow-growing members of the MTBC is approximately 12-24 hours, as opposed to *E. coli* or the fast growing *Mycobacterium abscessus*, which have doubling times of approximately 20 minutes^{20,21}. Slow growth rate is correlated with highly conserved genomes with high GC contents, which experience very low rates of single-nucleotide polymorphism mutations (SNPs)^{4,15}. The average mutation rate for *M. tuberculosis* is only 0.3-0.5 SNPs per genome per year^{2,11}.

Mycobacteria can be identified through microscopy using Ziehl-Neelsen staining, as the mycolic cell wall precludes absorption of *Gram* stains²². Curiously, this characteristic means that mycobacteria are not truly *Gram+* or *Gram-*. However, many still characterise mycobacteria as *Gram+* since mycobacteria are phylogenetically dissimilar to other *Gram-* organisms⁴.

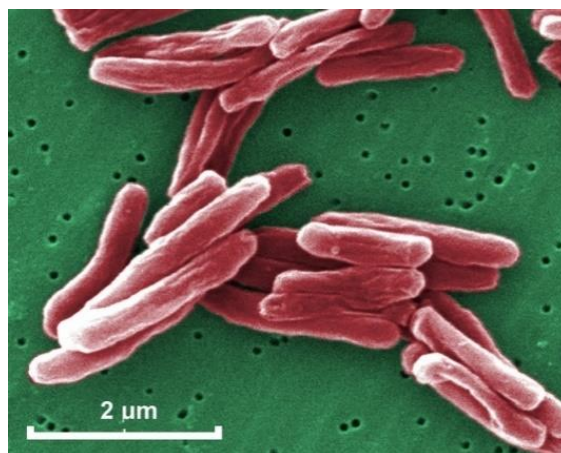


Figure 1.1: 15,549x magnification coloured scanning electron microscope image of *Mycobacterium tuberculosis*²³

The mycobacterial genus is thought to have first evolved around 150 million years ago during the Jurassic period ². *M. tuberculosis* and related species in the *Mycobacterium tuberculosis* complex (MTBC) are theorised to have emerged at least 11,000 years ago and have been co-evolving with their hosts since ^{2,13}. This timeline is a matter of debate, however, and relies on measurements of modern average mutation rates. Depending on the study and the mutation rate measures, the MTBC has been calculated to have emerged anywhere between 70,000 and 6,000 years ago ¹¹. Less contentious, on the other hand, is the proposed geographic region for the emergence of the MTBC, as studies of gene loss and mutation consistently indicate the nearest common MTBC ancestor evolved in Africa ¹¹.

Close co-evolution has resulted in a highly transmissible taxon of bacteria with “remarkable” longevity within hosts and advanced methods of immune system evasion ². Due to co-evolution, modern *M. tuberculosis* and members of the MTBC share numerous characteristics and are found in hosts in every known environment (excluding polar regions) along with non-tuberculous mycobacteria (NTM) species ^{2,24}. There are many hypotheses about the driving force behind emergence and co-evolution with humans, most of which revolve around the transition of human populations to larger societies. One example is that the harnessing of fire by early *Homo sapiens* created a perfect milieu for mycobacteria by increasing group population sizes while simultaneously increasing the prevalence of smoke-induced lung damage, lowering host resistance to pulmonary infection ¹¹.

The MTBC is currently comprised of 10 mycobacterial species capable of causing TB or TB-like disease within hosts (Figure 1.2). Three species specialise in human infection: *Mycobacterium tuberculosis* sensu stricto, *Mycobacterium canettii* and *Mycobacterium africanum* ^{1,2,15}. Additionally, bi-directional zoonotic TB transfer is well documented from cattle (*Mycobacterium bovis*) ¹³, goats and sheep (*Mycobacterium caprae*) ², seals and sea lions (*Mycobacterium pinnipedii*) ¹⁹, and rodents (*Mycobacterium microti*) ²⁵. Recently, three new species have been added to the

MTBC: *Mycobacterium mungi* from mongeese, *Mycobacterium suricattae* from meerkats, and *Mycobacterium orygis* from oryx^{11,26,27}.

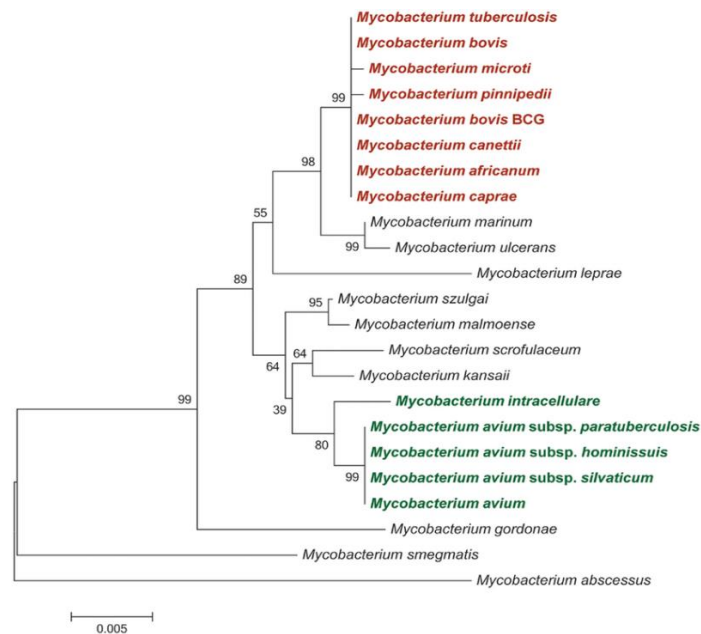


Figure 1.2: Phylogenetic tree of slow-growing mycobacteria anchored by two rapid-growing mycobacteria: *Mycobacterium smegmatis* and *Mycobacterium abscessus*. Select *Mycobacterium Tuberculosis* complex members are denoted in red²⁸.

MTBC members are highly homologous (~99.9% genetically identical) and have identical 16S rRNA sequences. This homology is evident when compared to NTMs; in the MTBC, the maximum genetic difference between members is approximately 2,000 SNPs while NTMs can vary up to 65,000 SNPs, a 32.5-fold difference¹¹. MTBC members are primarily clonal with little horizontal gene transfer. This makes differentiation between species difficult at the genetic level and impossible using microscopic methods^{19,29}. MTBC evolution to become obligate intracellular pathogens is a matter of much study with several hypotheses posited. However, it is generally agreed that a transition from environmental organism to intracellular pathogen likely occurred through numerous small steps, for example, a move from an environmental existence to free-living protozoa hosts such as amoebae¹¹. There is also evidence that a transition to a specialised pathogenic lifestyle was aided by large deletions within the MTBC species' genomes, reducing the average genome length to two thirds of that found in non-pathogenic mycobacteria, thereby increasing fitness¹¹.

1.2: Tuberculosis Epidemiology

1.2.1: What is TB?

Tuberculosis (TB), caused primarily by *Mycobacterium tuberculosis*, is an infectious respiratory disease of grave importance to global health ^{15,19,30}. Most commonly, TB presents as a pulmonary disease (84% of cases), although extrapulmonary and disseminated disease presentations also occur (16% of cases) ^{1,13,31}. Extrapulmonary TB infections are generally confined to the thorax; usually the pleura, pericardium, and perihilar lymph nodes ³². Disseminated TB infections create tubercles throughout the body, i.e., throughout the extremities or the nervous system ³². TB infections occur globally, with regional variations in incidence, prevalence, and causative agent.

As of the early 21st century, TB has surpassed HIV/AIDS as the global leading cause of death from a single infectious agent. The most recently available reports quantified annual TB fatalities at 1.4 million globally in 2019 ³³. Reports also identify TB as the 13th highest out of all causes of death globally (Figure 1.3) ³³. Retrospective studies have shown that 70% of smear-positive cases prove fatal within 10 years if untreated, as well as 20% of smear-negative, culture-positive cases ³³. In properly treated cases, mortality rates decrease to 14% across all active infections ³³.

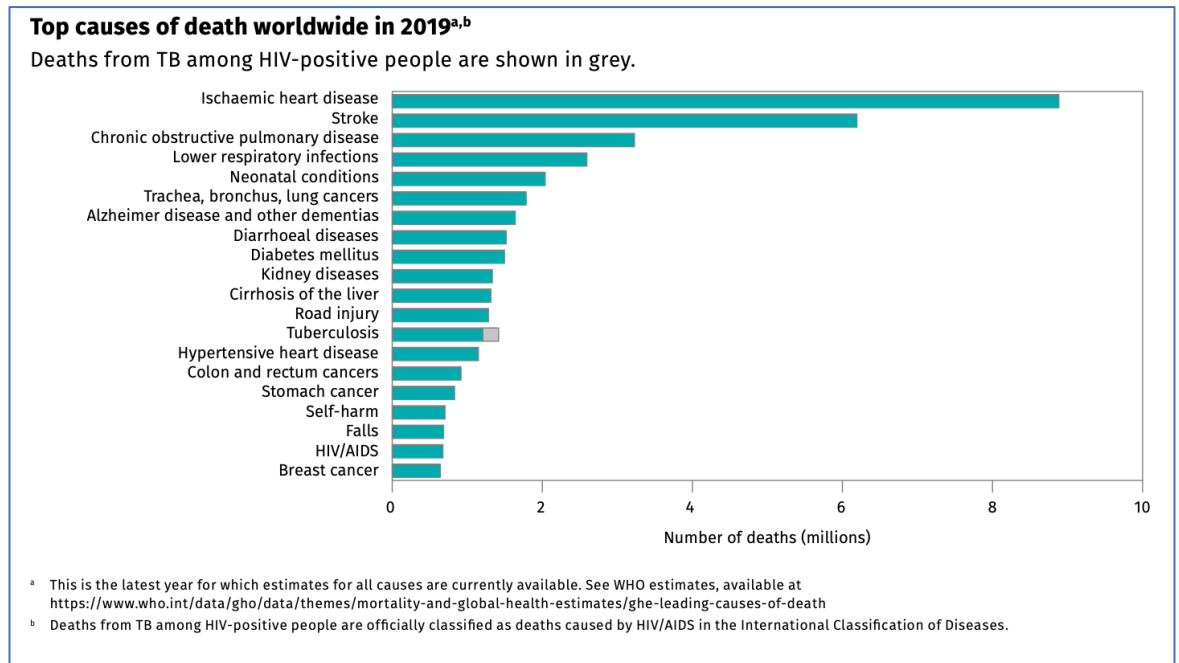


Figure 1.3: Causes of death globally in 2019 ³⁴

Beyond its mortality rate, latent TB infection (LTBI) contributes to global morbidity. Latent infections are defined as a state of persistent immune response to stimulation by *Mycobacterium tuberculosis* antigens with no evidence of clinically manifest active TB ³⁵. Approximately one-third of the global population harbour an LTBI with an incidence between nine and eleven million cases annually ^{2,24,31}. Exact numbers for LTBI are difficult to discern clinically, as the primary means of diagnosis is the Mantoux tuberculin skin test. A positive Mantoux test result is as likely to be due to previous exposure to TB bacilli, or vaccination, as it is to be due to live bacilli, resulting in limited diagnostic value ³⁶. Approximately 1% of LTBI cases will develop active TB annually ^{29,37}, while the WHO estimates that between 5%-10% of LTBI cases will develop into active TB during an individual's lifetime ³⁸.

1.2.2: TB Demographics

In the 2021 annual Global Tuberculosis Report, the WHO provided the most recent epidemiological data gathered from 198 countries, which was collated from internal reports provided by governmental health surveillance systems. The report covers approximately 99% of the global

population, and its findings show that TB disproportionately infects adults aged 15 and over (90% of cases). TB incidence is also slightly elevated in males aged over 15 (56% of new cases) compared females over 15 (32% of new cases) ³³.

TB infections in HIV-positive individuals are of marked epidemiological interest. HIV co-infections are separately analysed in the 2021 WHO Global TB Report and are often the focus of research studies ^{34,39,40}. Due to HIV's immunosuppressing nature, seroconversion of TB infection can happen earlier, resulting in symptomatic cases that may evade diagnostic detection ³⁸. This diagnostic evasion is correlated with paucibacillary infections, which fall below the limit of detection for smear-microscopy, and higher incidence of extrapulmonary disease among HIV+ individuals ³⁸. Diagnosis delay is highly correlated with adverse treatment outcomes. Aside from diagnostic difficulties, earlier seroconversion results in a 26-fold increase in the likelihood of HIV+ individuals developing active TB ³⁸.

Co-infection with HIV is most prevalent in Africa with rates >50% in many countries. In South Africa, for example, robust MDR and HIV testing systems identify 40%-80% of MDR and XDR cases are also HIV+ ^{38,41}. Accurate numbers for TB mortality in HIV+ individuals are difficult to obtain, since death due to TB in HIV+ individuals is often reported only as death by HIV ³³. However, a 2015 study found HIV/TB case fatalities are primarily (92.3%) due to multi-organ involvement and failure ⁴². These deaths are classified as deaths by HIV, however, they are still recorded for the WHO annual report.

Paediatric TB studies are less prevalent in the literature, but some existing studies place the incidence of TB attributable to children under 15 as 6-15% ⁴³. Lack of documentation is generally attributed to the paucibacillary nature of paediatric TB, increased presentation of extrapulmonary TB in paediatric patients, and difficulties in collecting diagnostic samples from paediatric patients ⁴¹. In children and adolescents, advancement from infection to active disease is rapid and the prevalence of extra-pulmonary and disseminated TB is increased ^{43,44}. A WHO report from 2015, the

last time paediatric TB was explicitly described, reported 210,000 deaths in children under 15 from TB globally per year. Of these 210,000 deaths, 17% were comorbid with HIV ⁴⁴.

The 2021 WHO annual report also summarised global incidence rates across all demographics (Figure 1.4). The annual incidence is estimated at 10.4 million cases globally ^{12,33}. Incidence rates vary by country, from 5/100,000 to 500/100,000 annually (global average 130/100,000). The incidence rate disparity is correlated with data that shows 87% of incident cases occurred in 30 high-incidence countries in 2019. Of these 30 countries, 8 account for approximately two thirds of global cases. Global incidence has declined 11% since 2015, largely driven by a 25% decrease in the WHO European region, although incidence is increasing in the WHO American region due to upward trends in Brazil ³⁴.

Estimated TB incidence rates, 2020

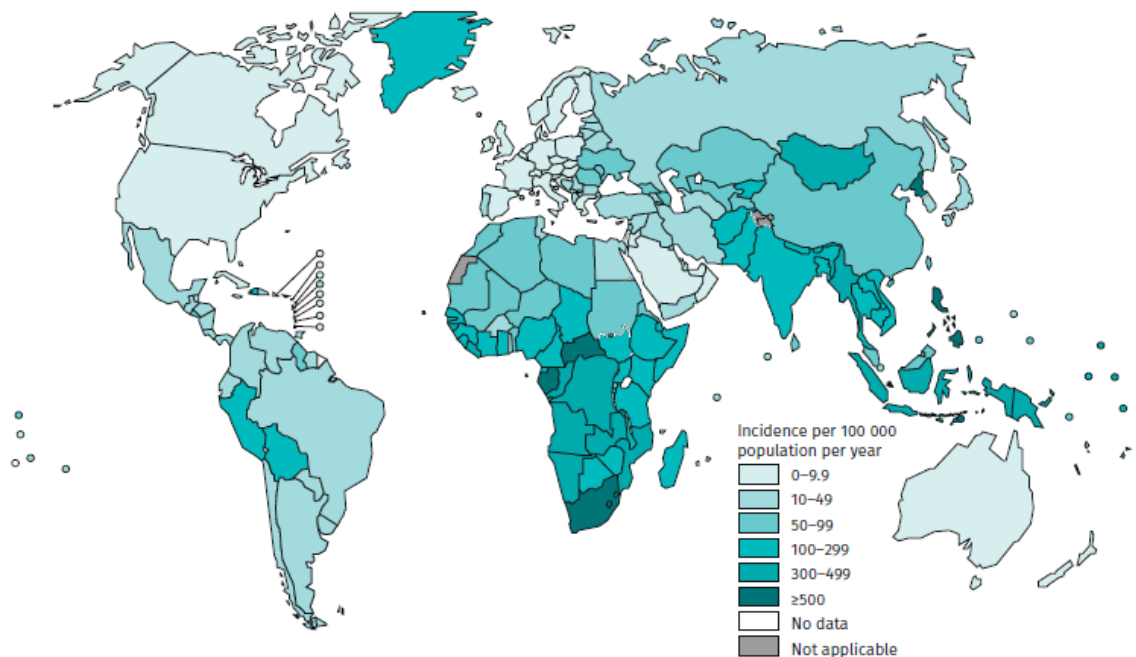


Figure 1.4: Global incidence rates of WHO reporting countries, 2021 ³⁴

1.2.3: Global TB Trends

The WHO have reported that over the past two decades TB incidence and mortality rates have been declining globally (Figure 1.5). Annual incidence has declined by an average of 1.7% per annum,

although the total reduction is still short of the 20% target for 2020. The decline in incidence is being monitored by increases in reporting rates in most countries, aiding in global case estimates³⁸. Likewise, the 2020 WHO Global TB Report saw a 14% reduction in mortality from 2001-2019, which still falls short of the 35% 2020 target³³.

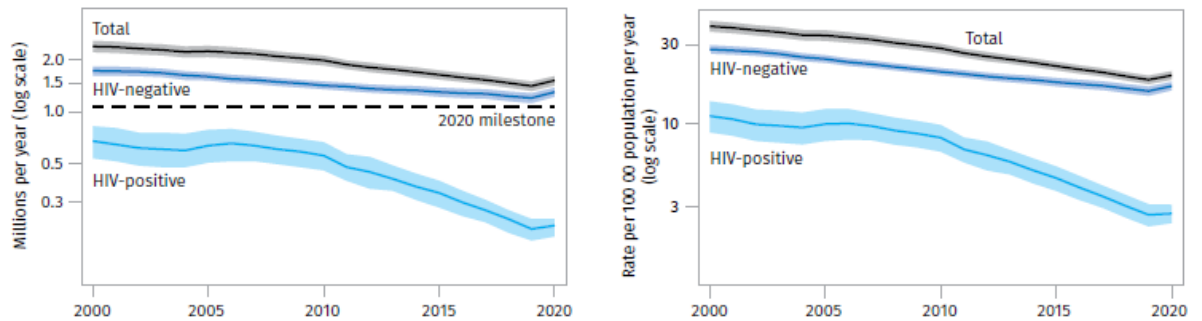


Figure 1.5: Global trends in the estimated number of TB deaths (left) and the mortality rate (right), 2000-20³⁴. Shaded areas represent uncertainty intervals. The horizontal dashed line shows the END TB Strategy 2020 milestone.

1.2.4: COVID and TB

The SARS-CoV-2 (Covid-19) pandemic has had a significant negative impact on global TB control and treatment efforts. Reports from the WHO and STOP TB Partnership predict mortality rates will likely return to either 2012 or 2015 levels (depending on the modelling system used). The STOP TB Partnership also calculates an increased incidence of 6 million cases and 1.4 million preventable deaths by 2025 as a direct result of the Covid-19 pandemic³³.

This increase in incidence and mortality is forecast for numerous reasons. For instance, detection rates are dropping by 20%-50%, in part due to the reallocation of resources and avoidance of healthcare by the public (Figure 1.6). Two examples are India and South Africa, both of which reported a drop in TB notification rates >50% over the 2019 calendar year. Major sources for TB resurgence have been cited to be the redirection of medical resources, such as molecular diagnostic tests, and the discouragement of those with either chronic conditions or mild symptoms from

seeking medical aid ³³. Moreover, loss of economic stability and major disruption to supply lines contribute to an increase in case rates ³³.



Figure 1.6: Trends in case notifications of individuals newly diagnosed with TB by WHO region, 2016-2020 ³⁴

1.3: Drug Resistance in TB

Drug-resistant TB is a growing issue, even when overall incidence of TB was in decline ⁴¹. The most recent WHO reports cited 3.3% of new cases and 18% of recurring cases globally were drug-resistant (Figure 1.7) ³³. A systematic review published in 2017 indicated that approximately one fifth of globally tested isolates are resistant to at least one first- or second-line drug ⁴¹. Rates of drug-resistance were highest in former Soviet republics (SSRs) where >25% of new cases and >50% of recurring cases demonstrated some form of drug-resistance ^{41,45}. Disparity in global rates can be attributed in part to historic factors, such as inconsistent supply lines and medication shortages in the former SSRs ^{46,47}.

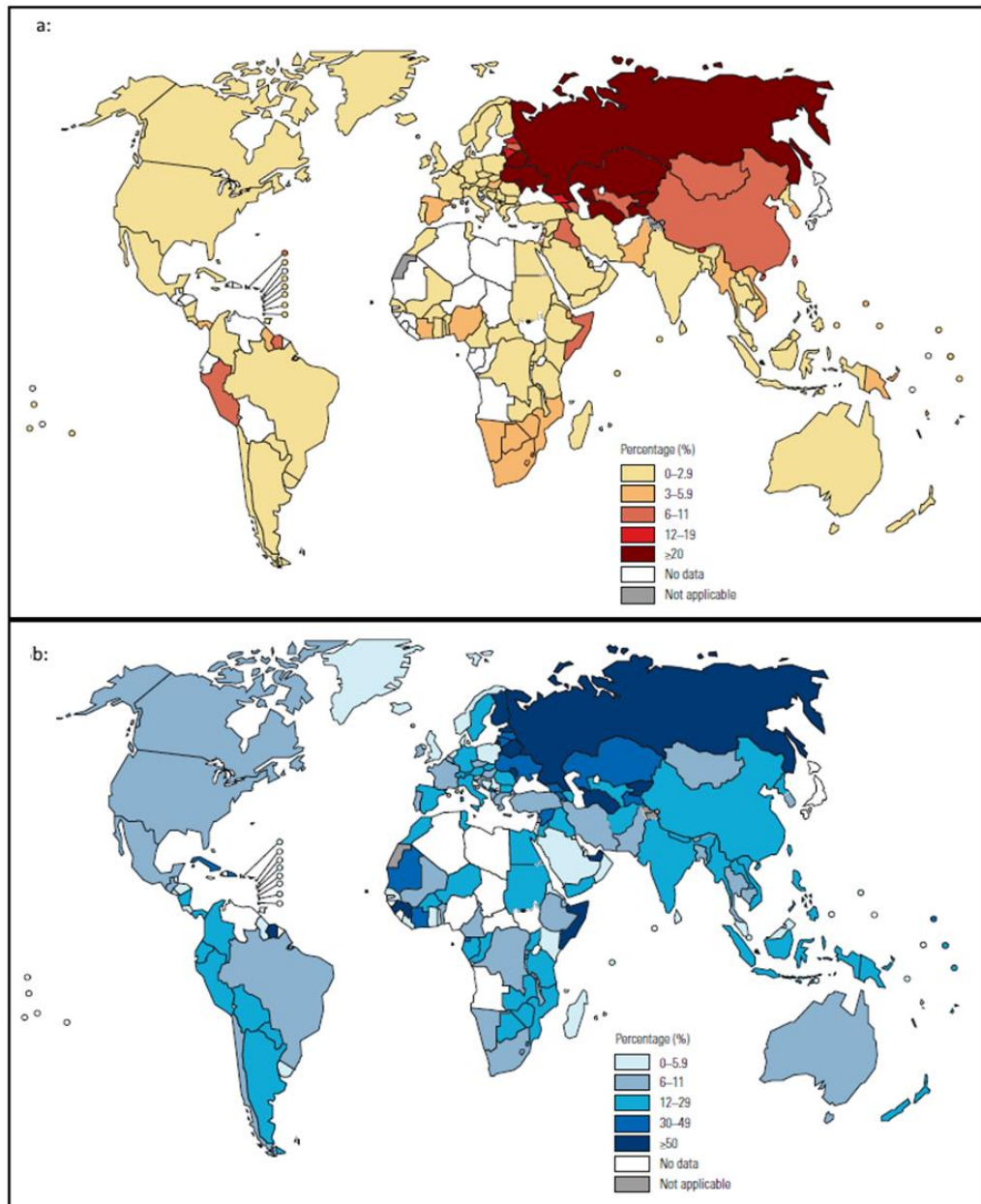


Figure 1.7: Global MDR/RR-TB rate in new (a) and previously treated (b) TB cases³³.

Drug-resistant TB can be broken down into different types (Figure 1.8); rifampicin-resistant (RR), multidrug-resistant (MDR), extensively drug-resistant (XDR), and “incurable” or totally drug-resistant (TDR)^{8,16}. Increasing incidence of DR-TB is a growing issue globally^{16,48,49}. All types of DR-TB are caused through genetic mutations owing to the clonal reproduction of mycobacteria^{13,29}.

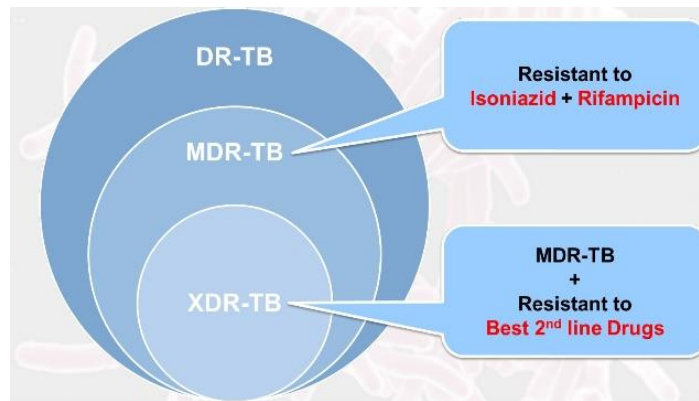


Figure 1.8: Visual representation of the relationship between the three most common types of drug-resistant TB ⁵⁰.

The first recognised occurrence of drug-resistance in TB was reported in the late 1940s, shortly after the introduction of streptomycin as an anti-tuberculous agent ^{41,45,51}. Since then, drug-resistance has been increasingly well-documented. Investigation into the types and severity of drug-resistance has become a pressing issue, with the WHO END TB Partnership placing special emphasis on further research.

Concerns are that drug-resistant infections will reverse progress made towards the eradication of TB ^{41,52}. The incidence of drug resistant infections worldwide has increased over 4-fold in the past decade alone. Only 4.9% of patients demonstrated drug resistance in 2009 compared to 20% in 2019 ⁴⁸. In 2015, the last year for which complete data was available from WHO, 580,000/10.5 million TB cases worldwide were identified as RR/MDR-TB ^{6,45}. Of those, 9.5% were XDR or worse.

1.3.1 RR/MDR TB

Rifampicin resistant TB (RR-TB) is the most common form of DR-TB and is defined as any TB infection which exhibits resistance to rifampicin or any of its related compounds, such as rifapentine. In 2015, there were an estimated 580,000 cases of RR-TB, although only 340,000 were reported. Of the cases reported, only a fraction (36.8%) were administered second-line treatment ⁴⁵. Isoniazid resistance is thought to be more common (9.5% of all TB infections), but testing for it does not yet exist in the same way as it does for rifampicin resistance ⁴¹.

MDR-TB is the second most common type of resistance after RR-TB^{8,16}. MDR-TB is defined as a TB infection that is resistant to at least isoniazid and rifampicin^{41,53}. In 2019, approximately 78% of rifampicin-resistant infections were further categorised as MDR following DST³³. Furthermore, between 2018 and 2019, the prevalence of MDR-TB increased by 10%³³.

Despite resistances, MDR-TB infections are still commonly treated with traditional WHO-endorsed DS-TB regimens in LMICs. These treatments require only a 6-month course of first-line antibiotics^{14,54}. However, an augmented 24-month, or a newly designed 12-month regimen, are recommended by the WHO in places with sufficient infrastructure and resources⁴¹.

There are several known risk factors for the development of RR/MDR-TB, the most significant being prior patient history of ≥ 1 month of anti-tuberculous treatment⁴⁵. Historically, this has been considered the primary force behind the selective evolution of drug-resistant bacilli, which become prevalent during reinfection^{41,45}. However, this does not account for the incidence of RR/MDR-TB in newly acquired TB infections.

Other risk factors for RR/MDR-TB include hospitalisation, incarceration, and HIV infection⁴⁵. These external factors can impact drug-resistance in both recurrent and new TB infections while other factors specifically affect community transmission. Geodemographic variations are also known risk factors, for example, in areas with large populations of formerly incarcerated individuals or lower socio-economic status, greater community prevalence of RR/MDR-TB has been recorded⁴⁵.

Mortality and morbidity are increased in MDR-TB cases when compared to drug susceptible cases. Mortality rates are calculated to be between 40%-50% in MDR cases and treatment difficulties often lead to affected individuals suffering from chronic disease^{41,53}.

1.3.2 XDR/TDR TB

XDR-TB was redefined in 2020 as a strain that fulfils the definition of MDR/RR-TB and which is also resistant to any fluoroquinolone and at least one additional Group A drug

(levofloxacin/moxifloxacin, bedaquiline, and linezolid) ⁵⁵. The first recorded outbreak of XDR-TB occurred in Tugela Ferry, South Africa in 2006 ⁴¹. The Tugela Ferry clone alerted the world to the severity of continued drug resistance in TB, and the incidence of XDR-TB has increased since this first outbreak. In 2019, 20% of reported MDR infections were also resistant to fluoroquinolones, a 2-fold increase from 2017 ^{33,41}.

TDR-TB is less formally defined than RR-, MDR-, or XDR-TB, although some sources do describe TDR as “programmatically incurable” owing to the lack of sufficient susceptible drugs for a curative regimen ⁴¹. The incidence of TDR-TB infections is increasing in three of the four highest incidence countries, which are China, India, and South Africa. This is particularly concerning to management programs and watch groups as these countries are generally poorly equipped to prevent onward transmission ⁴¹.

1.3.3 Factors in the Emergence of Drug Resistance

The emergence of drug resistance has been an officially recognised problem since 1994 when the WHO and the International Union Against Tuberculosis and Lung Disease (IUATL) launched the Global Project on Anti-Tuberculosis ^{41,51}. This project’s primary focus was to establish a surveillance network for the emergence of drug resistance, and this is still active today, making it the world’s oldest and largest antimicrobial resistance surveillance project ⁴⁵. This network is not without its limitations, however, as the most detailed and consistent data routinely comes from high-income countries, which are not representative of high-incidence LMICs ^{41,51,56}. This inconsistency in LMIC data reporting makes it difficult to accurately estimate the emergence of drug-resistance.

Primarily, drug resistance in *M. tuberculosis* and related species is attributable to SNPs ^{15,41}. This contrasts with many other bacterial species that acquire resistance through gene transfer systems. Because of this, development of resistant phenotypes in the MTBC is simplified while also limiting the spread of phenotypes because of the clonal nature of mycobacteria ¹⁵.

The development of DR-TB infections is primarily considered as a result of inconsistent treatment protocols, delayed treatment, lengthy treatment courses, and administration of drugs on already resistant strains; all of which lead to positive selection for drug-resistance and a higher incidence of resistant infection transfer between hosts ^{13,30,57}. This is especially evident where poorly funded and/or administered treatment programs with low cure rates (<50%) have increased the population of individuals with chronic disease ⁵⁸. Additionally, some species within the MTBC exhibit lineage-specific inherent resistance to pyrazinamide, like *M. bovis* and *M. canettii*, which, if misdiagnosed, can impede resistance-control methods ^{6,8,15}.

Multiple studies from 1994 through to the present have shown previous history of TB treatment to be the most consistent risk factor for MDR-TB emergence. This is further supported by geographic distribution maps of MDR-TB which overlap areas historically known for ineffective treatment ³³. Poor treatment can result in a large population with chronic TB and, in combination with steady selective pressures, this can lead to new MDR mutations with increased stability.

However, the development of DR-TB is not solely due to ineffective treatment. DR-TB hotspots, defined as regions where the prevalence of DR-TB is >5%, have brought increased interest to community and patient-to-patient evolution and transmission ^{45,56}.

Investigation of selective pressure leads to an interesting discussion on the development of DR-TB. Drug resistance is frequently thought of as an “end-point”, yet the development of drug resistance is a continuous biological process and is constrained by the biophysical properties of TB bacilli ⁵⁶. While external pressures may alter the relative fitness of a given bacilli, they cannot fundamentally change the underlying mutative processes which cause phenotypic variation. Thus, even constant selective pressure will not necessarily increase the rate of mutation emergence, however it will serve to fix those that do emerge more readily.

Studies into phylogeographic distribution of resistance types show significant differences in the prevalence of drug resistance between lineages and strains ^{41,56,59}. The most successful MTBC

lineage in prevalence and development of antimicrobial resistance is the Lineage 2 Beijing strain (Figure 1.9)⁵⁶. The exact biological link between lineage and development of resistance is unknown and the hypothesis that an elevated basal mutation rate may be involved has not been supported in the research^{56,59}.

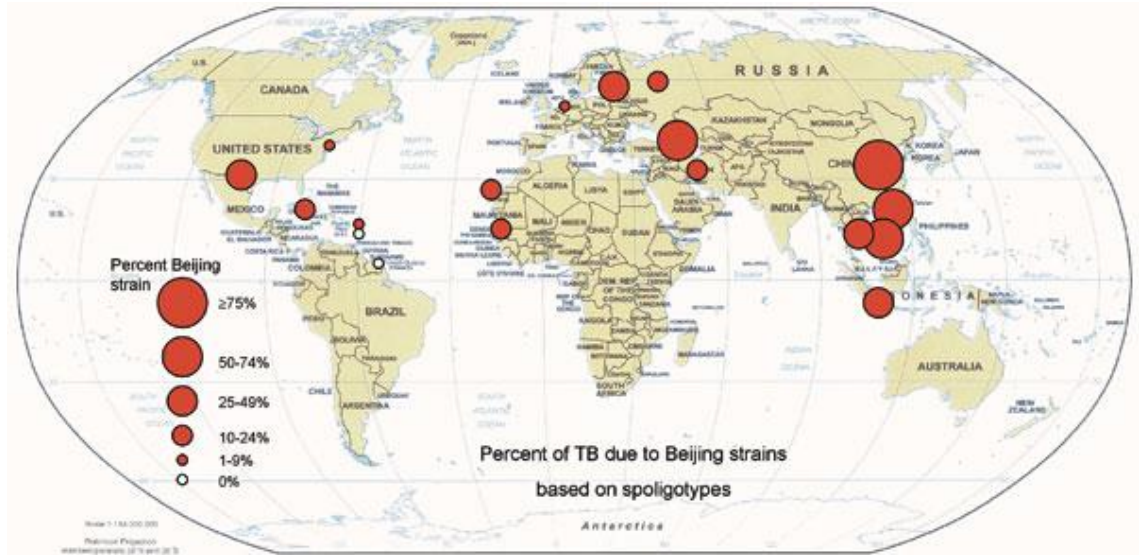


Figure 1.9: Global map showing the proportion of TB infections due to the Beijing Strain of *M. tuberculosis* in select geographic regions in 2002⁵⁹.

1.4: TB Treatment

1.4.1: First-Line Medications

TB treatment primarily relies on a combination of four drugs: rifampicin, isoniazid, pyrazinamide, and ethambutol. Per WHO guidelines, all four drugs are administered for a period of two months after which point only rifampicin and isoniazid are administered for a further four months. However, in the event of drug resistance, alternative methods of treatment are recommended. First-line treatment can additionally include streptomycin, yet this is less common given a 70-year history of streptomycin resistance in TB^{60,61}. These first-line medications benefit from oral administration, improving treatment compliance⁶¹.

Compliance with this treatment protocol has a documented success rate of approximately 85% in drug-susceptible patients⁶². Despite this high success rate, more effective medications and shorter treatments are continually under research. These research avenues aim to improve patient adherence and reduce patient/health system costs⁶². In 2021 the Guideline Development Group (GDG) convened to review evidence on the safety and efficacy of a reduced 4-month treatment protocol comprised of rifapentine, isoniazid, pyrazinamide, and moxifloxacin. This method was identified to be non-inferior to the existing 6-month protocol with equivalent side effect tolerance⁶². While this regimen benefits from being shorter and all-oral, the cost of rifapentine is currently a limiting factor for short- and medium-term implementation⁶².

1.4.2: Drug Resistant TB Treatment

In rifampicin-susceptible and isoniazid-resistant infections the treatment recommendation is amended to a six-month regimen of rifampicin, pyrazinamide, ethambutol, and levofloxacin. In this form of drug-resistant infection, streptomycin and other injectable medications are specifically advised against by the WHO. Similarly, in the event of rifampicin-resistant or MDR infection, an extended course of treatment is recommended, including levofloxacin or moxifloxacin to replace rifampicin. This extended course takes 24-months and relies on highly toxic injectable medications. The combination of length, administration complexity, and toxicity leads to lower treatment compliance and increased onward transmission⁴¹.

Extended treatments come with alternative guidelines set by the WHO. For example, kanamycin and capreomycin are discouraged for an extended drug treatment regimen, while bedaquiline is strongly recommended. Likewise, clofazamine and cycloserine are approved for extended treatment regimens when necessary³¹.

For MDR-TB, the goal has been to develop a consistent scalable treatment regimen, especially in LMICs, since the launch of the DOTS-Plus program by WHO in 1999. This program emphasised sustained commitment to MDR control and directly observed therapy to treat MDR positive

patients. In a trial in Bangladesh, the International Union Against Tuberculosis and Lung Diseases developed and tested an early recommendation to amend treatment protocols^{63,64}. This regimen consisted of a 4-6 month intensive phase using kanamycin, moxifloxacin, prothionamide, clofazimine, pyrazinamide, isoniazid, and ethambutol, followed by 5 months of moxifloxacin, clofazimine, pyrazinamide, and ethambutol⁶⁴. In areas with “simple” strains of MDR-TB, this regimen was found to perform consistently well; however, the efficacy fell in areas with mixed strains or a high proportion of pyrazinamide resistant strains⁶⁵⁻⁶⁸.

A meta-analysis of medications most associated with positive MDR/XDR-TB treatment outcomes identified linezolid, levofloxacin, carbapenems, moxifloxacin, bedaquiline and clofazimine as being most effective⁶⁹. The authors of the meta-analysis cited only modest benefits for the use of injectables and that the worst treatment outcomes occurred with the use of kanamycin and capreomycin. However, it is stressed, that the worse outcomes that arise when using injectables may be due to confounding factors, while the improved outcomes from the use of late generation medications like fluoroquinolones, bedaquiline, linezolid and clofazimine should be noted^{63,69}. While this meta-analysis strongly indicates that bedaquiline should be used in the treatment of MDR/XDR-TB, it must be accompanied by a monitoring of cardiac toxicity to avoid complications.

Using new studies available at the time, and the aforementioned meta-analysis, the WHO updated their treatment guidelines in 2019⁷⁰. These updated guidelines addressed both long and short regimens and reclassified available pharmaceuticals into A, B, and C groups based on toxicity, efficacy, and ease of administration⁶³. Further considerations for medication groupings included factors such as: reliability of DST methods, drug tolerability, population history of drug resistance, and potential interactions between drugs. In addition to ranking the medications, the WHO also stressed the need to stop the use of kanamycin and capreomycin, and to instead use amikacin if an injectable is still required for treatment^{63,70}.

One of the main takeaways from these reports is the continued need for research into new and optimised treatment regimens. One such avenue of research was the Nix-TB trial in South Africa, which showed promising results for treatment of XDR-TB using bedaquiline, linezolid, and pretomanid ⁷¹. This was innovative in that it was the first completely oral and short regimen for the treatment of XDR-TB and complex MDR-TB cases ⁶³. A follow-up analysis identified a treatment success rate of 88.78% after 6-months of treatment and a 6-month follow-up period ⁷². However, to maintain this degree of efficacy, extreme care will need to be taken to monitor for and avoid developing resistance to these newer medications, as has been the case with previously developed anti-tuberculous drugs. Likewise, increased patient monitoring is required, as linezolid is a highly toxic drug and can lead to cross-resistance with bedaquiline ⁶³.

A second new regimen under study, the SimpliciTB trial, uses bedaquiline, pretomanid, moxifloxacin, and pyrazinamide ⁷³. In drug-susceptible TB (DS-TB) patients, this regimen resulted in culture negativity within a mere two months, which is a third of the time in comparison to the normal short course TB treatment for DS-TB patients ⁶³. At the time of writing, results on the efficacy of this regimen have not been published though hopes are high that the inclusion of pretomanid will result in improved health outcomes by 2025 ⁷⁴.

These two studies provide evidence for the efficacy of reduced treatment times even for MDR/XDR-TB ⁶³. However, it is unlikely that either regimen will become the sole means of treatment for DR-TB cases, as strain variability and personal response to treatment will always prove to be confounding factors ^{63,65}. When coupled with rapid DST, through methods such as NGS, confounding factors can be mitigated and treatment can be summarily shortened. Reduction in treatment time would, in turn, promote improved health outcomes, increase treatment compliance, and reduce the financial burden of treatment for patients and health organisations.

1.5: Tuberculous Disease by Non-*M. tuberculosis* mycobacteria

1.5.1: Zoonotic TB

Zoonotic TB (zTB) transmission is also recognised as epidemiologically important, with an estimated 140,000 incident cases in 2019³³. This is similar to the reported incidence in 2016 (147,000 cases), indicating that as overall TB incidence decreases, zTB incidence remains stable²⁵. zTB incidence rates are calculated by identifying *M. bovis* infections, and are likely to be conservative as zoonotic species beyond *M. bovis* are not systematically identified and tracked³³. A review published in 2019 delved further into zTB transmission and infection, citing systematic and continued neglect for the condition in the WHO annual reports²⁵.

According to this review, published by Couto, et al., zTB is dispersed globally, though the majority of cases occur in Africa and Southeast Asia²⁵. Cases are likely underreported due to requisite diagnostic techniques being largely unavailable in LMICs where zTB is most prevalent. More frequently, zTB exhibits extrapulmonary presentation, making standard diagnostic methods such as smear-microscopy largely ineffective. In cases where zTB does present as a respiratory illness, it is often reported as a TB infection, as TB and zTB infections are indistinguishable without the use of advanced molecular techniques²⁵.

Most commonly, transmission of zTB is through ingestion of unpasteurized animal products, especially milk and cheese. This supports findings that zTB occurs more frequently in LMICs and immigrant populations within high-income countries where food safety standards are often less stringent²⁵. Due to this alternative exposure pathway, zTB primarily presents either as extrapulmonary or disseminated infection, as mentioned above. This contributes to the observed increase in mortality rate in *M. bovis* cases compared to *M. tuberculosis*, as miliary lymphatic and central nervous system infections are more common, and have inferior detection and treatment outcomes (Figure 1.10)²⁵.

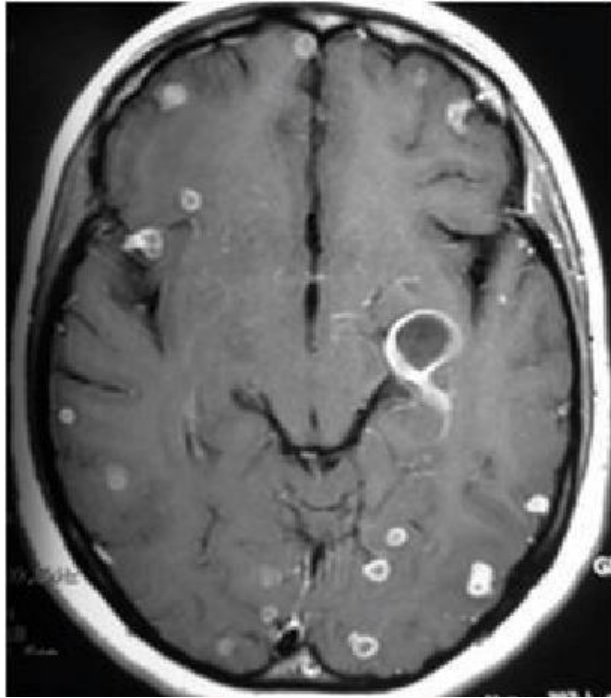


Figure 1.10: MRI of a disseminated central nervous system TB infection ⁷⁵.

1.5.2: Non-Tuberculous Mycobacteria

Beyond the varied types of TB infection, there are numerous diseases which have TB-like presentation but are not caused by the *Mycobacterium tuberculosis* complex (MTBC). Primarily, these are caused by NTMs which lead to pulmonary disease (NTM-PD). NTMs are defined as mycobacterial species which are not part of the MTBC or *Mycobacterium leprae*.

Increasing global incidence rates for NTM-PD create difficulties for diagnosis ^{76,77}. There is evidence that as global incidence rates for TB decline, incidence rates of NTM infections are increasing even more rapidly. One longitudinal study conducted from 1995 to 2012 identified an 8 fold increase in NTM infection throughout the United Kingdom, from 0.9/100,000 people to 7.6/100,000 people ⁷⁷.

NTM-PD epidemiology is hindered by the lack of reporting requirements in most countries ^{76,78}. These pathogens are generally ignored by health monitoring systems due to the long-held belief that patient-to-patient transmission does not occur, and thus any infections remain isolated. However, evidence from a longitudinal study conducted in cystic fibrosis centres beginning in 2012

showed genetic evidence of direct patient-to-patient transmission, either through fomites or long-lasting aerosols ⁷⁷. This makes early detection and differentiation between TB and NTM-PD increasingly important as the treatments are different and even the correct treatment course can result in negative side effects in patients such as nausea, vomiting, loss of sensation in extremities, and loss of eyesight ^{76,77}.

1.5.3: *M. tuberculosis*-Like Pathogens

Not all *M. tuberculosis*-like infections are caused by mycobacterial species. Another common cause of TB-like disease, which can complicate diagnosis and treatment, are bacteria from the genus *Nocardia*. *Nocardia* species are slow growing, *Gram*-positive, acid-fast bacteria similar to many mycobacteria (Figure 1.11) ⁷⁹. A 2020 review by Duggal and Chugh discussed this often neglected disease group in clinical settings ⁷⁹, focusing on 54 *Nocardia* species known to cause disease in humans, most frequently in immunocompromised individuals, with an overall global incidence rate of approximately 1/100,000 individuals. *Nocardia* infection presentation is primarily pulmonary, with symptoms such as pneumonia, inflammation, abscess formation, and deep structural cavitation; all these serve to mimic TB in clinical diagnosis. This symptom overlap, and subsequent difficulty in clinical diagnosis, are the basis for the genus nickname, “The Great Masquerader” ⁷⁹.

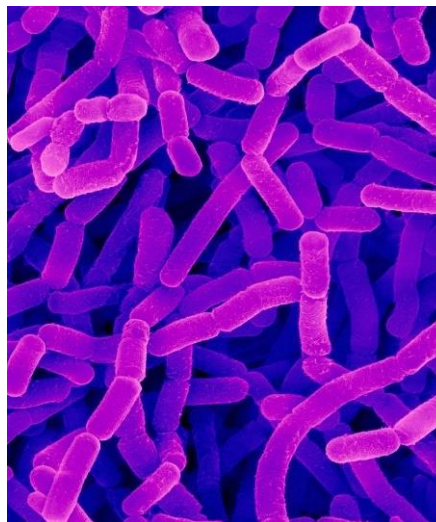


Figure 1.11: Colourised 1,600x magnification scanning electron microscope image of *Nocardia asteroides* structure ⁸⁰.

1.6: A Brief Overview of Molecular Epidemiology

Molecular epidemiology approaches have become the standard approach to study TB epidemiology and multiple methods have been developed. These methods have the advantage of being able to differentiate the species and strain causing TB while also providing data on transmission and reinfection.

1.6.1: IS6110 Typing

IS6110 has served as the gold standard for molecular epidemiology in TB infections since 1993⁸¹. This method of DNA speciation analyses the IS6110 insertion which is only found in members of the MTBC for differentiation of species. Related strains and linked cases will display extremely low levels of variability when analysed using RFLP techniques which analyse repetitive segments within the MTBC genomes. Unrelated cases will show a high degree of difference.

While useful for linking cases it ultimately displays limited utility compared to newer methods such as MIRU-VNTR due to its increased difficulty compared to this newer methodology. In further comparison, spoligotyping was developed concurrently with IS6110 and demonstrates poorer discrimination but is sufficient for many clinical and research purposes due to increased flexibility over IS6110.

1.6.2: MIRU-VNTR

Another molecular method is mycobacterial interspersed repetitive unit variable number tandem repeats (MIRU-VNTR) analysis. Mycobacterial genomes contain regions of 36bp direct repeat sequences interspersed with unique genomic segments which are PCR amplified and counted. Usually, this analysis is performed using twenty-four loci, the results of which are highly reproducible and easily compared between laboratories^{82,83}. MIRU-VNTR provides a high degree of discriminatory power to assays, allowing investigation of transmission dynamics and determination of whether a case is novel, relapse, or reinfection^{82,84}. However, this discriminatory power varies

by *M. tuberculosis* strain, requiring additional loci in a hypervariable region for the same diagnostic capability in the Beijing strain^{82,83}. As the Beijing strain is correlated with increased drug resistance, more complex loci sets would be required for routine diagnosis. An increase in complexity summarily limits the clinical utility.

MIRU-VNTR has further benefits, including its ease of use and its relatively low cost.

1.6.3: Spoligotyping

Like MIRU-VNTR analysis, spoligotyping uses non-coding identical direct repeat (DR) regions. However, unlike MIRU-VNTR, which looks for the number of repeats, spoligotyping identifies the unique spacer segments between each DR⁸⁵. Results are generally presented as a binary presence/absence, which allows direct comparison between isolates⁸². Identification of spacer segments also allows differentiation of *M. tuberculosis* strains; e.g., the Beijing strain lacks spacers 1 through 33, but contains spacers 34 through 43⁸².

The benefits of spoligotyping include high reproducibility and rapid turnaround times. Spoligotyping can produce a result within one day, as opposed to several weeks for IS6110 RFLP analysis⁸⁶. However, spoligotyping struggles to discriminate between strains in regions with a high prevalence of Beijing strain infections⁸². In a test of 118 clinical *M. tuberculosis* samples, spoligotyping identified 68 different strains, compared to a IS6110 analysis, which differentiated 88 strains. This study indicated that samples with multiple IS6110 copies are more difficult to differentiate by spoligotyping⁸⁵.

1.6.4: Whole Genome Sequencing

Unlike MIRU-VNTR and spoligotyping, which utilise only a small fraction of the *M. tuberculosis* genome, whole genome sequencing (WGS) analyses the entirety of an isolate's genetic sequence. WGS can be performed on clinical isolates for identification of species, strain, and drug-resistant mutations within a sample⁸⁷⁻⁸⁹.

WGS is useful for in-depth investigation of drug resistance, disease transfer, and lineage calling. However, WGS is not without its drawbacks. Firstly, WGS requires isolated cultures, thus increasing the time from suspected diagnosis of TB to obtain results ^{10,13}. Secondly, WGS requires extensive infrastructure and specialised staff training for accurate results and bioinformatic interpretation ^{16,54}. These drawbacks limit the clinical utility of WGS for drug resistance testing and diagnosis in resource limited areas outside of centralised reference laboratories.

These limitations are decreasing in severity with the development of new methodologies. For example, ONT has reduced the need for specialist skills and infrastructure, particularly with the use of the RBK kit. This kit allows library preparation from sample in 15 minutes. Likewise, new free software tools such as TB-profiler are available for sequencing analysis which decreases the need for specialist bioinformatic skills ^{90,91}. With these improvements WGS is becoming the new Gold Standard for TB diagnostics where resources are available.

1.7 Economics of TB

TB is extremely virulent and results in an excessive disease burden in LMICs ^{24,30}. The majority of global TB cases (95%) occur in countries with limited resources and health infrastructure (Figure 1.12) ²⁴. 43% of cases were reported in Southeast Asia, 25% in Africa, and 18% in the Western Pacific ³⁴. Despite this socio-economic link, the majority of TB research is conducted in high-income countries that exhibit low TB incidence ¹³. Numerous financial and economic factors also arise from TB infection and prevalence, both at the governmental and individual levels.

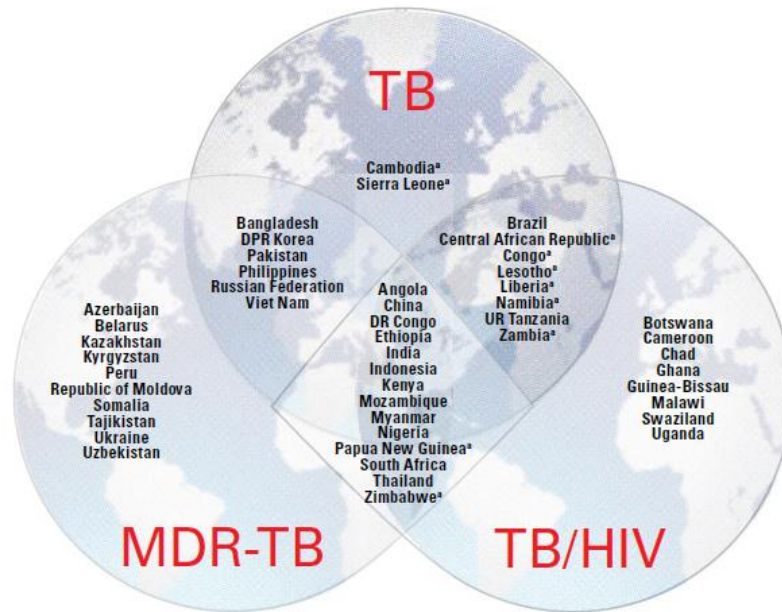


Figure 1.12: Countries in the three high-burden country lists for TB, TB/HIV, and MDR-TB between 2016 and 2020, with overlaps ³³.

Treatment for TB often places a large strain on medical infrastructure and governmental funding, especially for drug-resistant infections ⁴¹. For example, the cost of treatment for MDR-TB is approximately 100-fold that of DS-TB ⁵¹. Furthermore, despite accounting for only 5% of TB cases in South Africa, XDR-TB treatments consume over one third of South African national TB-program resources ⁴¹. To offset these burdens, many resources for combatting TB in high incidence countries come from extra-governmental sources, such as NGOs and foreign governments. One argument advocating for extra-national funding is that international travel and migration in the modern era compound to make drug-resistance and the spread of TB global issues ⁴¹. Programs to improve food access, housing, and general medical access, all of which are strongly linked to TB incidence, are also important for improving global TB outcomes and reducing the impact of TB on LMICs ⁵¹.

According to the WHO, in 2019 available funding for universal TB treatment access increased from \$5.6 billion to \$6.5 billion ³³. 57% of this funding was provided by five countries; Brazil, Russia, India, China, and South Africa. 97% of this was allocated for domestic use in combatting TB within their own borders. However, the funding total is still short of the \$13 billion goal for universal TB treatment access set by the WHO for 2022 ³³.

As previously mentioned, TB research is largely funded by organisations in low-incidence/high-income countries. In 2018, 56% of the total research funding available was supplied by the US Government as well as the Bill and Melinda Gates foundation. TB research funding is primarily allocated for treatment and infrastructure research, with approximately 9% earmarked for improving diagnostic methods ³³.

Aside from the burden on national healthcare and surveillance systems, at the individual level, TB diagnosis and treatment cause sizable financial burdens. The WHO calculated that, since 2015, 47% of global individuals treated for TB faced catastrophic healthcare costs (Figure 1.13), defined, in this context, as greater than or equal to 20% of annual household income. The percentage of cases facing such catastrophic costs is higher for individuals treated for drug-resistant TB infections (>87%) ³⁴. Costs disproportionately affect individuals in LMICs, compounding the burden seen at the national level ⁵¹.

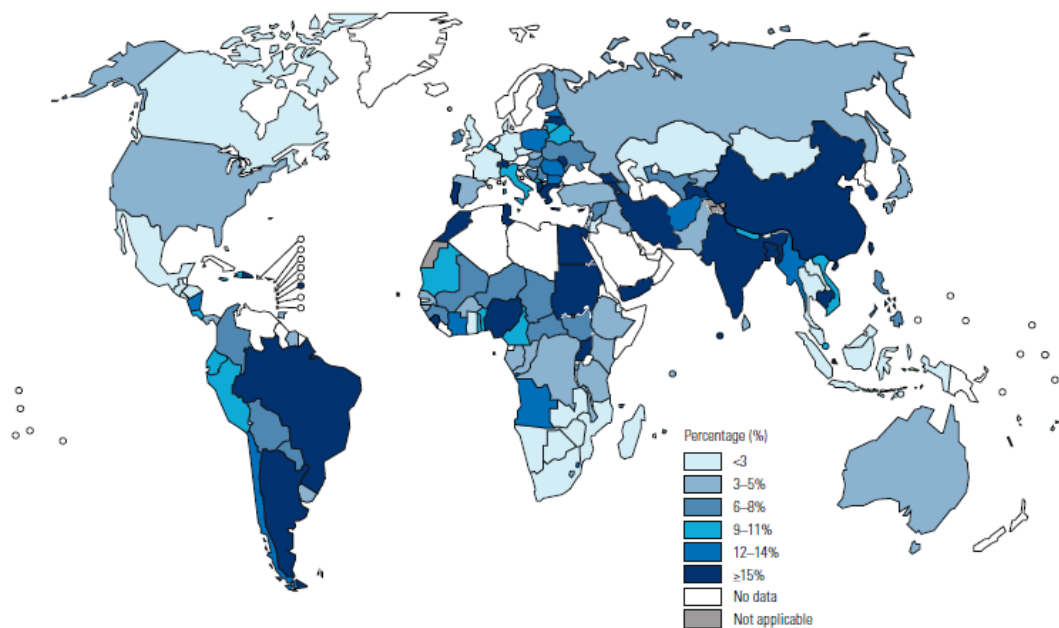


Figure 1.13: Percentage of the general population facing catastrophic health expenditure, according to the latest available data ³³.

1.8: Diagnosing TB and DR-TB

1.8.1: Drug-Susceptible TB Diagnosis

Over the past century, multiple diagnostic technologies have been developed or proposed. As technologies advance, so do hopes for faster, more accurate diagnostic methodologies.

1.8.1.1 Gold Standard

Effective TB diagnostics first emerged towards the end of the 19th century with the development of acid-fast staining, microscopy, and routine culture of clinical samples ^{15,92}. Standard microscopy is cheap and produces results quickly, though there are two key limitations: it is burdened with a high detection threshold, approximately 10⁵ colony forming units per millilitre (CFU/mL), and it is highly reliant on operator skill. Reliance on operator skill especially affects the sensitivity of microscopy diagnosis, which ranges from 20-80% for culture confirmed cases ⁹³. Despite these drawbacks, microscopy is still the only diagnostic tool commonly available in many low-income, high-incidence countries ^{3,13,14}.

In contrast, culture-based diagnostics, while slower, exhibit higher sensitivity and a lower limit of detection, approximately 10 CFU/mL, which is 10,000x lower than that of visual microscopy ^{14,94}. Though culture-based methods are highly sensitive, they still have significant drawbacks, the most prominent being the long turn-around time due to the slow growth of MTBC ¹³. For a summary of the strengths and weaknesses associated with various culture methods, see section 1.8.3.1.

These limitations demonstrate the requirement for new diagnostic and DST methods in order to improve TB control ^{29,95}.

1.8.1.2 PCR

One such method was developed in 1985 with the invention of polymerase chain reaction (PCR) by Kary Mullis. PCR methods show a marked increase in the speed of TB diagnosis, however, they still exhibit some weaknesses. For example, an inability to inform epidemiological studies renders PCR

tests less practical for disease control and tracking programs. Similarly, PCR methods are unable to detect co-infections or mixed infections, which can complicate treatment.

Some targets used for TB diagnosis have included IS6110, *rrs*, and *rpoB*⁹⁶. These genes are highly conserved in TB genomes and serve as consistent biomarkers for bacterial presence. Similarly, differentiation of virulent MTBC species and *M. bovis* BCG has targeted the deletion of the RD1 region⁹². These methods while sensitive and specific suffer from limited scope and breadth due to the conservative nature of PCR based diagnostics.

For a full review of the strengths and weakness of PCR techniques please see Wlodarska et al., or Schürch and van Soolingen^{13,97}. A brief summary of strengths and weaknesses is presented in section 1.8.3.2.

The next logical step in TB control was to move beyond the use of amplicons and aim towards deriving information from entire genome sequences. It was at the turn of the 21st century that the potential to routinely investigate drug-resistance and molecular epidemiology in this way emerged.

1.8.2: Drug-Resistant TB Diagnosis

1.8.2.1: Gold Standard

While useful for a rapid diagnosis of TB disease, microscopy is incapable of providing a drug-resistant or -susceptible diagnosis. Culture, however, is a powerful method for drug susceptibility testing (DST). MTBC cultures are grown in the presence of known antibiotic concentrations and the results are recorded as resistant or susceptible. Mycobacteria isolates are classified as phenotypically resistant if >1% of inoculated colonies on a plate grow in the presence of critical concentrations of a given drug⁴¹.

More recently an improved phenotypic method has come to the fore with the dissemination of the Bactec MGIT 960 manufactured by Beckton Dickenson in the USA. Using liquid medium and automated growth monitoring the reduction in oxygen attributable to the growth of aerobic

bacteria. This method reduces the phenotypic resistance calling time from several weeks to approximately one, greatly improving the turnaround time.

The use of MGIT technology has been further aided by research into broth microdilution methods. These methods have shown to increase the sensitivity and discriminatory power of MGIT diagnosis in the presence of heteroresistance, particularly for rifampicin, isoniazid, and ethambutol⁹⁸. This is managed by using geometrically increasing concentrations of antimicrobial agents within each culture, thereby more accurately identifying the MIC for a given sample⁹⁹.

Alongside research improving sensitivity and specificity the European Committee on Antimicrobial Susceptibility Testing (EUCAST) released a universal MGIT protocol in 2019¹⁰⁰. This protocol allowed for increased transparency between laboratories and facilitated ramping up of phenotypic testing utilising MGIT.

However, both phenotypic methods (culture and MGIT) suffer from the same limitations as culture diagnosis for drug-susceptible TB, and in fact take longer, since resistance cultures are performed following isolation of MTBC from sputum. Despite these drawbacks, culture-based phenotypic testing has remained the gold standard for identifying resistance to antibiotics¹²⁻¹⁵.

1.8.2.2: PCR

The WHO-endorsed Xpert MTB/RIF and new MTB Ultra assays are capable of diagnosing MTBC while also testing for resistance to rifampicin. WHO also endorsed the PCR based line-probe assays MTBDRplus and MTBDRsl DST which test MTBC isolates for first- and second-line drug resistance^{13,54}. While these assays have lower sensitivity for smear-negative samples; MTB/RIF: 84.48%, MTB/RIF Ultra: 81.8%, MTBDRPlus: 57%, MTBDRsl: 20-37%¹⁰¹⁻¹⁰³. Despite the decreased sensitivity, these assays are faster than gold standard methods and allow for antibiotic regimens to be implemented within clinically viable timeframes^{6,52,54}. Furthermore, these assays are currently the

only molecular methods endorsed by the WHO for use in LMICs ¹⁴. These factors demonstrate clear advantages over previous culture-only methods.

However, while rapid, these assays are only able to cover a very small percentage of the myriad SNPs associated with first- and second-line antibiotic resistance. This limitation, and low flexibility in targets, means that phenotypic resistance can be missed by omitting current and novel SNPs. In part due to this, it is common practice to utilise culture to confirm molecular DST findings, which largely negates the speed advantage of PCR methods.

1.8.3: Strength and Weakness Summary

1.8.3.1: Culture/Microscopy

Table 1.1: A summary of the primary strengths and weaknesses inherent with culture and microscopy for TB

Strengths	Weaknesses
Sensitive	Long processing time
Affordable	Risk of contamination and overgrowth
Able to perform simultaneous diagnosis and DST	Increased rate of false-negatives during diagnosis and DST
	Increased risk of laboratory transmitted illness
	Unable to differentiate species or strains

As mentioned previously culture serves as an extremely sensitive diagnostic procedure with a limit of detection of 1CFU/mL under ideal conditions ^{14,94}. Culture and microscopy also benefit from being cheap compared to molecular technologies. Further, culture can both serve as a diagnostic and DST test, although microscopy has no DST function.

Counter to these benefits culture and microscopy demonstrate numerous drawbacks. The most glaring of these is the long turnaround time for culture, approximately 8 weeks on average ^{15,104}. Further, the slow growth rate of TB increases the risk of overgrowth by commensal organisms ¹⁶, the risk of cross-contamination during incubation ¹⁷, and increases the likelihood of type 2 error ⁸. The low bacterial load required to result in active infection in TB also increases the likelihood of laboratory acquired infection during routine TB diagnostic and DST work by 6-9 fold over the general public ¹⁰⁵. Finally, neither culture nor microscopy is able to routinely differentiate causative

agents or strains within the MTBc in a clinically useful manner which can result in negative patient outcomes ⁵⁷.

These drawbacks often far outweigh the benefits of culture and microscopy prompting the use of more advanced diagnostic tools where available.

1.8.3.2: PCR

Table 1.2: A summary of the primary strengths and weaknesses inherent with PCR for TB

Strengths	Weaknesses
Rapid processing time	Reliance on highly conserved primers
Affordable	Unable to detect coinfection
Able to perform some DST	Requires culture followup for comprehensive DST
	Reduced sensitivity

PCR exhibits one major benefit over microbial culture for TB diagnosis, its speed. While culture takes weeks PCR has the potential to take mere hours to render a diagnosis ⁹⁴. This speed is aided by being only slightly more expensive than culture increasing the utility in laboratories of all sizes ¹⁰⁶. This speed and affordability is further enhanced by a limited ability to perform simultaneous DST during diagnosis with the proper design of primers.

However, as with culture, PCR is not without significant weaknesses. Firstly, the reliance of any PCR on highly reserved primers limits the breadth of a diagnostic assay. Similarly, this conservatism can reduce sensitivity in the presence of mutations ^{5,107}. The use of primers also limits the ability of an assay to determine coinfection as it is primarily a simple presence or absence of amplification which is detected ¹⁵. This presence/absence also means that anything beyond basic DST must be performed by follow up culture, largely negating the speed advantage of PCR ⁵².

In summation while PCR offers a distinct advantage over gold standard culture the drawbacks still necessitate the development and implementation of improved diagnostic and DST methods.

1.9: Whole Genome Sequencing (WGS) in TB

In 1998, over a century after the advent of acid-fast microscopy and culture-based methods, the first full *Mycobacterium tuberculosis* genome, *M. tuberculosis* H37Rv, was published ¹⁰⁸. This isolate

became the official reference genome for *M. tuberculosis* ²⁹. Since the publication of this original genome sequence, sequencing methods have become faster, cheaper, and simpler, resulting in a library of thousands of complete and partially assembled MTBC genomes within the National Center for Biotechnology Information (NCBI) database ^{3,29}. Many sequences were constructed using Sanger methodology, which formed the basis for the original genotypic diagnostic protocols, which have been increasingly used in the research and clinical management of TB ^{5,7,29}.

Sequencing allows for more in-depth research than previously possible through either culture or PCR. For example, the coverage of extra genome allows for molecular epidemiology and improved outbreak tracing and management. However, there are drawbacks to using WGS, preventing the widespread adoption of these techniques (section 1.9.2). Issues with WGS are driving research into quicker, cheaper, and more accurate molecular methods. Proponents for new techniques seek the advantages of sequencing without the drawbacks of culture, hoping to reduce the complexity and time required for these assays.

1.9.1: WGS DST

WGS diagnostics overcome the limitation of PCR, by targeting narrow sections of a genome. When coupled with information on resistance-conferring SNPs, this allows simultaneous DST for all anti-tuberculous medications ^{5,10}. However, this method still relies on the isolation of pure culture before DST can be performed and can often only be performed at larger reference laboratories ^{13,16,17}. Both limitations introduce delays for diagnosis, which can lead to poorer patient outcomes.

1.9.2: Strengths and Weaknesses of WGS

Table 1.3: A summary of the primary strengths and weaknesses inherent with WGS for TB

Strengths	Weaknesses
Can speciate mycobacteria	Requires culture
Can provide epidemiological data	Cannot determine transmission timing or directionality
Can simultaneously perform in-depth DST	Requires specialized infrastructure
High genomic resolution	Methods are unvalidated for use in LMICs

WGS demonstrates another large step in TB diagnostic and DST technology. This technology allows powerful and in-depth analysis of diagnostic samples which can generate multiple useful types of data. One such use of WGS is for the differentiation of mycobacteria and strains as WGS is able to supply information on the entire genome instead of the small sections previously possible²⁹. This genetic information can also be used to investigate epidemiological links with benefits for both clinicians and disease control organizations¹⁵. Finally, this whole genome coverage allows for simultaneous DST of all known mutation conferring SNPs, providing access to a suitable bioinformatic tool¹⁰⁹.

However, for all its strength WGS has a few notable weaknesses. Firstly, current WGS methods require pure culture which means that it is limited by the same slow processing time as traditional culture methods⁷. Also, WGS sequencing provides a snapshot look at a genome and as such comparison of genomes cannot determine time or direction of a transmission event¹⁰⁶. Further, coupled with the analytical strength of WGS is a summary increase in the expense of infrastructure required limiting the utility of these techniques outside of reference and research laboratories^{9,15}. In part due to the limitations imposed by these costs WGS is not validated for diagnostic use in LMICs where the power for DST is most sorely needed¹³.

As can be seen, there is currently no perfect tool for TB control. However, new assays and methodologies are continuously in development to improve the power, utility, and cost of TB diagnostics.

1.10: The Future of TB Diagnostics

Diagnostics and genomics are currently undergoing what Wlodarska et al. call a “Genomic Revolution” and what Tsalik et al. have named a “technological revolution”, phrases which indicate the rapid advancement and increasing analytical power of these methods in health related fields^{13,17}. Wlodarska et al. add that “the genomic revolution is set to dramatically alter the clinical

microbiology landscape, and we expect to see the first inroads in this area in the diagnosis, treatment, and epidemiology of tuberculosis in well-resourced settings.”¹³.

1.10.1 Metagenomic Diagnostics

Currently, one major use of next-generation metagenomic sequencing within diagnostics is identification of pathogen genomic sequences in a timely and cost effective manner^{1,7,8,15}. By investigating the large swathes of the genome, rather than smaller sections, biomarkers, or fingerprints, metagenomics allows for more detailed analysis than available through traditional sequencing methods^{10,30,54,110}. Single nucleotide resolution of large genome portions, available rapidly with metagenomic sequencing, stems from the ability of an assay to cover the majority of a genome with multiple read-depth within a single sequencing run without the need for culture isolation^{5,30}.

Rapid and accurate detection of SNPs has been transformative for clinical diagnosis and epidemiological efforts, as most resistance in TB is attributable to SNPs⁵. This is especially vital within the MTBC, as members have extraordinarily high levels of genomic homogeneity, making speciation by phenotypic methods or first-generation sequencing methods difficult^{1,12}. However, with SNP level resolution, differences are now identifiable within the MTBC, allowing for more accurate diagnosis and outbreak monitoring^{10,16,54,57}.

To achieve this level of resolution for pathogens the concentration of host DNA must be reduced. Samples will contain many-fold more host cells, and thereby host DNA, than bacterial cells which can overwhelm sequencing reads¹¹¹. However, the use of targeted depletion methods can reduce the proportion of host DNA in a sample, thereby allowing the detection and multiple-read depth of bacterial contributors¹¹¹⁻¹¹³.

The strengths and weaknesses of metagenomics can be summarised as follows:

Table 1.4: A summary of the primary strengths and weaknesses inherent with metagenomics for TB

Strengths	Weaknesses
High genomic resolution ¹¹⁰	Requires enrichment or host depletion ^{48,94}
Independent of culture ³	Expensive ¹⁶
Rapid turnaround time ^{3,49}	Requires complex infrastructure ¹⁴
Comprehensive DST ^{16,30}	Complex bioinformatic analysis required ^{8,88}

1.10.2 Targeted Next-Generation Sequencing

Use of targeted next-generation sequencing (tNGS) methods has allowed a shift from traditional Sanger sequencing for the detection and diagnosis of disease. High-throughput methods have dramatically reduced the cost per base of sequencing and, when combined with targeted amplification, have removed the barrier from low target DNA volumes in samples ^{114,115}. This has in turn altered the focus of molecular diagnosis away from single-gene related illnesses such as cystic fibrosis to diseases involving multiple genes concurrently. The new limitation is then on the pace of discovery and definition of genes for a given phenotype ¹¹⁴.

Diagnosis and DST of TB has directly benefited from this new focus with release of new commercial technologies like the Deeplex[®] Myc-TB from GenoScreen ¹¹⁶. The increase in defined drug-resistance associated genes allows products such as this to perform concurrent DST for more drugs than previous technologies. Because of this expanded target range the Deeplex[®] Myc-TB assay has seen success in Africa when compared to the GeneXpert MTB/RIF test ^{117,118}. One study also showed success in the detection of a drug-resistant TB strain using the Deeplex[®] Myc-TB kit which was undetected by WHO-endorsed methods ¹¹⁹. These trials demonstrated the potential for tNGS to detect DR-TB with greater accuracy than existing WHO-endorsed methods allowed.

Due to this diagnostic power WHO, in conjunction with FIND, have called for new diagnostic and DST methods using targeted next-generation sequencing (tNGS) to combat the increase in DR-TB

worldwide¹²⁰. Using existing PCR technology, combined with sequencing capabilities offered by systems such as those available from Illumina, ThermoFisher, and Oxford Nanopore Technologies (ONT), the aim is to create a specific and sensitive assay capable of accurately calling clinically relevant SNPs. By using a preliminary PCR step to enrich genetic regions of interest, assay specificity can be improved through careful primer design. Also, PCR amplification can improve assay sensitivity by facilitating deep, even, coverage of the target region ¹²¹.

Combined with rapid long-read sequencing this adds a new tool to the clinical genomics tool box.

1.11: Study Aims

Due to the increasing drug-resistance and prevalence of TB worldwide, new methods for diagnosis and epidemiological investigation are required. Existing methods have high sensitivity and specificity, yet are often hampered by slow turnaround times, complexity, and inability to rapidly detect MTBC and first and second line anti-TB resistance. This study seeks to address these issues by developing diagnostic tests that are rapid, user friendly, and affordable, in line with WHO/FIND aims.

Citing the need for novel techniques, this study aims to develop a standardised methodology for detection and sequencing of TB from primary sputum samples, using two NGS methods. Firstly, this study will seek to develop a tNGS assay for the detection of drug-resistant MTBC directly from clinical samples. Secondly, it seeks to develop a host depletion based rapid metagenomic sequencing test for MTBC and drug resistance detection. Both approaches will utilise nanopore sequencing and real-time analysis tools from ONT (Epi2Me) to develop sample-to-result pipelines for use directly on sputum. The tNGS approach will be developed for the FIND Seq&Treat programme – designed to generate evidence and boost in-country capacity to support the global adoption of commercial tNGS for affordable, scalable, and rapid TB DST (<https://www.finddx.org/at-risk-populations/seq-treat/>) – and will be evaluated as part of this programme.

Chapter 2 - Methods

2.1: Bacterial Culture Conditions for Method Development

M. bovis BCG and *M. smegmatis* were independently cultured for use in method development. The *M. bovis* BCG strain was provided by collaborators at the Norfolk and Norwich University Hospital (NNUH) Innovation Centre (section 2.2) where it was cultured in a BD BACTEC MGIT 960 until flagged positive ($\sim 10^5$ CFU/mL). A freeze-dried *M. smegmatis* sample (NCTC 8159) was purchased from the Public Health England (PHE) culture collection. *M. smegmatis* was reconstituted in 1mL of LB nutrient broth before inoculating 100 μ L into three 10mL of LB broth cultures in 15mL falcon tubes. An uninoculated 10mL sample of LB broth was also cultured as a contamination control. *M. smegmatis* samples, and the control, underwent incubation on an orbital shaker at 37°C. Cultures were incubated for four days until suspended bacteria became visible, at which time culture tubes were transferred to a 4°C refrigerator for downstream use.

Freeze-dried culture samples of *M. kansasii* (DSM 44162), *M. abscessus* (DSM 44196), and *M. avium* (DSM 44156) were sourced from the Deutsche Sammlung von Mikroorganismen und Zellkulturen (DSMZ) for use in specificity testing. These samples were each reconstituted in 1mL MiddleBrook 7H9 nutrient broth. 100 μ L of reconstituted samples were then inoculated into pre-aliquoted glass culture tubes containing MiddleBrook 7H9 nutrient broth from Hardy Diagnostics in triplicate (Catalog # C32). Inoculated cultures were grown in an orbital incubator at 37°C for 12 weeks, or until suspended bacteria became visible. An uninoculated culture tube underwent the same growth conditions as contamination control.

A second strain of *M. bovis* BCG was grown by collaborators at the NNUH Innovation Centre under specific conditions to inhibit clumping and promote even distribution of bacterial cells throughout a liquid culture¹²². Freeze-dried *M. bovis* BCG was reconstituted in 1mL of MiddleBrook 7H9 nutrient broth. 10 μ L of the reconstituted sample was inoculated into a BACTEC MGIT liquid growth tube with PANTA (supplemental polymyxin B, amphotericin B, nalidixic acid, trimethoprim and

azlocillin) and left to grow for 30 days. After this period the MGIT tube was removed from the machine and vortexed vigorously to resuspend cells. The culture was left to sit for 10 minutes, allowing large clumps of cells to settle. After this settling period, 200µL of supernatant was removed and reinoculated into a fresh MGIT tube to which 100µL of 0.5% Tween-80 had been added. The newly inoculated MGIT tube was returned to the BACTEC MGIT machine and left to incubate for a further 18 days, after which time the tube was removed and the cultured *M. bovis* BCG was ready for further experimentation.

For solid media growth, MiddleBrook 7H10 agar plates were purchased from Trafalgar Scientific (Catalogue #7046). 100µL of each liquid BCG culture, serially diluted in phosphate buffered saline (PBS), was aliquoted into the centre of an agar plate. The liquid dilution was spread using a disposable sterile cell spreader before the plates were covered and placed into a 37°C incubator for 8-12 weeks, until bacterial growth became visible. An uninoculated agar plate was also prepared as a contamination control.

In silico sequences for *M. caprae* (GCF_001941665.1) and *M. pinnipedii* (GCF_002982275.1) were sourced from the NCBI database for use in specificity testing to avoid the necessity of culturing BSL-3 organisms. Likewise, *M. leprae* (GCF_003253775.1), *M. ulcerans* (GCF_020616615.1), and *M. marinum* (GCF_016745295.1) were also sourced *in silico* to simplify specificity testing and reduce the lead-time needed to grow new cultures from freeze-dried stock.

2.2: Clinical Sample Ethics

Excess diagnostic sputum was obtained from the NNUH Innovation Center for all contrived sample experiments. Contrived samples were created by spiking known quantities of known organisms (*M. bovis* BCG, *M. avium*, *M. abscessus*, and/or *M. kansasii*) into these sputum samples (further described in section 2.6). Sputum was pooled at the Innovation Center and no identifying information was provided. The use of excess diagnostic samples for TB diagnostics research was approved by HRA and Cambridge East Research Ethics Committee under IRAS project ID 255463.

2.3: DNA Extraction

DNA was extracted using automated systems to simplify sample preparation and minimize the risk of contamination. Two automated methods were used through the course of the study, the MagNA Pure Compact System and the Promega Maxwell Rapid Sample Concentrator (RSC) 48.

2.3.1: MagNA Pure Extraction

DNA was extracted from pure liquid cultures for use in method development and positive controls using the MagNA Pure compact system. When extracting from pure liquid culture a sample size of 200µL was used. Samples were pelleted in a benchtop centrifuge at 6,000g for 3 minutes before carefully removing the supernatant. It was standard practice to leave approximately 50µL of supernatant behind to avoid loss of sample. The pellet was then resuspended in 500µL of MagNA Pure Bacterial Lysis Buffer (BLB) available from Roche Life Science (Catalogue # 04659180001). The resuspended sample was then transferred to a Lysis Matrix E tube available from MP Biomedicals (Catalogue # 116914050-CF) for mechanical cell-lysis and sample homogenization. The samples were then bead-beaten in a Qiagen TissueLyser LT (Catalogue # 85600) at maximum speed for 15 minutes to maximize mechanical cellular lysis. Following lysis the samples were again pelleted in a benchtop centrifuge, at 21,000g for 3 minutes. After centrifugation, 230µL of supernatant was carefully removed and aliquoted into a fresh MagNA Pure tube for use in the automated extraction system. This was done by removing two volumes of 115µL to minimize the risk of transferring any of the lysis matrix which can inhibit subsequent DNA extraction. An additional 170µL BLB was added along with 20µL of Proteinase K and the mixture was incubated on an Eppendorf ThermoMixer C (Catalogue #5382000031) at 65°C, 800rpm, for 5 minutes. Finally, the sample in the MagNA Pure tube was loaded into the MagNA Pure Compact according to the manufacturer's protocol and eluted in 50µL.

NRF sputum spiked with liquid culture [*M. bovis* BCG], and contrived clinical samples received from FIND, were initially extracted using the MagNA Pure Compact. For these sample types, the initial

sample volume used was between 750µL and 1mL. After aliquoting the desired volume of sample into a clean Eppendorf it was centrifuged at 8,000g for 5 minutes to create a pellet.

The pellet was resuspended in 700µL of BLB. This resuspended sample was then transferred to a Lysis Matrix E tube [MP Biomedicals] for mechanical lysis. The sample was then bead-beaten in a MP Biomedicals FastPrep-24 5G lysis system (Catalogue # 116005500) at 6m/s for two cycles of 45 seconds each. The bead-beaten samples were then centrifuged in a benchtop centrifuge at 21,000g for 3 minutes. Following centrifugation, 400µL of the supernatant was carefully transferred to a barcoded MagNA Pure tube in two batches of 200µL each. 20µL of Proteinase K was then added to the sample and the mixture was incubated on an Eppendorf ThermoMixer C at 65°C, 800rpm, for 5 minutes. The incubated sample was then loaded into the MagNA Pure Compact following the manufacturer's protocol and eluted in 50µL for downstream use.

2.3.2: Promega Maxwell Extraction

NRF sputum spiked with liquid culture [*M. bovis* BCG], and contrived clinical samples received from FIND, were also extracted using the Maxwell RSC 48. For these sample types, the initial sample volume used was between 750µL and 1mL. After aliquoting the desired volume of sample into a clean Eppendorf it was centrifuged at 8,000g for 5 minutes to create a pellet.

The pellet was resuspended in 700µL of PBS and transferred to a MP Biomedicals Lysis Matrix E tube for mechanical lysis and homogenization. As with the samples being prepared for the MagNA Pure, these samples were processed in a MP Biomedicals FastPrep-24 5G system at 6m/s for two cycles of 45 seconds each. After lysis, the samples underwent centrifugation in a benchtop centrifuge at maximum speed for 3 minutes before 400µL of supernatant was carefully aliquoted into a fresh 1.5mL Eppendorf tube in two 200µL volumes. The sample then had 40µL of Proteinase K and 200µL of Lysis Buffer A from the Promega Maxwell RSC PureFood Pathogen Kit (Catalogue #AS1660) added and pipette mixed. This mixture was then incubated in an Eppendorf ThermoMixer C at 65°C, 800rpm, for 10 minutes. Following this incubation, 400µL of PBS and 300µL of Lysis Buffer

from the Promega Maxwell RSC PureFood Pathogen Kit were added to the sample. Finally, the entire mixed sample was loaded into the Promega Maxwell RSC following manufacturer's protocols and eluted into 50µL for downstream use.

2.4: DNA Quantification

Quantification of nucleic acid was performed using two methods; the Invitrogen Qubit 4 Fluorometer (ThermoFisher Scientific Catalogue #Q33238) and the Promega GloMax Discover microplate reader (Catalogue #GM3000) using Qubit reagents.

2.4.1: Qubit

Quantification using the Qubit 4 Fluorometer was performed with 2µL of extracted elute. High sensitivity Qubit reagents from the Qubit dsDNA HS Assay Kit (Catalogue #Q33231) were mixed in a 200:1 Buffer:Dye ratio according to manufacturer specifications. For the two recommended standards in the kit, 190µL of the mixed buffer was aliquoted into two Qubit tubes. These tubes then had 10µL of the included standards 1 and 2 added, one to each. Next, 198µL of the buffer mix was aliquoted into Qubit tubes, one for each sample being quantified. 2µL of sample were then added to each of the tubes to bring all tubes to a total volume of 200µL. The samples and controls were then briefly vortexed and centrifuged before being incubated in the dark for 2 minutes. Finally, the samples were read individually on the Qubit 4 Fluorometer, standards first, according to the manufacturer instructions. The resulting DNA concentrations were recorded for analysis and quality control.

2.4.2: Promega

The Promega GloMax quantification method was used when high throughput was required as it could be performed in a 96 well plate. As with the Qubit 4 Fluorometer method, Qubit dsDNA HS Assay Kit reagents were used and mixed in the 200:1 Buffer:Dye ratio. A clear flat-bottomed 96-well CytoOne plate from StarLab [Catalogue #CC7682-7596] was used and 198µL of prepared

buffer/dye solution was added to each well for the number of samples being quantified. 2µL of sample elute was then added to each well to bring the total volume of each up to 200µL. The plate was then sealed with a foil, mixed by vortex, and spun down briefly in a benchtop centrifuge to ensure thorough mixing of each sample. Following this mixing process, the plate was incubated in the dark for 2 minutes before carefully removing the film and inserting the plate into the Promega GloMax as instructed by the manufacturer protocols. The dsDNA fluorescence protocol was selected, run, and the subsequent results were transferred to a computer for analysis using a custom excel spreadsheet created by Dave Baker of the QIB sequencing service. The resulting nucleic acid concentrations were recorded for analysis.

2.4.3: Bacterial Cell Equivalent Calculation

As the Qubit 4 Fluorometer and Promega Glomax methods yielded only DNA concentrations within a sample, a conversion formula was created to determine the number of cell equivalencies (CE) within each sample. This was possible as *M. bovis* and *M. tuberculosis* have haploid genomes, allowing the number of cell equivalents to be determined by dividing the weight of DNA detected by the weight of a single *M. bovis* or *M. tuberculosis* genome. One megabase of DNA weighs 1.09fg. The length of the *M bovis* BCG genome is 4.27 megabases. Thus, the average weight of the *M bovis* BCG genome is 4.654fg. This translates to 214,855.08 CE per ng of detected DNA. Then, as only 2µL of DNA from the 50µL elute was used for quantification, the detected concentration (in ng) was multiplied by 25. This resulted in the equation below which would yield the total number of cell equivalents extracted from a given sample.

$$(X * 25) * 214,855.08 = CE \text{ per Extracted Sample}$$

2.5: DNA Quantification by qPCR

qPCR was used for quantification of host, commensal, and target DNA. Nested qPCR reactions were also used for relative quantification of target amplicons following multiplex amplification.

2.5.1: SYBR Green qPCR

Per reaction, 2 μ L of DNA was used as template with a working mix of SYBR Green Master Mix, forward primer, reverse primer, and molecular H₂O prepared in the concentrations detailed below (Table 2.1).

Table 2.1: SYBR Green qPCR working solution formula per sample

Reagent	Volume per Sample (μ L)
SYBR Green Master Mix	10
20 μ M Forward Primer	1
20 μ M Reverse Primer	1
Molecular Grade H ₂ O	6
DNA template	2
Total volume	20

The master mix used for these assays was the LightCycler® 480 SYBR Green 1 Master Mix from Roche Life Science (Catalogue # 04707516001). The primers targeted the BCG RD1 region, the human RNA polymerase A gene, and the bacterial 16S gene V3-V4 fragment (Table 2.2). 18 μ L of the mastermix and 2 μ L of the template DNA were loaded into a 96-well LightCycler plate. The plates were then sealed with clear foil, vortexed, and briefly spun down prior to insertion into the LightCycler® 480 system for analysis. The reactions were then amplified using the cycling conditions detailed below (Table 2.3).

Table 2.2: SYBR Green qPCR amplification primers for the amplification of three targets of interest

Amplification Target	Forward Primer (5'-3')	Reverse Primer (5'-3')
BCG RD1 Region	AAGCGGTTGCCGCCGACCGACC	GAGGCGATCTGGCGGTTTGGGG
Human RNA polymerase A Gene	TGAAGCCGTGCGGAAGG	ACAAGAGAGCCAAGTGTCG
Bacterial 16S V3-V4 Fragment	CCTACGGGDGGCWGCA	GGACTACHVGGGTMTCTAATC

Table 2.3: Cycling conditions for SYBR Green qPCR amplification

Step	Temperature (°C)	Time (mm:ss)	Cycles (#)
Pre-Incubation	95	05:00	1
Amplification	95	00:30	40
	55	00:30	
	72	00:30	
Final Extension	72	05:00	1
Melt Curve	95	00:05	1
	65	01:00	
	95	Continuous	
Cooling	37	00:01	1

2.5.2: TaqMan Probe-based qPCR

Per probe reaction, 5µL of DNA was used as template with a working solution of Roche probe master mix, forward primer, reverse primer, fluorescence probe, and molecular H₂O (Table 2.4).

Table 2.4: Probe-based qPCR working solution formula per sample

Reagent	Volume per Sample (μL)
Roche Probe Master Mix	10
20μM Forward Primer	0.5
20μM Reverse Primer	0.5
10μM Fluorescence Probe	0.4
Molecular H ₂ O	3.6
DNA template	5
Total volume	20

The master mix used for the probe assays was the LightCycler® 480 Probe Master Mix from Roche Life Science (Catalogue #04707494001). The primers targeted the BCG RD1 region, the human RNA polymerase A gene, and the bacterial 16S gene V3-V4 fragment with Taqman FAM probes selected to fit within each amplicon (Table 2.5). 15μL of the master mix and 5μL of template were added to wells of a 96-well LightCycler plate. The plate was then covered with a clear LightCycler foil, vortexed, and briefly spun down prior to insertion into the LightCycler® 480 system for analysis. The reactions were then amplified using the cycling conditions detailed below (Table 2.6).

Table 2.5: Primer/Probe sets selected for the qPCR amplification of three DNA targets

Amplification Target	Forward Primer (5'-3')	Reverse Primer (5'-3')	Fluorescence Probe (5'-3')
BCG RD1 Region	AAGCGGTTGCCGCCGACCGA CC	GAGGCGATCTGGCGGTTTGG GG	[6FAM]GTGCTTCTGGTCGACGATTG[BHQ1]
Human RNA Polymerase A	TGAAGCCGTGCGGAAGG	ACAAGAGAGCCAAGTGTCG	[6FAM]TACCACGTCATCTCCTTTGATGGCTCCTAT[BHQ1]
Bacterial 16S V3-V4 Fragment	CCTACGGDGGCGWGCA	GGACTACHVGGTMTCTAAT C	[6FAM]CAGCAGCCCGGTA[BHQ1]

Table 2.6: Probe-based qPCR Cycling Conditions

Cycle Step	Time (mm:ss)	Temperature (°C)	Cycles (#)
Initial Denaturation	05:00	95	1
Denaturation	00:30	95	40
Annealing	00:30	55	
Extension	00:30	72	
Final Extension	05:00	72	1

2.5.3: Nested qPCR Amplification

Nested qPCR was used for the relative quantification of TB multiplex PCR products. Multiplex product DNA was diluted 1:100 with molecular H₂O and used as template for SYBR Green qPCR amplification. Amplification was performed as described in section 2.5.1.

2.5.4: qPCR Amplification Analysis

The qPCR data was analysed using the Abs Quant/2nd Derivative Max analysis program in the LightCycler® software which calculated the cycle threshold (C_T) and graphed the amplification curve for each sample. This C_T was then used to compare the relative starting concentration of DNA between samples. Assuming that the PCRs were efficient, template concentration doubles every cycle, hence the relative difference in starting concentration between 2 samples could be calculated using $2^{\Delta C_T}$.

2.5.5: Melt Curve Analysis

Amplification by SYBR Green included a melt curve step for the identification of primer dimers or non-specific amplification. Melt curves were assessed visually for signs of secondary or tertiary peaks (at lower or higher melting temperatures than the expected amplicon peak) which would indicate the presence of non-target amplification or primer dimers (Figure 2.1).

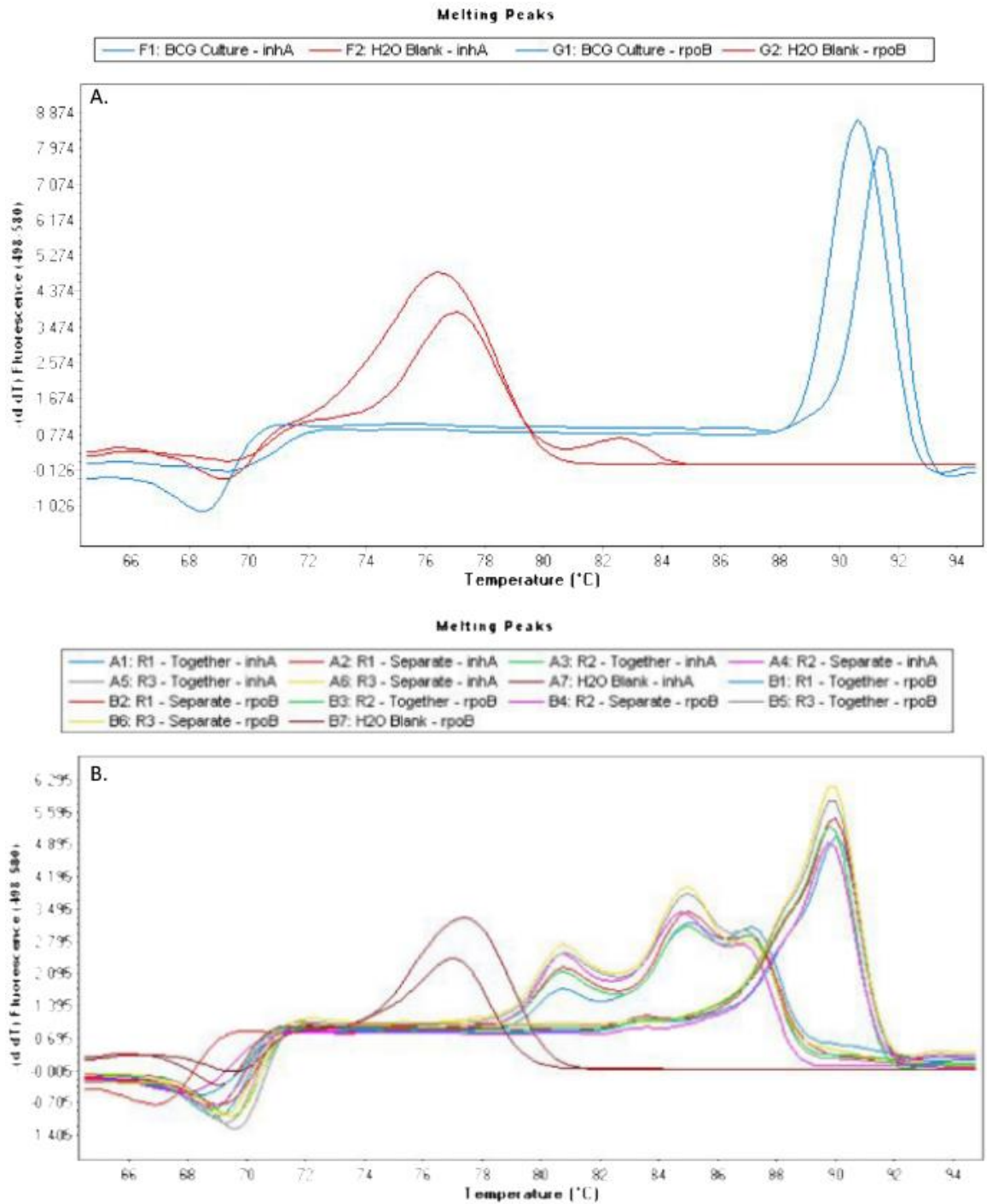


Figure 2.1: Example of qPCR melt curve analysis from two experiments. A: Clear difference between primer dimer peak in water controls and expected melt peak in BCG samples with no evidence of double peaks. B: Multiple samples exhibiting secondary and tertiary peaks

2.6: Fragment Size Analysis

Assessment of amplicon size was performed using the TapeStation 2200 platform [Agilent].

Analysis was performed using HS D5000 reagents [Catalogue #5067-5592] for improved resolution of amplicon sizes compared to Genomic DNA reagents. Electrophoresis followed manufacturer protocols and fragment size analysis was performed using the Agilent TapeStation native software.

2.7: Contrived Clinical Samples

Sputasol treated sputum samples determined to be free of respiratory pathogens (normal respiratory flora – NRF) at the NNUH Innovation Centre microbiology laboratory were used for all spiking experiments. Prior to use, all NRF sputum samples received on the same date were pooled and homogenized by vortexing for 5 minutes at maximum speed to thoroughly combine and homogenise the samples.

For spiking of samples, 900µL of homogenized NRF sputum was aliquoted into a clean 1.5mL Eppendorf tube. To this aliquot, 100µL of liquid culture of the desired microorganism and concentration was added to bring the total volume to 1mL. Spiked samples were then mixed thoroughly by vortexing for 30 seconds at medium speed before use in downstream experimentation. In the event a spiked sample would be used over multiple days it was stored at 4°C between uses.

2.8: Design of tNGS PCR Primers

PCR primers for tNGS were designed using Primer-BLAST software available from a collaboration between NCBI and Primer3 developers. Results on the specifics of primer design for assay targets is presented in Results section 3.2.2

2.9: Nucleic Acid Host Depletion

Saponin-based host depletion methods were used to remove host DNA from contrived clinical samples prior to metagenomic sequencing. Initially, the depletion method described by Charalampous, et al ¹¹¹ was used, followed by a further optimized one-pot saponin depletion method.

Both methods use Saponin as the active chemical agent, which works by creating pores in cellular membranes thereby exposing the DNA to enzymatic degradation. Saponin must be made fresh weekly and protected from light to prevent denaturation. For a 5% working solution of saponin, as required in the Charalampous method, 500mg of saponin was suspended in 10mL of PBS. This solution was mixed by vortexing and filtered through 0.22 μ M syringe filter prior to experimental use and storage. The optimized one-pot method required a 1% saponin working solution, made by suspending 100mg of saponin in 10mL of PBS. This working solution was then vortexed, however, no subsequent filtration was used before use or storage according to protocol.

In the depletion method published by Charalampous, et al., 200 μ L primary samples were centrifuged at 8,000g for 5 minutes to create a pellet. The supernatant was then carefully removed, leaving approximately 50 μ L around the pellet, before resuspending the pellet in 250 μ L of PBS. 200 μ L of 5% saponin was then added and the sample was briefly vortexed before being left to incubate at room temperature for 10 minutes. After incubation, 350 μ L of molecular grade H₂O was added, followed 30 seconds later by 12 μ L of a 5M NaCl solution. The sample was then vortexed and pelleted at 8,000g for 5 minutes. After pelleting, the supernatant was carefully removed, again leaving approximately 50 μ L around the pellet, and the sample was resuspended in 100 μ L PBS. 100 μ L of HL-SAN 5.5M buffer solution [5.5M NaCl and 100mM MgCl₂ in molecular H₂O], and 10 μ L of HL-SAN DNase were then added and the mixture was incubated on an Eppendorf ThermoMixer C at 37°C, 800rpm for 15 minutes. After incubation, 800 μ L of PBS was added and the sample was

pelleted in a centrifuge at 6,000g for 3 minutes. The pellet was then processed for DNA extraction as per section 2.2.

In the one-pot host depletion method 200µL of primary sample, 40µL of a 1% saponin solution, 200µL of a 5Mol HL-SAN buffer (5M NaCl and 100mM MgCl₂ in molecular H₂O), and 10µL of HL-SAN DNase were combined in a clean 1.5mL Eppendorf. This mixture was then incubated on an Eppendorf ThermoMixer C at 37°C and 1,000rpm for 10 minutes. Following incubation, 1mL of PBS was added to the sample and it was pelleted in a centrifuge at 12,000g for 3 minutes. The supernatant was then carefully removed from the pellet, leaving approximately 50µL around the pellet. As above, the pellet was then processed for DNA extraction as per section 2.3.

2.10: Sputum NaOH/NALC-Na Decontamination and Sedimentation

Sedimented sputum samples are commonly used in diagnostics laboratories for the investigation of TB infection. Spiked sputum samples underwent a decontamination protocol to prove the TB tNGS test would work on this sample type. The method chosen was published in the Stop TB Partnership Mycobacteriology Laboratory Manual ¹²³.

This method used a combination of Sodium Hydroxide (NaOH), Sodium Citrate Dihydrate (HOC(COONa)(CH₂COONa)₂ · 2H₂O), and NALC (C₅H₉NO₃S) solutions to render non-mycobacterial cells nonviable. A 6% stock solution of NaOH was made by suspending 30g of NaOH in 500mL of molecular grade H₂O. A 2.9% Na Citrate Dihydrate stock solution was also made by suspending 14.5g Na Citrate Dihydrate in 500mL of molecular grade H₂O. The working NaOH/NALC-Na Citrate digestant solution was mixed daily by combining equal volumes of 6% NaOH and 2.9% Na Citrate Dihydrate with a specific amount of NALC (ranging from 0.25-5g) according to Table 2.7.

Table 2.7: Preparation of NaOH/NALC-Na Citrate Digestant Solution

Volume of Digestant Needed (mL)	6% NaOH (mL)	2.9% Na Citrate Dihydrate (mL)	Amount of NALC to Add (g)
50	25	25	0.25
100	50	50	0.50
200	100	100	1.00
250	125	125	1.25
500	250	250	2.50
1,000	500	500	5.00

A neutralizing phosphate buffer solution was used to stop the decontamination reaction. This buffer was made by combining 7.1g Disodium Phosphate (Na_2HPO_4) and 6.8g Monopotassium Phosphate (KH_2PO_4) in 1.5L of molecular grade H_2O . This suspension was then autoclaved to ensure sterility and aliquoted into 50mL falcon tubes.

For decontamination, 250 μL of spiked sputum and 250 μL of digestant solution were combined in a clean 1.5mL Eppendorf. The samples were then vortexed at medium speed for 30 seconds before incubating for 15 minutes at room temperature on an orbital shaker at 500rpm. In the absence of a shaker plate for incubation, samples were vortexed at low speed for 10 seconds every two minutes to ensure thorough mixture. After incubation, the digestant reaction was neutralized by adding 1mL of phosphate buffer solution. The samples were then pelleted in a refrigerated centrifuge at 14,000g and 4°C for 5 minutes. The supernatant was carefully removed, leaving approximately 50 μL around the pellet to prevent loss of sample. Finally, the pellet was resuspended in 700 μL of PBS for immediate DNA extraction (as described in section 2.3).

2.11: Determining Analytical Limit-of-Detection

Analytical limit-of-detection (LoD) for metagenomic and targeted sequencing methods was determined using two methods, qPCR and MinION sequencing.

2.11.1: qPCR Determination of the Metagenomic LoD

For qPCR LoD experiments, a series of 10-fold serial dilutions were made from liquid *M. bovis* BCG culture stock. Serial dilutions from 1×10^6 CFU/mL to 1×10^1 CFU/mL were used to spike NRF sputum to create contrived clinical samples as described in section 2.6. After either host and/or commensal depletion the samples underwent SYBR Green qPCR amplification using the BCG RD1 primer pair described in section 2.4.

Using the Abs Quant/2nd Derivative Max analysis software, the C_T of each sample was calculated. Any sample which failed to amplify prior to the included negative H₂O control was classified as a failure to detect. Also, a melt curve analysis was performed to identify amplification and detection due to primer dimers or non-specific amplification, determined by the existence of a secondary peak. Using these two analysis methods the lower bound of the LoD was identified for further investigation and optimization.

2.11.2: MinION Sequencing for Determination of the tNGS Drug Resistance Assay LoD

LoD determination by MinION sequencing used duplicate *M. tuberculosis* dilutions of 1000, 500, 100, 50 and 1 CFU/mL. Contrived samples underwent the tNGS multiplex protocol and were prepared for ligation-based MinION sequencing (section 2.13). Sequencing was performed for 3 hours with live-basecalling, after which all reads were uploaded to the ONT Epi2Me FASTQ TB Resistance Profile for analysis and interpretation. Successful detection was classified as a read depth of at least 50x for all gene targets as determined by the Epi2Me software.

2.12: Multiplex PCR Using Qiagen Kit

Multiplex groups for the tNGS assay were amplified using an Applied Biosystems™ MiniAmp™ thermal cycler (Catalogue #15856152). Reactions were prepared in the QIB Extra laboratory as a separate clean environment where no Mycobacterium DNA had been used. The multiplex reactions were prepared in 0.2mL thin-walled PCR tubes or plates, depending on the number of samples, as described in Table 2.8. Template DNA was added in a separate room (the QIB Tissue Processing

laboratory) before immediately sealing the samples. Sealed samples were then mixed by vortex before being briefly spun down in a benchtop centrifuge. The mixed reactions were then placed into a thermal cycler for amplification under the cycling conditions in Table 2.9.

Table 2.8: Multiplex group amplification reaction formula per sample

Reagent	Volume per Sample (μL)
2x Qiagen Multiplex Master Mix	25
10x Primer Mix (0.2μM per primer)	5
5x Qiagen Q-Solution	10
Nuclease-Free H ₂ O	5
Template DNA	5
Total volume	50

Table 2.9: Multiplex group amplification cycling conditions

Step	Time (mm:ss)	Temperature (°C)	# of Cycles
Heat Activation	20:00	95	1
Denaturation	00:30	94	35
Annealing	01:30	60	
Extension	01:30	72	
Final Extension	10:00	72	1
Hold	∞	4	1

2.13: DNA Purification and Concentration with AMPure XP Beads

During sequencing library preparation samples underwent repeated Ampure XP bead washes in different concentrations (Table 2.10).

Table 2.10: Example table of AMPure XP Beads Used for Different Bead Wash Concentrations

Bead Wash Concentration	Volume of Beads to Add ($\mu\text{L}/100\mu\text{L}$ of Sample)
1x	100
0.8x	80
0.6x	60
0.4x	40

The required volume of resuspended AMPure XP beads at room temperature were added to the sample. The samples were then incubated at room temperature for 5 minutes before being placed onto a magnetic rack for 2 minutes. Following magnetic pelleting, the supernatant was then carefully removed, and the bead pellet was washed with 500 μL of 70% ethanol. After 30 seconds the ethanol was carefully removed, and the pellet was washed with a further 500 μL of 70% ethanol. Again, the supernatant was carefully removed, and any residual supernatant was removed using a p10 pipette. The pellet was left to air dry for approximately 30 seconds, being careful not to let the pellet dry too much and crack, before being removed from the magnetic rack and resuspended in the desired volume. This suspension was then incubated at room temperature for 5 minutes before being returned to the magnetic rack and left to pellet for a further 2 minutes.

DNA was resuspended in either molecular H₂O or elution buffer (EB) during the final library preparation step. Likewise, elution volume was variable dependent on requirements.

2.14: MinION Library Preparation

For sequencing of tNGS assay amplicons, multiplex groups were pooled after amplification to a total of ~1 μg in 100 μl (10ng/ μl). MinION sequencing was then performed with the library preparation method depending on the application (metagenomic or tNGS). The release of a new sequencing kit by ONT before validation of the tNGS assay also led to a change in the library prep kit used (Figure 2.2). Metagenomic sequencing libraries were barcoded using the ONT PCR barcoding kit [Catalogue

#SQK-RPB004]. Meanwhile, tNGS sequencing libraries were originally barcoded using the ONT PCR 96-Expansion barcoding kit [Catalogue #EXP-PBC096] and later the ONT Native barcoding kit after the release of the native barcoding 96-expansion [Catalogue #EXP-NBD196]. All sequencing libraries were made using the ONT Ligation Sequencing Kit [Catalogue #SQK-LSK109].

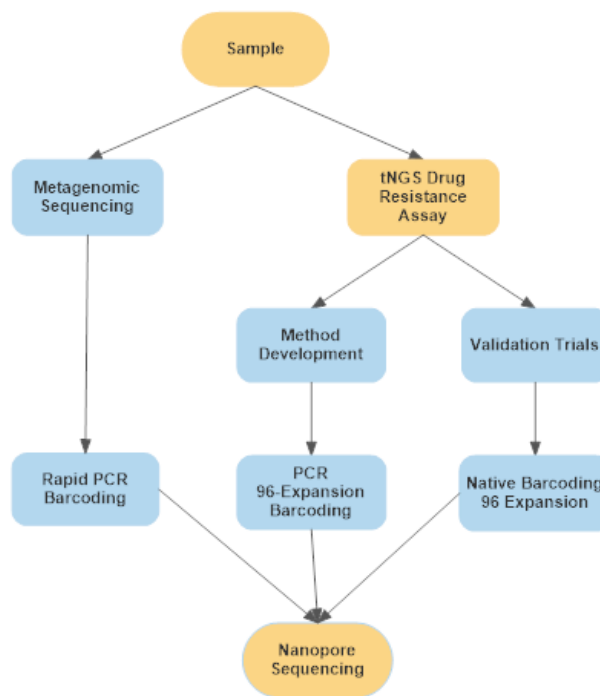


Figure 2.2: Flowchart illustrating the usage of three nanopore sequencing library barcoding methods depending on the sequencing purpose

2.14.1: Rapid PCR Barcoding Kit Library Preparation for Metagenomics

The PCR barcoding kit protocol used to prepare metagenomic samples was altered from manufacturer protocols to improve performance with respiratory samples. To start, 30µL of eluted DNA from the automated extraction was aliquoted into a fresh 1.5mL LoBind Eppendorf tube. A 1.2x bead wash (as per section 2.12) was then performed and the sample resuspended in 16µL molecular H₂O for elution. Following magnetic pelleting, 15µL of elute was carefully removed and retained for library preparation.

To prepare samples for sequencing using the PCR barcoding kit, 7.5µL of template DNA and 2.5µL of fragmentation mix (FRM) were combined in 0.2mL thin-walled PCR tubes. The tubes were then

gently mixed and spun down to remove air bubbles prior to incubating for 1 minute at 30°C and 1 minute at 80°C. Following this incubation, samples were cooled at 4°C in the PCR machine for approximately 1 minute. Next, 38µL of nuclease-free H₂O, 2µL of PCR barcode (RLB), and 50µL of LongAmp Taq 2x Master Mix (NEB) [Catalogue #M0287L] were added to each sample bringing the total volume of each to 100µL. The samples were then briefly vortexed and spun down before amplifying under the following conditions (Table 2.11).

Table 2.11: Cycling conditions for ONT PCR Barcoding

Step	Time (mm:ss)	Temperature (°C)	# of Cycles
Initial Denaturation	03:00	95	1
Denaturation	00:15	95	25
Annealing	00:15	56	
Extension	04:00	65	
Final Extension	06:00	65	1
Hold	∞	4	1

After tagmentation of adapters and barcodes followed by PCR amplification of the library, all samples were quantified using the qubit, as described in section 2.3, and pooled equimolar in a fresh 1.5mL Eppendorf. The pooled sample then underwent a 0.6x bead wash with elution in 14µL MinION Buffer (10mM Tris-HCl pH 8.0 with 50mM NaCl). 13µL of this elute was transferred to a fresh 1.5mL Eppendorf for QC and flow cell loading (section 2.14).

2.14.2: LSK109 Ligation with PCR Barcoding Expansion

Library preparation of tNGS samples initially used the ONT LSK109 ligation kit with PCR Barcoding Expansion 1-96 for higher throughput. To begin, 45µL of the pooled 100µL template DNA for each sample was combined in a 0.2mL thin-walled PCR tube with 7µL of Ultra II End-Prep Buffer [NEB], 3µL Ultra II End-Prep Enzyme Mix [NEB] (Catalogue #E7546L), and 5µL of molecular grade H₂O for a

total reaction volume of 60 μ L. These samples were pipette mixed prior to being briefly spun down and incubated for 5 minutes at 20°C followed by 5 minutes at 65°C. Each sample was then transferred to its own 1.5mL Eppendorf for a 1x bead wash. Samples were resuspended in 31 μ L molecular H₂O before retaining 30 μ L of the elute for barcode adapter ligation.

Following on, samples underwent barcode adapter ligation by combining 30 μ L of end-prepped elute from the previous step with 20 μ L of barcode adapter (BCA) [ONT] and 50 μ L of Blunt/TA Ligase Master Mix (NEB) [Catalogue #M0367L]. Samples were mixed by pipetting and briefly spun down prior to a 10-minute incubation at room temperature. After incubation, a 0.8x bead wash was performed and samples were eluted in 25 μ L molecular H₂O. The elute was carefully removed after magnetic pelleting and 1 μ L of each was quantified by Qubit to allow dilution of samples to 10ng/ μ L prior to the barcoding PCR.

To attach the PCR barcodes to each sample, reactions were prepared in 0.2mL thin-walled PCR tubes in the following concentrations (Table 2.12). The samples were briefly mixed by vortexing and pulse centrifuged followed by amplification under the cycling conditions in Table 2.13.

Table 2.12: PCR Barcoding 96-Expansion reaction reagent concentrations

Reagent	Volume (μL)
10 μ M PCR Barcode	1
10ng/ μ L Adapter Ligated Template DNA	2
LongAmp Taq 2x Master Mix	25
Nuclease-Free H ₂ O	22
Total volume	50

Table 2.13: PCR Barcoding 96-Expansion cycling conditions

Step	Time (mm:ss)	Temperature (°C)	# of Cycles
Initial Denaturation	03:00	95	1
Denaturation	00:15	95	15
Annealing	00:15	62	
Extension	01:30	65	
Final Extension	05:00	65	1
Hold	∞	4	1

After the barcoding amplification was completed, samples were quantified by Qubit before being pooled equimolar in a clean 1.5mL Eppendorf. A 0.8x wash was then performed on the pooled, barcoded, samples with the washed product being resuspended in 48µL molecular grade H₂O.

45µL of elute was transferred to a new 0.2mL Eppendorf for End-Prep. 7µL Ultra II End-Prep Buffer, 3µL Ultra II End-Prep Enzyme Mix, and 5µL molecular grade H₂O were then added for a total reaction volume of 60µL. The sample was then briefly mixed by vortexing before being pulse centrifuged. Following this, the sample was incubated in a thermal cycler at 20°C for 5 minutes followed by 65°C for 5 minutes. The end-prepped sample was then transferred to a clean 1.5mL Eppendorf where it underwent a 0.8x bead wash after which the sample was eluted into 61µL of molecular H₂O.

For ligation of the sequencing adapter Quick T4 Ligase [NEB #M2200L], adapter mix (AMX) [ONT], ligation buffer (LNB) [ONT], elution buffer (EB) [ONT], and short fragment buffer (SFB) [ONT] were all thawed, vortexed, spun down, and stored on ice. For the ligation reaction, 60µL of end-prepped DNA had 25µL LNB, 10µL quick T4 DNA ligase, and 5µL AMX added to it creating a total reaction volume of 100µL. This reaction was gently mixed by flicking and then pulse centrifuged prior to incubating at room temperature for 10 minutes. Following incubation, a 0.4x bead wash was performed with the use of 125µL SFB resuspension washes instead of 70% Ethanol. The sample was

finally resuspended in 15µL EB for elution, all of which was carefully retained for use in flow cell loading (section 2.14).

2.14.3: Native Barcoding 96 Expansion Kit Library Preparation

On the 21st of May, 2020, ONT released the Native Barcoding 96-Expansion [ONT #EXP-NBD196] removing the need for PCR barcoding. This method was then used as the barcoding method of choice for tNGS samples.

To begin, 12.5µL (approximately 125ng) of DNA was aliquoted from each sample into thin-walled PCR plate wells. An end-prep solution was then mixed using 1.75µL Ultra II End-Prep Buffer and 0.75µL Ultra II End-Prep Enzyme Mix per sample. 2.5µL of this mix was then aliquoted to each sample well before sealing the plate, vortexing it, and briefly spinning the plate down in a benchtop centrifuge. The mixed plate was then incubated in a thermal mixer at 20°C for 5 minutes followed by 65°C for 5 minutes.

The end-prepped samples then had a barcode ligated directly on. 0.75µL of end-prepped DNA from each sample was transferred to a clean thin-walled 96-well PCR plate. Each sample then had 3µL molecular grade H₂O, 1.25µL native barcode [ONT], and 5µL Blunt/TA Ligase master mix [NEB] added, in order. The plate was then sealed with foil, vortexed, spun down in a benchtop centrifuge, and was incubated in a thermal cycler at 20°C for 20 minutes followed by 65°C for 10 minutes. After this incubation, all samples were pooled in a clean 1.5mL Eppendorf tube and, when running 96 samples, 480µL of the pooled, barcoded, DNA was aliquoted into another 1.5mL Eppendorf. This aliquot then underwent a 0.4x bead wash with two resuspension washes in 700µL of SFB. The sample was then eluted into 35µL of molecular H₂O once the elute was again clear and colourless, 35µL was removed and retained in a fresh 1.5mL Eppendorf for adapter ligation.

The final step prior to loading is ligation of the sequencing adapter to the template DNA. To perform this step Quick Ligation Reaction Buffer [NEB], Quick T4 DNA Ligase [NEB], adapter mix (AMII)

[ONT], EB [ONT], and SFB [ONT] were thawed, mixed, briefly spun down, and stored on ice. The reaction was then prepared in a 1.5mL Eppendorf by adding the following reagents in order; 30µL pooled, barcoded, template DNA, 10µL Quick Ligation Reaction Buffer, 5µL Quick T4 DNA ligase, and 5µL AMII. The reaction was mixed by vortexing and pulse centrifuged before incubating at room temperature for 20 minutes. Following incubation, a 0.6x bead wash was performed with resuspension washes in 125µL SFB. After washes, the pellet was resuspended in 15µL EB and the clear elute was carefully retained for flow cell loading (section 2.15).

2.15: MinION Loading

The MinION flow cell was loaded according to manufacturer protocols using the Flow Cell Priming Kit (ONT) [Catalogue #EXP-FLP002]. The prepared library was quantified by Qubit using the method detailed in section 2.4 and the number of fmols/µL was calculated for loading using the online tool available at https://www.bioline.com/media/calculator/01_07.html. Optimally, between 100 and 200 fmols were loaded.

2.16: Sequencing Analysis

Drug resistance in samples was identified through the ONT Epi2Me FastQ TB Resistance Profile pipeline. Sequencing fastQ reads were uploaded using the ONT desktop agent available at <http://epi2me.nanoporetech.com>. Using fastQ data, the pipeline identifies genes and SNPs responsible for drug resistance against a curated database. After automated analysis through this pipeline, results were obtained from the ONT Epi2Me website and visual examination of wild-type and mutant reads was conducted to determine resistance to drugs and the existence of hetero-resistant samples (Figure 2.3). This pipeline is now discontinued; however, a similar method is currently available in Epi2Me Labs.

Drugs

- EMB ethambutol
- INH isoniazid
- PZA pyrazinamide
- RIF rifampicin
- STM streptomycin
- AMI amikacin
- BDQ bedaquiline
- CP capreomycin
- CIP ciprofloxacin
- CLM clofazimine
- ETO ethionamide
- KAN kanamycin
- LZD linezolid
- MOX moxifloxacin
- OFX ofloxacin
- PAS para-aminosalicylic-acid
- QUI quinolones

		katG_S315T		
REFERENCE		G	C	T
SAMPLE		G	G	T
POSITION		2155167	2155168	2155169
BASECALLED COUNTS	A	7		
	C		3	1
	G	658	679	1
	T	2	2	673
		rpoB_S450L		
REFERENCE		T	C	G
SAMPLE		T	T	G
POSITION		761154	761155	761156
BASECALLED COUNTS	A	3	3	6
	C	31	37	4
	G	9	13	2392
	T	2111	2118	9

Figure 2.3: Example Epi2Me TB Resistance Pipeline Output for Resistant Samples

For QC, reads were also mapped to a concatenated fastA reference of assay target sequences using MiniMap2 and Qualimap (Figure 2.4). Visual examination for equal coverage of targets, dropouts, and coverage greater than 50x was performed using this mapping method.

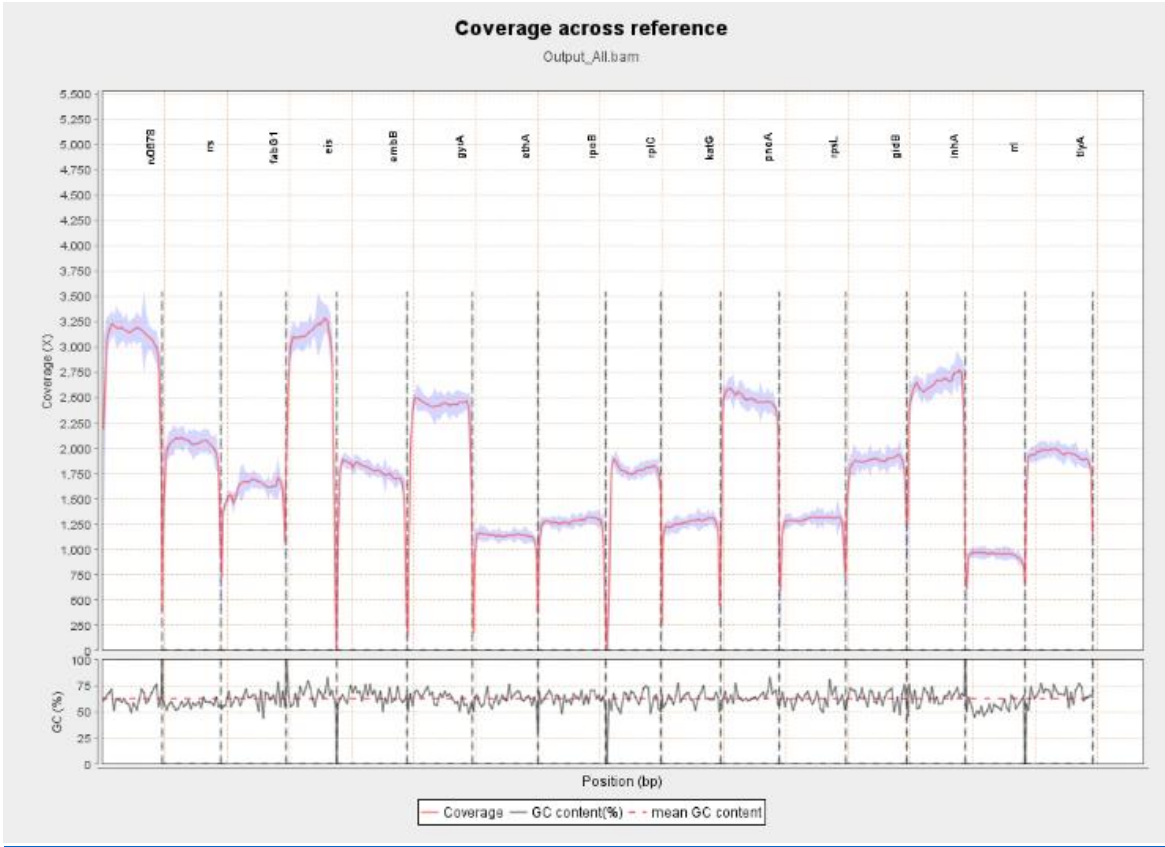


Figure 2.4: Example output of sequencing reads mapped to a concatenated assay reference for visualization of coverage in samples.

Chapter 3 – Results and Discussion

With the global incidence of drug-resistant TB increasing (from 5% in 2008 to ~12.5% in 2020) the need for rapid and accurate DST methods is increasing in urgency^{34,124}. Molecular diagnostic technologies provide the speed, accuracy, and cost-effectiveness to meet this need. Earlier molecular diagnostic tools such as Line Probe Assays (MTBDRplus and MTBDRsl) have narrow foci and limited flexibility inhibiting long-term viability. While PCR based tests like Xpert MTB/RIF and MTB/RIF Ultra also have narrow DST foci their performance as fast and accurate first-line tests will make them important in TB control for the foreseeable future.

To compensate for limitations in DST coverage the use of NGS has increased the breadth of investigation and the flexibility to detect new SNPs. Specifically, three avenues of sequencing and analysis for DST have come to the fore; whole genome sequencing (which requires cultured TB), targeted sequencing (which utilizes PCR amplification of target regions) and metagenomic sequencing (which sequences whole genomes directly from sample extractions). While WGS is a powerful tool for epidemiology, the reliance on *M. tuberculosis* culture makes it too slow to be useful clinically. The remaining two avenues were investigated throughout this research with the most viable being identified as tNGS due to the ability to specifically amplify MTBC DNA even in the presence of commensal bacterial DNA and host DNA.

The aim of the study was to develop rapid and sensitive diagnostic tests for TB. The key to this is efficient DNA extraction from primary samples. This took multiple steps from optimisation of DNA extraction to design of targeted primers and troubleshooting the bioinformatic pipeline.

3.1: Comparison of Extraction and Purification Methods for Optimization of Mycobacterial DNA

Yields

Firstly, molecular methods require effective sample preparation to isolate pathogen nucleic acid in replacement of culture for successful utilization. Consequently, metagenomic and tNGS methods are reliant on efficient extraction of mycobacterial DNA. Metagenomic assays are more sensitive to

issues of extraction than tNGS, as they sequence extracted DNA directly without enrichment. Thus, if extraction is inefficient, clinical applications are limited by a decreased limit of detection. However, tNGS assays amplify target DNA prior to sequencing, reducing the impact of extraction inefficiency and competing commensal and human nucleic acid on the clinical utility of an assay. Due to the correlation of DNA extraction to LoD, optimising extraction is essential. Generally, extraction efficiency of mycobacteria using standard methods is estimated at 30-50%, due to the hardness of the cells ^{125,126}. However, recent studies have demonstrated extraction efficiencies of 75-90% are possible under optimised conditions ¹²⁷.

3.1.1: DNA Purification Method Comparison

The MagNA Pure Compact automated extraction system was compared with the MagMAX manual extraction method for purifying bead-beaten samples. Testing was performed on *M. smegmatis* (*M. smegmatis* was used for extraction optimization as it is non-pathogenic, fast growing, and structurally similar to *M. tb*¹²⁸) liquid culture aliquots. Dual sets of triplicate 175µL samples of overnight *M. smegmatis* culture were aliquoted for each method. Following mechanical lysis (Methods section 2.3) samples were extracted following manufacturer specifications for each method. Extractions were quantified by high sensitivity Qubit (section 2.4.1), showing a concentration ~2-fold higher from MagNA Pure compared to MagMAX (Table 3.1).

Table 3.1: Qubit quantification comparing nucleic acid extraction methods using duplicate sample sets, MagMax and MagNA Pure Compact

Extraction Method	Replicate 1 Mean Concentration (ng/µL)	Replicate 2 Mean Concentration (ng/µL)	Replicate 3 Mean Concentration (ng/µL)
MagMax	0.162	0.136	0.146
MagNA Pure Compact	0.234	0.230	0.230

A second test compared the MagNA Pure Compact system against the Promega Maxwell RSC system. Two triplicate 500µL *M. smegmatis* liquid culture aliquots were prepared and bead beaten

(Methods section 2.3). Analysis indicated the MagNA Pure system yielded a statistically significant (Paired T-Test: $p < 0.0001$) average of 5.4 fold more nucleic acid than the Promega Maxwell (Table 3.2).

Table 3.2: Qubit quantification comparing nucleic acid extraction methods for triplicate samples, MagNA Pure Compact and Promega Maxwell RSC

Extraction Method	Mean Qubit DNA Concentration (ng/ μ L)
MagNA Pure Compact	8.58
Promega Maxwell RSC	1.58

MagNA Pure was subsequently tested with increasing bead-beating times to ascertain which yielded the highest concentration of nucleic acids. Triplicate liquid *M. smegmatis* culture samples were bead beaten for 5 minutes, 10 minutes, and 15 minutes at maximum Qiagen TissueLyser LT speed ($\sim 6\text{m/s}$). A linear increase in nucleic acid yield was observed with increasing mechanical lysis time (Figure 3.1).

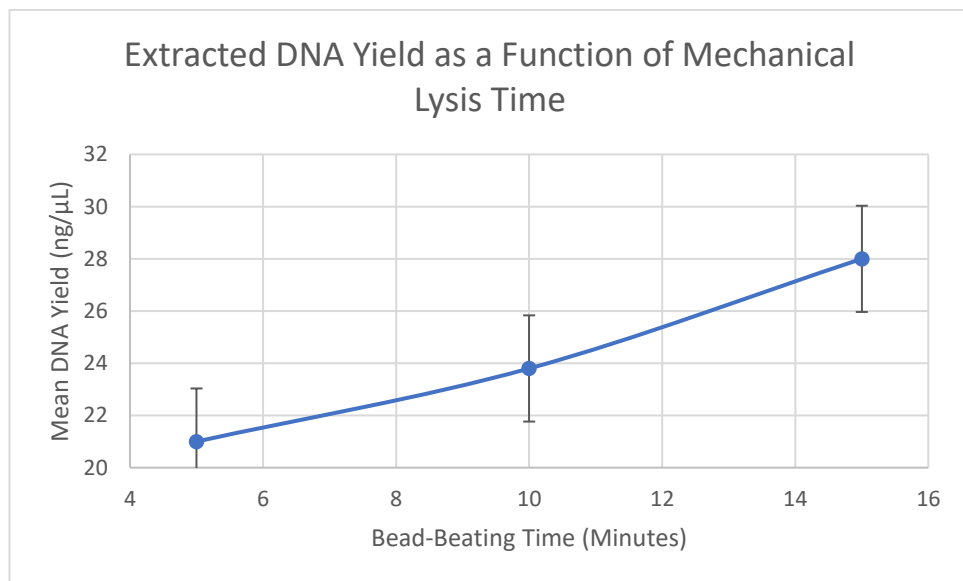


Figure 3.1: Line chart showing the increase in mean DNA yield by MagNA Pure extraction as a function of mechanical lysis time using triplicate samples. Error bars indicate one standard deviation

Different bead beaters were then assessed, in conjunction with MagNA Pure extraction. Two 1mL sets of liquid overnight *M. smegmatis* culture were prepared - one set underwent 15 minutes full-speed bead-beating in a Qiagen TissueLyser and the other underwent two 45-second full-speed cycles in an MP Biomedicals Fast-Prep 24, before extraction by MagNA Pure Compact. Results

showed 15-minute lysis in the Qiagen machine yielded a mean 24.6ng/μL DNA and two 45-second cycles in the MP Biomedicals machine yielded a mean 29.4ng/μL DNA (Table 3.3). This was an increase of 4.8ng/μL using the MP Biomedicals device with a shorter protocol. The MP Biomedicals FastPrep-24 method was chosen for subsequent extractions.

Table 3.3: Post-extraction DNA concentrations after using two mechanical cell disruption protocols.

	Extracted DNA Concentration (ng/μL)
Qiagen TissueLyser	24.6
MP Biomedicals Fast-Prep 24	29.4

3.1.2: Importance of Automated Extraction

For a test to be adopted for routine use in a clinical setting an automated extraction system is optimal; as automated sample preparation increases throughput while reducing the risk of contamination or human error. Thus, the optimal preparation for extraction in automated systems needed to be identified as automated systems allow little internal optimization. Emphasis was placed on mechanical lysis pre-extraction, as the primary impediment to efficient automated mycobacterial DNA extraction is the toughness of the cells ^{129,130}.

The automated methods tested were selected based on availability and use in previous studies of respiratory and systemic infections. The MagNA Pure Compact was released in the early 2000s and was adopted as a rapid and easy means of nucleic acid isolation ¹³¹. Preliminary results were inconsistent and one early study cited a reduction in PCR sensitivity when using nucleic acids isolated by this means ¹³². Further, the MagNA Pure Compact system can only extract 8 samples per run. Despite these limitations MagNA Pure Compact automated kits have been used for numerous studies of respiratory diseases using both targeted and metagenomic methodologies ^{111,133,134} and so was the extraction machine of choice at the beginning of the study. Future use of this system will be limited, however, due to discontinuation of the line and support by Roche.

Comparatively, the Maxwell RSC 48 system is capable of processing 48 samples concurrently, increasing utility in high-throughput studies. There are numerous automated kits, optimized by the manufacturer for extraction of DNA and RNA from different sample types ¹³⁵. During the ongoing SARS-CoV-2 pandemic, the Maxwell RSC has been heavily used for RNA extraction from patient samples and waste water for diagnostics and monitoring in multiple laboratories ^{136–139}. The discontinuation of the MagNA Pure forced a switch in extraction technology during the study.

3.1.3: Comparison of Bead Beating Matrices for DNA Extraction

We compared bead-beating matrices from MP Biomedical for the mechanical disruption of the *M. tb* cell wall. Matrices were selected based on manufacturer’s descriptions of organisms/sample types they are optimized for. This selection process identified seven matrices for comparison to Matrix E, the standard used in the Justin O’Grady (JOG) laboratory (Table 3.4).

Table 3.4: Bead-beating matrices chosen for comparison of mycobacterial cell lysis efficiency and their material compositions

Bead-Beating Matrix	Matrix Components
A	Garnet matrix with ¼” Ceramic Sphere
B	0.1mm Silica Spheres
C	1mm Silica Spheres
E*	1.4mm Ceramic Spheres, 0.1mm Silica Spheres, 4mm Glass Bead
G	1.6mm Silicon Carbide Particles and 2mm Glass Beads
K	0.8mm Zirconium Silicate Beads
Y	0.5mm Yttria-Stabilized Zirconium Oxide Beads

*The bead-beating matrix regularly used in the JOG laboratory group

Two triplicate (~10⁴ CFU/mL) sets were prepared and processed in two different bead-beating machines, the Qiagen TissueLyser and the MP Biomedical FastPrep. Aliquoted samples were subjected to mechanical lysis for either 15 minutes in the TissueLyser or two cycles of 45 seconds in the FastPrep prior to further extraction and clean-up on the MagNA Pure Compact. Qubit quantification results indicated matrix Y was superior to matrix E by a mean of 14ng/μL (Table 3.5).

However, assessment by *M. smegmatis* Sybr green qPCR showed that matrix E and Y were equally efficient in extracting *M. smegmatis* DNA.

Table 3.5: DNA quantifications by Qubit and qPCR from various bead-beating matrices on two homogenizers, the MP Biomedicals FastPrep-24 and the Qiagen TissueLyser.

Bead-Beating Matrix	FastPrep Mean DNA Concentration (ng/μL)	TissueLyser Mean DNA Concentration (ng/μL)	FastPrep SYBR Green qPCR (\bar{x} CT)	TissueLyser SYBR Green qPCR (\bar{x} CT)
A	23.6	5.58	16.36	18.19
B	22.6	4.84	17.29	19.91
C	25.6	19.1	16.92	17.82
E	32.6	19.8	16.58	17.55
G	17.7	15.5	16.57	17.77
K	28.2	23.6	16.79	17.59
Y	38.8	41.6	16.82	17.33

A follow-up experiment retested matrix E and matrix Y. Triplicate 500μL overnight *M. smegmatis* culture samples ($\sim 10^5$ CFU/mL) were prepared and bead beaten on the two machines as described above. Quantifications indicated the difference between Matrix Y and Matrix E was not consistent (Table 3.6) And that the high concentrations observed in Qubit were not DNA, but perhaps RNA or protein, and these may have inhibited the qPCR results in the FastPrep sample.

Table 3.6: DNA quantifications by Qubit and qPCR of two MP Biomedicals bead-beating matrices on two homogenizers, the MP Biomedicals FastPrep-24 and the Qiagen TissueLyser using triplicate samples.

Bead-Beating Matrix	FastPrep Mean DNA Concentration (ng/μL)	TissueLyser Mean DNA Concentration (ng/μL)	FastPrep SYBR Green qPCR (\bar{x} CT)	TissueLyser SYBR Green qPCR (\bar{x} CT)
E	80.0	23.6	18.89	17.27
Y	37.0	25.4	16.41	17.34

One further experiment was performed using samples containing human and commensal bacterial cells. Normal respiratory flora (NRF) samples were spiked with *M. smegmatis* DNA (Section 2.7) to create contrived clinical samples. Matrices E, K, and Y were tested in triplicate, using the FastPrep-24 method, to determine relative lysing and extraction efficiencies in the presence of non-mycobacterial cells and sputum matrix. Matrix E was superior for DNA yield ($\geq 0.14 \text{ ng}/\mu\text{L}$ improvement) and comparative concentration (mean $\Delta\text{CT} = \geq 0.48$, 1.48-fold increase) (Table 3.7). On this evidence, lysis matrix E was chosen for subsequent extractions.

Table 3.7: DNA quantifications by Qubit and qPCR of spiked NRF sputum lysed in three MP Biomedicals bead-beating matrices using triplicate samples

Bead-Beating Matrix	Qubit Mean DNA Concentration (ng/μL)	SYBR Green <i>M. smegmatis</i> Assay (\bar{x} C_T)
E	8.30	19.63
K	6.50	20.51
Y	8.16	20.11
Negative Control	Too Low	35.00

3.1.4: Mechanical Disruption Optimisation Summary

As seen in section 3.1.1, without pretreatment neither automated method performed efficiently on mycobacterial cells. Incorporating bead-beating prior to automated extraction significantly increases nucleic acid yield^{140,141}. A previous study run in the O’Grady laboratory, INHALE, indicated that MP Biomedicals lysis matrix E performed optimally for respiratory samples¹¹³. However, as the INHALE study focused on lysis and identification of pneumonia pathogens, efficiency for MTBC extraction could not be assumed.

The proprietary oscillating technology of MP Biomedicals FastPrep proved more efficient for cellular disruption than technology used by other bead beating devices (section 3.1.1). When paired with lysing matrix optimisation (section 3.1.3) this proved an effective method for rupturing the lipid-

rich cell wall of mycobacterial cells for DNA extraction. Reviewing the literature also showed bead-beating is consistently the most efficient means of mycobacterial lysis, over chemical lysis or enzymatic extraction^{125,127,140}. Lysing matrix E, designed for environmental samples, performed optimally for mycobacterial lysis over matrices explicitly designed for other hardy organisms such as yeast and fungi.

3.2: Targeted Next-Generation Sequencing

Design and testing of the tNGS assay began with selection of target genes and concluded with validation and troubleshooting using a set of 392 blinded samples (Figure 3.2). Redesign of gene target primer pairs and formulation of multiplex groups occurred in parallel with redesign of one frequently dictating a redesign of the other. Despite the complex nature of this design process the end product resulted in a highly sensitive and specific assay with the potential for implementation in clinical conditions.

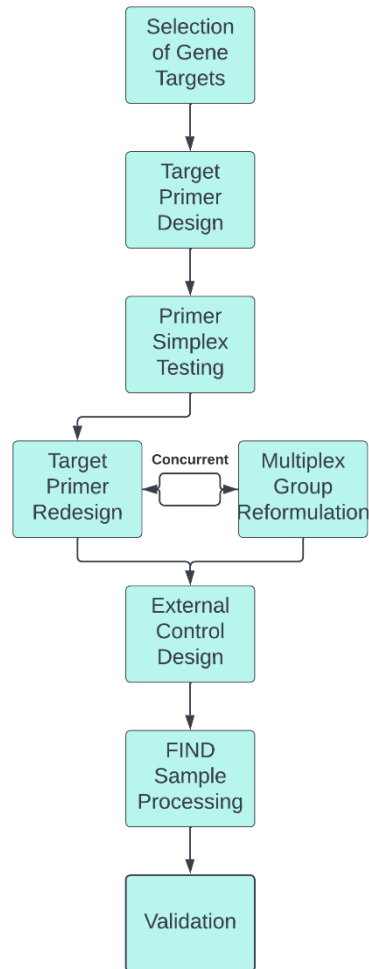


Figure 3.2: A flowchart illustrating the general progression and timeline of development for the tNGS assay. As indicated target primer redesign and multiplex group reformulation were an iterative process occurring concurrently. When both were performing to specifications development moved on and incorporated external controls.

3.2.1: Selection of Resistance Associated Mutations for Development of a tNGS Test for Drug-Resistant TB

Selection of gene targets for a tNGS drug resistance assay was predicated on a publication available from the WHO, as well as a systematic review by Miotto, *et al*^{142,143}. These reports identified high, medium, and low confidence mutations in 12 genes when calculating odds-ratios (OR) of phenotypic resistance, accounting for resistance to 9 drugs (Table 3.8). High confidence mutations were defined by Miotto, *et al* as having an OR higher than 10, medium confidence mutations had

an OR $5 < \dots \leq 10$, and low confidence mutations had an OR $1 < \dots \leq 5$. Additionally, 4 gene targets for 4 more anti-tuberculosis drugs were identified (Table 3.9) from the Deeplex MYC-TB (GenoScreen, France) test and a study by Zhao, et al. and included in the assay design ^{116,144}.

Table 3.8: Anti-tuberculosis drugs and the genes which are known to harbor resistance mutations as informed by two international studies

Drug	Gene Target	Source
Isoniazid	<i>inhA</i>	WHO & Miotto, et al.
	<i>katG</i>	WHO & Miotto, et al.
	<i>fabG1</i>	WHO
Rifampicin	<i>rpoB</i>	WHO & Miotto, et al.
Fluoroquinolones	<i>gyrA</i>	WHO & Miotto, et al.
Pyrazinamide	<i>pncA</i>	WHO & Miotto, et al.
Amikacin	<i>rrs</i>	WHO & Miotto, et al.
	<i>eis</i>	WHO
Kanamycin	<i>rrs</i>	WHO & Miotto, et al.
	<i>eis</i>	WHO & Miotto, et al.
Capreomycin	<i>rrs</i>	WHO & Miotto, et al.
	<i>tlyA</i>	WHO & Miotto, et al.
Ethionamide	<i>ethA</i>	Miotto, et al.
Streptomycin	<i>rpsL</i>	Miotto, et al.
	<i>rrs</i>	Miotto, et al.
	<i>gidB</i>	Miotto, et al.

Table 3.9: Anti-tuberculosis drugs and the genes which are known to harbour resistance mutations as informed by existing literature

Drug	Gene Target	Source
Ethambutol	<i>embB</i>	Zhao, et al.
Bedaquiline	<i>rv0678</i>	Villellas, et al., Andries, et al., & Ismail, et al.
Clofazamine	<i>rv0678</i>	Villellas, et al., Andries, et al., & Ismail, et al.
Linezolid	<i>rrl</i>	Wasserman, et al.
	<i>rplC</i>	Beckert, et al., & Wasserman, et al.

Using this list of genes, the regions required to cover the mutations of interest were identified. To this end, a comprehensive list of high and medium confidence mutations within each gene was created. On review, it was decided to focus assay design to capture high confidence mutations and include medium confidence mutations where possible. This list included both amino acid mutations within genes and single nucleotide mutations outside genes and totaled 448 individual mutations (Appendix I). The largest proportion of mutations occurred within the *pncA* gene (37.3%), the second highest proportion within the *rpoB* gene (10%), and the lowest proportion within the *rplC* gene (0.002%).

3.2.1.1: Assay Target Selection Sources

As referenced in section 3.2.1, the primary source for selection of assay targets was a systematic review conducted by the WHO ¹⁴². This was primarily augmented by a second systematic review by Miotto, et al. recommended by collaborators at FIND ¹⁴³. In addition, several non-WHO reviewed targets were included in assay formulation for newer drugs.

The primary WHO source provided gene targets for resistance to rifampicin, isoniazid, fluoroquinolones, pyrazinamide, amikacin, capreomycin, and kanamycin. The Miotto report

reviewed gene targets for resistance to ethionamide and streptomycin in addition to supporting the findings in the WHO report. In total these two reports provided confidence estimates for SNPs in 12 genes with strong correlations to drug resistance. It is of interest to note that despite its role as a first-line anti-tuberculous medication there were no SNPs or genes for ethambutol covered in either the WHO or Miotto reports.

Selection of ethambutol resistance conferring gene targets was instead supported by a 2015 study by Zhao, *et al.* investigating the embCAB genes ¹⁴⁴. This report found little correlation between ethambutol resistance and mutations in *embA* or *embC* genes, however, it did find a strong correlation between ethambutol resistance and SNPs within *embB*.

Finally, coverage of genes correlated with resistance to bedaquiline and clofazimine were informed by studies by Andries, *et al.*, Villellas, *et al.*, and Ismail, *et al.* ¹⁴⁵⁻¹⁴⁷. Genes correlated with linezolid resistance were informed by two studies; one by Beckert, *et al.* in 2012 and one by Wasserman, *et al.* in 2019 ^{148,149}. The assay covers three genes associated with resistance to these antibiotics, one for bedaquiline and clofazimine and two for linezolid. With these drugs included, gene targets for the assay were set and the SNPs requiring coverage were catalogued.

3.2.1.2: Target SNP Selection

The principal document used for SNP identification, as with gene selection, was the 2018 WHO/FIND report on sequencing technology for detection of drug resistance ¹⁴². This systematic review of MTBC mutation publications included analysis utilizing the global ReSeqTB Data Sharing Platform. This analysis used a consensus approach to grade drug-resistance associated SNPs into high, medium, and low confidence using likelihood and odds ratios. Similarly, the systematic review of 52 MTBC sequencing and DST studies by Miotto, *et al.* was further used to identify resistance conferring SNPs. As with the WHO/FIND report, these SNPs were graded into high, medium, and low confidence.

Resistance associated SNPs in *embB* were catalogued by Sreevatsan, *et al.* in a 1997 study, Plinke, *et al.* in a 2006 study, and Zhao, *et al.*, in a 2015 study^{144,150,151}. Each study performed phenotypic DST testing before sequencing to identify SNPs in *embB* correlated with ethambutol resistance. Resistance conferring SNPs for bedaquiline and clofazimine associated gene *rv0678* were identified using an analysis of 359 clinical isolates by Villellas, *et al.*¹⁴⁵. This analysis identified minimum inhibition concentrations (MICs) above clinical dosages, indicating drug resistance, occurred in 2.3% of isolates. In these resistant isolates the only mutations detected occurred within *rv0678* at codon 63 (serine to arginine), supporting the gene's role in drug resistance. Bedaquiline and clofazimine resistance was further supported by the studies from Andries, *et al.* and Ismail, *et al.*^{146,147}.

Finally, resistance associated SNPs for linezolid were identified in *rplC* using studies by Beckert, *et al.*, Wasserman, *et al.*, Locke, *et al.*, and Locke, *et al.*^{148,149,152,153}. Phenotypic DST and WGS identified a change in codon 154 (cysteine to arginine) was the sole *rplC* mutation correlated with resistance to linezolid. The two studies performed by Locke, *et al.* also indicated codons 152, 155, 157, 159, and 169 were correlated with resistance to Linezolid in *Staphylococcus* strains and were covered to ensure full coverage of potential linezolid resistance SNPs^{152,153}.

This suite of identified SNPs associated with drug resistance were used as the backbone of the assay. As research continues and new treatments are developed, new target genes and SNPs can, and must, be incorporated into the assay and analysis pipeline. For example, the recent success of a regimen in the Nix-TB trial using bedaquiline, linezolid, and pretomanid for XDR-TB will require careful monitoring for the emergence of resistance-conferring SNPs. This trial showed successful treatment for XDR-TB in 88.78% of patients after 6-months of treatment and a 6-month follow-up period^{71,72}. Pretomanid is a new drug and the resistance mechanisms and mutations leading to resistance are not yet fully understood. Early research has linked at least 6 genes to potential resistance to pretomanid which will need to be monitored in tNGS assays to prevent treatment failure (*fgd1*, *ddn*, *fbiA*, *fbiB*, *fbiC*, and *fbiD*)^{154,155}.

The recent release of an official mutation target list from the WHO will help to standardise the mutations reported by tNGS assays – this list will evolve with more sequence data and new TB drugs

156

3.2.2: Design and Optimization of PCR Primers for target resistance genes

3.2.2.1: Design of PCR Primers

Using the list of mutations, outlined in section 3.2.1, a map was created for each target gene highlighting the location of every high-confidence resistance conferring mutation site (Figure 3.3). Each gene map used the annotated *M. tuberculosis* H37Rv reference genome (NC_000962.3) available from the NCBI database. Primers were designed using these maps and an amplicon size ranging from 900 to 1,100 base pairs, a size chosen to allow efficient amplification, be suitable for nanopore sequencing, and cover all the necessary SNPs in a single amplicon. Size range was kept consistent across all amplicons to promote consistent amplification efficiency across targets.

```

AATGCACTTCGCTTTTCATCGCTTACGTCC TTGCCGGCGGTTTCCTTGCCCTGCGGTGGCGACGCACGATG
TGGCTGCATGTTCCGGCGGTGATATGGGGGATCGGCATCGCCGCTAAGCGGGTCGACTGCCCGCTGACCT
GGGTGGAGCGCTGGGCTCGCAACCAAGGCCGCGATGACACCTCTGTCACCGGACGGATTTGTGCGCTCACTA
CATCACCGGCGTGATCTATCCCGCCGGTGGGTGGCCGCCGCTCAGCTGGTCATGTTGCGGATCGTCCGG
GCGTCATGGACCCTATATCTGTGGCTGCCGCGTCGGTAGGCCAAACTGCCCGGGCAGTCGCCCGAACGTAT
GGTGGACGTTATGCGG GCGTTGATC ATCGTTCGAC GTG CAGAAC GACTTC TGC GAGGGT GGC TCG CTC GCGG
TAACCGGT GGC GCCGCGCTGGCCCGCGCCATCAGCGACTAC CTGGCCGAAGCGGCGGACTACCATCACGT
CGTG GCAACCAAGGACTTC CACATCGAC CCG GGTGAC CACTTC TCC GGCACACCG GAC TATTCTCG TCG
TGGCCACCG CATTGC GTCAGCGGT ACT CCCGGCGCGGACTTC CATCCAGT CTG GACACGTCGGCAATCG
AGGCGGTG TTC TAC AAGGGT GCCTACACCGGAGCGTAC AGCGGCTTCGAA GAG TCGACGAGAACGGCAC
GCCACTGTGAATTGG CTC CGGCAA CGC GGC CTC GATGAG GTC GATGTGGTCGGT ATT GCCACC GAT CAT
TGTGTG CGC CAGACC GCCGAGGACGCGGTACGCAATGGCTTGGCCACCAGG CTC CTGGTGGACCTGACAG
CGGGTGTGTCGGCCGATAACCACCGTCGCCGCG CTC GAGGAG ATG CGCACCGCCAGC GTC GAGTTGGTTTG
CAGCTCCTGATGGCACCGCCGAACCGGGATGAACTGTTGGCGGCGGTGGAGCGCTCGCCCGAAGCGGCGC
CCGCGCACGACCGCGCCGGCTGGGTGCGGTTGTTCACCGGTGACGCGCGGTTCGAAGACCCGGTGGGTTT
GCAGCCGCAGGTGGGCATGAGGCCATCGCCGCTTCTACGACACCTTCATCGGGCCGCGGGATATCACG
TTCCATCGCGATCTGGATATCGTCTCCGGCACGGTGGTGTGCGCGATCTCGAACTCGAGGTCGCGATGG
ACTCGGCTGTGACGGTTCATTCCCCTTCTACGCTATGACCTACGACCGGTTACCGGCGAGTGGCA
GATTGCCGCACTGCCGGCGTACTGGGAGTTGCCGGCGATGA

```

Figure 3.3: Example of a gene map showing the locations of known high-confidence resistance mutations in the *pncA* gene. Areas highlighted in grey are extragenic regions included to make the amplicon >900bp long.

Target gene primer pairs were designed using Primer-BLAST, a web-based software tool created collaboratively between the NCBI and the Primer3 developers. Strict parameters were set to increase the likelihood of primers amplifying with equivalent efficiency when in a multiplex (Table

3.10). The FASTA sequence maps were used to design PCR primers. In genes less than 900bp, 500bp extragenic regions were included on both the 5' and 3' ends to allow design of amplicons of a similar length.

Table 3.10: Primer design parameters for use in designing target gene primer pairs in Primer-BLAST

Parameter	Minimum Value	Optimum Value	Maximum Value
Primer Size (bp)	15	18	20
Primer Melting Temperature (°C)	59	60	61
Primer GC%	40	50	60
Product Size (bp)	900	1000	1100
Consecutive GC Clamp Length	1	3	N/A

All primer pairs were QC tested in simplex format using SYBR Green qPCR on *M. bovis* BCG DNA (Table 3.11). As equal amount of BCG DNA was used in all reactions, PCR assay efficiency could be assessed comparatively. The results below are from the first primer design iteration, there were 73 more (described in section 3.2.2.2).

Table 3.11: tNGS Target Gene Primer Simplex QC Test for Original Primers Using Triplicate Samples

Gene Target	qPCR Amplification ($\bar{X} C_T$)
<i>eis</i>	24.47
<i>pncA</i>	25.80
<i>fabG1</i> & <i>inhA</i>	19.49
<i>rv0678</i>	19.15
<i>tlyA</i>	21.89
<i>ethA</i>	35.00
<i>gyrA</i>	19.97
<i>rrs</i>	8.80
<i>rplC</i>	15.91
<i>rpsL</i>	20.19
<i>embB</i>	12.72
<i>rpoB</i>	16.46
<i>gidB</i>	18.93
<i>katG</i>	16.06
<i>rri</i>	19.66

3.2.2.2: Gene Target Primer Pair Redesign

Primers were redesigned multiple times during multiplex group optimization (section 3.2.3). Redesigns resulted in a total of 90 primer pairs (176 individual redesigned primers). For assessment of redesigned primers all amplifications were performed on triplicate samples and mean C_T s were used to quantify amplification efficiency. Likewise, when sequencing was performed it was in duplicate for each amplification resulting in a total n of six for each sample in analysis.

Design of gene target primer pairs was highly iterative (section 3.2.2) and primer performance was assessed both in simplex and in multiplex. However, multiple targets were suitable following initial design or with a single redesign for improved target coverage (*gyrA*, *gidB*, *inhA*, *pncA*, and *rpoB*).

Conversely, several targets required extensive optimization before they performed well in multiplex format.

Amplicons were designed to be approximately 1kb to capture all the necessary SNPs in some genes and to keep a consistent length for multiplexing – 1kb is also an optimal length for nanopore sequencing. Use of 1kb targets allowed total gene coverage of 8 targets reducing the need to redesign if new drug resistant SNPs are identified in these genes.

The tNGS assay is limited by reliance on conserved primers which can lower sensitivity if a mutation occurs within the primer site or outside the targeted section of the genome ^{5,19}. However, the risk is reduced due to the highly conserved clonal genomes of mycobacteria, unlike many other bacterial pathogens.

However, during sequencing of contrived samples a mutation within the *katG* forward primer site was identified, resulting in a loss of sensitivity and requiring primer redesign (section 3.2.11). This was a known mutation site, but it is a mutation not associated with resistance and therefore was overlooked – it is important to consider all known mutation sites when designing tNGS primers to avoid this issue. Primer site mutations can prove especially problematic in the event of mixed infection, where primer competition will result in only one strain being detected.

3.2.2.3: Redesign of *inhA* primer pair

Primers for gene target *inhA* were redesigned once. Redesign was necessary as the original primer set combined coverage of *inhA* and *fabG1* but didn't cover all necessary target SNPs. Splitting into two separate primer pairs enabled greater coverage of target mutations for both genes (Table 3.12). New primers covered 96% of the *inhA* gene as well as the 5' gene promoter region to cover all high confidence mutations listed in appendix I.

Table 3.12: Redesign history for *inhA* primers

<i>inhA</i> Redesign Version	Forward Primer (5'-3')	Reverse Primer (5'-3')	Amplicon Length (bp)
Original	GGGCGCTGCAATTTATCCC	GGCGTAGATGATGTCACCCG	941
Redesign 1*	GGCGTAGATGATGTCACCCGT	GGGCGCTGCAATTTATCCC	942

*Redesign version selected for use

3.2.2.4: Redesign of *pncA* primer pair

Primers for *pncA* were also redesigned once during optimization. The primers were moved to encompass the entire *pncA* gene and cover all known high confidence resistance-conferring mutations (Table 3.13).

Table 3.13: Redesign history for *pncA* primers

<i>pncA</i> Redesign Version	Forward Primer (5'-3')	Reverse Primer (5'-3')	Amplicon Length (bp)
Original	TCAGCTGGTCATGTTTCGCG	ATGAACACCGTCACAGCCG	960
Redesign 1*	TCCAGATCGCGATGGAACG	TCACCGGACGGATTTGTCG	953

*Redesign version selected for use

3.2.2.5: Redesign of *rpoB* primer pair

To ensure coverage of the rifampicin resistance determining region (RRDR), a FASTA copy of the gene was used to map the location of each known mutation (Appendix II). This map was used to identify potential primer sites which centered the amplicon on the *rpoB* variable region, while also increasing coverage from 27% to 31% of the *rpoB* gene (Table 3.14).

Table 3.14: Redesign history for *rpoB* primers

<i>rpoB</i> Redesign Version	Forward Primer (5'-3')	Reverse Primer (5'-3')	Amplicon Length (bp)
Original	TAGTCCTAGTCCGAGTCGCC	ACGTCTTCTTCGGTCAGCG	963
Redesign 1*	TCATCATCAACGGGACCGAG	ACACGATCTCGTCGCTAACC	1092

*Redesign version selected for use

3.2.2.6: Redesign of *rrl* primer pair

Optimisation of primers for *rrl* (23S rRNA) required two rounds of redesign. The first redesign was to position the high confidence mutation sites more centrally within the amplicon. This alteration reduced the risk of having low coverage for mutations of clinical interest. Specificity testing with DNA template extracted from NRF sputum demonstrated this primer pair cross-reacted with human or commensal bacterial 28S or 23S rRNA genes ($\bar{X} C_T = 13.02$). Using Primer-BLAST (Section 2.8), *rrl* primers were redesigned to increase specificity using *M. tuberculosis* H37Rv as the reference

genome. This redesign resulted in an amplicon which covered all known high-confidence mutation locations and an improved 33% coverage of the 3,138bp *rrl* gene. Specificity testing of the new primer pair demonstrated no cross-reactivity with human/commensal DNA and was selected for continued use (Table 3.15).

Table 3.15: Redesign history for *rrl* primers

<i>rrl</i> Redesign Version	Forward Primer (5'-3')	Reverse Primer (5'-3')	Amplicon Length (bp)
Original	TGAGAGGTGACGCATAGCC	GATCAGCCTGTTATCCCCGG	948
Redesign 1	AACACAGGTCCGTGCGAA	TATCCTGACCGAACGTGGC	959
Redesign 2*	GGTCCGTGCGAAGTCGC	TGAACCCGTGTTCTGCGG	1044

*Redesign version selected for use

3.2.2.7: Redesign of *rplC* primer pair

rplC primers underwent two redesigns. The first redesign reduced amplicon size from 1088bp to 902bp to improve amplification speed and efficiency, while still covering the full 654bp *rplC* gene. This redesign version was used for multiplex configurations 1 through 5 until testing by nested qPCR highlighted that *rplC* was amplifying >2CTs later than other primer pairs in the group. The *rplC* gene was then redesigned using Primer-BLAST.

The redesign covered the entire *rplC* gene as well as a 153bp buffer on the 5' end and a 171bp buffer on the 3' end. This improved efficiency in line with other targets and no cross-reactivity with human or commensal bacterial DNA was detected (Table 3.16).

Table 3.16: Redesign history for *rplC* primers

<i>rplC</i> Redesign Version	Forward Primer (5'-3')	Reverse Primer (5'-3')	Amplicon Length (bp)
Original	ACATCATCGATCCCACGCC	CATCTTCTTGGGTGTGCGC	1088
Redesign 1	CCGCTACCGACTGAGAAGAA	GGCGTCTTGACGTGATTTT	902
Redesign 2*	AGTACAAGGACTCGCGGGA	TCGAGTGGGTACCCTGGC	978

*Redesign version selected for use with increased working concentration of 3µM

3.2.2.8: Redesign of *tlyA* primer pair

tlyA required four rounds of redesign. Redesign of *tlyA* was initially performed to preferentially detect high-confidence mutation sites over medium-confidence mutation sites, except as convenient. This redesign encompassed the full 807bp gene but cross-reacted with human/commensal DNA in NRF sputum when assessed by qPCR ($\bar{X} C_T = 17.42$). Therefore, a second redesign was performed using Primer-BLAST. Testing was conducted with both *M. bovis* BCG culture and NRF sputum spiked with *M. bovis* BCG. This assay was less efficient than others in its group and needed further optimisation.

Increased concentrations of *tlyA* primers were tested to improve efficiency. Three samples with varying concentrations of *tlyA* were tested and assessed by qPCR (Table 3.17). Increasing *tlyA* primer concentration from 2 μ M to 3 μ M improved the uniformity of the multiplex group amplification, from a mean range of 3.33 to 1.59 C_T s, hence 3 μ M *tlyA* primers were used for subsequent experiments.

Table 3.17: Nested qPCR mean C_T results for comparison of multiplex amplification efficiency in multiplex with various *tlyA* concentrations

Gene Target	2.5 μ M <i>tlyA</i> Stock Concentration qPCR ($\bar{X} C_T$)	3 μ M <i>tlyA</i> Stock Concentration qPCR ($\bar{X} C_T$)	4 μ M <i>tlyA</i> Stock Concentration qPCR ($\bar{X} C_T$)	Control Stock Concentration qPCR ($\bar{X} C_T$)
<i>gidB</i>	11.52	7.39	8.13	7.79
<i>inhA</i>	8.21	8.09	7.98	9.83
<i>rri</i>	9.35	8.54	10.56	9.45
<i>pncA</i>	12.53	8.80	10.85	9.18
<i>rpsL</i>	8.11	8.56	7.99	8.11
<i>tlyA</i>	30.13	8.98	8.93	11.12

Two further primer redesigns were tested (Table 3.18) but neither performed better than redesign 2 at 3 μ M concentration.

Table 3.18: Redesign history for *tlyA* primers

<i>tlyA</i> Redesign Version	Forward Primer (5'-3')	Reverse Primer (5'-3')	Amplicon Length (bp)
Original	TGTGGGTTTCCTTCCTTGGG	AGCAGTACTTCGGTGAACCC	1041
Redesign 1	CATCGCACGTCGTCTTTCC	GTGTGGACGACCAGCAGAA	921
Redesign 2 *	CGTTGATGCGCAGCGATC	GGTCTCGGTGGCTTCGTC	1096
Redesign 3	ATCGACGCCCTACTTGCTT	CTCCAATCCCTGGCCGAC	922
Redesign 4	TCCGGTGACTAGCGTAGGAA	ACCGCATCCTCCAATCCCT	987

*Redesign version selected for use with increased working concentration of 3 μ M

3.2.2.9: Redesign of *rv0678* gene primer pair

Four *rv0678* primer pairs were designed. Low coverage for the *rv0678* mutation sites were observed when performing sensitivity testing (Figure 3.4). Primer-BLAST was used to design 4 primer pairs as described previously as the original forward primer was proximal to the high confidence mutation site. Four new primer pairs were designed to encompass the entire 498bp *rv0678* gene, keeping primers sufficient distance from the important mutations.

Rv0678_S63R				
REFERENCE		A	G	C
SAMPLE		A	G	C
POSITION		779176	779177	779178
BASECALLED COUNTS	A	44		1
	C			20
	G	1	27	
	T			3

katG_S315*				
REFERENCE		G	C	T
SAMPLE		G	C	T
POSITION		2155167	2155168	2155169
BASECALLED COUNTS	A	10	2	5
	C		1907	5
	G	3176	1244	5
	T	4	5	3209

Figure 3.4: Example output from the Epi2Me TB Resistance Profile pipeline for the mutation in Rv0678 associated with resistance to bedaquiline and clofazimine compared to that for katG associated with resistance to isoniazid.

Primers were compared in multiplex mixes using *M. bovis* BCG spiked sputum. Analysis by qPCR showed that redesign versions 2 and 3 were most efficient ($\bar{X} C_T < 5$). Mean C_T results for all multiplex targets showed that version 2 was best but some of the PCRs were still inhibited ($\bar{X} C_T$ range = 9.66CTs). This indicated a need for further optimisation of the multiplex as a whole. However, the redesigned *rv0678* primers were within tolerances and version 2 primers were used for subsequent experiments (Table 3.19)

Table 3.19: Redesign history for rv0678 primers

rv0678 Redesign Version	Forward Primer (5'-3')	Reverse Primer (5'-3')	Amplicon Length (bp)
Original	CGGAACCAAAGAAAGTGCGG	GGTGACATGCTGACCTACGG	1010
Redesign 1	CGTGGTCTTCAAGGTGAGCG	ACAAGGAGTGACCACAGGC	933
Redesign 2 *	GCTCGTCCTTCACTTCGCC	ATCAGTCGTCTCTCCGGT	959
Redesign 3	ATCGACGGTGATTGGCAG	CCACCTCGGTCAGATTGCG	968
Redesign 4	CGGAGCCGGAAACTTCGTA	AAGTCACTGAACGTGGCCG	1037

*Redesign version selected for use

3.2.2.10 Redesign of *fabG1* primer pair

Redesign of *fabG1* primers was initially required to separate the combined *inhA/fabG1* primer set. The amplicon was shifted to completely cover the 744bp *fabG1* gene along with short buffer regions on both the 5' and 3' ends. Further redesigns were required to improve amplification efficiency in different multiplex configurations. As with other primers, PrimerBLAST was used to design 4 primer pairs as described previously.

Multiplex mixes were tested using *M. bovis* BCG spiked sputum. Redesign version 3 was most efficient with a $\bar{X} C_T < 5$. Results indicated further optimization of multiplex group 1 was required ($\bar{X} C_T$ range = 9.66 C_T s). However, *fabG1* redesign version 3 was within tolerance and used for subsequent experimentation (Table 3.20).

Table 3.20: Redesign history for *fabG1* primers

<i>fabG1</i> Redesign Version	Forward Primer (5'-3')	Reverse Primer (5'-3')	Amplicon Length (bp)
Original	GGGCGCTGCAATTTATCCC	GGCGTAGATGATGTCACCCG	941
Redesign 1	ACCTTCAAATCGGTGGCCT	AATCACTCCGGCCTTGGAG	1060
Redesign 2	TACGCTCGTGGACATACCG	GGTGCTCCTCGTTTTGCAC	1030
Redesign 3 *	CTTTTGCACGCAATTGCGC	AGCAGTCCTGTCATGTGCG	1058
Redesign 4	CGACAAACGTCACGAGCG	GTGCTCCTCGTTTTGCACG	1089
Redesign 5	TAGCGCGACATACCTGCTG	GTGGCCCATACCCATGCC	1066

*Redesign version selected for use

3.2.2.11: Redesign of *ethA* primer pair

Redesign of *ethA* primers was performed to improve identification of mutations and primer specificity. Primer-BLAST was used to design 5 primer pairs as described above. Primer mixes were used to amplify *M. bovis* BCG spiked sputum and *ethA* redesigns were tested in multiplex PCR (Table 3.21). Redesign version 3 was selected for subsequent experimentation as it had the narrowest \bar{X} C_T range (Table 3.22).

Table 3.21: Nested mean qPCR C_T s for five multiplexes testing redesigned *ethA* primer pairs using triplicate samples

<i>ethA</i> Redesign Version	<i>gyrA</i> Nested qPCR (\bar{X} C_T)	<i>rpoB</i> Nested qPCR (\bar{X} C_T)	<i>ethA</i> Nested qPCR (\bar{X} C_T)	<i>rplC</i> Nested qPCR (\bar{X} C_T)	<i>katG</i> Nested qPCR (\bar{X} C_T)	<i>hsp65</i> Nested qPCR (\bar{X} C_T)	Nested qPCR Range (\bar{X} C_T)
1	12.94	14.02	9.91	10.66	11.62	11.27	4.11
2	13.36	11.19	13.61	12.64	11.85	11.54	2.42
3	11.96	12.11	12.62	11.53	11.47	11.78	1.15
4	12.00	12.09	10.84	11.96	10.83	11.13	1.26
5	12.02	12.76	12.29	29.60	11.27	11.29	18.33

Table 3.22: Redesign history for *ethA* primers

<i>ethA</i> Redesign Version	Forward Primer (5'-3')	Reverse Primer (5'-3')	Amplicon Length (bp)
Original	TCGGCTTGATTGACCACCC	ACGATGTAGGTGGGTGAGC	964
Redesign 1	GTCCAGGAGGCATTGGTGT	CGGAATTCGCTCCGACTCC	1023
Redesign 2	GTCCAGGAGGCATTGGTGT	TGACGGCCTCGACATTACG	1191
Redesign 3 *	GTCCAGGAGGCATTGGTGT	TGGATCCATGACCGAGCAC	1163
Redesign 4	TCAACCCCGTTGCGGTAAT	TGGATCCATGACCGAGCAC	1040
Redesign 5	ACCCCGTTGCGGTAATGAT	GAGCTACGCCATCCTGGAA	941

*Redesign version selected for use

3.2.2.12: Redesign of *rrs* (16S rRNA gene) primer pair

Initial redesign of *rrs* primer pairs was performed to improve coverage of a mutation proximal to the reverse primer. Redesigned primers included a 3' buffer region. Specificity testing identified cross-reactivity with human/commensal DNA when amplifying unspiked NRF sputum (\bar{X} C_T = 23.77).

Using Primer-BLAST a new primer pair was designed covering 60% of the *rrs* gene and retaining a 3' buffer region. This primer pair negatively impacted amplification of *eis* and *embB* targets in the multiplex.

New primers were designed for all multiplex group 1 targets concurrently. During these redesigns 4 new *rrs* primer pairs were designed. Design used 2 manually selected forward primers and 2 manually selected reverse primers. Primers included a minimum 3bp GC clamp on the 3' end. *rrs* gene coverage ranged from 60% to 68% and included a 3' buffer.

Primers were tested using *M. bovis* BCG spiked sputum and analyzed by nested qPCR (amplicons diluted 1:100 using nuclease-free H₂O). qPCR results indicated that redesign version 4 amplified most efficiently (\bar{X} C_T < 5) (Table 3.23).

Table 3.23: Nested mean qPCR C_Ts for four multiplexes testing redesigned *rrs* primer pairs

<i>rrs</i> Redesign Version	<i>eis</i> Nested qPCR (\bar{X} C _T)	<i>embB</i> Nested qPCR (\bar{X} C _T)	<i>rrs</i> Nested qPCR (\bar{X} C _T)	<i>rv0678</i> Nested qPCR (\bar{X} C _T)	<i>fabG1</i> Nested qPCR (\bar{X} C _T)
3	13.51	6.00	8.20	9.90	7.48
4	14.77	5.00	5.00	5.00	5.00
5	13.67	40.00	5.00	5.00	7.66
6	40.00	19.81	40.00	8.84	6.00

Inclusion of this *rrs* primer pair also improved the efficiency of 4/5 of the remaining multiplex group targets. The multiplex group required further optimisation as a whole, but primer redesign version 4 was selected for subsequent experimentation (Table 3.24).

Table 3.24: Redesign history for *rrs* primers

<i>rrs</i> Redesign Version	Forward Primer (5'-3')	Reverse Primer (5'-3')	Amplicon Length (bp)
Original	GCTTAACTGTGAGCGTGCG	CTTTGTTGTCATGCACCCGG	1023
Redesign 1	TTCCCTTGTGGCCTGTGTG	ATGTTTCACTTCCCCGCGT	998
Redesign 2	CGTTCCTTGTGGCCTGT	GCACGACATCACTCGTGC	947
Redesign 3	AATACGTAGGGTGCAGCG	AAAGGAGGTGATCCAGCCG	1013
Redesign 4*	CTCTGGGCAGTAACTGACGC	GAGTGTTGCCTCAGGACCC	942
Redesign 5	TTGTCCGGAATTACTGGGCG	GACAAGAACCCTCACGGC	1054
Redesign 6	TGGAATTCCTGGTGTAGCGG	AGTGTTCCTCAGGACCCA	1006

* Redesign version selected for use

3.2.2.13: Redesign of *rpsL* primer pair

Initial redesign of *rpsL* primers was performed to address cross-reactivity with human/commensal DNA. Primer redesign was performed using Primer-BLAST. A primer pair covering the full 375bp *rpsL* gene and 5' and 3' buffer regions was designed.

Specificity testing exhibited no cross-reactivity when assessed by qPCR. However, sensitivity testing in mixed samples identified low sequencing coverage of *rpsL*. Analysis using the Epi2Me TB Resistance Profile pipeline showed an average coverage depth of 84x in *rpsL* while *gidB* and *rrs* showed a mean coverage of 684x for the same sample. To improve coverage depth 5 primer pairs were designed ranging in size from 933bp to 1077bp. All primer pairs covered the full *rpsL* gene and included buffer regions on 5' and 3' ends.

Analysis showed variability in *rpsL*, and other multiplex target, amplification efficiency (Table 3.25). Redesign version 3 minimized disruption to the multiplex group and had the lowest mean *rpsL* C_T . Further multiplex group optimisation was required but redesign version 3 was selected for use in subsequent experimentation (Table 3.26).

*Table 3.25: Nested mean qPCR amplification C_T s of five multiplexes testing redesigned *rpsL* primer pairs using triplicate samples*

<i>rpsL</i> Redesign Version	<i>gidB</i> Nested qPCR (\bar{X} C_T)	<i>inhA</i> Nested qPCR (\bar{X} C_T)	<i>rrl</i> Nested qPCR (\bar{X} C_T)	<i>pncA</i> Nested qPCR (\bar{X} C_T)	<i>rpsL</i> Nested qPCR (\bar{X} C_T)	<i>tlyA</i> Nested qPCR (\bar{X} C_T)	Nested qPCR Range (\bar{X} C_T)
2	13.11	9.17	11.76	11.65	29.26	16.09	20.09
3	10.35	9.64	13.14	12.53	11.84	18.54	8.90
4	10.34	9.60	11.73	11.47	29.11	14.63	19.51
5	11.44	9.29	13.53	12.88	13.31	17.33	8.04
6	11.69	9.92	12.84	14.01	28.95	18.26	19.03

Table 3.26: Redesign history for *rpsL* primers

<i>rpsL</i> Redesign Version	Forward Primer (5'-3')	Reverse Primer (5'-3')	Amplicon Length (bp)
Original	GAGTTTTGGTCGGCACTGC	GGGCGGGTTTGACATTGTC	992
Redesign 1	GCGGCGGGTATTGTGGTT	TAACCGGCGCTTCTCACC	1063
Redesign 2	AGGCAAGCTATGCGACACA	GTTGCGGACCCTACTCAGG	1064
Redesign 3*	CGCTTTGACCTGCCAGACT	GCGCTTCTCACCAGCGATA	1077
Redesign 4	CGATGCCTCGGATGAGACG	TCAGCACGTCCTTCTGTGC	1071
Redesign 5	TACGCTTGATGTAGGGGCG	TAATGCGCAAAGGCTCGGT	1005
Redesign 6	GGCAAGCTATGCGACACAC	AGCGATAATGCGCAAAGGC	933

* Redesign version selected for use

3.2.2.14: Redesign of *embB* primer pair

embB underwent seven redesigns for optimising performance in multiplex. The first redesign was performed to prioritise all high-confidence SNPs over medium confidence SNPs. Multiplex amplifications using *M. bovis* BCG culture were assessed post-sequencing by Qualimap visualization. Analysis showed *embB* had 7-fold lower mean coverage depth relative to other group targets (Figure 3.5).

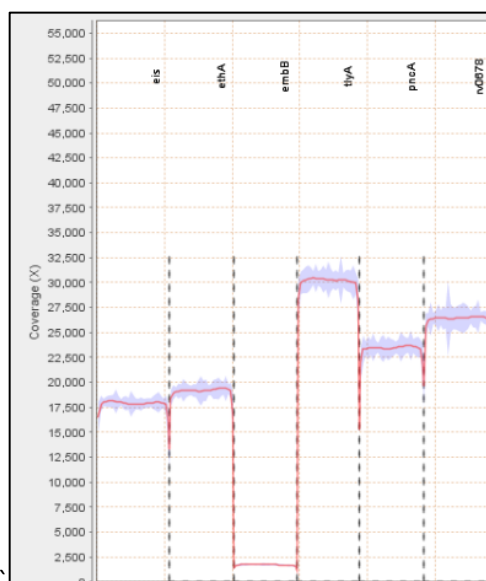


Figure 3.5: Qualimap coverage map of genes targeted by primers within multiplex group 1 after tNGS amplification and sequencing with *embB* primer iteration 1

A new primer pair was designed using Primer-BLAST to address this low coverage. Redesigned primers covered all known high-confidence SNP sites and 28.9% of the full gene. Redesigned primers were incorporated into multiplex group 1 and tested using *M. bovis* BCG DNA. Product was sequenced by Flongle and FASTQ files were mapped (see Methods section 2.16) to visualize relative coverage within the multiplex (Figure 3.6). Mapping showed this redesign resulted in an *embB* drop out. This redesign version also correlated with lower sequencing coverage of *rrs* and increased coverage of *hsp65*.

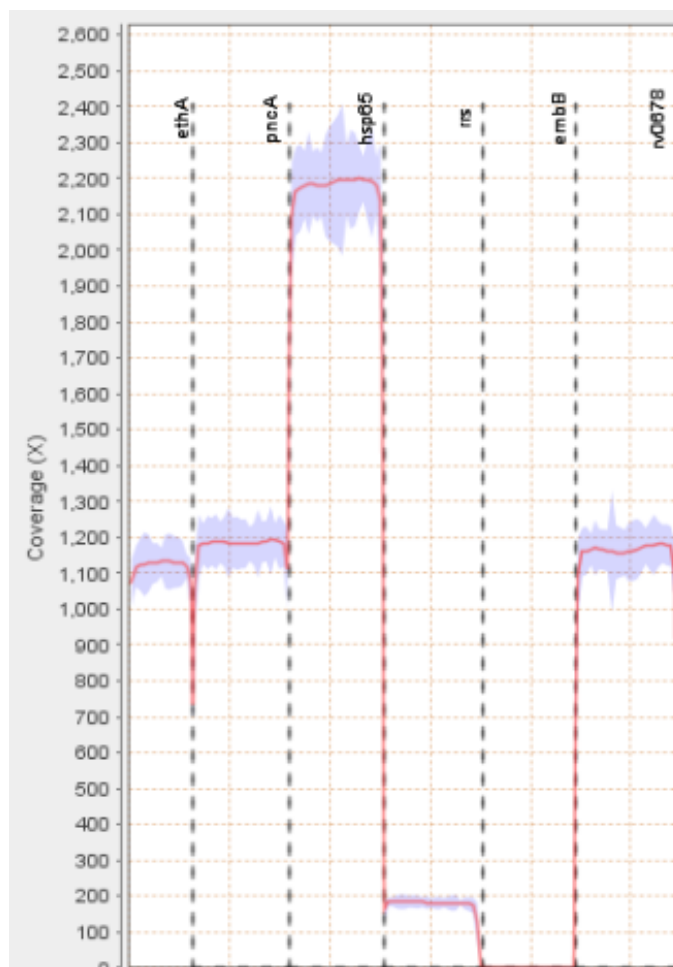


Figure 3.6: Qualimap coverage map of genes targeted by primers in the group 1 multiplex after tNGS amplification and sequencing with *embB* redesign iteration 2 primers

A third primer pair was designed to improve target and multiplex performance. Redesign version 3 reduced amplicon size in an attempt to improve amplification efficiency. Testing using *M. bovis* BCG spiked sputum showed poor *embB* coverage in the multiplex by PCR and sequencing.

A further 4 primer pairs were designed using Primer-BLAST. Multiplex amplification using *M. bovis* BCG spiked NRF sputum DNA were assessed by nested qPCR. *embB* redesign version 5 yielded the most efficient amplification ($\bar{X} C_T \leq 5$) (Table 3.27) and the smallest mean C_T range with 4/5 of primer pairs demonstrating a mean $C_T < 5$. Hence, *embB* redesign version 5 was selected for inclusion in the final multiplex and use subsequent experimentation (Table 3.28).

Table 3.27: Mean nested qPCR C_T s for four multiplexes testing redesigned *embB* primer pairs using triplicate samples

<i>embB</i> Redesign Version	<i>eis</i> Nested qPCR ($\bar{X} C_T$)	<i>embB</i> Nested qPCR ($\bar{X} C_T$)	<i>rrs</i> Nested qPCR ($\bar{X} C_T$)	<i>rv0678</i> Nested qPCR ($\bar{X} C_T$)	<i>fabG1</i> Nested qPCR ($\bar{X} C_T$)
4	13.51	6.00	8.20	9.90	7.48
5	14.77	5.00	5.00	5.00	5.00
6	13.67	40.00	5.00	5.00	7.66
7	40.00	19.81	40.00	8.84	6.00

Table 3.28: Redesign history for *embB* primers

<i>embB</i> Redesign Version	Forward Primer (5'-3')	Reverse Primer (5'-3')	Amplicon Length (bp)
Original	TGGTGATCTTGTCCGTGCC	ACCAAGATCCGCAGCATCG	1012
Redesign 1	GGGCTGATTGGCTTTGTGTT	GTCGCTGACATGGGTCACTCA	936
Redesign 2	CTCAATTGCCAGCTCCTCC	TGGGCGTGAACATCAGGAA	1031
Redesign 3	GGGGTGTTACCGACCTG	GGTCAGGATGACGGTGCC	915
Redesign 4	CGCCGTGGTGATATTCGGC	GGGATACCAACACCGTCGT	1007
Redesign 5*	CGCCGTGGTGATATTCGGC	GCACACCGTAGCTGGAGAC	1124
Redesign 6	CTCTGGCATGTCATCGGCG	GGAGACATACCACCGCCG	1086
Redesign 7	CCCAGCTCCTCCTCAGGC	TGGTGGGCGTGAACATCAG	1026

* Redesign version selected for use

3.2.2.15: Redesign of *katG* primer pair

A FASTA *katG* gene sequence was annotated to identify positions of the high-confidence mutation sites within the 2,223bp gene. Five new primer pairs were designed using Primer-BLAST to prioritize the high confidence mutations over medium and low confidence mutations.

Primers were compared to determine the most efficient amplification and least disruption to existing multiplex reactions. Redesign version 3 had the best amplification efficiency ($\bar{X} C_T = 10.3$) and redesign version 4 had the least impact on the other targets in the multiplex ($\bar{X} C_T$ range = 5.16 C_T s) (Table 3.29). However, inconsistent assay performance required further redesign of the multiplex.

Table 3.29: Mean nested qPCR C_T s for five multiplexes testing redesigned *katG* primer pairs using triplicate samples

<i>katG</i> Redesign Version	<i>gyrA</i> Nested qPCR ($\bar{X} C_T$)	<i>rpoB</i> Nested qPCR ($\bar{X} C_T$)	<i>ethA</i> Nested qPCR ($\bar{X} C_T$)	<i>rplC</i> Nested qPCR ($\bar{X} C_T$)	<i>katG</i> Nested qPCR ($\bar{X} C_T$)	<i>hsp65</i> Nested qPCR ($\bar{X} C_T$)	Nested qPCR Range ($\bar{X} C_T$ s)
2	13.76	11.92	8.43	9.76	17.77	10.45	9.34
3	11.33	12.27	9.60	18.26	10.30	11.53	8.66
4	10.91	9.57	9.34	8.49	13.65	9.69	5.16
5	12.11	10.69	8.74	10.23	18.95	10.99	10.21
6	11.77	11.61	9.04	11.66	15.08	11.60	6.04

The *hsp65* target was included to help speciate non-tuberculous mycobacteria if present. Other targets in the multiples (such as *gyrA*, *rrs*, and *rrl*) were also capable of providing that information, so the decision was made to remove the *hsp65* target from the multiplex to ease optimisation. Redesign versions 2-6 were amplified without *hsp65* using spiked NRF sputum. Nested qPCR analysis showed removal of *hsp65* primers resulted in failure to amplify in 4/5 of multiplex options (Table 3.30). However, redesign version 6 without *hsp65* primers showed consistent amplification for all targets ($\bar{X} C_T$ range = 1.45 C_T s).

Table 3.30: Mean nested qPCR C_Ts for five multiplexes testing redesigned *katG* primer pairs with the removal of *hsp65* primers using triplicate samples

<i>katG</i> Redesign Version	<i>gyrA</i> Nested qPCR (\bar{X} C _T)	<i>rpoB</i> Nested qPCR (\bar{X} C _T)	<i>ethA</i> Nested qPCR (\bar{X} C _T)	<i>rp1C</i> Nested qPCR (\bar{X} C _T)	<i>katG</i> Nested qPCR (\bar{X} C _T)
2	40.00	40.00	40.00	40.00	40.00
3	40.00	40.00	40.00	40.00	40.00
4	40.00	40.00	40.00	40.00	40.00
5	40.00	40.00	40.00	40.00	40.00
6	15.06	15.32	14.62	13.87	14.60

3.2.2.16: Redesign of *eis* primer pair

The first *eis* primers were redesigned to correct poor sensitivity for high-confidence mutations in the gene promoter region. Primer-BLAST was used to design a new primer pair containing the promoter region SNP sites. The new primers resulted in an amplicon covering 59% of the *eis* gene in addition to the 5' promoter region.

An NRF sputum DNA sample was amplified and sequenced by Flongle and analysed using the Epi2Me TB Resistance Profile pipeline (section 2.16). Epi2Me results showed low coverage of *eis* targets compared to other group 1 multiplex targets, indicating a need for further redesign. Four additional primer pairs were designed and compared using nested qPCR. Version 3 performed best overall but the *eis* target was amplifying inefficiently and required further redesign (Table 3.31).

Table 3.31: Mean nested qPCR C_Ts testing redesigned *eis* primer pairs using triplicate samples

<i>eis</i> Redesign Version	<i>eis</i> Nested qPCR (\bar{X} C_T)	<i>embB</i> Nested qPCR (\bar{X} C_T)	<i>rrs</i> Nested qPCR (\bar{X} C_T)	<i>rv0678</i> Nested qPCR (\bar{X} C_T)	<i>fabG1</i> Nested qPCR (\bar{X} C_T)
2	13.51	6.00	8.20	9.90	7.48
3	14.77	5.00	5.00	5.00	5.00
4	13.67	40.00	5.00	5.00	7.66
5	40.00	19.81	40.00	8.84	6.00

Ten primer pairs were designed by Primer-BLAST, 7 as normal and 3 were designed with reduced amplicon size (400-600bp) for improved amplification efficiency. Redesigns generated amplicons ranging in gene coverage from 11.7% to 73.5%. Primer performance was tested in multiplex qPCR (Table 3.32). Redesign version 8 was judged to be the best primer pair overall, with a low mean *eis* C_T and early mean C_Ts for all other targets.

Table 3.32: Mean nested qPCR C_Ts testing redesigned *eis* primer pairs using triplicate samples

<i>eis</i> Redesign Version	<i>eis</i> Nested qPCR (\bar{X} C_T)	<i>embB</i> Nested qPCR (\bar{X} C_T)	<i>rrs</i> Nested qPCR (\bar{X} C_T)	<i>fabG1</i> Nested qPCR (\bar{X} C_T)	<i>rv0678</i> Nested qPCR (\bar{X} C_T)
6	12.62	8.87	6.84	8.76	7.45
7	12.01	35.00	7.02	9.10	7.77
8	12.33	9.58	6.40	9.67	7.91
9	11.06	9.48	7.51	9.66	7.15
10	12.60	9.53	7.80	10.14	8.02
11	13.87	8.83	6.72	8.58	7.05
12	11.46	9.43	7.64	9.77	8.03
13	11.26	9.61	7.46	9.73	7.65
14	10.67	9.51	7.38	9.14	7.63
15	12.07	12.70	6.99	8.98	7.97

Sequencing by MinION was used to corroborate these results. The *eis* target had the highest coverage within the multiplex group despite poor nested qPCR performance (Figure 3.7). This was a surprising result and didn't match the qPCR data. There may have been an issue with the nested qPCR for *eis*, or there may have been some bias in the sequencing for the *eis* amplicon. Investigation identified a base in the forward nested primer was misdesigned creating overly conservative efficiency judgements. Therefore, version 8 was selected for use in subsequent experimentation (Table 3.33).

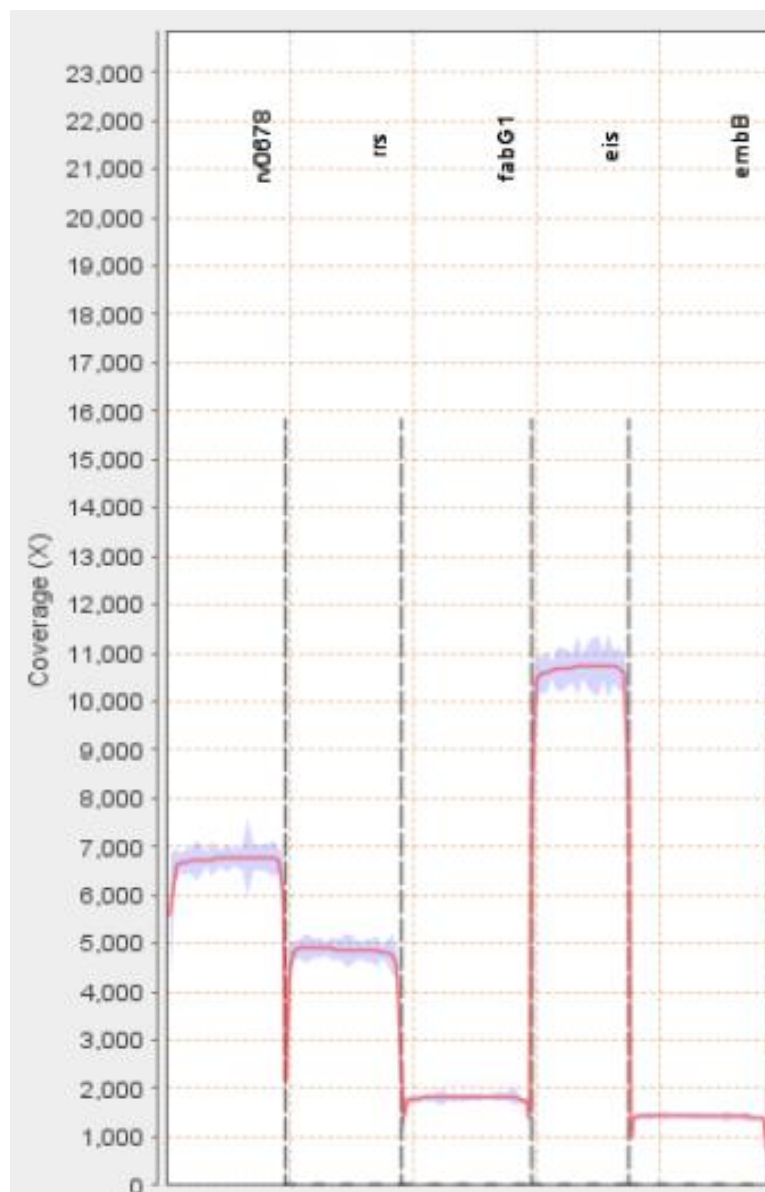


Figure 3.7: Qualimap coverage map of group 1 gene targets using *eis* redesign 8 primers from pooled triplicate samples for improved resolution

Table 3.33: Redesign history for *eis* primer pairs

<i>eis</i> Redesign Version	Forward Primer (5'-3')	Reverse Primer (5'-3)	Amplicon Length (bp)
Original	GCGCTGTACATGGATCTGC	AAAAGCCCGTCAGCCTAGC	1063
Redesign 1	ACCGCGACGAAACTGAGAC	GGTAGTGGCGGTGCACATT	1009
Redesign 2	CCAGTAGGAACATCCCCGG	ATGACATCCACAAGCGCCA	904
Redesign 3	AGATCGCCTCAAACCTCGCC	GATTACGCGTTCGTGCGC	1074
Redesign 4	CCGGAATCGGCTATGCGG	GTCGGGTACCTTTCGAGCC	1054
Redesign 5	GGACCGTGAAAACTCGCC	TCGCTGATTCTCGCAGTGG	1083
Redesign 6	GGTGAGCAGGTGGGGTAAC	ACCGGTACTTGCTCTGCAC	1055
Redesign 7	TCATGCAAGGTGGTAGCGG	GTTGCGACTGTGAGCAACG	810
Redesign 8*	TCCATGTACAGCGCCATCC	TGTCGGGTACCTTTCGAGC	917
Redesign 9	CAGTAGGAACATCCCCGGC	GGTAGTGGCGGTGCACATT	806
Redesign 10	GGGATGCAGTAACGCGAAC	ATGGGACCGGTACTTGCTC	880
Redesign 11	TACCCGTCGGGATGCAGTA	TGTAGCGCGGTTGGACAAT	1189
Redesign 12	CTTCACCAGGCACCGTCAA	TGGGACCGGTACTTGCTCT	442
Redesign 13	GCCAGTAGGAACATCCCCG	GTTGCGACTGTGAGCAACG	453
Redesign 14	TCCCGACCACCTCAGAACC	CTTGTCTGGTCCAACGGGT	593
Redesign 15	TCAGCTCATGCAAGGTGGT	TCGTCGCTGATTCTCGCAG	546

* Redesign version selected for use

3.2.2.17: Final Targets and Primers

Following primer redesign the assay consisted of 16 gene targets in 3 multiplex groups (Table 3.34).

The removal of *hsp65* to improve *katG* performance, and the separation of *fabG1* and *inhA* into individual targets altered the total number of targets during optimization. Specificity, sensitivity, and LoD experiments were then performed using the optimized primer designs.

Table 3.34: Final optimized gene target primer sets for tNGS multiplex assay

Assay Drug Resistance Gene Target	Multiplex Group	Forward Primer (5'-3')	Reverse Primer (5'-3')
<i>eis</i>	1	TCCATGTACAGCGCCATCC	TGTCGGGTACCTTTCGAGC
<i>embB</i>		CGCCGTGGTGATATTCGGC	GCACACCGTAGCTGGAGAC
<i>rrs</i>		CTCTGGGCAGTAACTGACGC	GAGTGTTGCCTCAGGACCC
<i>rv0678</i>		GCTCGTCCTTCACTTCGCC	ATCAGTCGTCCTCTCCGGT
<i>fabG1</i>		CTTTTGACGCAATTGCGC	AGCAGTCCTGTCATGTGCG
<i>gyrA</i>	2	TGACAGACACGACGTTGCC	CGATCGCTAGCATGTTGGC
<i>rpoB</i>		TCATCATCAACGGGACCGAG	ACACGATCTCGTCGCTAACC
<i>ethA</i>		GTCAGGAGGCATTGGTGT	TGGATCCATGACCGAGCAC
<i>rplC</i>		AGTACAAGGACTCGCGGGA	TCGAGTGGGTACCCTGGC
<i>katG</i>		TGCCCCGATCTGGCTCTTA	CTGTGGCCGGTCAAGAAGA
<i>gidB</i>	3	TGACACAGACCTCAGGAGC	GCCCTTCTGATTCGCGATG
<i>inhA</i>		GGGCGCTGCAATTTATCCC	GGCGTAGATGATGTCACCC
<i>rrl</i>		GGTCCGTGCGAAGTCGC	TGAACCCGTGTTCTGCGG
<i>pncA</i>		TCACCGGACGGATTTGTCG	TCCAGATCGCGATGGAACG
<i>rpsL</i>		GCGGCGGGTATTGTGGTT	TAACCGGCGCTTCTCACC
<i>tlyA</i>		CGTTGATGCGCAGCGATC	GGTCTCGGTGGCTTCGTC

3.2.3: Optimization of Multiplex Groups for tNGS based DR-TB detection

3.2.3.1: *in silico* Multiplex Grouping

Multiplex PCRs are powerful diagnostic and research tools, however, this power comes with increased complexity and design difficulties. A 1997 paper by Henegariu, *et al.*, summarized the four primary issues associated with multiplex PCR; namely if all products are weak, only long products are weak, only short products are weak, or if non-specific amplification occurs¹⁵⁷. These issues can often be attributed to primer-dimer formation and/or formation of unwanted products, both of which lower target amplification efficiency^{158,159}. Unfortunately, in the 25 years since this

publication few methods have been developed to effectively remove the trial-and-error nature of multiplex design and optimization. This is especially so for design of multiplex primers, as unknown variables in DNA interactions make definitive design of non-competitive or -interactive primers difficult.

Software developers and bioinformaticians have developed several software tools to minimize the risk of non-specific interactions and streamline multiplex design. Examples include Oli2Go, PRIMEval, MultiPLX 2.1, and Ultiplex; all of which claim to remove the risk of primer interactions and allow greater multiplexing¹⁶⁰⁻¹⁶³. Oli2Go performs simultaneous cross-dimer checking as well as specificity testing against multiple Kingdoms and Phyla for increased assay performance in shotgun sequencing and environmental sampling projects¹⁶⁰.

MultiPLX 2.1 uses nearest neighbour DNA binding thermodynamic analysis to identify the optimal multiplex groupings of pre-designed primers¹⁶³. This analysis aims to reduce primer-dimer formation and inhibition of primers while designing optimal multiplex groupings according to user defined parameters. Despite this, when tested on primers designed for the tNGS assay it returned only triplex mixes, regardless of parameters set. This prompted use of an alternative primer analysis and grouping tool.

PRIMEval, developed by many of the same individuals behind Oli2Go, also performs specificity and cross-dimer checks. However, PRIMEval improves on Oli2Go with added assessment of non-specific hybridization events, primer depletion, and amplification efficiency prediction¹⁶¹. This added utility was why PRIMEval was selected for *in silico* evaluation of Primer-BLAST designed primers for the tNGS assay.

More recently, Ultiplex multiplex analysis software was released by developers in China in 2021¹⁶². Ultiplex surpasses PRIMEval or Oli2Go with incorporation of primer design directly in the program, as opposed to being solely a post-hoc analysis tool¹⁶². Validation testing by the developers saw successful design of a 108-plex through use of the Ultiplex pipeline; a degree of multiplicity that if

replicable could greatly improve efficiency of molecular assay design. This tool, however, wasn't available until 2021 after we had finished designing the primers ¹⁶².

Primers designed as described in section 3.2.2 were organized into multiplex groups. Initially, groups were selected using MultiPLX 2.1 web-based software program described previously ¹⁶³. This program assessed all the simplex primers *in silico* for interactions and chose those least most likely to work well in a multiplex reaction. The program suggested 5 triplex reactions would be most efficient (Table 3.35).

Table 3.35: Triplex groups as designed by use of MultiPLX 2.1 software

Triplex Group	Gene Target 1	Gene Target 2	Gene Target 3
1	<i>eis</i>	<i>ethA</i>	<i>embB</i>
2	<i>pncA</i>	<i>gyrA</i>	<i>rpoB</i>
3	<i>fabG1/inhA</i>	<i>rrs</i>	<i>gidB</i>
4	<i>rv0678</i>	<i>rplC</i>	<i>katG</i>
5	<i>tlyA</i>	<i>rpsL</i>	<i>rrl</i>

However, *in silico* analysis is generally insufficient on its own to guarantee a viable multiplex. Optimisation and troubleshooting must be performed *in vitro* to detect issues which software programs overlook. As seen in sections 3.2.2 and 3.2.3, even with the use of *in silico* analysis, extensive optimization was still required to create viable 5- and 6-plexes. Non-specific priming was not typically the reason for multiplex group redesign. Rather, variable primer efficiencies and primer interactions (homo/hetero-dimer formation) were more commonly the cause of multiplex failure.

3.2.3.2: *in vitro* Multiplex Optimisation

The decision was made to consolidate the triplexes into larger multiplexes to reduce assay complexity, cost, and risk of contamination. A set of three 5-plex reactions were created using

triplex groups 1, 2, and 3 as the backbone (Table 3.36). An additional multiplex mix was included in testing combining all target primers in a single reaction for comparison to the new 5-plex groups.

Table 3.36: Configuration 1 of the 5-plex primer mixes for the tNGS assay

5-Plex Group	Gene Target 1	Gene Target 2	Gene Target 3	Gene Target 4	Gene Target 5
1	<i>eis</i>	<i>ethA</i>	<i>embB</i>	<i>tlyA</i>	<i>rv0678</i>
2	<i>pncA</i>	<i>gyrA</i>	<i>rpoB</i>	<i>rpsL</i>	<i>rplC</i>
3	<i>fabG1</i> & <i>inhA</i> *	<i>rrs</i>	<i>gidB</i>	<i>rrl</i>	<i>katG</i>

*Due to genomic proximity, targets for *fabG1* and *inhA* were covered in a single primer set

The 5-plex mixes were tested in duplicate using *M. bovis* BCG DNA. The performance of each 5-plex group, and the 15-plex, was measured by qPCR of *M. bovis* BCG specific RD1 and RD3 region primers and TapeStation. Analysis by RD1/RD3 qPCR acted as a nested measure of amplification and identified an increase in variance in 5-plex groups, as compared to the triplex groups (mean range increase = 1.06 C_Ts). However, there was no evidence of amplification failure as detected by qPCR (Table 3.37). Analysis of 5-plex and multiplex amplification products by TapeStation demonstrated evidence of non-specific amplification in all 5-plex groups. Furthermore, this analysis showed a total lack of target amplification in 5-plex group 2 and the 15-plex mix (Figure 3.8).

Table 3.37: SYBR Green qPCR results for evaluation of 5-plex configuration 1 amplification performance on *M. bovis* BCG DNA using dual sets of triplicate samples

Sample Replicate Set	5-Plex Group 1 \bar{X} C _T	5-Plex Group 2 \bar{X} C _T	5-Plex Group 3 \bar{X} C _T
1	19.60	17.12	19.82
2	19.60	17.11	19.84

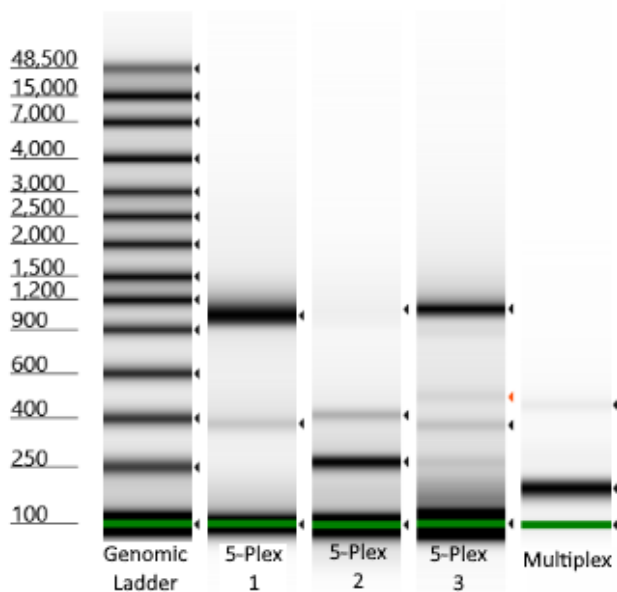


Figure 3.8: TapeStation gel image of 5-plex configuration 1 indicating non-specific amplification identified as of secondary and tertiary banding as well as, indicating no target amplicons in 5-plex 2 or the 15-plex reaction.

The 5-plex groups were then reconfigured to improve performance. This reconfiguration, and all subsequent reconfigurations, occurred in parallel to the primer redesigns covered in section 3.2.2. To improve assessment of multiplex performance a set of nested qPCR primers for each target were designed. This allowed us to measure the performance of each gene target in the multiplex without the need for sequencing (Table 3.38). Nested primers were designed to be approximately 100bp and have similar design characteristics to each other and the multiplex primers.

Table 3.38: Nested primer sequences for tNGS amplification analysis with design parameters

Nested Primer	Primer Length	Melting Temperature (°C)	GC%	Sequence (5'-3')	Amplicon Size (bp)
<i>inhA</i> & <i>fabG1</i> Forward	18	59.97	61.11	CAACAAGCTCGACGGGGT	101
<i>inhA</i> & <i>fabG1</i> Reverse	18	60.05	61.11	CCTTGGACACATCCGCGT	
<i>pncA</i> Forward	18	60.05	66.67	GGTGACCACTTCTCCGGC	110
<i>pncA</i> Reverse	18	60.13	61.11	TCGATTGCCGACGTGTCC	
<i>katG</i> Forward	18	59.89	61.11	TTATCCGGATGGCGTGGC	106
<i>katG</i> Reverse	18	60.05	61.11	TCGGGCCAGCTGTAAAGC	
<i>eis</i> Forward	19	60.08	57.89	CCGCTACCACCTTGCATGA	107
<i>eis</i> Reverse	18	59.65	66.67	GGTCTGACCAACCGGAC	
<i>rrs</i> Forward	18	59.97	61.11	TTGTACACACCGCCCGTC	106
<i>rrs</i> Reverse	18	60.13	61.11	ACTTCGTCCAATCGCCG	
<i>tlyA</i> Forward	18	60.13	66.67	GTCCTCGAGCGGACCAAC	108
<i>tlyA</i> Reverse	18	60.28	61.11	GGGCAACACGGTAGCCAA	
<i>gyrA</i> Forward	19	60.00	57.89	GGTCATGGGGCGGGTAAA	92
<i>gyrA</i> Reverse	18	59.13	61.11	CGCGGCCAGTTTTGTAGG	
<i>gidB</i> Forward	18	60.13	61.11	CGTGGCCGTTGAGATCGT	109
<i>gidB</i> Reverse	18	60.05	61.11	CAACTTGTCCAACGCGGC	
<i>rpsL</i> Forward	18	59.81	61.11	ACGCTTGATGTAGGGGCG	100
<i>rpsL</i> Reverse	18	60.89	66.67	GCCGGGTGTGTGCATAG	
<i>ethA</i> Forward	18	60.05	61.11	CCGCTGGACCGTTCACAT	110
<i>ethA</i> Reverse	18	59.80	61.11	ATCTCGGCGAGTAGCCCT	
<i>rv0678</i> Forward	18	59.89	61.11	TGACCGTGTTGTCCAGCC	104
<i>rv0678</i> Reverse	18	60.05	61.11	CAACGGCACCTGCGAAAC	
<i>rrl</i> Forward	18	59.57	61.11	CGCCCAAAGGTTCCCTCA	103
<i>rrl</i> Reverse	18	59.34	61.11	CCGACTTTCGTCCCTGCT	
<i>rplC</i> Forward	18	60.05	61.11	ATCAGCCCACGCAAGGTC	103
<i>rplC</i> Reverse	18	59.89	66.67	CATCCGAGTCGTCCAGCC	
<i>embB</i> Forward	18	60.05	61.11	CGACTTTACCGCCACCGT	108
<i>embB</i> Reverse	18	60.13	61.11	GCCTGCAAATTGGCGTCC	
<i>rpoB</i> Forward	18	60.13	66.67	GAGCGGTTCTGGGTTCTCC	100
<i>rpoB</i> Reverse	18	60.13	61.11	GACGCAGCTTGCGGTAGA	

To determine the cause of the non-specific band in 5-plex group 1 a series of duplex reactions were examined. Each of the 5 primer pairs were included in a duplex PCR with each other, creating 10 total reactions, to identify which pairs were interacting. The interaction was identified between primers for *eis* and *rv0678*. Therefore, a second tNGS multiplex configuration was designed, swapping the primers for *pncA* in 5-plex group 2 with those for *rv0678* in 5-plex group 1 resulting in another three 5-plex mixes (Table 3.39).

Table 3.39: Configuration 2 of 5-plex primer mixes for tNGS amplification

5-Plex Group	Gene Target 1	Gene Target 2	Gene Target 3	Gene Target 4	Gene Target 5
1	<i>eis</i>	<i>ethA</i>	<i>embB</i>	<i>tlyA</i>	<i>pncA</i>
2	<i>gyrA</i>	<i>rpoB</i>	<i>rpsL</i>	<i>rplC</i>	<i>rv0678</i>
3	<i>fabG1 & inhA</i>	<i>rrs</i>	<i>gidB</i>	<i>rriI</i>	<i>katG</i>

tNGS amplification results were assessed by both qPCR and TapeStation. Use of the nested primers to determine performance of each of the targets in the 3 multiplexes identified a single inhibited target in 5-plex group 1, *embB*. The remaining four group 1 targets had mean nested C_Ts between 8.68 to 11.38 while *embB* had a mean C_T of 19.77 (Table 3.40). TapeStation of this multiplex configuration did not show evidence of non-specific amplification indicating the swap of *pncA* for *rv0678* was successful (Figure 3.9). The swap also had a major impact on 5-plex group 2, which was now performing as desired.

Table 3.40: Mean results of nested SYBR Green qPCR analysis on amplification of assay targets using multiplex primer group configuration 2 using triplicate samples

Multiplex Group	Gene Target	Nested qPCR Amplification (\bar{X} C _T)
1	<i>eis</i>	9.73
	<i>ethA</i>	8.82
	<i>embB</i>	19.77
	<i>tlyA</i>	8.99
	<i>pncA</i>	11.38

2	<i>gyrA</i>	10.56
	<i>rpoB</i>	9.31
	<i>rpsL</i>	10.04
	<i>rplC</i>	9.80
	<i>rv0678</i>	9.98
3	<i>fabG1 & inhA</i>	8.68
	<i>rrs</i>	9.27
	<i>gidB</i>	10.34
	<i>rrl</i>	9.09
	<i>katG</i>	9.75

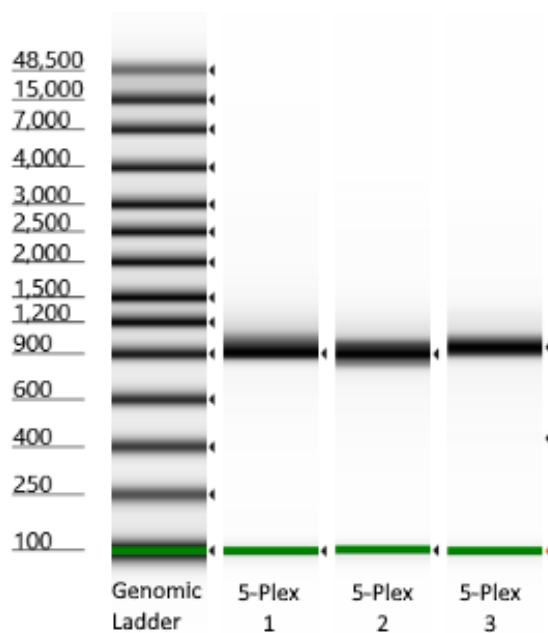


Figure 3.9: 5-plex configuration 2 TapeStation gel image showing no evidence of non-specific amplification identified as dual banding or loss of target amplicon in pooled triplicate samples for improved resolution.

Evidence of the *embB* target dropout (\bar{X} C_T 8 later than the rest of the 5-plex group as shown in table 3.40) necessitated development of a third multiplex configuration. During reconfiguration, *fabG1* and *inhA* targets were separated due to lack of coverage of some important *fabG1* targets, and a *hsp65* primer pair was added for speciation of non-tuberculous mycobacteria (NTMs - see section 3.2.7). These changes resulted in two 6-plex primer mixes and one 5-plex primer mix (Table 3.41).

Table 3.41: Configuration 3 of multiplex primer mixes for tNGS amplification

Multiplex Group	Gene Target 1	Gene Target 2	Gene Target 3	Gene Target 4	Gene Target 5	Gene Target 6
1	<i>eis</i>	<i>embB</i>	<i>ethA</i>	<i>pncA</i>	<i>tlyA</i>	<i>hsp65</i>
2	<i>gyrA</i>	<i>rpoB</i>	<i>fabG1</i>	<i>rpsL</i>	<i>rplC</i>	<i>rv0678</i>
3	<i>inhA</i>	<i>rrs</i>	<i>gidB</i>	<i>rriI</i>	<i>katG</i>	N/A

M. bovis BCG spiked normal respiratory flora (NRF) sputum collected from the NNUH clinical microbiology laboratory was used for testing this multiplex configuration to simulate clinical samples. qPCR analysis identified that multiplex group 1 had two inhibited targets (*eis* and *embB*), while multiplex group 2 had one slightly inhibited target (*fabG1*). There was no inhibition evident in multiplex group 3 (Table 3.42). TapeStation analysis showed no evidence of non-specific amplification with this group configuration (Figure 3.10).

Table 3.42: Mean results of nested SYBR Green qPCR analysis on amplification of assay targets using multiplex primer group configuration 3 using triplicate samples

Multiplex Group	Gene Target	Nested qPCR Amplification (\bar{X} C _T)
1	<i>eis</i>	15.12
	<i>embB</i>	22.75
	<i>ethA</i>	7.38
	<i>pncA</i>	8.60
	<i>tlyA</i>	7.22
	<i>hsp65</i>	9.13
2	<i>rv0678</i>	7.76
	<i>gyrA</i>	8.10
	<i>rpoB</i>	8.50
	<i>fabG1</i>	10.55
	<i>rpsL</i>	8.95
	<i>rplC</i>	7.26
3	<i>katG</i>	7.77
	<i>gidB</i>	7.99
	<i>inhA</i>	8.19
	<i>rrs</i>	8.91
	<i>rriI</i>	7.91

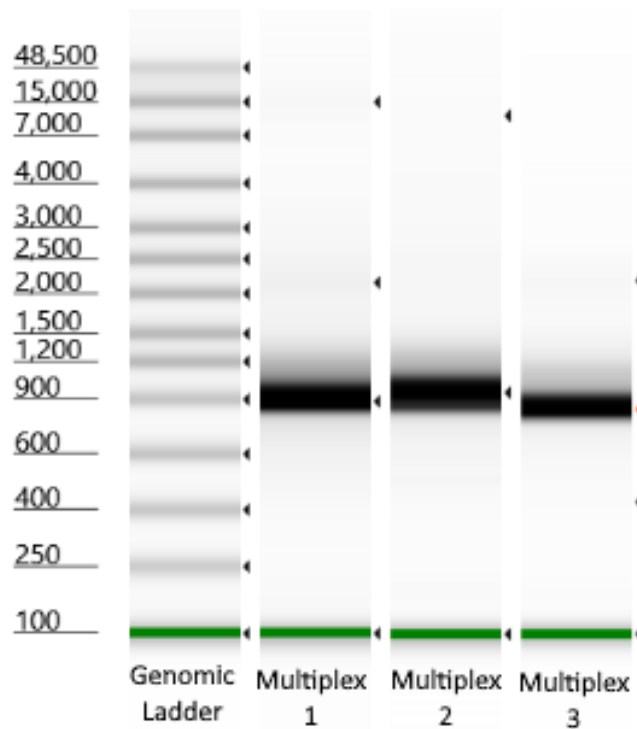


Figure 3.10: Multiplex configuration 3 TapeStation gel image showing no evidence of non-specific amplification identified as dual banding or loss of target amplicon in pooled triplicate samples for improved resolution.

A fourth multiplex configuration was then designed swapping *embB* from multiplex group 1 with *fabG1* from multiplex group 2 (Table 3.43). Redesigned primers for *rrs*, *rri*, *tlyA*, *rpsL*, and *embB* were also introduced to normalize sequencing coverage between targets.

Table 3.43: Configuration 4 of multiplex primer mixes for tNGS amplification

Multiplex Group	Gene Target 1	Gene Target 2	Gene Target 3	Gene Target 4	Gene Target 5	Gene Target 6
1	<i>eis</i>	<i>fabG1</i>	<i>ethA</i>	<i>pncA</i>	<i>tlyA</i>	<i>hsp65</i>
2	<i>gyrA</i>	<i>rpoB</i>	<i>rpsL</i>	<i>embB</i>	<i>rplC</i>	<i>rv0678</i>
3	<i>katG</i>	<i>gidB</i>	<i>inhA</i>	<i>rrs</i>	<i>rri</i>	N/A

Reconfigured multiplex groups were again tested using *M. bovis* BCG spiked NRF sputum. Nested qPCR identified inhibition of some multiplex group 1 (*eis*, *fabG1*, and *tlyA*), multiplex group 2

(*embB*), and multiplex group 3 (*rrs*) targets (Table 3.44). TapeStation analysis showed no evidence of non-specific amplification. (Figure 3.11).

Table 3.44: Mean results of nested SYBR Green qPCR experiment on amplification of multiplex configuration 4 multiplex primer group formulation using triplicate samples

Multiplex Group	Gene Target	Nested qPCR Amplification (\bar{X} C _T)
1	<i>eis</i>	17.43
	<i>fabG1</i>	11.49
	<i>ethA</i>	8.01
	<i>pncA</i>	9.65
	<i>tlyA</i>	12.39
	<i>hsp65</i>	9.22
2	<i>rv0678</i>	9.63
	<i>gyrA</i>	11.06
	<i>rpoB</i>	10.52
	<i>rpsL</i>	10.71
	<i>embB</i>	14.86
	<i>rplC</i>	10.42
3	<i>katG</i>	8.60
	<i>gidB</i>	9.50
	<i>inhA</i>	8.75
	<i>rrs</i>	13.75
	<i>rrl</i>	8.40

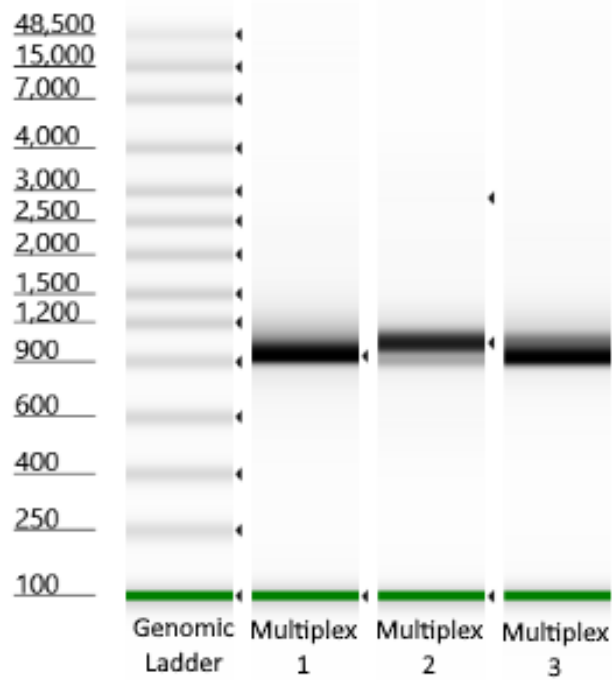


Figure 3.11: Multiplex configuration 4 TapeStation gel image showing no evidence of non-specific amplification identified as dual banding or loss of target amplicon in pooled triplicate samples for improved resolution.

Multiplex group 1 primer pairs worked well together. All but one primer pair in multiplex group 2 and multiplex group 3 amplified efficiently. Therefore, these groupings were chosen as the backbone for the next group configuration, and the poor performing primer pairs for *eis*, *fabG1*, *tlyA*, *embB*, and *rrs* were relocated (Table 3.45).

Table 3.45: Configuration 5 of multiplex primer mixes for tNGS amplification

Multiplex Group	Gene Target 1	Gene Target 2	Gene Target 3	Gene Target 4	Gene Target 5	Gene Target 6
1	<i>ethA</i>	<i>pncA</i>	<i>hsp65</i>	<i>rrs</i>	<i>embB</i>	N/A
2	<i>rv0678</i>	<i>gyrA</i>	<i>rpoB</i>	<i>rpsL</i>	<i>rplC</i>	<i>fabG1</i>
3	<i>katG</i>	<i>gidB</i>	<i>inhA</i>	<i>rriI</i>	<i>eis</i>	<i>tlyA</i>

This multiplex configuration was tested on *M. bovis* BCG spiked NRF sputum and assessed by TapeStation. Fragment size analysis identified no non-specific amplification or evidence of amplification failure. Multiplex performance was also tested using MinION sequencing. This

methodology allowed assessment of the breadth of coverage and relative amplification efficiency of each target. The samples were pooled and sequenced on the MinION as described in methods section 2.14. Reads were mapped against a reference FASTA file created by concatenating each target region (Methods section 2.16). Mapping with MiniMap2 and Qualimap (Methods section 2.16) identified a near total dropout of *embB*, low coverage of *fabG1*, *rrs* and *tlyA*, and notably high coverage of *hsp65* (Figure 3.12).

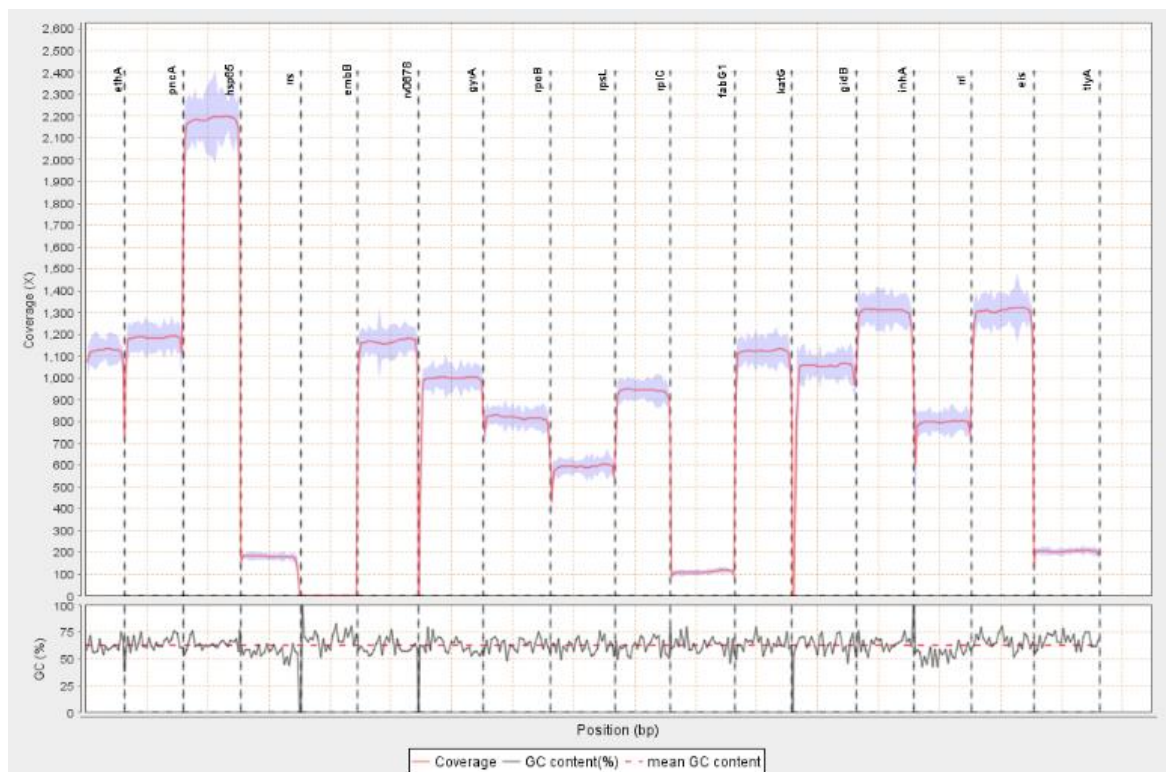


Figure 3.12: QualiMap visualization of multiplex configuration 5 sequenced reads mapped to a concatenated reference of assay gene targets using pooled triplicate samples for improved resolution.

Next, the problem *fabG1*, *rrs*, and *tlyA* target primers were grouped with *hsp65* (the best performing target) to promote even coverage in the other groups. The primer pair for *rpsL* was added to this group to create a five-plex. *embB* was moved out of multiplex group 1 into multiplex group 2 and the remainder of targets moved from multiplex group 1 were split between multiplex groups 2 and 3 (Table 3.46).

Table 3.46: Configuration 6 of multiplex primer mixes for tNGS amplification

Multiplex Group	Gene Target 1	Gene Target 2	Gene Target 3	Gene Target 4	Gene Target 5	Gene Target 6
1	<i>hsp65</i>	<i>rrs</i>	<i>rpsL</i>	<i>fabG1</i>	<i>tlyA</i>	N/A
2	<i>rv0678</i>	<i>gyrA</i>	<i>rpoB</i>	<i>ethA</i>	<i>rplC</i>	<i>embB</i>
3	<i>katG</i>	<i>gidB</i>	<i>inhA</i>	<i>rrl</i>	<i>eis</i>	<i>pncA</i>

The relative amplification efficiency of each target was assessed by nested qPCR. Results indicated inhibition of both *eis* and *embB*. The remainder of targets amplified with a mean range of 2.78 C_Ts, apart from *rpsL* which was a mean 2.29 C_Ts earlier than the next target (Table 3.47).

Table 3.47: Mean results of nested SYBR Green qPCR experiment on amplification of multiplex configuration 6 multiplex primer group formulation using triplicate samples

Multiplex Group	Gene Target	Nested qPCR Amplification (\bar{X} C _T)
1	<i>hsp65</i>	10.86
	<i>rrs</i>	11.76
	<i>rpsL</i>	6.69
	<i>fabG1</i>	9.80
	<i>tlyA</i>	10.53
2	<i>rv0678</i>	10.98
	<i>gyrA</i>	9.23
	<i>rpoB</i>	10.22
	<i>ethA</i>	9.35
	<i>rplC</i>	9.58
	<i>embB</i>	19.77
3	<i>katG</i>	10.99
	<i>gidB</i>	8.98
	<i>inhA</i>	10.02
	<i>rrl</i>	9.93
	<i>eis</i>	18.94
	<i>pncA</i>	10.85

Multiple experiments indicated *eis* and *embB* were consistently inhibited. These target primer pairs were placed into a multiplex group together for focused redesign along with *rv0678*, *rrs*, and *fabG1*. *katG* and *hsp65* primers replaced *rv0678* and *embB* in multiplex group 2. Multiplex group 3 was completed with the addition of *tlyA* and *rpsL* (Table 3.48).

Table 3.48: Configuration 7 of multiplex primer mixes for tNGS amplification

Multiplex Group	Gene Target 1	Gene Target 2	Gene Target 3	Gene Target 4	Gene Target 5	Gene Target 6
1	<i>rv0678</i>	<i>eis</i>	<i>embB</i>	<i>rrs</i>	<i>fabG1</i>	N/A
2	<i>gyrA</i>	<i>rpoB</i>	<i>ethA</i>	<i>rplC</i>	<i>katG</i>	<i>hsp65</i>
3	<i>gidB</i>	<i>inhA</i>	<i>rriI</i>	<i>pncA</i>	<i>rpsL</i>	<i>tlyA</i>

Analysis of nested qPCR data showed inhibition in *eis* and *embB* primers (7.38 and 13.93 mean C_T s later than the overall mean, respectively). The remainder of targets amplified more consistently exhibiting a total mean C_T range of 3.97 (Table 3.49).

Table 3.49: Mean results of nested SYBR Green qPCR experiment on amplification of multiplex configuration 7 multiplex primer group formulation using triplicate samples

Multiplex Group	Gene Target	Nested qPCR Amplification (\bar{X} C _T)
1	<i>rv0678</i>	8.84
	<i>eis</i>	17.73
	<i>embB</i>	24.28
	<i>rrs</i>	10.95
	<i>fabG1</i>	10.63
2	<i>gyrA</i>	10.64
	<i>rpoB</i>	10.88
	<i>ethA</i>	7.7
	<i>rplC</i>	11.08
	<i>katG</i>	10.61
	<i>hsp65</i>	11.67
3	<i>gidB</i>	10.27
	<i>inhA</i>	9.62
	<i>rrl</i>	9.92
	<i>pncA</i>	11.26
	<i>rpsL</i>	9.57
	<i>tlyA</i>	11.66

Results indicated that while there was still some variation, e.g. multiplex group 2 with the early mean *ethA* C_T (7.7), multiplex groups 2 and 3 had relatively consistent amplification efficiency. There were continued issues with inhibition and/or competition with primers for *eis* and *embB*. Two experiments were performed in an attempt to solve these issues. First was the design of configuration 7 with doubled concentrations of primers for *eis* and *embB* (Table 3.50). Second, *embB* primers were swapped with multiplex group 2 member *ethA* and *eis* was swapped with *inhA* in multiplex group 3 to see if that would resolve primer interactions (Tables 3.51 & 3.52). Neither experiment improved the amplification efficiency of *eis* or *embB*. Doubling the primer concentrations caused significantly more inhibition in all groups.

Table 3.50: Mean results of nested SYBR Green qPCR experiment on amplification of multiplex configuration 7 multiplex primer group formulation with doubled *eis* and *embB* primer concentrations using triplicate samples

Multiplex Group	Gene Target	Nested qPCR Amplification (\bar{X} C _T)
1	<i>rv0678</i>	18.46
	<i>eis</i>	25.22
	<i>embB</i>	27.29
	<i>rrs</i>	25.07
	<i>fabG1</i>	24.55
2	<i>gyrA</i>	19.84
	<i>rpoB</i>	20.89
	<i>ethA</i>	18.78
	<i>rplC</i>	22.62
	<i>katG</i>	20.51
	<i>hsp65</i>	21.23
3	<i>gidB</i>	18.77
	<i>inhA</i>	16.03
	<i>rrl</i>	16.26
	<i>pncA</i>	17.48
	<i>rpsL</i>	10.95
	<i>tlyA</i>	24.42

Table 3.51: Configuration 8 of multiplex primer mixes for tNGS amplification

Multiplex Group	Gene Target 1	Gene Target 2	Gene Target 3	Gene Target 4	Gene Target 5	Gene Target 6
1	<i>rv0678</i>	<i>rrs</i>	<i>fabG1</i>	<i>ethA</i>	<i>inhA</i>	N/A
2	<i>gyrA</i>	<i>rpoB</i>	<i>rplC</i>	<i>katG</i>	<i>hsp65</i>	<i>embB</i>
3	<i>gidB</i>	<i>rrl</i>	<i>pncA</i>	<i>rpsL</i>	<i>tlyA</i>	<i>eis</i>

Table 3.52: Mean results of nested SYBR Green qPCR experiment on amplification of multiplex configuration 8 multiplex primer group formulation using triplicate samples

Multiplex Group	Gene Target	Nested qPCR Amplification (\bar{X} C _T)
1	<i>rv0678</i>	17.55
	<i>rrs</i>	16.16
	<i>fabG1</i>	10.94
	<i>ethA</i>	26.42
	<i>inhA</i>	15.88
2	<i>gyrA</i>	16.14
	<i>rpoB</i>	18.75
	<i>rplC</i>	22.43
	<i>katG</i>	20.30
	<i>hsp65</i>	20.69
	<i>embB</i>	24.97
3	<i>gidB</i>	15.78
	<i>rrl</i>	18.26
	<i>pncA</i>	17.04
	<i>rpsL</i>	21.12
	<i>tlyA</i>	24.83
	<i>eis</i>	25.31

Inefficient amplification of certain targets was a continuing issue, so alternative solutions were tested. Firstly, the multiplexes were reverted to configuration 7. Secondly, we tested increased MgCl₂ concentration to reduce stringency and improve efficiency. Three duplicate contrived clinical samples were prepared with additional 60mM MgCl₂; the first with 1μL, the second with 2μL, and the third with 3μL.

Increasing MgCl₂ concentrations reduced amplification efficiency in *eis* and *embB* compared to the control. No significant change in amplification efficiency for *rrs*, *rv0678*, or *fabG1* was detected with increased MgCl₂ concentrations (Table 3.53).

Table 3.53: Mean results of a nested SYBR Green qPCR experiment on the relative amplification of multiplex group 1 targets using multiplex primer configuration 7 with increased MgCl₂ concentrations using two sets of triplicate samples

Sample	Replicate	<i>eis</i> Nested qPCR Amplification (\bar{X} Cr)	<i>embB</i> Nested qPCR Amplification (\bar{X} Cr)	<i>rrs</i> Nested qPCR Amplification (\bar{X} Cr)	<i>rv0678</i> Nested qPCR Amplification (\bar{X} Cr)	<i>fabG1</i> Nested qPCR Amplification (\bar{X} Cr)
1μL 50mM MgCl ₂	1	17.48	20.19	10.20	8.53	10.12
	2	18.12	20.80	10.83	8.29	10.64
2μL 50mM MgCl ₂	1	18.84	21.57	10.00	8.74	9.87
	2	17.78	21.50	10.88	8.22	10.53
3μL 50mM MgCl ₂	1	18.43	20.11	10.97	9.53	35.00
	2	19.13	20.83	10.51	9.04	10.62
Control	N/A	17.22	17.76	11.52	8.76	10.74

The most viable remaining option was to redesign the *eis* and *embB* primers. Multiple primer pairs were designed and tested for both targets – as detailed in section 3.2.2. The final primer design was selected by nested qPCR using configuration 7 groupings (Table 3.54). The inclusion of new primers resulted in efficient amplification of all multiplex group 1 targets, with the exception of *eis*. Primer design option 1 in multiplex configuration 7 was used for subsequent experimentation on specificity, sensitivity, LoD, and clinical validation. *eis* was redesigned to provide better amplification efficiency as described in section 3.2.2.

Table 3.54: Configuration 7 mean qPCR amplification results for relative amplification of multiplex group 1 targets using three redesigned *eis* primer pair options using triplicate samples

Sample	<i>eis</i> Nested qPCR Amplification (\bar{X} C _T)	<i>embB</i> Nested qPCR Amplification (\bar{X} C _T)	<i>rrs</i> Nested qPCR Amplification (\bar{X} C _T)	<i>rv0678</i> Nested qPCR Amplification (\bar{X} C _T)	<i>fabG1</i> Nested qPCR Amplification (\bar{X} C _T)
Option 1	13.61	8.03	6.00	6.00	7.39
Option 2	35.00	9.73	6.94	7.49	8.77
Option 3	16.70	9.82	6.51	6.00	8.19
H ₂ O Control	35.00	35.00	31.87	29.13	35.00

3.2.3.3: Multiplex Optimisation Summary

As presented throughout section 3.2.3, creating a sensitive multiplex configuration which yielded amplicons for all targets required multiple iterations. 5-plex PCRs were chosen as the minimum multiplex level to limit the number of total PCR reactions required per test. More PCR reactions would increase assay cost and increase risk of contamination. Early experiments to consolidate all primers into a single multiplex proved unsuccessful. These attempts consistently resulted in dropout of multiple target amplicons and would have required extensive redesign of target primers. Due to time limitations, one 5-plex and two 6-plex PCRs were designed and optimised for the assay. This use of multiple reactions is a disadvantage compared to e.g. the GenoScreen test that has a single multiplex PCR reaction. However, the sensitivity is better and the turnaround time significantly shorter than reported by GenoScreen ¹¹⁶. It should be noted that the 3 multiplexes have since been consolidated into one by colleagues in the O'Grady Group.

3.2.4: Optimization of Sample Extraction for Amplification of Drug Resistance Gene Targets in Multiplex

3.2.4.1: Comparison of Nucleic Acid Extraction Methods for Sedimented Samples

Towards the end of the study the MagNA Pure was being discontinued by Roche so it was important to choose an alternative automated extraction device. The MagNA Pure was compared to the Promega Maxwell RSC from decontaminated sedimented samples (as our diagnostic methods needed to be capable of working on both sputum and sedimented decontaminated sputum for Seq&Treat). DNA yield for each system was compared by qPCR using two gene targets, *eis*, and *tlyA* (Table 3.55). Results showed a mean loss of 1.55 C_Ts (2.9 fold) for *eis* and a mean increase of 2.37 C_Ts (5.2 fold) for *tlyA* in Maxwell over MagNA Pure. As this did not indicate a significant difference in extraction efficiency (Paired T-Test: p>0.05) performance of the two machines was deemed similar, so MagNA Pure could safely be replaced with Maxwell.

Table 3.55: Comparison of two automated extraction methods for extraction of nucleic acids from sedimented spiked NRF sputum samples using triplicate samples

Nucleic Acid Extraction Method	qPCR Amplification Nested Primer Set	SYBR Green qPCR Assay (\bar{X} C _T)
MagNA Pure Compact	<i>eis</i>	21.18
	<i>tlyA</i>	25.65
Promega Maxwell RSC	<i>eis</i>	22.73
	<i>tlyA</i>	23.28

The Promega Maxwell Extraction was superior to the MagNA Pure for extraction of sedimented samples. The cause for this difference is currently unknown. This superiority is potentially due to differences in bead concentration between machine reagent cartridges. Alternatively, the use of Roche BLB during mechanical lysis during both extraction methods may prove more compatible with the Roche MagNA Pure than the Promega Maxwell improving the DNA yield in the former. Use

of an alternative buffer during mechanical lysis may potentially improve DNA yields in the Promega Maxwell to the level seen in the MagNA Pure Compact. However, results were consistently better for MagNA Pure in raw sputum samples, and Promega Maxwell in sedimented sputum samples.

Optimisation of sedimented sample extraction (section 3.2.4.3) showed that altering the reagent in which bead-beating was performed, and adjusting the pre-extraction reagent volumes, increased Maxwell extraction efficiency.

3.2.4.2: Comparison of Maxwell Extraction Kits for Mycobacterial Extraction

To identify the most efficient Maxwell DNA extraction kit, two kits were tested; PureFood Pathogen and Cultured Cells. Two NaOH/NALC-NA decontaminated samples were bead beaten in PBS and another two were bead beaten in BLB (Bacterial Lysis Buffer, Roche) followed by extraction (one of each sample type) using the 2 Maxwell kits. Resulting elutes were quantified by SYBR Green qPCR using hsp65 primers to detect mycobacterial DNA (Table 3.56).

qPCR results showed PBS prepared samples were a mean 3.12 C_T s earlier than BLB bead-beaten samples. This difference represented a significant difference in efficiency between the two kits (Paired T-Test: $p < 0.0001$). Also, if PBS is used during mechanical lysis then the PureFood Pathogen and Cultured Cells kits perform similarly well but cultured cells kit had poorer extraction efficiency bead beating in BLB. The Maxwell PureFood Pathogen method using PBS was chosen for subsequent use.

Table 3.56: Mean qPCR quantification C_T results for comparison of two automated nucleic acid extraction kits using two different buffers during bead-beating using triplicate samples

Sample	Sample Treatment	SYBR Green qPCR Assay ($\bar{X} C_T$)	Difference between BLB and PBS ($\bar{X} \Delta C_T$)
PureFood Pathogen	BLB	23.93	0.72 (1.6 fold)
	PBS	23.21	
Cultured Cells	BLB	27.05	4.15

	PBS	22.90	(17.7 fold)
--	-----	-------	-------------

3.2.4.3: Optimization of NaOH/NALC-Na Decontamination Protocol for Use with Low Sample Volumes

FIND initially provided us with sputum (~1.5ml/sample) for tNGS assay validation but later requested that validation be performed on decontaminated sputum. The WHO recommended sputum decontamination method is designed for 2-5mL sputum. We used half of the sample volume for sputum testing so had only 750ul sputum remaining for decontamination and testing. Therefore, working volumes were reduced and adjustments were made to avoid loss of biomass when working with invisible pellets.

The first method was approached mathematically to determine the maximum sample size effective within a 1.5mL Eppendorf to accommodate the maximum tube size for the benchtop centrifuge available and biosafety requirements of screw-cap tubes in the QIB CL3 facility. The decontamination method calls for equal volumes of liquid sample and NaOH/NALC-Na solution to be added, followed by a 2x volume of phosphate buffer solution, so 250µL of sample and 250µL decontaminant solution plus 1mL of phosphate buffer solution fit in the 1.5mL tube.

Following the change to 1.5mL Eppendorfs a direct comparison was conducted between decanting and pipetting supernatant (duplicate samples tested). Results indicated no significant difference (Paired T-Test: $p > 0.05$) in nucleic acid yields between pipetting or decanting and so the more easily replicable pipetting method was selected (Table 3.57).

Table 3.57: Mean qubit quantification of paired samples for comparison of decanting and pipetting supernatant in a head-to-head trial using two sets of triplicate samples

Sample Set	Sample Treatment	Mean Qubit Concentration (ng/µL)	Mean Difference Between Decanting and Pipetting (Δ ng/µL)
Replicate 1	Decanted	0.14	0.03
	Pipetted	0.11	

Replicate 2	Decanted	0.11	0.01
	Pipetted	0.10	

Further experimentation was performed to determine the amount of target DNA (*M. bovis* BCG) lost during NaOH/NALC-Na decontamination. Nucleic acid yield from non-decontaminated controls and decontaminated samples were quantified by SYBR Green qPCR using two target genes, *inhA* and *eis* (Table 3.58). Results showed that decontamination, even under optimized conditions, resulted in a significant loss of nucleic acid of approximately 380-fold (Paired T-Test: $p < 0.0001$). However, prior to optimization the DNA loss was approximately 10,733-fold. Therefore, despite the continued loss of nucleic acid the optimized method was significantly improved over the original (Paired T-Test: $p < 0.0001$).

Table 3.58: Mean qPCR C_T results of two M. bovis BCG gene targets for comparison of nucleic acid yields in decontaminated versus non-decontaminated samples using triplicate samples.

Sample	qPCR Target	Sample Treatment	NaOH/NALC-Na qPCR Assay (\bar{X} C _T)	DNA Loss (\bar{X} Δ C _T)
A338	eis	Decontaminated	24.77	9.21 (592.2 fold)
		Not Decontaminated	15.56	
	inhA	Decontaminated	25.19	7.40 (168.9 fold)
		Not Decontaminated	17.79	

Further optimization of decontaminated sample extraction adjusted incubation time and reagent volumes used prior to Maxwell extraction. 400 μ L of mechanically lysed sample was combined with 40 μ L Proteinase K and 200 μ L Lysis Buffer A from the Promega PureFood Pathogen kit. The mixture was incubated for 10 minutes at 65°C before adding 400 μ L of PBS and 300 μ L of Promega lysis buffer. The 1,300 μ L sample was loaded into the Maxwell cartridge instead of the smaller 400 μ L sample, 300 μ L lysis buffer, and 20 μ L Proteinase K (720 μ L total) sample used previously. This optimisation facilitated an LoD of 50-100 CFU/mL, equivalent to the Cepheid GeneXpert (Xpert) MTB/RIF test ¹⁶⁴, and better than GenoScreen Deeplex Myc-TB (100-1,000 CFU/mL) ¹⁶⁵ and was used for subsequent

extraction of decontaminated samples. However, for improved LoDs and extraction a selective depletion protocol would need to be developed to reduce competition and inhibition from commensal organisms.

3.2.4.3.1: Why Optimise Sputum Decontamination?

The tNGS assay was initially validated using primary sputum samples. This would be practical in settings where the tNGS assay is used for primary diagnosis and DST, as it decreases complexity and the risk of contamination. However, most labs will continue to perform culture and smear microscopy, alongside molecular techniques, requiring initial decontamination to inactivate commensal bacteria and concentrate samples. To accommodate these workflows, the tNGS assay also required validation with existing sample preparation protocols.

Preliminary testing of the decontamination and sedimentation protocol resulted in significant loss (99%) of available sample DNA, making optimisation a priority. While the protocol as written is practical for clinical sample volumes (>5mL), small volumes (<1mL) such as those used for experimentation and optimization are more sensitive to sample loss (section 3.2.4.3). One area of concern was loss of pellet mass during transfer of the supernatant. Experimentation with supernatant removal methods (decanting and pipetting) indicated that this was unlikely to be a cause of DNA loss, as both protocols yielded similar extracted DNA concentrations under experimental conditions.

Improved sample concentrations following optimisation of working volumes and tube size indicated that this may have been the source of sample loss. Use of smaller working volumes in a 15mL falcon tube was identified as the probable issue. Scaling down the reaction and performing decontamination in a 1.5mL Eppendorf tube reduced DNA loss by approximately 10,400 fold, resulting in similar performance of the test in decontaminated sputum compared to sputum.

3.2.5: Optimisation of PCR Conditions

Experimentation was performed to optimise reagents and cycling conditions for sensitive and specific amplification of *M. tuberculosis* DNA. Simplex reactions were initially amplified using Takara PrimeSTAR Max master mix with SYBR Green dye for quantification. 18µL of working master mix and 2µL *M. bovis* BCG DNA template were amplified in a LightCycler 480 following Takara protocols (Table 3.59)

Table 3.59: Cycling conditions for Takara simplex amplification of tNGS assay primers

Step	Temperature (°C)	Time (mm:ss)	Cycles (#)
Initial Denaturation	95	05:00	1
Denaturation	98	00:10	35
Annealing	60	00:05	
Extension	72	00:10	
Final Extension	72	05:00	1

Analysis identified no amplification failures, though amplification efficiency varied by target (Figure 3.13). However, TapeStation analysis showed non-specific amplification in 8/15 simplexes (Figure 3.14).

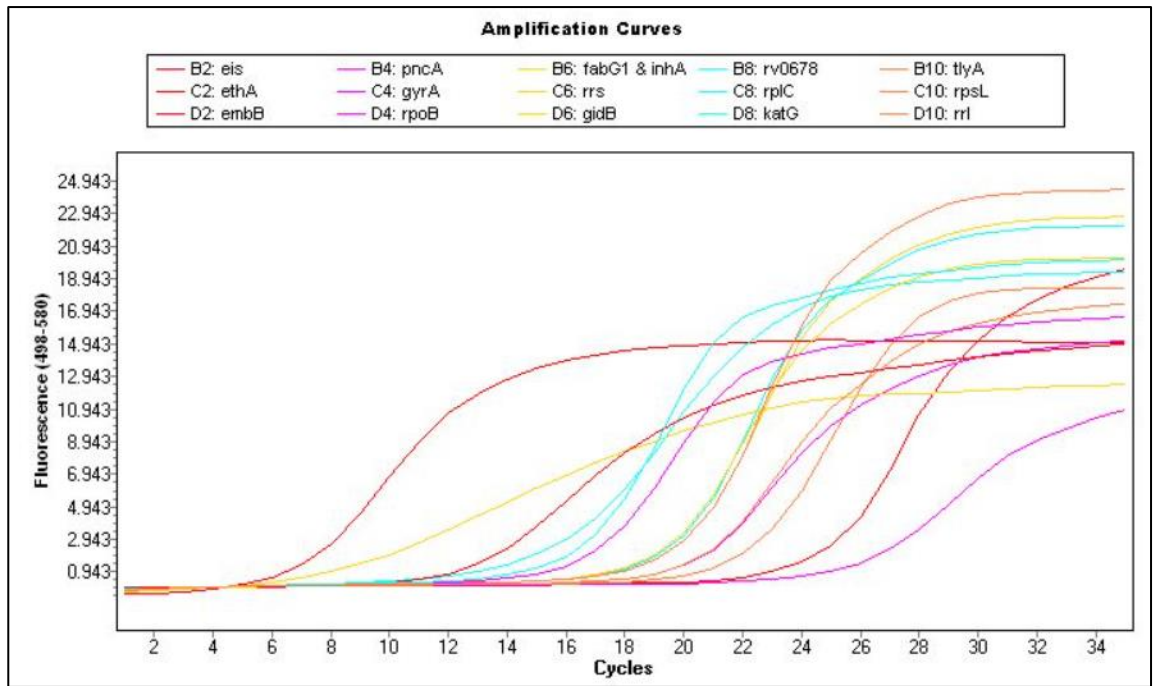


Figure 3.13: One of a triplicate set of qPCR amplification curves for simplex assay primers using Takara amplification

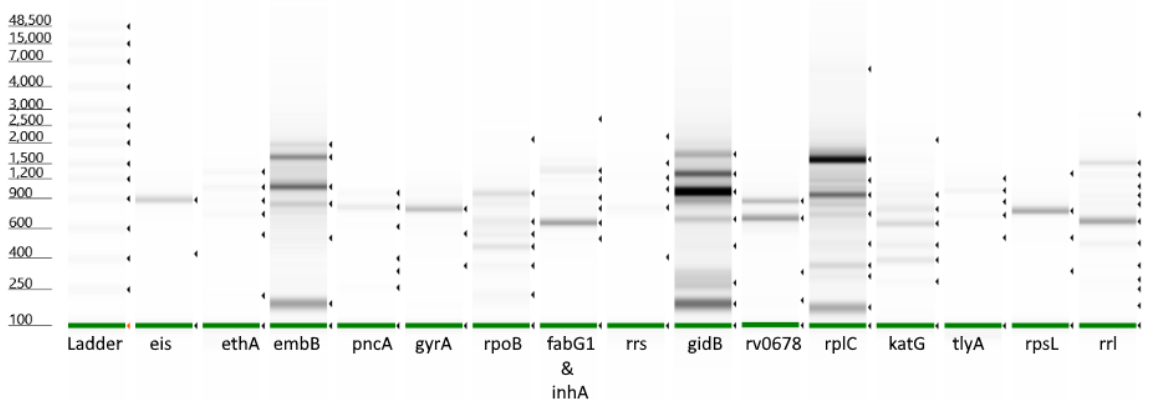


Figure 3.14: TapeStation analysis of PCR products indicating non-specific amplification in *embB*, *rpoB*, *fabG1/inhA*, *gidB*, *rv0678*, *rplC*, and *katG* reactions using pooled triplicate samples for improved resolution

To determine if the non-specific amplification was related to the mastermix; *ethA*, *embB*, *gidB*, and *rplC* were amplified using Roche SYBR Green master mix and recommended cycling conditions (Table 3.60). Analysis by TapeStation showed use of the SYBR Green master mix reduced non-specific amplification in all targets (Figure 3.15). These results demonstrated that the Takara mix was the cause of the non-specific amplification and an alternative was required.

Table 3.60: Cycling conditions for SYBR Green simplex amplification with Takara temperatures

Step	Temperature (°C)	Time (mm:ss)	Cycles (#)
Initial Denaturation	95	05:00	1
Denaturation	98	00:15	35
Annealing	60	00:15	
Extension	72	01:00	
Final Extension	72	05:00	1

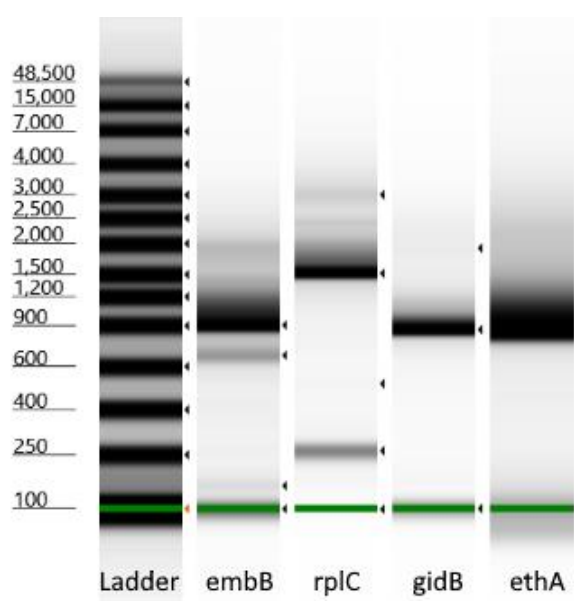


Figure 3.15: TapeStation analysis of PCR for *embB*, *rplC*, *gidB*, and *ethA* using Sybr Green mastermix using pooled triplicate samples for improved resolution

The SYBR Green master mix was used to amplify targets in triplex reactions. Cycling conditions were amended to be more suitable for the multiplex reaction (Table 3.61). Melt-curve analysis was included to identify non-specific amplification and primer dimers.

Table 3.61: NEB cycling conditions used for triplex amplification with SYBR Green master mix

Step	Time (mm:ss)	Temperature (°C)	Cycles
Initial Denaturation	05:00	98	1
Denaturation	00:30	98	35
Annealing	01:00	62	
Elongation	01:00	72	
Final Elongation	10:00	72	1
Melt	N/A	98	1

Cooling	01:00	37	1
---------	-------	----	---

Analysis showed triplex groups amplified at similar C_T s with no evident inhibition or competition within groups (Figure 3.16). Melt-curve analysis showed some evidence of non-specific amplification and primer-dimer formation within triplex reactions (Figure 3.17). TapeStation analysis was also performed (Figure 3.18), showing no non-specific amplification in triplexes 1, 3, and 5. Triplex 2 had extra bands at 250bp and 400bp while triplex 4 had smearing from 1,000bp to approximately 1,400bp.

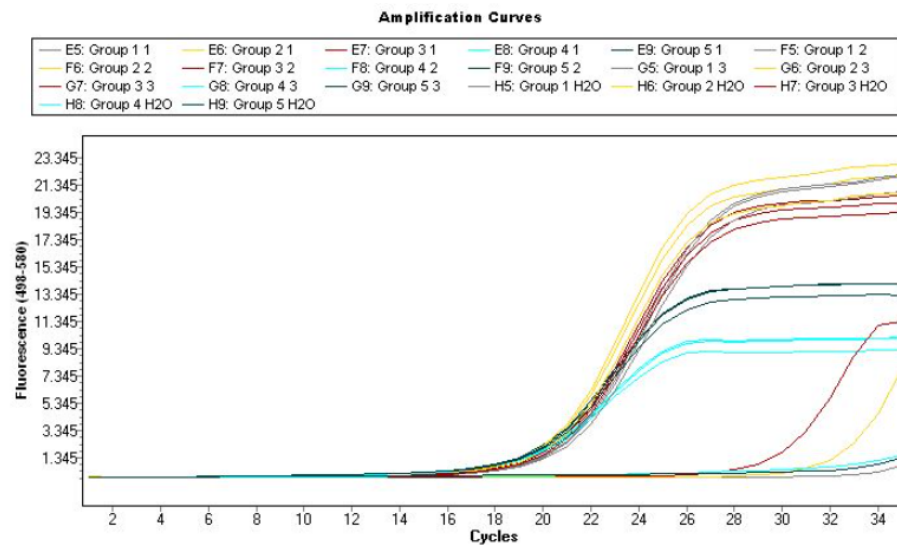


Figure 3.16: qPCR amplification curves for one of a triplicate set of triplex reactions amplified using NEB cycling conditions with SYBR Green master mix

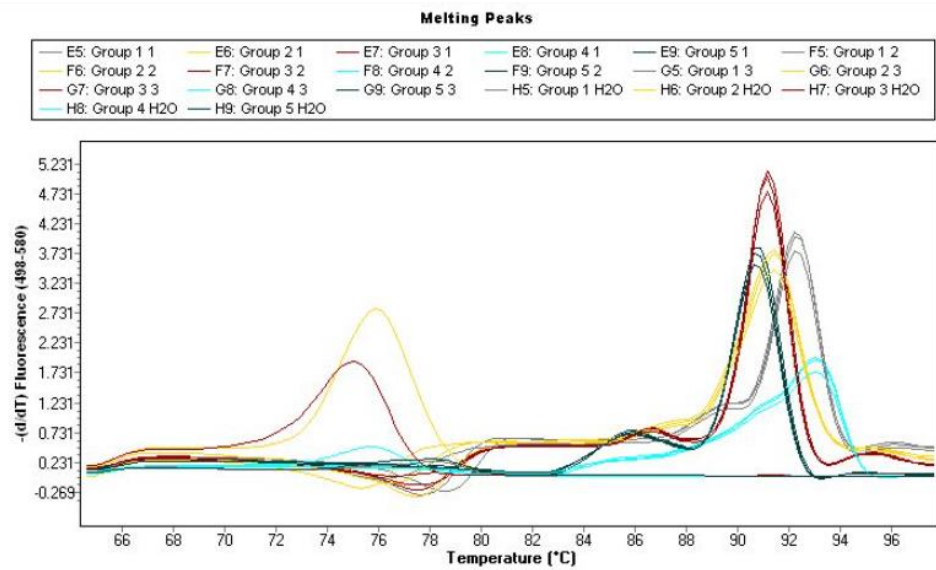


Figure 3.17: qPCR melt curves for one of a triplicate set of triplex reactions amplified using NEB cycling conditions with SYBR Green master mix

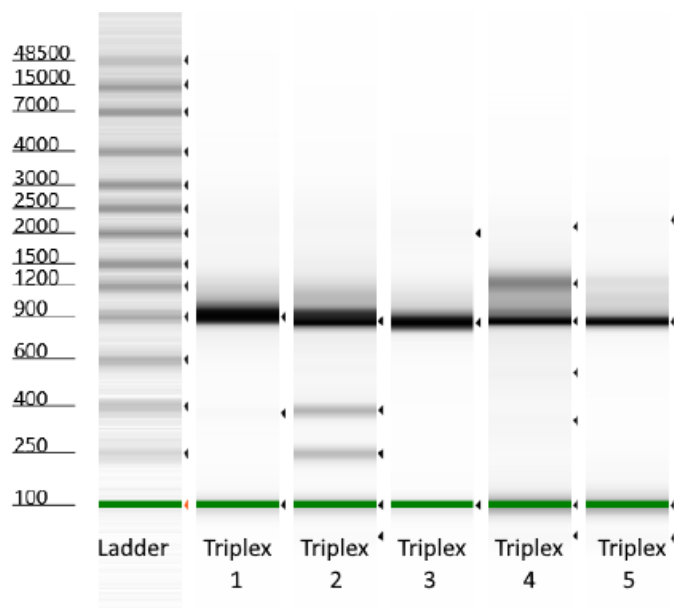


Figure 3.18: TapeStation analysis of five triplex PCRs amplified using the SYBR Green kit using pooled triplicate samples for improved resolution

Five triplex reactions would be too costly and laborious to perform, so it was decided to develop 3 multiplex assays each containing 5 targets instead. Roche probe master PCR mix was substituted for SYBR Green master mix (as the PCR products could not be sequenced with Sybr Green dye intercalated into the DNA backbone) using the same PCR conditions. qPCR incorporating *M. bovis* BCG probes showed similar amplification between each 5-plex groups (Figure 3.19). TapeStation

showed 5-plex group 1 exhibited no non-specific amplification. However, 5-plex group 2 failed to generate amplicons of the desired size and 5-plex group 3 exhibited smearing from 100bp to 1,000bp (Figure 3.20).

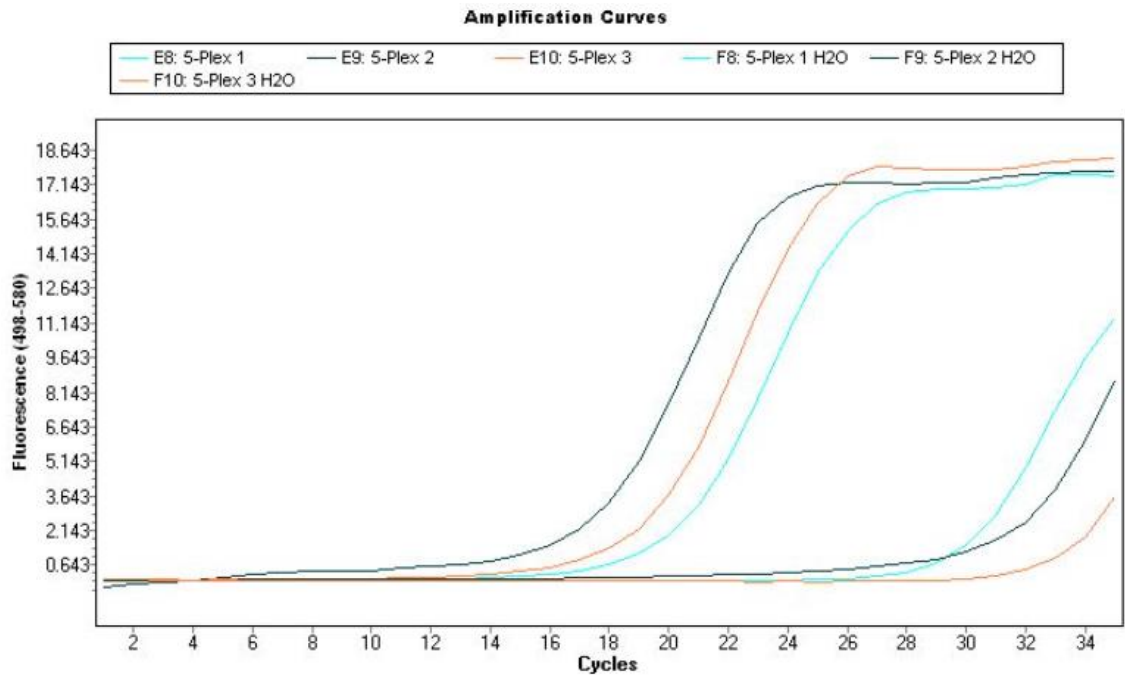


Figure 3.19: qPCR amplification curves for one of a triplicate set of 5-plex reactions

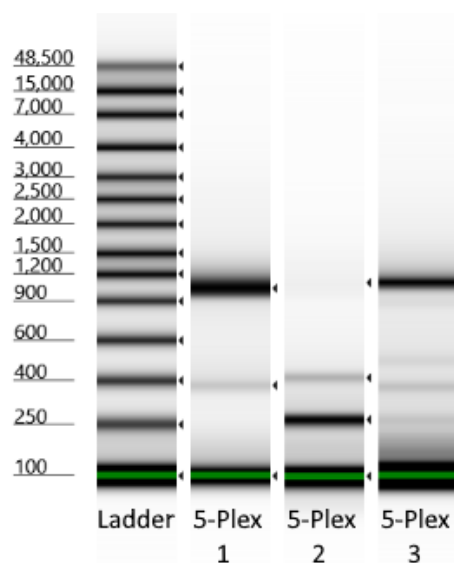


Figure 3.20: TapeStation fragment size analysis of three 5-plex reactions using pooled triplicate samples for improved resolution

Further amplification optimization was performed using master mixes designed specifically for multiplex amplification. The first was a multiplex kit from Qiagen and the second from NEB. Both methods were tested to determine the one with the best amplification yield and specificity. DNA from spiked NRF sputum was amplified according to manufacturers' protocols (Tables 3.62 & 3.63). Comparison by TapeStation indicated NEB exhibited greater variability in amplification specificity than Qiagen (Figure 3.21). Analysis also showed variability in amplicon yield for NEB (Range = 34.24 ng/ μ L) while Qiagen yields were generally higher and more consistent (Range = 6.3 ng/ μ L) with slightly less non-specific amplification and a cleaner negative control (Table 3.64).

Table 3.62: Qiagen Multiplex kit PCR cycling conditions

Step	Time (mm:ss)	Temperature (°C)	Cycles
Heat Activation	15:00	95	1
Denaturation	00:30	94	35
Annealing	01:30	60	
Extension	01:30	72	
Final Extension	10:00	72	1

Table 3.63: NEB Multiplex master mix PCR cycling conditions

Step	Time (mm:ss)	Temperature (°C)	Cycles
Initial Denaturation	01:00	95	1
Denaturation	00:20	95	35
Annealing	01:00	60	
Extension	01:30	68	
Final Extension	05:00	68	1

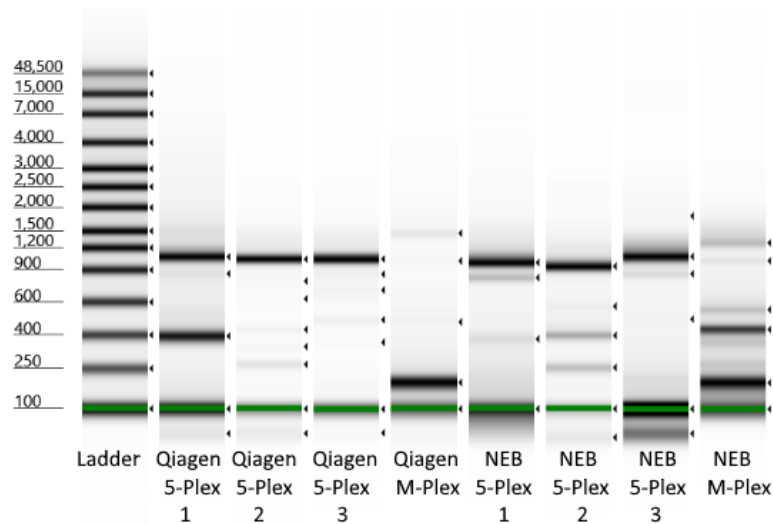


Figure 3.21: TapeStation analysis of the 3 5-plex reactions using Qiagen and NEB mastermixes (including a negative control for each mastermix) using pooled triplicate samples for improved resolution

Table 3.64: Mean post-amplification DNA concentrations for Qiagen and NEB mastermixes

Amplification Kit	Sample	DNA Concentration (\bar{X} ng/ μ L)
Qiagen	5-Plex Group 1	17.9
	5-Plex Group 2	20.0
	5-Plex Group 3	13.7
NEB	5-Plex Group 1	7.46
	5-Plex Group 2	41.7
	5-Plex Group 3	8.08

The Qiagen kit was determined to be superior in sensitivity and specificity and was selected for multiplex PCR for the remainder of the study.

3.2.5.1: Why PCR Reagent Optimisation Matters

While metagenomic tests don't specifically amplify target DNA prior to sequencing, tNGS assays are defined by it. Identification of the optimal amplification protocol for target amplicons was needed, especially for multiplex reactions. Simplex and duplex qPCR assays can use most PCR master mixes

without a loss of sensitivity or specificity. However, as reaction complexity increases, tolerances decrease, requiring more careful selection of PCR reagents to avoid target loss, amplification failure, and/or non-specific amplification.

As addressed in section 3.2.5, use of PCR master mixes designed for simplex reactions [SYBR Green and Roche Probe] resulted in loss of target amplicons and significant non-specific amplification in multiplex. Two pre-optimised multiplex master mixes were tested. The Qiagen multiplex kit tested has been used in screening for genetic disorders and forensic investigation ^{166,167}. In addition, a study from 2014 showed this multiplex kit performed optimally for detection of bacterial infections ¹⁶⁸.

The NEB multiplex master-mix tested has been used in conjunction with NGS for diagnosis and monitoring of cancers as well as assessing bacteria in environmental samples ¹⁶⁹⁻¹⁷¹. It has also been used in experiments directly diagnosing TB from clinical samples ¹⁷². The combination of manufacturer optimised reagent concentrations and use of proprietary Q-solution for improved amplification of GC-rich template resulted in the Qiagen kit outperforming the NEB master mix for multiplex amplifications in our hands.

3.2.6: Development of External Assay Controls

To ensure all steps following DNA extraction performed as expected in every tNGS run, a set of external controls were designed in collaboration with the Garvan Institute for Medical Research in Australia. Three controls were created, one for each multiplex group. Controls were designed using concatenated gene target sequences approximately 6,000bp each (Appendix III). Controls were synthesized by Invitrogen and received at a stock concentration of 5ng/μL, approximately 758×10^6 DNA copies per μL. Stocks were diluted to approximately 10,000 copies per μL using three dilution steps. The controls were used as template in 3 multiplex groups, then combined and sequenced as with test samples. Amplification and sequencing indicated control sequences performed as expected for a fully susceptible target profile when assessed using the Epi2Me TB

Resistance Profile Pipeline (Figure 3.22). External controls were subsequently incorporated into every sequencing run. All 16 gene targets in the control must be detected, without any mutations, for the sequencing run to be considered valid.

	POSITION	2155572	2155573	2155574
BASECALLED COUNTS	A	1	18	2
	C	3914		12
	G	1	3863	2
	T	6		3860
katG_I335V				
REFERENCE		G	A	T
SAMPLE		G	A	T
POSITION		2155107	2155108	2155109
BASECALLED COUNTS	A	7	3733	1
	C	1	3	18
	G	3740	11	
	T		4	3586

Figure 3.22: Screenshot of Epi2Me TB Resistance Profile Pipeline output for external controls showing expected fully susceptible profile as designed

As the multiplex amplifies multiple targets of a similar size it can be difficult to identify when a problem occurs, especially as there are a number of steps in library preparation that can lead to loss of amplicon; e.g. the bead washes. Contamination is also a concern as PCR is highly sensitive and TB amplicons will be present in the laboratory after the test starts to be used. These issues can lead to false positive and negative results, which are dangerous in a clinical setting - it is important the assay can monitor for problems that would lead to incorrect results. To monitor the test process post DNA extraction, three external controls (one per multiplex reaction) were developed for inclusion in the assay as discussed previously. These consisted of synthetic fragments of DNA containing all the targets for the relevant multiplex (approx. 6Kb long). The relevant control was added to a separate external control reaction for each multiplex and these were then processed in the exact same way as the test samples. The expected result for the external positive control after

sequencing and analysis was fully susceptible *M. tuberculosis* reads with minimum 20x coverage of all 17 targets. If there were target dropouts or any resistance SNPs detected, the run was considered invalid due to the risk of false positive or false negative results. The external controls are highly concentrated and the preparation and use of them needed to be performed with caution. Throughout testing and validation no contamination events were detected, however, for future implementation the use of internal controls (a human target or a spiked difficult to lyse bacterium that is not clinically relevant) is preferable.

Replacement of external controls with internal controls will further improve the viability of the tNGS assay in clinical settings. Removing the need for extra reagents, especially highly concentrated ones such as the controls, decreases risk of cross-contamination and false positives. The cost of controls will need to be addressed however as incorporation will likely increase the tNGS assay's cost per sample.

A no-template control, which swapped molecular grade water for template DNA, was also included for every test run to monitor for contamination. If more than three targets had >20 reads in the no-template control, the run was deemed invalid.

3.2.7: Inclusivity and Specificity Testing

After finalizing tNGS assay primer pairs and multiplex groups, specificity testing was performed. Inclusivity testing was included to assure the coverage of non *M. tuberculosis* members of the MTBC were detectable by the assay. Initial inclusivity/specificity testing used NRF sputum spiked with *M. tuberculosis* and *M. bovis* BCG DNA. Samples were extracted, multiplexed, and sequenced before uploading basecalled fastQ files to the Epi2Me WIMP pipeline for identification of reads. Any species identified above 1% of the microbial reads were recorded (Table 3.65).

Table 3.65: Total identified reads across all samples for mixed samples analyzed using the Epi2Me WIMP pipeline

Organism Identified at 1% Cutoff	Reads Reported by Epi2Me WIMP Pipeline (#)	% of Total Reads
<i>Mycobacterium tuberculosis</i>	148,365	45.9
<i>Mycobacterium bovis</i>	17,139	5.3
<i>Pseudomonas aeruginosa</i>	3,865	1.2
<i>Homo sapiens</i>	3,714	1.15

The tNGS assay amplified both *M. tuberculosis* and *M. bovis* as expected, however, there were also a small percentage of *Pseudomonas aeruginosa* reads identified. BLAST analysis of the reads revealed these to be 16S and 23S regions of the *P. aeruginosa* genome. Mapping the reads to our tNGS TB amplicon reference sequence using Qualimap (Figure 3.23) confirmed this to be the case, mapping to the *rrs* (16S) and *rrl* (23S) gene targets. Some low-level non-specific amplification of 16S and 23S regions of other bacteria wasn't unexpected and didn't affect the detection of the target species.

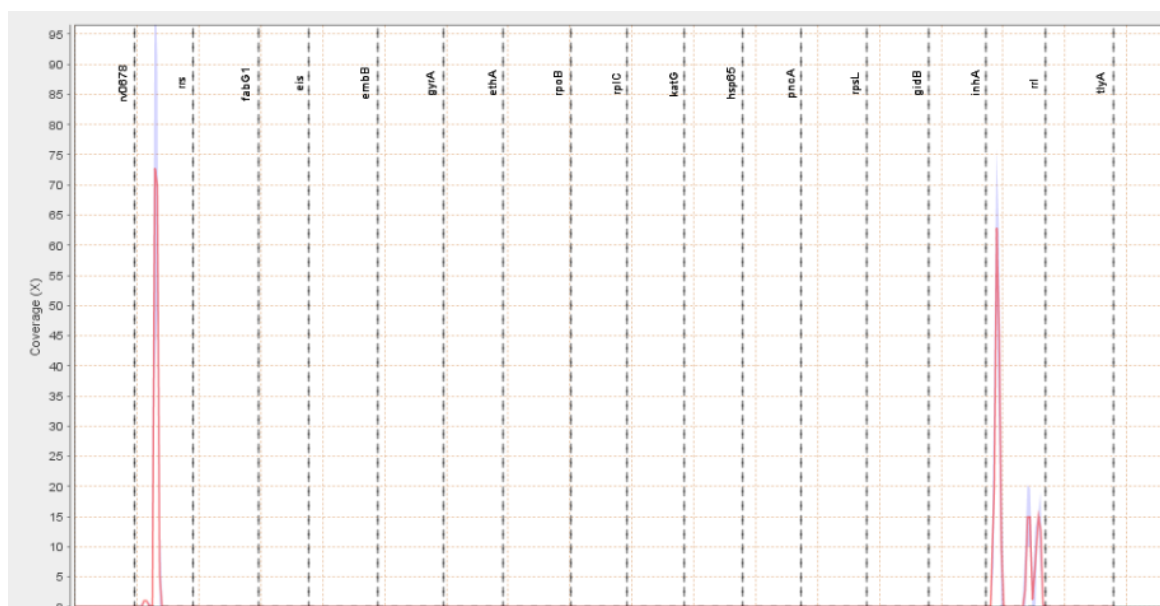


Figure 3.23: QualiMap visualization of *Pseudomonas aeruginosa* reads mapped onto the TB tNGS assay gene target reference to identify areas of cross-reactivity

A second inclusivity experiment used *Mycobacterium africanum* DNA to assess assay performance in other MTBC members. Approximately 100 cell equivalents (CE) of *M. africanum* DNA was spiked into an NRF sputum sample. Following amplification and sequencing reads were analysed by both Epi2Me WIMP and Epi2Me TB Resistance Profile pipelines.

WIMP analysis identified no non-target reads above the 1% cutoff. Due to the high homology between MTBC organisms, all *M. africanum* reads were identified as *M. tuberculosis* by the automated pipeline (Table 3.66). The TB Resistance Profile analysis did not identify any target dropouts and reads were also mapped for visualization of target coverage. This indicated that all resistance gene targets had at least 500x coverage with a relatively low input of 100 CE. Inclusion of non-*M. tuberculosis* MTBc species did not negatively impact the target coverage of the assay (Figure 3.24).

Table 3.66: Identified reads in three multiplex group samples spiked with *M. africanum* analyzed using the Epi2Me WIMP Pipeline

Sample	Organism Identified at 1% Cutoff	Reads Reported by Epi2Me WIMP Pipeline (#)	% of Sample Reads

Multiplex Group 1	<i>Mycobacterium tuberculosis</i>	4,390	44.6
Multiplex Group 2	<i>Mycobacterium tuberculosis</i>	5,506	37.9
Multiplex Group 3	<i>Mycobacterium tuberculosis</i>	5,754	41.8

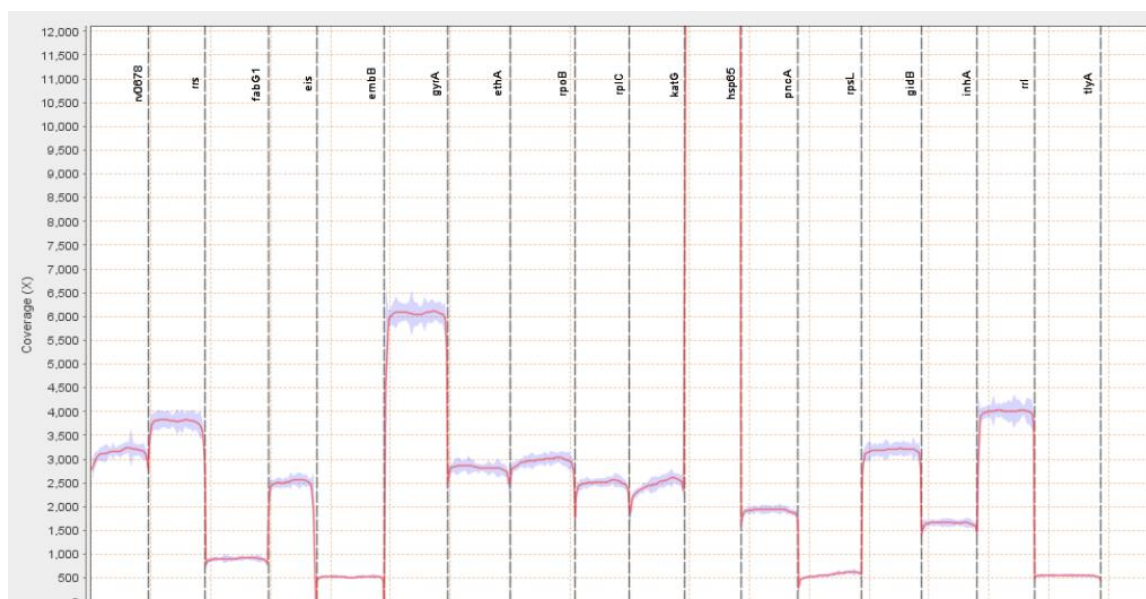


Figure 3.24: QualiMap visualization of *M. africanum* reads mapped onto the TB tNGS assay gene target reference

Further specificity experimentation was performed *in silico* using fastQ files of clinically important NTMs obtained from the NCBI database. Five NTM species as well as *M. leprae* were selected, the reads for each covered the full breadth of each genome (Table 3.67). Organism fastQ files were mapped to the tNGS assay reference using MiniMap2 and Qualimap (Figure 3.25). Locations exhibiting most non-specific reactivity were *rrs* and *rrl* gene targets which correspond with the 16S and 23S genes.

Table 3.67: A list of NTM and *M. leprae* genomes used for *in-silico* specificity testing

Organisms with Reference fastQ Files Obtained
<i>Mycobacterium avium</i>
<i>Mycobacterium kansasii</i>
<i>Mycobacterium leprae</i>

Mycobacterium marinum

Mycobacterium ulcerans

Mycobacterium abscessus

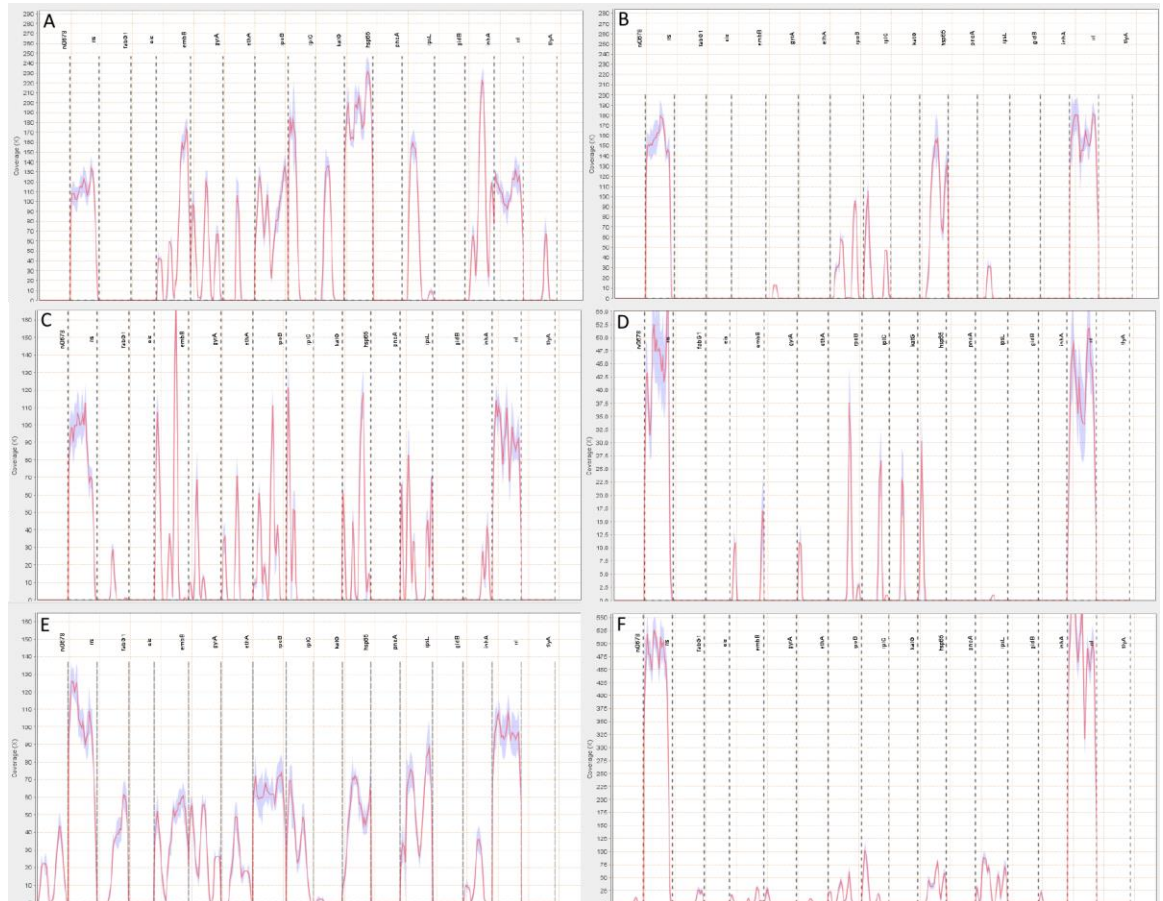


Figure 3.25: QualiMap visualization of 5 NTM genomes and *M. leprae* mapped onto the TB tNGS assay gene target reference to identify areas of potential nonspecific assay reactivity. A: *M. avium*, B: *M. abscessus*, C: *M. kansasii*, D: *M. leprae*, E: *M. ulcerans*, and F: *M. marinum*

Inclusivity of the assay in members of the MTBc was also tested *in silico*. As before, fastQ files were obtained from the NIH database for 6 MTBc members; *M. tuberculosis*, *M. africanum*, *M. bovis*, *M. bovis* BCG, *M. caprae*, and *M. pinnipedii*. fastQ files were mapped against the tNGS reference for identification of target dropouts (Figure 3.26). Analysis identified no target dropouts in the tested MTBc members. Lower coverage of *rrl* and *rrs* was detected in both *M. bovis* and *M. pinnipedii*, approximately 2- and 4- fold lower, respectively. The underlying cause for this discrepancy was unclear as all MTBc have identical 16S and 23S sequences.

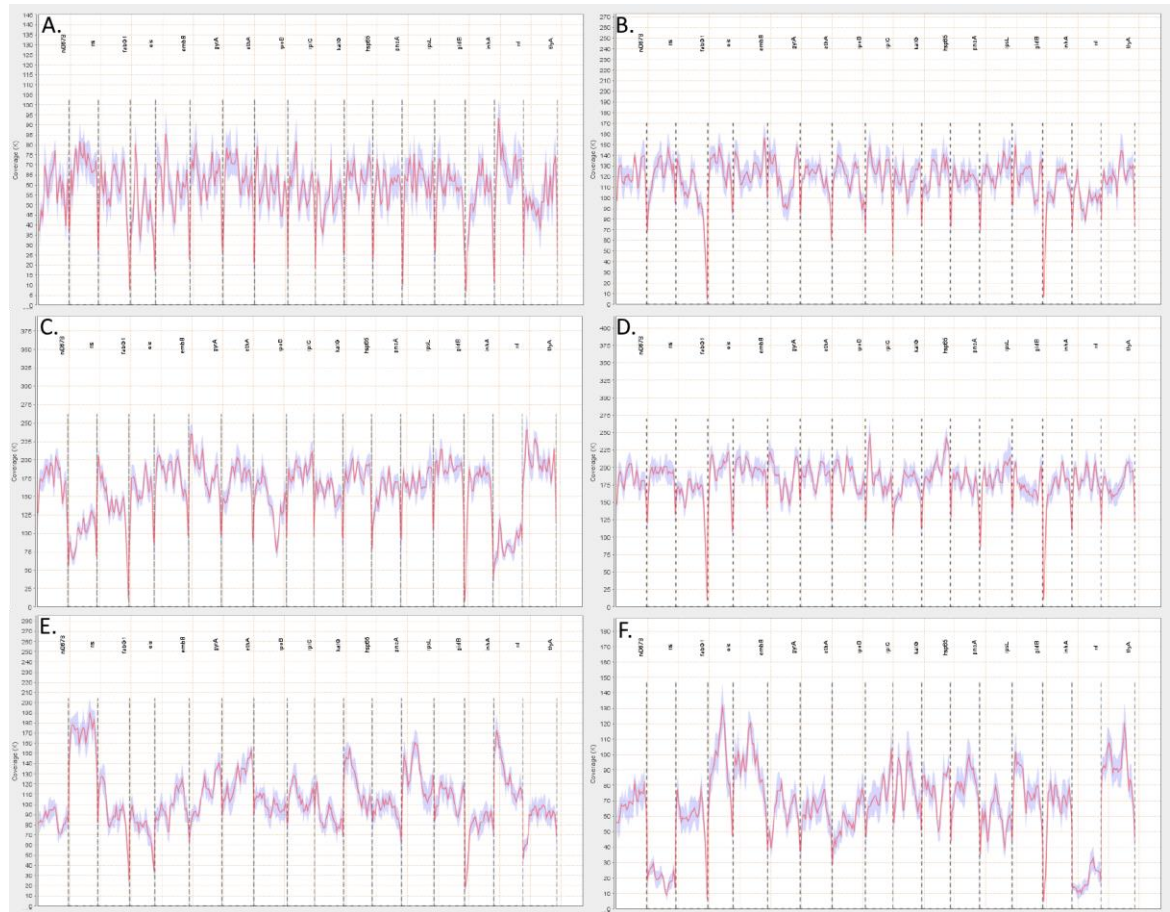


Figure 3.26: QualiMap visualization of 6 MTBC species genomes mapped onto the TB tNGS assay gene target reference. A: *M. tuberculosis*, B: *M. africanum*, C: *M. bovis*, D: *M. bovis* BCG, E: *M. caprae*, and F: *M. pinnipedii*

M. abscessus and *M. kansasii* were further used *in vitro* to test specificity of the tNGS assay in the presence of NTMs in sputum. Known concentrations of DNA (3.33×10^4 CFU) from the two NTMs were spiked into NRF sputum along with *M. tuberculosis* DNA (Table 3.68).

Table 3.68: Testing assay specificity in a sample containing equal concentrations of three mycobacteria

Sample Name	Volume of 10^4 CE/ μ L <i>M. tuberculosis</i> DNA Added (μ L)	Volume of 10^4 CE/ μ L <i>M. abscessus</i> DNA Added (μ L)	Volume of 10^4 CE/ μ L <i>M. kansasii</i> DNA Added (μ L)
Mixed NTM Test	3.33	3.33	3.33

The triplicate samples were DNA extracted, amplified, sequenced, and reads were uploaded to the Epi2Me WIMP pipeline to assess detection of target DNA in the presence NTMs. Analysis identified

MTBC as the only microbes in the samples. No reads were identified as either *M. abscessus* or *M. kansasii*, indicating the tNGS assay is specific for *M. tuberculosis* even in samples with a high proportion of NTM DNA.

3.2.7.1: Specificity and Inclusivity Summary

As covered in throughout section 3.2.7, inclusivity and specificity of the tNGS assay were assessed repeatedly during development. Preliminary *in silico* analysis indicated the tNGS assay was highly specific in 15/17 targets with only *rrs* and *rrl*, (16S and 23S genes respectively), demonstrating nonspecific amplification. This was expected, as these genes are highly conserved in the genus and designing specific primers that are also compatible in the multiplex is extremely difficult. The non-specific amplification did not, however, cover the entirety of either target region and was non-disruptive to the assay. *In silico* analysis using 5 NTM and *M. leprae* fastQ files also demonstrated non-MTBC mycobacteria were not consistently or evenly covered by assay targets, indicating pulmonary infections by non-target mycobacteria do not negatively impact assay specificity. This also indicates the assay is incapable of accurately identifying NTM infections as currently designed.

In silico analysis of MTBC sequencing reads from the NCBI database mapped against a concatenated sequence of assay targets demonstrated full target region coverage. This coverage thereby indicates that the assay would work in true clinical samples regardless of MTBC causative agent assuming effective DNA extraction.

Following *in silico* testing, analytical specificity was assessed *in vitro* using cultures of *M. bovis* BCG, *M. kansasii*, and *M. abscessus* as well as pre-extracted *M. africanum* DNA. Extraction and sequencing of *M. kansasii* and *M. abscessus* culture did show full *rrs* and *rrl* target coverage. This is due to the highly conserved 16S and 23S genes in all mycobacteria mentioned previously. However, the specific MTBC targets did not see uniform target coverage demonstrating a high level of analytical specificity.

3.2.8: Limit of Detection

Experimentation after clinical validation was conducted to determine the minimum limit of detection (LoD) of the tNGS assay. NRF sputum was spiked with *M. bovis* BCG culture to simulate clinical samples. *M. bovis* BCG was cultured under conditions detailed in section 2.1 with the addition of Tween-80 to minimize clumping of mycobacterial cells. A dilution series from 1,000 CFU/mL – 10 CFU/mL was prepared (Table 3.69).

Table 3.69: Metagenomic sequencing LoD culture dilution series and spiking with Tween grown M. bovis BCG culture

Sample	Mycobacterial Culture Concentration (CFU/mL)	Post-Spike Sample Mycobacterial Culture Concentration (CFU/mL)
Dilution 1	1,000	100
Dilution 2	500	50
Dilution 3	100	10
Dilution 4	50	5
Dilution 5	10	1

Paired samples were prepared by spiking 100µL of each dilution into 900µL of NRF sputum. Spiked samples were extracted, amplified, and quantified by Promega GloMax for a preliminary assessment of LoD for each dilution step (Table 3.70). No sample quantified lower than the negative control. There was no significant (Paired T-Test: $p > 0.05$) difference in amplification within each multiplex regardless of starting concentration, indicating uniformity at all concentrations.

Table 3.70: Mean DNA concentration quantifications for LoD determination of tNGS assay multiplex amplifications from two triplicate sets of 5 contrived clinical sample dilutions

Sample	Replicate	Multiplex Group 1 Post-Amplification Concentration (\bar{X} ng/ μ L)	Multiplex Group 2 Post-Amplification Concentration (\bar{X} ng/ μ L)	Multiplex Group 3 Post-Amplification Concentration (\bar{X} ng/ μ L)
Dilution 1	1	48.88	7.42	15.00
	2	48.30	6.61	12.18
Dilution 2	1	50.37	5.40	10.08
	2	40.49	3.89	6.66
Dilution 3	1	50.07	4.89	8.64
	2	45.40	3.25	7.17
Dilution 4	1	48.54	4.72	8.23
	2	34.36	3.35	6.20
Dilution 5	1	46.74	3.30	6.91
	2	28.73	3.70	6.29
Negative Control	N/A	4.93	1.47	4.37

Multiplex groups were pooled and sequenced using the ONT Native Barcoding 96 Expansion kit as described in methods section 2.14.3. Analysis of reads indicated that at two hours of sequencing, only the 100 CFU/mL sample surpassed 50x coverage (mean gene target coverage = 1,733x). The 50, 10, 5, and 1 CFU/mL concentration samples failed to achieve 50x coverage for any gene target after 2 hours.

The gold standard for TB diagnostic analytical sensitivity (limit of detection/LoD) remains culture which is capable of detecting of 1-10 CFU/mL under optimal conditions¹⁷³. For comparison, the LoD of the Xpert MTB/RIF assay is ~131 CFU/mL from primary sputum samples and between 10-100 CFU/mL from concentrated culture while the Xpert MTB/RIF Ultra assay has an LoD of 11.8 CFU/mL^{174,175}. Likewise, the GenoType MTBDRplus assay exhibits an analytical LoD of 160 CFU/mL¹⁷⁶.

For further comparison, the tNGS multiplex assay demonstrates an LoD of 50-100 CFU/mL from primary sputum samples. With improved nucleic acid extraction efficiency it should be possible to reduce the tNGS assay LoD from primary samples yet further.

3.2.9: Clinical Validation of the tNGS Drug Resistance Assay

A set of 392 well characterized (phenotypic and genotypic {Illumina sequenced} susceptibility data), blinded, spiked sputum samples were provided by FIND for validation of the tNGS assay. Samples were unblinded after initial assessment of the assay by FIND. Samples were divided into three categories for assessing different properties of the tNGS assay. The largest set (A samples; n=312) consisted of triplicate samples of *M. tuberculosis* variants with resistance mutations for testing the assay's ability to detect a diverse range of drug-resistance associated SNPs. The second set (B samples) consisted of five triplicate mixtures of an XDR strain with a Pan-Susceptible strain including 50:50, 80:20, 90:10, 99:1, and 99.9:0.1 ratios at two concentrations ($\sim 10^5$ and $\sim 10^7$ CFU/mL; n=30). This set was designed to determine the tNGS assay's ability to detect heteroresistance and measure what proportion of minor variants the assay can detect. Finally, five replicates of serial dilutions ($10^7 - 10^3$ CFU/mL) of a susceptible and a resistant strain spiked into sputum (C samples; n=50) were provided to test the dynamic range of the test.

The target product profile (TPP) set by FIND during validation for genotypic sensitivity and specificity was 98% for detection of drug-resistance associated SNPs against the genetic reference standard obtained by Illumina sequencing. In comparison, the TPPs for phenotypic sensitivity varied by drug, though all drugs were set at 95% phenotypic specificity. The phenotypic TPP for rifampicin sensitivity was highest at 95% while the desired sensitivity for isoniazid and fluoroquinolones was 90%. Finally, the desired amikacin, kanamycin, capreomycin, and pyrazinamide sensitivities were lowest (85%). The disparity between genotypic and phenotypic TPPs is due to variable resistance predictability by SNPs and that SNP based resistance prediction is better for some drugs than others.

For analytical sensitivity (limit of detection/LoD) the target was 1.8×10^3 CFU/mL in pan-susceptible samples and 4.7×10^3 CFU/mL in XDR samples. In mixed samples the TPP for accurate genotypic resistance calls was at the 10% XDR to 90% pan-susceptible ratio. This is due to this being the

approximate cut-off at which phenotypic resistance can become dominant in mixed samples as determined by FIND.

3.2.9.1: Sequencing and Analysis of FIND Samples

All samples were processed for sequencing as described in methods section 2.14.2. Eighty samples were sequenced per MinION run for a minimum of 6 hours (resulting in 5 total sequencing runs). Analysis was performed using the Epi2ME TB Resistance Profile pipeline for resistance calling. During detailed analysis of the data in Epi2Me, we discovered that not all resistance SNPs were being reported by the software automatically. Therefore, the Epi2Me data had to be visualized and analysed manually to ensure SNPs were not omitted.

Appendix IV consists of the complete results compiled for FIND including genotypic and phenotypic results for 392 blinded samples. To make resistance calls the proportion of wildtype bases was compared to the proportion of resistance bases at each locus. Initially, resistance calls were divided into three categories; loci with resistance bases contributing $\geq 80\%$ of reads were called resistant and were entered into a spreadsheet in red, loci with resistance bases contributing $\geq 50\%$ - $<80\%$ of reads were called as mixed infections but primarily resistant and were noted in orange, loci with resistance bases contributing $\geq 20\%$ - $<50\%$ were called as mixed infections but non-resistant and were noted in green, any loci with $<20\%$ bases resistant were called pan-susceptible. This was summarily simplified to loci with resistance bases $\geq 15\%$ being called phenotypically resistant regardless of mixed infection status (Table 3.71).

Table 3.71: Example results for phenotypic resistance prediction based on a 15% read threshold

Sample	Ethambutol	Isoniazid	Pyrazinamide	Rifampicin	Streptomycin	Amikacin	Bedaquiline	Capreomycin
A405	Resistant	Resistant	Resistant	Resistant	Resistant	Susceptible	Susceptible	Susceptible
A798	Resistant	Resistant	Resistant	Resistant	Resistant	Susceptible	Susceptible	Susceptible

Secondarily, Epi2Me WIMP analysis was performed to detect different MTBC members and check for contamination. This analysis identified only *M. tuberculosis* in each sample with no other MTBC causative agents or coinfectious agents.

Following initial analysis, all 392 samples were sequenced a second time using extractions from sedimented sputum to test assay reproducibility. Analysis identified no differences in resistance SNPs calls between replicates and the results were submitted to FIND for validation.

3.2.9.2: Genotypic Sensitivity and Specificity

One hundred and four “A” samples (pooled sputum) were spiked with *M. tuberculosis* strains with a wide selection of drug resistance mutations grown to an OD₆₀₀ of 1 by FIND and aliquoted into 3 replicates. The majority call from each replicate set was used to determine sensitivity and specificity compared to the WGS reference. As mentioned previously the TPP criteria set by FIND required a minimum 98% sensitivity and specificity for detection of targeted SNPs. FIND assessed mutations for isoniazid, pyrazinamide, rifampicin, kanamycin, amikacin, and fluoroquinolones. Sensitivity and specificity results for each SNP were recorded, of which 95% exhibited sensitivity above the 98% threshold, while 99% exhibited specificity above the 98% threshold (Table 3.72).

Table 3.72: Overall genotypic sensitivity and specificity results for XDR+PZA resistance SNPs

Testing Criteria	Sensitivity	Specificity
Percent of Mutations Above 98%	95%	99%
Mutations at or Above 98%	70	73
Mutations Below 98%	4	1
Total	74	74

Four mutations fell below the 98% sensitivity threshold, of which one showed 0% sensitivity. This mutation (*rpoB* D435A) was one of a double mutation at this codon, the other of which was D435Y. On review of Epi2Me results we found that both mutations occurred above the 15% reporting threshold in sample A361 and the loss in sensitivity was attributable to reporting error during manual analysis. Excluding this outlier, the sensitivity of the remaining three mutations (*rpoB* D435Y, *inhA* I194T, and *gyrA* D94A) ranged from 50%-80%. Related to the previous loss of sensitivity

in sample A361, a 66.7% sensitivity was calculated. This was again related to an error in reporting due to a double mutation which was remedied. The loss of sensitivity (50%) in *inhA* I194T was called wildtype in our test results for sample A229 but was a mixed infection (20%) in WGS indicating a false negative. Epi2Me results for sample A229 were reevaluated and were still identified as wildtype (10.1% reads resistant) indicating a potentially lowered LoD at this locus for mixed infections. Finally, sample A229 also exhibited 80% sensitivity for *gyrA* D94A. As before, Epi2Me results were reevaluated and found to be consistent, indicating a potential issue with intermittent dropouts for mixed infections at this locus.

One mutation fell below the 98% specificity threshold (*katG* S315T; 94.1%). In assay sequencing and analysis of sample A229 this locus was found to exhibit a proportion of resistance SNPs between 20-50%. In the WGS for comparison sample A229 this locus was categorized as wildtype. This disparity lead to reevaluation of Epi2Me results for this resistance call and resistance SNPs were found to account for 13.2% of reads. As this is below the 15% threshold the specificity loss was determined to be due to reporting error and summarily amended. The overall range in sensitivity was 67%-100% and in specificity was 75%-100% (Table 3.73).

Table 3.73: Overall genotypic sensitivity and specificity results for each tNGS assay gene target calculated from reported SNP findings

Gene Target	Sensitivity		Specificity	
	Meet Criteria/Total	% Meet Criteria	Meet Criteria/Total	% Meet Criteria
<i>rpoB</i>	22/24	92%	24/24	100%
<i>fabG1</i>	4/4	100%	4/4	100%
<i>inhA</i>	2/3	67%	3/3	100%
<i>katG</i>	4/4	100%	3/4	75%
<i>gyrA</i>	9/10	90%	10/10	100%
<i>eis</i>	1/1	100%	1/1	100%
<i>rrs</i>	5/5	100%	5/5	100%
<i>pncA</i>	25/25	100%	25/25	100%
<i>embB</i>	11/11	100%	11/11	100%
<i>ethA</i>	2/2	100%	2/2	100%
<i>rpsL</i>	2/2	100%	2/2	100%

Genotypic specificity and sensitivity were determined by FIND using comparison to Illumina sequences. Clinical validation quantified a genotypic specificity of 94-100% across all targets with an overall assay specificity of 99%. This demonstrated parity with existing Xpert MTB/RIF (99%), GenoType MTBDRplus (100%), and GenoType MTBDRsl (98.6%) assays ¹⁷⁷⁻¹⁸². Analysis further indicates improved accuracy of resistance calls in second-line anti-tuberculous drugs compared to technologies currently on the market.

Clinical validation of the tNGS assay quantified a total genotypic sensitivity of 95%. However, detailed analysis of validation results identified disparities in sensitivity among assay targets. Discussion with FIND researchers and manual analysis of results identified loss of genotypic sensitivity in individual targets was primarily attributable to issues in the Epi2Me analysis pipeline which omitted several pyrazinamide and kanamycin SNPs. Omitted SNPs have since been added to a newly developed analysis pipeline by collaborators at ONT. This new pipeline utilises the official curated list of resistance conferring SNPs from the WHO, standardising the SNPs detected ¹⁵⁶.

3.2.9.3: Phenotypic Sensitivity and Specificity

Phenotypic sensitivity and specificity calling were performed using the same 104 triplicate samples as for the genotypic testing. Phenotypic DST was performed on all 104 *M. tuberculosis* strains by FIND using MGIT DST culture. Each drug had different optimal and minimum TPPs for phenotypic sensitivity and specificity assigned by FIND (Table 3.74). Kanamycin and pyrazinamide phenotypic resistance detection fell below the minimum sensitivity threshold. However, no phenotypic call fell beneath the required specificity threshold (Table 3.75). Thus, 4/6 tested drugs surpassed requirements for phenotypic resistance calling while 2/6 fell below the required sensitivity threshold.

Table 3.74: Optimum and minimum acceptable sensitivity and specificity TPPs for phenotypic resistance calling as determined by FIND for the analysis of the tNGS assay

Anti-TB Drug	Sensitivity		Specificity	
	Optimal Sensitivity (%)	Minimum Sensitivity (%)	Optimal Specificity (%)	Minimum Specificity (%)
Rifampicin	99	95	98	95
Isoniazid	90	90	98	95
Fluoroquinolones	90	90	98	95
Amikacin	90	85	98	95
Kanamycin	90	85	98	95
Capreomycin	90	85	98	95
Pyrazinamide	90	85	98	95

Table 3.75: Overall calculated phenotypic sensitivity and specificity of tNGS assay resistance calls as compared to a phenotypic DST reference

Drug	Sensitivity		Specificity	
	Calculated Sensitivity (%)	95% Confidence Interval (%)	Calculated Specificity (%)	95% Confidence Interval (%)
Rifampicin	97	91.5 – 99.0	100	20.7 - 100
Isoniazid	96	90.3 – 98.5	100	34.2 - 100
Fluoroquinolones	91	80.7 – 96.1	96	86.0 – 98.8
Amikacin	97	84.7 – 99.5	97	89.8 – 99.2
Kanamycin	66	52.7 – 76.4	100	92.3 - 100
Pyrazinamide	63	51.4 – 73.7	97	83.8 – 99.4

In kanamycin, poor sensitivity was related to failure of the Epi2Me TB Resistance Profile pipeline to detect a resistance SNP 10bp before the start of the *eis* gene in the promoter region. The loss of sensitivity in pyrazinamide was attributed to the Epi2Me pipeline not analysing 7 high-confidence mutations in *pncA*. A new resistance calling pipeline has now been developed which raises the phenotypic sensitivity above the required 90% threshold for both drugs.

Comparison to line-probe assay (LPA) DST performed by FIND demonstrated the tNGS assay is superior for making phenotypic resistance calls. According to this FIND analysis LPAs fell below the FIND specificity TPP for fluoroquinolones, amikacin, and kanamycin, and omitted pyrazinamide. In contrast, the tNGS assay met the FIND specificity TPP for all drugs; however, it fell below the sensitivity TPP for kanamycin and pyrazinamide (Table 3.76). As mentioned previously the development of a new analytical pipeline has since raised the sensitivity in phenotypic resistance calls for both of these drugs above the required threshold (90%).

Table 3.76: Comparison of tNGS DST assay to LPA DST as performed by FIND

Drug	tNGS DST Assay			LPA DST		
	# of Samples	Sensitivity	Specificity	# of Samples	Sensitivity	Specificity
Rifampicin	101	0.97	1.00	101	0.97	1.00
Isoniazid	104	0.96	1.00	103	0.97	1.00
Fluoroquinolones	104	0.91	0.96	104	0.96	0.91
Amikacin	100	0.97	0.97	100	0.97	0.90
Kanamycin	104	0.66	1.00	104	0.93	0.90
Pyrazinamide	99	0.63	0.97	---	---	---

Phenotypic specificity was assessed by comparison to culture. In comparison to the genotypic specificity, the tNGS assay showed a range of 96%-100% phenotypic specificity across all targets. This corroborates well with the genotypic specificity determined previously. Further, comparison of the tNGS assay to existing molecular diagnostic methods also demonstrated specificity superior to existing line probe assays for fluoroquinolones, amikacin, and kanamycin ^{103,183,184}.

In comparison, the tNGS assay exhibited discrepancies between genotypic and phenotypic sensitivity, primarily when analysing mixed samples (section 3.2.9.5). One source of this discrepancy was the phenotypic resistance calling threshold initially selected, where only mutation SNPs greater

than 50% of total site reads were categorized as phenotypically resistant. Reduction of the threshold from 50% to 15% improved assay phenotypic sensitivity in mixed samples for all tested samples. This alteration improved the assay's phenotypic sensitivity to meet the FIND Seq&Treat TPP for each resistance.

Phenotypic sensitivity for rifampicin was of particular interest for comparison to the WHO endorsed Xpert MTB/RIF and Xpert MTB/RIF Ultra assays. A 2020 systematic review of the MTB/RIF Ultra test found a phenotypic sensitivity of 91.15% for rifampicin drug resistance ¹⁸⁵. For comparison, phenotypic sensitivity for rifampicin resistance was 79.2% for the GenoType MTBDRplus LPA ^{180,183}. However, the tNGS assay demonstrated a superior phenotypic sensitivity of 97% for rifampicin resistance compared to culture.

An issue with accurate phenotypic resistance calling in mixed samples was shown due to a non-resistance conferring mutation in the *katG* forward primer binding site. This mutation, which occurred only in one of the strains in the mixed sample, lowered the amplification efficiency of that strain effectively rendering the assay only able to detect one of the two strains present. Redesign of the forward primer to avoid this mutation locus (section 3.2.11) resolved this issue allowing accurate detection of mixed infections with *katG* involvement.

3.2.9.4: Indeterminate Rates and Reproducibility

The reproducibility of the tNGS assay was assessed using panels A and B (mixture panel; n=30). Individual mutations within targets demonstrated a disagreement rate of 0.16% (2 disagreement calls / 1,248 replicate calls). The first of these was in A139 with a mutation detected at *embB* M206I while the other two replicates had a mutation at *embB* M306I. This disagreement was due to reporting error during manual analysis and was corrected. The second disagreement occurred in A379 with the report of two double mutations at codon 445 while the other two replicates detected a single mutation at this codon. This double mutation was only 15% of reads which suggests that it

may be a false positive due to sequencing noise. Despite these two disagreement calls results indicated a very high level of assay reproducibility.

Analysis of samples and replicates demonstrated a 0% indeterminate rate across panels A and B, well below the FIND TPP of <5%. The overall target indeterminate rate was also assessed finding a 0% target indeterminate rate in panel B but a 1% (36/3,744) target indeterminate rate in panel A. By distinguishing between target failure and gene deletions in the targets the target indeterminate rate was reduced to 0.3% (12/3,744). Of the remaining 12 indeterminate targets, 3 came from sample A262 which was identified as a multiplex group 1 failure. The final 9 indeterminates occurred in targets *gidB* and *pncA*.

3.2.9.5: Mixed Clinical Samples to Measure Heteroresistance Detection

Mixed infection samples were created using a pan-susceptible and an XDR strain of *M. tuberculosis*, both grown to OD₆₀₀=1 and mixed in several different proportions; 50%, 20%, 10%, 1%, and 0.1% XDR:Pan-Susceptible. A 1/100 dilution of each stock was also prepared. Pooled sputum samples were then spiked in triplicate with neat and 1/100 dilutions of the 5 mixed samples resulting in 30 samples total. The minimum criteria according to TPP was accurate resistance calls in mixed samples with ≤10% XDR.

Initial resistance calls for mixed samples were accurate for *rpoB* (rifampicin), *fabG1* (isoniazid), *gyrA* (fluoroquinolones), and *rrs* (amikacin). However, initial resistance calls were unable to accurately call *katG* (isoniazid) and *pncA* (pyrazinamide) resistance (Figure 3.27). Multiple optimization methods were tested to improve sensitivity in *katG* and *pncA*. Firstly, adjustment of the call threshold from 20% to 15% of reads helped improve sensitivity in mixed samples. Additionally, optimization of the *katG* forward primer to mitigate the impact of a non-resistance conferring SNP improved sensitivity to *katG* mutations in mixed samples (Section 3.2.11). The loss of sensitivity in *pncA* was determined to be due to reporting error where *pncA* codon 171 results were mistakenly reported for *pncA* codon 71. Repeating analysis and reporting using reads from the correct codon

demonstrated accurate detection of mixed infection to the 10% threshold. Repeat analysis of results with the amended threshold showed the assay met requirements for calling phenotypic resistance in mixed (Figure 3.28).

ONT	rpoB 450L	katG 315T	fabG1 15T	gyrA 94G	rrs 1484	pncA 71R
B-0.1%	0/3	0/3	0/3	0/3	0/3	0/3
B-0.1DIL	0/3	0/3	0/3	0/3	0/3	0/3
B-1%	0/3	0/3	0/3	0/3	0/3	0/3
B-1DIL	0/3	0/3	0/3	0/3	0/3	0/3
B-10%	1/3	0/3	3/3	3/3	3/3	0/3
B-10DIL	3/3	0/3	3/3	3/3	3/3	0/3
B-20%	3/3	0/3	3/3	3/3	3/3	0/3
B-20DIL	3/3	0/3	3/3	3/3	3/3	0/3
B-50%	3/3	0/3	3/3	3/3	3/3	3/3
B-50DIL	3/3	0/3	3/3	3/3	3/3	3/3
pure XDR	3/3	3/3	3/3	3/3	3/3	3/3
pure SUS	3/3	3/3	3/3	3/3	3/3	3/3

Figure 3.27: Initial FIND analysis of mixed infection detection. Green indicates both genotypic and phenotypic resistance calls were correct. Blue indicates genotypic calls were correct but phenotypic calls were incorrect. Red indicates neither genotypic nor phenotypic calls were correct.

ONT	rpoB 450L	katG 315T	fabG1 -15T	gyrA 94G	rrs 1484	pncA 71R
B-0.1%	0/3	0/3	0/3	0/3	0/3	0/3
B-0.1DIL	0/3	0/3	0/3	0/3	0/3	0/3
B-1%	0/3	0/3	0/3	0/3	0/3	0/3
B-1DIL	0/3	0/3	0/3	0/3	0/3	0/3
B-10%	3/3	3/3	3/3	3/3	3/3	3/3
B-10DIL	3/3	3/3	3/3	3/3	3/3	3/3
B-20%	3/3	3/3	3/3	3/3	3/3	3/3
B-20DIL	3/3	3/3	3/3	3/3	3/3	3/3
B-50%	3/3	3/3	3/3	3/3	3/3	3/3
B-50DIL	3/3	3/3	3/3	3/3	3/3	3/3
pure XDR	3/3	3/3	3/3	3/3	3/3	3/3
pure SUS	3/3	3/3	3/3	3/3	3/3	3/3

Figure 3.28: Analysis of mixed infection detection following adjustment of the phenotypic resistance threshold and correction of errors in katG and pncA calling. Green indicates both genotypic and phenotypic resistance calls were correct. Red indicates neither genotypic nor phenotypic calls were correct.

3.2.9.6: Dynamic Range

Dynamic range of the tNGS assay was determined using five serial dilutions of two *M. tuberculosis* strains; one XDR and one pan-susceptible. Dilutions ranged from 1.8×10^7 CFU/mL to 1.8×10^3 CFU/mL for the pan-susceptible strain and from 4.7×10^7 – 4.7×10^3 CFU/mL for the XDR strain. Diluted strains were spiked into sputum by FIND and five replicates were prepared for each dilution (n=50 samples total).

Analysis through the Epi2Me TB Resistance Profile pipeline showed no target dropouts at any dilution level. Assessment was repeated using decontaminated/sedimented samples for comparison with raw sputum results. Comparison identified no loss of detection at any dilution level when using sedimented sputum samples. Results indicated the clinical LoD of the tNGS assay is below 1.8×10^3 CFU/mL. It should be noted that only 700 μ L sputum was used for extraction and only 1/10 of the extracted DNA was used for the PCR. Therefore, the analytical LoD of the PCR is <120 CE.

Dynamic range was also compared to three current molecular technologies by FIND; Genotype MTBDRPlus, GenoType MTBDRsl, and GeneXpert MTB/RIF. Analysis indicated that the dynamic range for the tNGS assay is equivalent to all three existing tests in the range tested (Table 3.77). Likewise, the dynamic range for DR-TB strain dilutions was equivalent to all three existing tests in the range tested (Table 3.78). However, despite 100% dynamic range sensitivity results the 1.8×10^4 CFU/mL concentration produced a small number of incorrect resistance calls. The reason for this is currently under investigation by collaborators at ONT.

Table 3.77: Results for comparison of dynamic detection range performed by FIND in pan-susceptible samples. Green indicates 100% detection by the test at the selected concentration.

	Concentration of Pan-Susceptible Strain (CFU/mL)				
	1.8×10^3	1.8×10^4	1.8×10^5	1.8×10^6	1.8×10^7
tNGS Assay	5/5	5/5	5/5	5/5	5/5
MTBDR Plus	1/1	1/1	1/1	1/1	1/1
MTBDR sl	1/1	1/1	1/1	1/1	1/1
GeneXpert MTB/RIF	1/1	1/1	1/1	1/1	1/1

Table 3.78: Results for comparison of dynamic detection range performed by FIND in XDR samples. Green indicates 100% detection by the test at the selected concentration.

	Concentration of XDR Strain (CFU/mL)				
	4.7×10^3	4.7×10^4	4.7×10^5	4.7×10^6	4.7×10^7
tNGS Assay	5/5	5/5	5/5	5/5	5/5
MTBDR Plus	1/1	1/1	1/1	1/1	1/1
MTBDR sl	1/1	1/1	1/1	1/1	1/1
GeneXpert MTB/RIF	1/1	1/1	1/1	1/1	1/1

The assay was shown to be capable of detecting all sample concentrations provided (minimum 1.8×10^3 CFU/mL for pan-susceptible strains and 4.7×10^3 CFU/mL for XDR strains) – the LoD of the assay is therefore $<10^3$ CFU/ml.

3.2.10: Assay Performance Summary

In assay phenotypic sensitivity for rifampicin (97%) the tNGS multiplex assay matched or outperformed all existing diagnostic assays to which it was compared, with the nearest being the Xpert MTB/RIF (97.6 %), Xpert MTB/RIF Ultra (92.7%) and GenoType MTBDRplus tests (96.2%)

^{184,186,187}. Likewise, overall phenotypic specificity (99%) was equivalent to existing assays, with the nearest being smear microscopy (99.8%) and the Xpert MTB/RIF assay (99%) ^{177,188}. Phenotypic specificity for rifampicin resistance (100%) was superior to Xpert MTB/RIF and Xpert MTB/RIF Ultra (99% and 98% respectively) ^{186,187}. Culture based diagnosis and DST were excluded from comparison of sensitivity and specificity as they are the baseline by which all other assays are validated.

In direct comparison, the tNGS assay LoD was superior to Xpert MTB/RIF for primary sputum samples and second only to culture ^{173,174}. These findings indicate the tNGS multiplex assay is highly competitive for paucibacillary samples.

3.2.11: Post-Validation Optimisation

During clinical validation, *katG* primers required redesign to include a high confidence SNP at codon 315. To improve integration of redesigned *katG* primers with group 2 removal of *hsp65* was necessary. This was deemed an acceptable change during validation as the *hsp65* target was only present to help speciate NTM if present and other targets could theoretically be used for the same purpose if necessary. The final multiplex configuration (config 9) is presented in Table 3.79 along with nested qPCR results (Figure 3.29) and QualiMap visualization (Figure 3.30).

Table 3.79: Configuration 9 of multiplex primer mixes for tNGS amplification following

Multiplex Group	Gene Target 1	Gene Target 2	Gene Target 3	Gene Target 4	Gene Target 5	Gene Target 6
1	<i>rv0678</i>	<i>eis</i>	<i>embB</i>	<i>rrs</i>	<i>fabG1</i>	N/A
2	<i>gyrA</i>	<i>rpoB</i>	<i>ethA</i>	<i>rplC</i>	<i>katG</i>	N/A
3	<i>gidB</i>	<i>inhA</i>	<i>rrl</i>	<i>pncA</i>	<i>rpsL</i>	<i>tlyA</i>

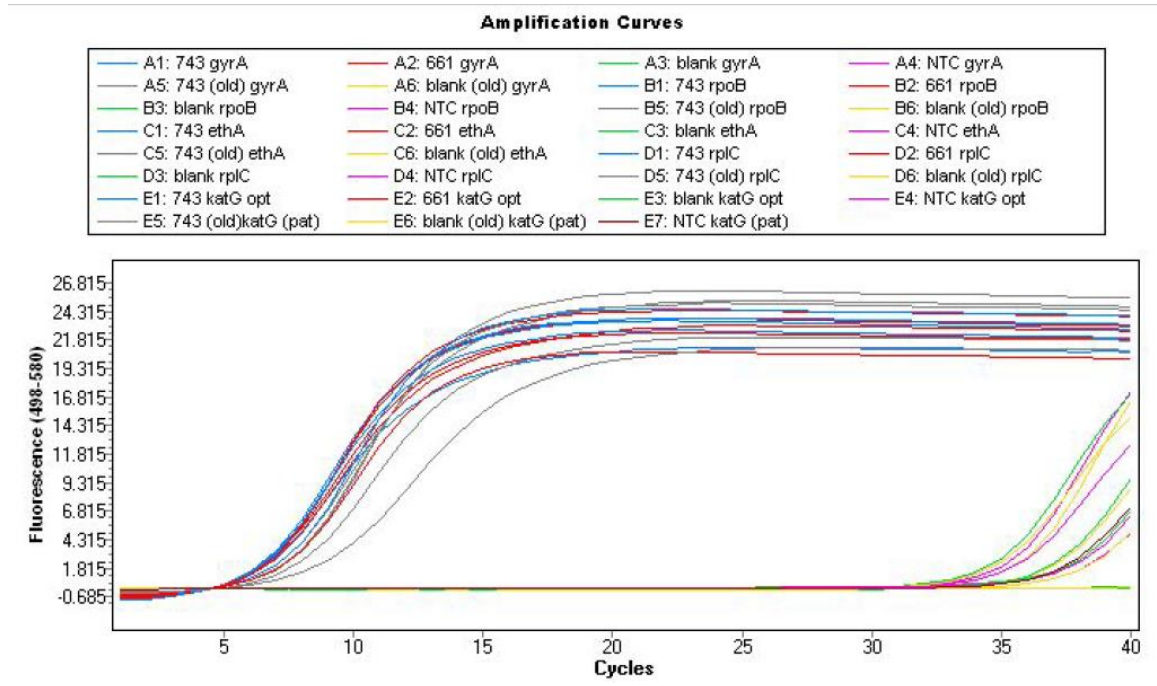


Figure 3.29: One of a triplicate set of nested qPCR C_T s for configuration 9 multiplex group 2 gene targets with original and reformulated *katG* primer pairs. Used for visualization of amplification efficiency with the removal of *hsp65*

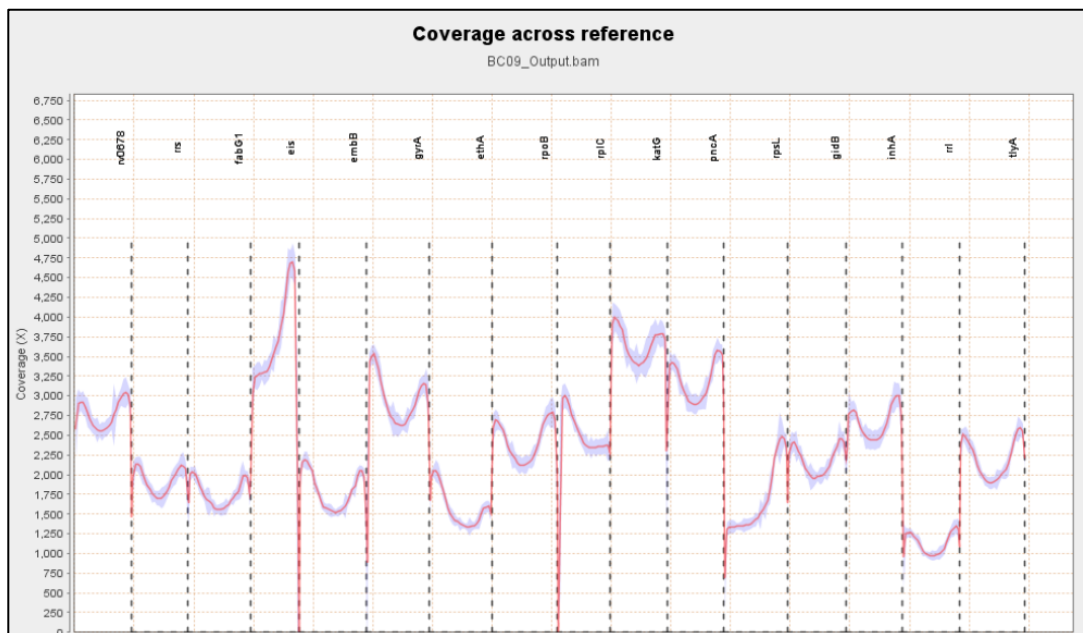


Figure 3.30: QualiMap visualization sequencing of a mixed infection sample showing equivalent coverage of all targets when using multiplex configuration 9 using one of a set of triplicate samples

Clinical validation experimentation identified a common, but non-resistance conferring, *katG* mutation in the forward primer site. This SNP promoted preferential amplification resulting in a loss of sensitivity in mixed infections. The mutation was located 5bp from the 5' end of the primer

requiring alternative forward primers to avoid its inclusion. A set of 5 primers were designed which shifted the primer location by 1bp each. All primer lengths were adjusted as needed to maintain melting temperature (Table 3.80). Alternative primers were tested on 50/50 mixed samples and analysed by sequencing. Analysis identified that primers which placed the SNP in the final 5' position, or excluded it entirely, were most sensitive to mixed infection (Table 3.81). As both primers performed similarly, the one completely avoiding the mutation site was selected for subsequent use (Table 3.82).

Table 3.80: Redesigned primers to mitigate and avoid the non-resistance conferring mutation site. The site of the SNP is bolded in red.

Base Pair Positions Shifted Toward 3' End	Primer
Original Primer	TGCC CG GATCTGGCTCTTA
1	GCC CG GATCTGGCTCTTAA
2	CC CG GATCTGGCTCTTAAGG
3	CG GATCTGGCTCTTAAGGC
4	CG GATCTGGCTCTTAAGGCTG
5	GGATCTGGCTCTTAAGGCTGG

Table 3.81: Detection of heteroresistant reads using a forward primer shifted to mitigate the non-resistance conferring SNP site in 50/50 mixed samples.

Base Pair Positions Shifted Toward 3' End	Mixed Resistance Reads Detected (Mutant/Wild-Type)
Original Primer	102/1029
1	197/1029
2	451/381
3	906/414
4	1210/581
5	1365/608

Table 3.82: Redesign history for katG primers

katG Redesign Version	Forward Primer (5'-3')	Reverse Primer (5'-3')	Amplicon Length (bp)
Original	TCCTCGAGATCCTGTACGGC	TGATACCCATGTGAGCAGG	1005
Redesign 1	ATCGCGTCCTTACCGTTC	GCAACACCCACCCATTACAG	930
Redesign 2	TAAGGCTGGCAATCTCGGC	CTTAACAGCTGGCCCGACA	982
Redesign 3	GGCCCAAGGTATCTCGCAA	TACGGGCCGCTGTTTATCC	995
Redesign 4	CCGCCTTTGCTGCTTTCTC	GTTACAGCGGTAAGCGGGA	1050
Redesign 5	TTGTCGCTACCACGGAACG	TAACAGCTGGCCCGACAAC	1068
Redesign 6	TGCCCCGATCTGGCTCTTA	CTGTGGCCGGTCAAGAAGA	951
Redesign 7	GCCCCGATCTGGCTCTTAA	CTGTGGCCGGTCAAGAAGA	950
Redesign 8	CCCGGATCTGGCTCTTAAGG	CTGTGGCCGGTCAAGAAGA	949
Redesign 9	CCGGATCTGGCTCTTAAGGC	CTGTGGCCGGTCAAGAAGA	948
Redesign 10	CGGATCTGGCTCTTAAGGCTG	CTGTGGCCGGTCAAGAAGA	947
Redesign 11*	GGATCTGGCTCTTAAGGCTGG	CTGTGGCCGGTCAAGAAGA	946

* Redesign version selected for use

3.2.12: Continuing Research

The tNGS project has the potential to generate sizable impact on the field of TB diagnostics through the opportunities afforded by the FIND/WHO Seq&Treat project. From multiple NGS technologies developed by varied research and development entities, our tNGS assay was chosen for further evaluation along with 2 others. The remaining three have moved into phase II trials where they will be assessed in reference laboratories in India, South Africa, and Georgia. Phase II trials will test the performance and viability of the assays in real-world high incidence conditions, after which the results will be analysed by FIND ¹⁸⁹. Assays which achieve FIND TPPs during this evaluation will undergo phase III trials globally where, if they perform as required, will receive WHO endorsement. Additionally, a patent has been filed for the tNGS assay method. This is in the process of being licensed by ONT for use in continuing development of the multiplex assay.

Consolidating reactions into a single multiplex must be a priority moving forward. While the assay as designed is comparable to existing technologies in sensitivity, specificity, and cost; the complexity and risk of contamination within the assay from three separate amplifications limits

practicality in clinical settings. By combining reagents into a single reaction; time, complexity, and cost may all be reduced. This in turn would increase the prospective implementation and reach of the assay for laboratories of all levels. Combination of the 3 multiplex reactions into a single reaction would reduce costs by an estimated £3.50 per sample. Colleagues in the O'Grady group have recently achieved this goal and continue to improve the assay moving forward.

3.3: Metagenomic Sequencing

Metagenomic sequencing has proven useful in the diagnosis of lower respiratory diseases and generation of epidemiological data in a single test^{111,113}. This speed and breadth of information would be a boon both for clinical TB treatment and TB control efforts within populations. To that end, a metagenomic assay was designed using host and experimental commensal bacterial depletion methods to improve detection of *M. tb* and MTBC DNA.

3.3.1: Assessment of a Host DNA Depletion Method for Diagnosis of TB and Drug Resistance by Metagenomic Sequencing

The first step for the metagenomic approach for detecting *M. tuberculosis* in sputum was to remove human DNA. A saponin-based host depletion method, described by Charalampous, et al.¹¹¹, was tested on a spiked NRF sputum sample. Triplicate samples were spiked with 10-fold serial dilution of *M. bovis* BCG culture (~150-150,000 CE/mL). Post-depletion, samples were extracted and removal of human DNA was analysed by qPCR targeting the human RNA polymerase A gene. Analysis identified host depletion up to ~99.99%, or 10⁴ fold, with a mean 3,257.5-fold reduction (Range = 159.8 – 6,165.5 fold) (Table 3.83).

Loss of target and overall bacterial DNA during depletion was also quantified (Tables 3.84 and 3.85). The loss of BCG ranged from 1.5-50 fold. This inconsistency is likely due to processing rather than an issue with saponin lysing *M. bovis* BCG. Commensal bacteria reduction was also monitored as

commensal bacteria would compete with target bacteria for sequencing reads. The saponin method showed reduction in commensal bacteria was similar to loss of target bacteria as expected.

Table 3.83: Mean human DNA qPCR results and calculated host depletion levels using triplicate samples

Sample	Approximate Number of <i>M. bovis</i> BCG Cells per Sample (CFU/mL)	Sample Treatment	Human RNA polymerase A qPCR Assay ($\bar{X} C_T$)	Human DNA Depletion ($\bar{X} \Delta C_T$)
BCG 10 ⁵	150,000	Depleted	32.57	12.59 (6,165.5 fold Reduction)
		Undepleted	19.98	
BCG 10 ⁴	15,000	Depleted	32.52	11.91 (3,848.3 fold Reduction)
		Undepleted	20.61	
BCG 10 ³	1,500	Depleted	31.19	11.48 (2,856.4 fold Reduction)
		Undepleted	19.71	
BCG 10 ²	150	Depleted	28.18	7.32 (159.8 fold Reduction)
		Undepleted	20.86	

Table 3.84: Mean *M. bovis* BCG DNA qPCR results and calculated target loss using triplicate samples

Sample	Approximate Number of <i>M. bovis</i> BCG Cells per Sample (CFU/mL)	Sample Treatment	<i>M. bovis</i> BCG RD1 gene qPCR Assay ($\bar{X} C_T$)	<i>M. bovis</i> BCG DNA Loss/Gain ($\bar{X} \Delta C_T$)
BCG 10 ⁵	150,000	Depleted	24.76	2.36 (5.1 fold Loss)
		Undepleted	22.4	
BCG 10 ⁴	15,000	Depleted	29.15	2.19 (4.6 fold Loss)
		Undepleted	26.96	
BCG 10 ³	1,500	Depleted	30.66	0.62 (1.5 fold Loss)
		Undepleted	30.04	
BCG 10 ²	150	Depleted	40	5.49 (44.9 fold Loss)
		Undepleted	34.51	

Table 3.85: Mean 16S rRNA gene qPCR results and calculated bacterial loss using triplicate samples

Sample	Approximate Number of <i>M. bovis</i> BCG Cells per Sample (CFU/mL)	Sample Treatment	Bacterial 16S gene qPCR Assay ($\bar{X} C_T$)	Total Bacterial DNA Loss/Gain ($\bar{X} \Delta C_T$)
BCG 10 ⁵	150,000	Depleted	26.32	2.15 (4.4 fold Loss)
		Undepleted	24.17	
BCG 10 ⁴	15,000	Depleted	26.38	2.35 (5.1 fold Loss)
		Undepleted	24.03	
BCG 10 ³	1,500	Depleted	25.77	1.63 (3.1 fold Loss)
		Undepleted	24.14	
BCG 10 ²	150	Depleted	26.73	1.9 (3.7 fold Loss)
		Undepleted	24.83	

To test reproducibility of host depletion in spiked NRF sputum the experiment was repeated with a second set of triplicate samples (Table 3.86). Analysis by qPCR showed host DNA was depleted up to ~99.99%, or 10⁴, with a mean fold reduction of 5,742.9 (Range = 3,821.7 – 7,750.1 fold).

Target and overall bacterial DNA loss from the saponin method were assessed as before (Tables 3.87 & 3.88). Loss of target bacterial DNA was less than observed previously. However, a significant loss of total bacterial DNA was detected (Paired T-Test: p=0.016).

Table 3.86: Mean human DNA qPCR results and calculated host depletion levels using triplicate samples

Sample	Approximate Number of <i>M. bovis</i> BCG Cells per Sample (CFU/mL)	Sample Treatment	Human RNA polymerase A qPCR Assay ($\bar{X} C_T$)	Human DNA Depletion ($\bar{X} \Delta C_T$)
BCG 10 ⁵	150,000	Depleted	34.79	12.92 (7,750.1 fold Loss)
		Undepleted	21.87	
BCG 10 ⁴	15,000	Depleted	33.65	12.24 (4,837.3 fold Loss)
		Undepleted	21.41	
BCG 10 ³	1,500	Depleted	33.67	11.9 (3,821.7 fold Loss)
		Undepleted	21.77	
BCG 10 ²	150	Depleted	34.31	12.68 (6,562.4 fold Loss)
		Undepleted	21.63	

Table 3.87: Mean *M. bovis* BCG DNA qPCR results and calculated bacterial loss using triplicate samples

Sample	Approximate Number of <i>M. bovis</i> BCG Cells per Sample (CFU/mL)	Sample Treatment	<i>M. bovis</i> BCG RD1 gene qPCR Assay ($\bar{X} C_T$)	<i>M. bovis</i> BCG DNA Loss/Gain ($\bar{X} \Delta C_T$)
BCG 10 ⁵	150,000	Depleted	24.97	1.75 (3.4 fold Loss)
		Undepleted	23.22	
BCG 10 ⁴	15,000	Depleted	30.41	2.82 (7.1 fold Loss)
		Undepleted	27.59	
BCG 10 ³	1,500	Depleted	29.63	0.71 (1.6 fold Gain)
		Undepleted	30.34	
BCG 10 ²	150	Depleted	34.60	0.05 (1.0 fold Loss)
		Undepleted	34.55	

Table 3.88: Mean 16S rRNA gene qPCR results and calculated bacterial loss using triplicate samples

Sample	Approximate Number of <i>M. bovis</i> BCG Cells per Sample (CFU/mL)	Sample Treatment	Bacterial 16S gene qPCR Assay ($\bar{X} C_T$)	Total Bacterial DNA Loss/Gain ($\bar{X} \Delta C_T$)
BCG 10 ⁵	150,000	Depleted	26.90	3.87 (14.6 fold Loss)
		Undepleted	23.03	
BCG 10 ⁴	15,000	Depleted	28.85	4.93 (30.5 fold Loss)
		Undepleted	23.92	
BCG 10 ³	1,500	Depleted	28.09	4.90 (29.9 fold Loss)
		Undepleted	23.19	
BCG 10 ²	150	Depleted	28.90	4.60 (24.2 fold Loss)
		Undepleted	24.30	

Significant host depletion (Paired T-Test: $p < 0.0001$) indicated this method did not require further optimization. However, there was need to develop a depletion protocol for commensal bacterial DNA for efficient and sensitive mycobacterial detection.

3.3.2: Development of a Commensal Bacteria DNA Depletion Method for Mycobacterial Samples

As the results previously demonstrated, there was a need for an optimized method for the removal of unwanted commensal DNA. We aimed to develop an additional depletion step to remove commensal bacteria within sputum samples without any loss of target (*M. bovis* BCG).

3.3.2.1: Assessment of Lysis Buffers for the Depletion of Commensal Bacterial DNA in Sputum Samples

Initially, two lysis buffers (MagNA Pure and Qiagen) were tested with and without the addition of lysozyme (Table 3.89). Triplicate samples were suspended in the lysis buffer solution for 10 minutes before undergoing host nucleic acid depletion. Following depletion, samples were amplified and assessed by qPCR to quantify DNA reduction.

Table 3.89: Lysis buffer solutions designed for testing in the optimization of commensal bacterial DNA depletion

Sample	Lysis Buffer Solution
BCG 10 ⁵ 1	400µL MagNA Pure Bacterial Lysis Buffer
BCG 10 ⁵ 2	200µL MagNA Pure Bacterial Lysis Buffer + 200µL 5M Lysozyme
BCG 10 ⁵ 3	400µL Qiagen Lysis Buffer
BCG 10 ⁵ 4	200µL Qiagen Lysis Buffer + 200µL 5M Lysozyme

Analysis indicated no significant depletion of commensal bacterial DNA (Paired T-Test: $p > 0.05$), while host depletion remained significant (Tables 3.90 & 3.91) (Paired T-Test: $p = 0.0099$). Target DNA (*M. bovis* BCG) was detected with no significant loss (mean loss = 3.57 fold) (Table 3.92).

MagNA Pure bacterial lysis buffer improved host DNA depletion (mean effect size = 162,491-fold) compared to Qiagen lysis buffer (mean effect size = 781.6-fold).

Table 3.90: Mean 16S rRNA gene qPCR results and calculated bacterial reduction using two sets of triplicate samples

Sample	Replicate Set	Approximate Number of <i>M. bovis</i> BCG Cells per Sample (CFU/mL)	Sample Treatment	Bacterial 16S gene qPCR Assay ($\bar{X} C_T$)	Total Bacterial DNA Depletion ($\bar{X} \Delta C_T$)
BCG 10 ⁵ 1	1	150,000	Depleted	25.66	1.26
			Undepleted	24.40	(2.4 fold Reduction)
	2	150,000	Depleted	24.35	1.14
			Undepleted	23.21	(2.2 fold Reduction)
BCG 10 ⁵ 2	1	150,000	Depleted	27.37	2.97
			Undepleted	24.40	(7.8 fold Reduction)
	2	150,000	Depleted	24.89	1.68
			Undepleted	23.21	(3.2 fold Reduction)
BCG 10 ⁵ 3	1	150,000	Depleted	23.88	0.52
			Undepleted	24.40	(1.4 fold Gain)
	2	150,000	Depleted	24.56	1.35
			Undepleted	23.21	(2.5 fold Reduction)
BCG 10 ⁵ 4	1	150,000	Depleted	25.03	0.63
			Undepleted	24.40	(1.5 fold Reduction)
	2	150,000	Depleted	24.74	1.53
			Undepleted	23.21	(2.9 fold Reduction)

Table 3.91: Mean human RNA Polymerase A gene qPCR results and calculated host depletion levels using four sets of triplicate samples

Sample	Approximate Number of <i>M. bovis</i> BCG Cells per Sample (CFU/mL)	Sample Treatment	Human RNA polymerase A DNA Probe qPCR Assay (\bar{X} C _T)	Human DNA Depletion (\bar{X} ΔC _T)
BCG 10 ⁵ 1	150,000	Depleted	40.00	17.31 (162,491.0 fold Reduction)
		Undepleted	22.69	
BCG 10 ⁵ 2	150,000	Depleted	40.00	17.31 (162,491.0 fold Reduction)
		Undepleted	22.69	
BCG 10 ⁵ 3	150,000	Depleted	31.48	8.79 (442.6 fold Reduction)
		Undepleted	22.69	
BCG 10 ⁵ 4	150,000	Depleted	32.82	10.13 (1,120.6 fold Reduction)
		Undepleted	22.69	

Table 3.92: Mean *M. bovis* BCG qPCR results and calculated bacterial loss using two sets of triplicate samples

Sample	Replicate Set	<i>M. bovis</i> BCG Cells per Sample (CFU/mL)	Sample Treatment	<i>M. bovis</i> BCG RD1 Region Probe qPCR Assay (\bar{X} C _T)	<i>M. bovis</i> BCG DNA Loss/Gain (\bar{X} ΔC _T)
BCG 10 ⁵ 1	1	150,000	Depleted	27.49	5.18 (36.2 fold Loss)
			Undepleted	22.31	
	2	150,000	Depleted	24.13	1.01 (2.0 fold Loss)
			Undepleted	23.12	
BCG 10 ⁵ 2	1	150,000	Depleted	26.34	4.03 (16.3 fold Loss)
			Undepleted	22.31	
	2	150,000	Depleted	24.54	1.42 (2.7 fold Loss)
			Undepleted	23.12	
BCG 10 ⁵ 3	1	150,000	Depleted	22.69	0.38 (1.3 fold Loss)
			Undepleted	22.31	
	2	150,000	Depleted	24.27	1.15 (2.2 fold Loss)
			Undepleted	23.12	
BCG 10 ⁵ 4	1	150,000	Depleted	22.83	0.52 (1.4 fold Loss)
			Undepleted	22.31	
	2	150,000	Depleted	24.11	0.99 (2.0 fold Loss)
			Undepleted	23.12	

Analysis by ANOVA with a Tukey post-hoc test showed use of bacterial lysis buffers resulted in significantly less commensal depletion than using saponin treatment alone (ANOVA: $p=0.001$). This was shown for both MagNA Pure lysis buffer and Qiagen lysis buffer (Table 3.93) and was surprising, as these lysis buffers were predicted to lyse commensal bacteria and result in bacterial DNA depletion. Analysis further showed no significant difference in commensal DNA depletion between MagNA Pure buffer or Qiagen buffer (ANOVA: $p=0.899$).

Table 3.93: Tukey HSD Post-Hoc test results for commensal bacterial DNA depletion using two bacterial lysis buffer incubations

Commensal Depletion Comparison	ANOVA P-Value	Tukey HSD Q-Value	$\alpha=0.05$ Critical Q Value
Saponin Only vs. MagnaPure Lysis Buffer Incubation	0.0010053	7.0872	3.4202
Saponin Only vs. Qiagen Lysis Buffer Incubation	0.0010053	6.8234	3.4202
MagnaPure Lysis Buffer Inclusion vs. Qiagen Lysis Buffer Incubation	0.8999947	0.2242	3.4202

3.3.2.2: Assessment of Reagents for the Depletion of Commensal Bacterial DNA in Sputum Samples

The effect of two detergents (triton x-100 and tween) and one reduction agent (DTT) was investigated for targeted depletion of commensal bacteria. Triplicate samples were incubated in each reagent for 10min followed by host nucleic acid depletion and DNA extraction. Extracted samples were amplified by qPCR to assess quantity of host DNA, commensal DNA, and target DNA in each sample with and without depletion.

Analysis showed a significant increase in commensal bacterial DNA following pre-incubation with 0.1% Tween, a 6.7 fold increase (Table 3.94). Exposure to 0.025% Triton, 1% DTT, and 0.1% DTT

showed no significant difference (Paired T-Test: $p > 0.05$) in the amplification of commensal bacterial DNA during qPCR. Depletion of commensal bacterial DNA was only observed after exposure to triton x-100 (~99.99% reduction). However, this was observed only in a single replicate.

Table 3.94: Mean 16S rRNA gene qPCR results and calculated bacterial reduction using three sets of triplicate samples

Sample	Replicate Set	Approximate Number of <i>M. bovis</i> BCG Cells per Sample (CFU/mL)	Sample Treatment	Bacterial 16S DNA Probe qPCR Assay ($\bar{X} C_T$)	Total Bacterial DNA Depletion ($\bar{X} \Delta C_T$)
Triton 0.025%	1	150,000	Depleted	32.19	13.33 (10,297.4 fold Reduction)
			Undepleted	18.86	
	2	150,000	Depleted	16.32	-2.54 (5.8 fold Gain)
			Undepleted	18.86	
	3	150,000	Depleted	16.39	-2.47 (5.5 fold Gain)
			Undepleted	18.86	
Tween 0.1%	1	150,000	Depleted	16.40	-2.46 (5.5 fold Gain)
			Undepleted	18.86	
	2	150,000	Depleted	16.13	-2.73 (6.6 fold Gain)
			Undepleted	18.86	
	3	150,000	Depleted	15.88	-2.98 (7.9 fold Gain)
			Undepleted	18.86	
DTT 1%	1	150,000	Depleted	15.80	-0.18 (1.1 fold Gain)
			Undepleted	15.98	
	2	150,000	Depleted	15.40	-0.58 (1.5 fold Gain)
			Undepleted	15.98	
	3	150,000	Depleted	15.39	-0.59 (1.5 fold Gain)
			Undepleted	15.98	
DTT 0.1%	1	150,000	Depleted	15.34	-0.64 (1.6 fold Gain)
			Undepleted	15.98	
	2	150,000	Depleted	16.05	0.07 (1.1 fold Reduction)
			Undepleted	15.98	
	3	150,000	Depleted	15.72	-0.26 (1.2 fold Gain)
			Undepleted	15.98	

Assessment of host nucleic acid depletion found inclusion of detergents prior to depletion did not negatively impact performance (Table 3.95). There was no significant loss (Paired T-Test: $p>0.05$) of target DNA (*M. bovis* BCG) following exposure to 0.025% Triton (2.7 fold), 0.1% Tween (2.2 fold), and 0.1% DTT (1.7 fold) (Table 3.96). Findings indicate inclusion of these reagents does not effectively deplete commensal bacterial DNA. The increased concentration of bacterial DNA in most of the samples tested may indicate that commensals are being lysed more efficiently but that the commensal DNA is not being digested.

Table 3.95: Mean human RNA polymerase A qPCR for assessing DNA depletion using four pre-host depletion detergent incubations using three sets of triplicate samples

Sample	Replicate Set	<i>M. bovis</i> BCG Cells per Sample (CFU/mL)	Sample Treatment	Human DNA Probe qPCR Assay (\bar{X} C _T)	Human DNA Depletion (\bar{X} Δ C _T)
Triton 0.025%	1	150,000	Depleted	40	15.18 (37,122.3 fold Reduction)
			Undepleted	24.82	
	2	150,000	Depleted	40	15.18 (37,122.3 fold Reduction)
			Undepleted	24.82	
	3	150,000	Depleted	40	15.18 (37,122.3 fold Reduction)
			Undepleted	24.82	
Tween 0.1%	1	150,000	Depleted	40	15.18 (37,122.3 fold Reduction)
			Undepleted	24.82	
	2	150,000	Depleted	40	15.18 (37,122.3 fold Reduction)
			Undepleted	24.82	
	3	150,000	Depleted	40	15.18 (37,122.3 fold Reduction)
			Undepleted	24.82	
DTT 1%	1	150,000	Depleted	40	15.03 (33,456.5 fold Reduction)
			Undepleted	24.97	
	2	150,000	Depleted	40	15.03 (33,456.5 fold Reduction)
			Undepleted	24.97	
	3	150,000	Depleted	40	15.03 (33,456.5 fold Reduction)
			Undepleted	24.97	
DTT 0.1%	1	150,000	Depleted	40	15.03 (33,456.5 fold Reduction)
			Undepleted	24.97	
	2	150,000	Depleted	40	15.03 (33,456.5 fold Reduction)
			Undepleted	24.97	
	3	150,000	Depleted	40	15.03 (33,456.5 fold Reduction)
			Undepleted	24.97	

Table 3.96: Mean *M. bovis* BCG qPCR for assessing DNA loss using four pre-host depletion detergent incubations using three sets of triplicate samples

Sample	Replicate Set	Approximate Number of <i>M. bovis</i> BCG Cells per Sample (CFU/mL)	Sample Treatment	<i>M. bovis</i> BCG DNA Probe qPCR Assay ($\bar{X} C_T$)	<i>M. bovis</i> BCG DNA Loss/Gain ($\bar{X} \Delta C_T$)
Triton 0.025%	1	150,000	Depleted	25.91	1.09 (2.1 fold Loss)
			Undepleted	24.82	
	2	150,000	Depleted	26.79	1.97 (3.9 fold Loss)
			Undepleted	24.82	
	3	150,000	Depleted	25.87	1.05 (2.1 fold Loss)
			Undepleted	24.82	
Tween 0.1%	1	150,000	Depleted	25.75	0.93 (1.9 fold Loss)
			Undepleted	24.82	
	2	150,000	Depleted	26.03	1.21 (2.3 fold Loss)
			Undepleted	24.82	
	3	150,000	Depleted	26.14	1.32 (2.5 fold Loss)
			Undepleted	24.82	
DTT 1%	1	150,000	Depleted	25.83	0.86 (1.8 fold Loss)
			Undepleted	24.97	
	2	150,000	Depleted	24.58	-0.39 (1.3 fold Gain)
			Undepleted	24.97	
	3	150,000	Depleted	25.87	0.90 (1.9 fold Loss)
			Undepleted	24.97	
DTT 0.1%	1	150,000	Depleted	25.52	0.55 (1.5 fold Loss)
			Undepleted	24.97	
	2	150,000	Depleted	25.71	0.74 (1.7 fold Loss)
			Undepleted	24.97	
	3	150,000	Depleted	25.93	0.96 (1.9 fold Loss)
			Undepleted	24.97	

3.3.2.3: Effectiveness of Depletion Methodologies

Assessment of host DNA depletion methods developed by Charalampous, *et al.*, proved effective in sputum samples containing mycobacteria¹¹¹. However, this method is designed to remove human cells/DNA and to avoid disruption and depletion of any bacterial DNA. Optimisation and development of the method to remove commensal bacterial DNA and improve relative concentration of target DNA (*M. bovis* BCG) for sequencing proved ineffective.

Saponin depletion of host DNA works by creating pores in cell and nuclear membranes (phospholipid bilayers)¹¹¹. These pores allow high salt HL-SAN buffer (which assists in DNA release from chromatin) and DNase into the cell to digest the DNA. Saponin cannot penetrate bacterial cell walls, so while this method is effective for removal of host DNA (*H. sapiens*) it is unable to deplete bacterial DNA. This is useful for metagenomic diagnosis or microbiome studies but is a limitation when targeting a single pathogen, especially in infections where the pathogen can account for only a small proportion of the bacterial community present in the sample.

To improve the relative concentration of mycobacterial DNA in contrived sputum samples several lysis and depletion methods¹¹¹ were tested. Initially, lysis buffers used in automated DNA extraction were tested (Section 3.3.2.1). Two buffers were tested, one for the MagNA Pure system and one from Qiagen. As these buffers are designed to lyse bacterial cells, but are inefficient for mycobacterial cells without mechanical disruption, it was hypothesized that these would preferentially lyse commensal bacterial. However, exposure to these buffers didn't result in reduction of commensal DNA.

Following these experiments the effects of three reagents (triton x-100, tween, and DTT) were assessed for depletion of commensal DNA in sputum samples. Rather than decrease the relative concentration of commensal bacteria DNA after extraction, tween instead increased the yield of commensal bacterial DNA. One hypothesis for why this occurred was that Tween improved bacterial cell lysis but inhibited HL-SAN DNase¹⁹⁰. In comparison, exposure of sputum samples to DTT resulted in no significant change in the extraction of commensal bacterial DNA or the relative concentration of mycobacterial DNA. Finally, one replicate which was exposed to triton x-100 did show significant depletion of commensal bacteria, however this result was not replicable and the other two replicates showed slight increases in extracted commensal DNA. While this result indicates that further investigation into triton x-100 is warranted, the results were not consistent enough for continued research during this project.

While none of these reagents were effective for selective depletion of commensal bacteria, neither did they negatively impact depletion of host cells. This indicates that use of a detergent prior to saponin depletion does not inhibit saponin or DNase.

3.3.2.4: Future Depletion Research

Future research to improve the relative concentration of mycobacterial DNA or remove commensal bacterial DNA for metagenomic sequencing can follow multiple paths. Two such options are development of a selective lysing and depletion process, or development of a hybridization capture system, as for enrichment in clinical samples for parasite and viral DNA ^{191–193}. Development of a targeted depletion methodology would allow efficient extraction of mycobacterial DNA from any primary sample type for sequencing. Hybridization capture allows highly specific enrichment of free DNA following mechanical lysis, removing the need for pre-processing for host or commensal depletion. Hybridization capture can streamline diagnostic workflows, however, use of specific bait molecules limits the breadth of coverage by sequencing in most samples ¹⁹⁴.

Targeted enrichment using hybridization capture can be useful for detection and diagnosis of drug resistance mutations. However, in addition to the limited fragment sizes, hybridization capture methods also require longer sequencing runs to generate equivalent read-depth to targeted amplification. For example, Horn estimates that 20x coverage of a 1kb genetic fragment requires approximately 500,000 Illumina reads ¹⁹⁴. This inefficiency in sequencing hybridization captured DNA is therefore compounded in analysis of multiple targets in concurrent samples.

3.3.3: Preliminary Limit of Detection Experiment

LoD for the metagenomic assay was assessed by qPCR of triplicate samples and sequencing of two sets of triplicate *M. bovis* BCG spiked NRF sputum. Serial 10-fold dilutions of *M. bovis* BCG culture (10^5 to 10^1 CFU/mL) were spiked into sputum – host DNA depletion was performed, DNA extracted and then qPCR amplified using a BCG probe based qPCR assay. Results showed target DNA was only

detectable in samples containing 10^4 CFU/mL spikes and above (Table 3.97). This was surprising as previous experiments showed detection of BCG DNA down to 10^2 CFU/mL (e.g. Table 3.84)

Table 3.97: Mean Roche probe-based qPCR results for M. bovis BCG testing the concentration of DNA available for metagenomic sequencing following depletion protocols using triplicate samples

Sample	BCG Probe qPCR Amplification (\bar{X} C_T)
10 ⁵ BCG Spiked Sputum	26.49
10 ⁴ BCG Spiked Sputum	28.90
10 ³ BCG Spiked Sputum	37.31
10 ² BCG Spiked Sputum	40.00
10 ¹ BCG Spiked Sputum	40.00
Non-Depleted 10 ⁵ Positive Control	25.85
Negative NRF Sputum Control	37.97

Following qPCR analysis 10^5 CFU/mL – 10^3 CFU/mL spiked extracted samples were sequenced to determine the working LoD of the method. Following 6 hours of sequencing, reads were uploaded to the Epi2Me WIMP pipeline and MTBC reads were recorded (Table 3.98).

Lack of amplification observed in the 10^3 CFU/mL spiked sample correlated with lack of coverage from sequencing. Analysis also showed amplification during qPCR did not directly correlate with sequencing coverage. MTBC reads accounted for only 7.62% of total reads in the 1×10^5 CFU/mL spiked sample but 41.48% of total reads in the 1×10^4 CFU/mL spiked sample, despite a qPCR product concentration 5.3 fold greater in the 1×10^5 CFU/mL sample. This is likely related to varying levels of bacterial and commensal DNA present in the samples. These preliminary results demonstrate an LoD of approximately 10,000 CFU/mL.

Table 3.98: Epi2Me WIMP pipeline results of three 10-fold serially diluted *M. bovis* BCG samples in NRF sputum

Sample	MTBC Reads (#)	Total Mycobacterial Reads (% of Total Reads)
1x10 ⁵ BCG Spiked Sputum	802	7.62
1x10 ⁴ BCG Spiked Sputum	23,709	41.48
1x10 ³ BCG Spiked Sputum	0	0

Based on these results focus was returned to the tNGS method to minimize the impact of commensal bacteria on diagnosis and DST.

3.3.4: Metagenomic Assay Performance Summary

The metagenomic protocol exhibits an LoD of approximately 10,000 CFU/mL; roughly equivalent to smear microscopy, though with increased complexity¹⁸⁸. This poor analytical sensitivity largely precludes competition with existing molecular technologies. One method for improving the LoD is by increasing sequencing times, although this would quickly inflate turnaround time (TaT) for the assay.

Currently, the metagenomic method does exhibit a TaT of approximately 8 hours from receipt of sample for majority genome coverage. Use of this method following a positive smear test could prove clinically useful given the depth and breadth of information possible. This use is limited, however, by the poor analytical specificity seen during preliminary testing. As with the analytical sensitivity, the metagenomic method displayed poor analytical specificity (41%).

The poor analytical performance of the metagenomic assay is further hampered by its cost.

Current metagenomic techniques have an average cost of £25.57/sample¹¹¹. This price point is higher than existing molecular techniques on the market and would need to be significantly reduced to promote uptake of the method.

Chapter 4 – Implementation and Conclusion

4.1: Implementation of the tNGS Assay

4.1.1: Current tNGS Assay Landscape

Although primarily new diagnostics for TB have utilized amplification without sequencing, tNGS assays have been developed for DST. The GenoScreen® Deeplex Myc-TB and the TGEN® Next-Gen RDST assay are both currently on the market although neither is, as yet, endorsed by the WHO ^{116,195,196}. Each test is used following a positive TB diagnosis for comprehensive DST. The Deeplex Myc-TB has a cited genotypic sensitivity of 97.1% ¹⁶⁵. This test also exhibits a high phenotypic sensitivity and specificity (95.3% and 97.4% respectively) for first and second-line medications ¹⁶⁵.

A 2016 study of the Next-Gen RDST method showed a genotypic sensitivity of 97.8% as compared to pyrosequencing ¹⁹⁶. This study also cited phenotypic sensitivities and specificities for three first-line medications; isoniazid (95%, 100%), rifampicin (97.6%, 98.9%) , and kanamycin (96.2%, 93.9%) ¹⁹⁶. For second-line medications phenotypic sensitivity ranged from 42.9% (amikacin) to 86.7% (moxifloxacin). The phenotypic specificity had a narrower range in second-line medications from 85.7% (oxifloxacin) to 98% (capreomycin) ¹⁹⁶.

However, neither of these methods is currently endorsed by the WHO. This means that the primary molecular methods for TB diagnosis and DST remain amplification or line-probe based.

4.1.2: TB Diagnostic Time Requirements

One of the primary limitations with gold standard culture techniques for TB is the time required. This is frequently compounded by patient delays in seeking treatment which average a median 23 days from the onset of symptoms ¹⁹⁷. In LMICs where frequently the only DST tool routinely available is culture the turnaround time (TaT) is often seen as unavoidable. Delays in diagnosis can result in negative patient outcomes, increased community transmission, and an increased risk of

drug resistance emerging. Conversely, while smear microscopy is rapid it suffers from low sensitivity and an inability to inform drug regimens. These limitations have been primary motivators behind the development of improved technologies.

The most widely used of these, the Xpert MTB/RIF assay, reduces diagnosis and rifampicin resistance calling TaT to 24 hours on average, although under optimal conditions it can take as little as 1 hour^{185,198}. The primary source of delays for the performance of an Xpert MTB/RIF assay lie in infrastructure, both physical and human. The median delay attributable to such issues within the healthcare system is 7 days¹⁹⁷. However, this ability to rapidly provide a TB diagnosis, and basic DST in the MTB/RIF assay, can result in improved patient outcomes. While this assay is only able to detect resistance to rifampicin, this is often a good surrogate for MDR increasing the utility possible within the rapid timeframe^{199,200}.

Another such technology, the Genotype MTBDRplus line probe assay, reduced time from sample to diagnosis of TB and drug resistance to 1 week on average²⁰¹. While this marked a significant decrease in TaT from culture it is still longer than preferable for optimal patient outcomes. Often, by the one-week mark, patients have already begun a treatment regimen based on clinical diagnosis. However, as a treatment course for TB currently takes several months of concerted effort, one week of ineffective treatment will have minimal healthcare implications except in the most extreme of cases.

Delays in the use of the Genotype MTBDRplus line probe assay are exacerbated by its use as a reflexive test following a positive TB diagnosis by either culture or Xpert MTB/RIF which further extends the time between diagnosis and comprehensive DST result. This is a concern when using the Genotype assay as administration of drugs despite resistance, or later alteration of a treatment regimen, can increase the risk of drug-resistance propagation in patients and the population. However, use of the MTBDRplus and MTBDRsl (second-line) assays do provide comprehensive drug resistance information and should not be discounted due to this lag time.

The tNGS multiplex assay can reduce the TaT of diagnosis and provide comprehensive DST in ~13 hours from the receipt of samples (Figure 4.1) when testing 80 samples at a time. However, in real lab conditions this is likely to translate to approximately two days from sample to patient. This can provide clinically useful treatment information the day after a TB diagnosis. The TaT is dependent on the number of samples tested and can be cut to approximately 8 hours when testing 24 samples. Further development of the test by colleagues in the O’Grady group has further reduced the TaT and it is now possible to test 24 samples in approximately 4 hours.

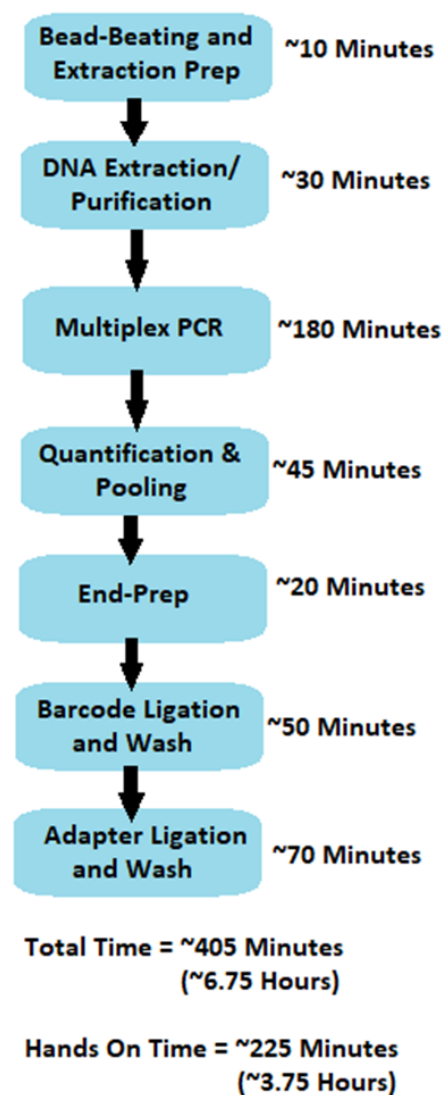


Figure 4.1: Flow and time requirements for each step of the tNGS multiplex assay following receipt of a sample excluding 6 hour recommended sequencing time

As mentioned previously, TaT is not solely impacted by the length of a diagnostic procedure. Rather, numerous factors from collection of the sample, distance to the appropriate laboratory, and levels of staffing play large roles in the TaT of any given assay.

4.1.3: Cost of TB Diagnosis

Beyond the clinical utility and performance of a diagnostic and DST assay, cost per sample is an essential factor in implementation. Any new assays should first be compared to the gold standards of culture and smear microscopy. Culture, due to necessary sample preparation and biosafety considerations, costs between £10.02 and £21.58, depending on if DST is conducted ^{201,202}. Smear microscopy is significantly cheaper at an average £1.77– £1.85 per sample and generally requires less infrastructure increasing accessibility ²⁰¹. When combined, fluorescent smear microscopy with culture DST costs approximately £13.91 per sample ²⁰¹. The majority of the costs for these methods lies in consumables which can fluctuate from country to country ²⁰³. However, these costs are not absolute and can be subsidized in LMICs to improve access and remove barriers to diagnostic care and improve patient outcomes.

New diagnostic and DST tests are also likely to be compared to existing WHO endorsed assays such as the previously discussed Xpert MTB/RIF, MTB/RIF Ultra, GenoType MTBDRplus and MTBDRsl. Of these, the Xpert MTB/RIF has the lowest average cost per sample (£12.30 – £27.58) when including privatised healthcare markets in India and Brazil, two high-incidence countries ^{198,201,204,205}. The GenoType MTBDRplus assay is more expensive at £18.47 – £19.33 per sample ^{201,206}. Unlike culture and smear microscopy the bulk of the cost for these tests lies not with consumables but instead with the equipment and assay cartridges themselves ²⁰³. Also, staff costs accounted for approximately 29% of the cost for an Xpert MTB/RIF assay compared to only 5.4% of the cost for smear microscopy in one study from 2021 ²⁰³. However, as with culture and smear microscopy, endorsed molecular assays are often subsidized by the WHO for use in LMICs to improve global health outcomes. These costs make the currently endorsed assays equivalent to, or slightly better

than, culture with DST. However, no molecular assay has yet approached the cost-effectiveness of smear microscopy.

WHO has called for new NGS technologies with costs below £49.43/sample²⁰⁷. The tNGS assay has calculated costs slightly higher than culture but which fall below the desired threshold; £23.22/sample for 80-samples/run, less than half of WHO's upper cost limit. This calculated cost would decrease to £19.52/sample, equivalent to the MTBDRplus assay, should all three multiplex reactions be combined into a single reaction. Cost could potentially be further reduced by sequencing with alternative library preparation methods, sequencing more samples per flow cell and washing/reusing flowcells.

4.2: Benefits of Nanopore Sequencing for TB Diagnosis

Both tNGS and metagenomic methods benefit from the use of Nanopore sequencing instead of Illumina or pyrosequencing. Nanopore sequencing allows real-time results which improves TaT of assays and can decrease costs by ceasing runs after adequate results have been generated. This allows wash and reuse of flowcells reducing per sample costs²⁰⁸. Illumina, however, requires completion of a run before results can be analysed decreasing analytical flexibility.

One major advantage of nanopore sequencing is cost-effectiveness. Starter kits from ONT cost £823.80 and don't require service contracts²⁰⁸. In comparison the iSeq 100 from Illumina has a list price of £16393.62 and requires a service contract for operation²⁰⁹. This cost disparity limits the uptake of Illumina in LMICs outside of central reference laboratories but can allow for use of nanopore methods at the point-of-care.

Another benefit of nanopore sequencing which can assist uptake at point-of-care and near-patient facilities is its portability. Both the tNGS and metagenomic methods utilise the MinION sequencing platform which is highly portable (10.5cm x 2.3cm x 3.3cm, 85g) and has been used in remote locations around the world, and above it (the ISS)²¹⁰. Use of the MinION only requires connection

to a laptop and a power source, one study performed 24 hours of sequencing off of portable solar panels, demonstrating utility in remote areas with limited infrastructure ²¹¹. The new MinION Mk1C removes the requirement for an external laptop for use further improving portability.

All of these factors make nanopore sequencing in general, and the MinION platform in particular, powerful resources for disease control in LMICs.

4.3: Conservation and Ecology Applications

Use of the tNGS assay for monitoring TB status in livestock and wildlife is a potential avenue of investigation for future consideration. In conversation with zoo keepers at the National Zoonotic Gardens of South Africa and Brandywine Zoo in Delaware, as well as trackers and game keepers at the Phinda Private Game Reserve I was told that herd animals have a high incidence of TB which is largely undetectable until the infection is terminal. This is especially problematic in zoos where death by TB can result in a cull of the entire herd ²¹². By using high throughput sequencing such as used in validation of the tNGS assay, it should be feasible to include TB screening in annual wellness checks.

Using the assay in such a way would require some measure of redesign in the targets to optimize coverage of *M. bovis*, *M. orygis*, and *M. caprae*. This redesign would also need to reincorporate a speciation target to improve determination of an infection's causative agent. However, the drug resistance detection pipeline is not predicted to require modification simplifying adaptation of the tNGS assay for use in animals instead of humans.

4.4: Conclusions

While TB will continue to be a global health issue for the foreseeable future, constant research and development of new diagnostic technologies and treatment regimens should help stem the increase in DR-TB. The tNGS assay developed in this study will help in the fight against DR-TB. This was effectively shown compared to existing diagnostic assays where the tNGS assay exhibited

equivalent or superior sensitivity, specificity and LoD. However, the metagenomic methodology, despite showing promise for lower respiratory infections in general ¹¹³, proved ineffective for TB specific diagnoses due to commensal bacteria. Design of a targeted depletion or capture methodology for metagenomic sequencing could improve this technology's viability in coming years.

As molecular methods continue to improve the use of culture and smear microscopy should be phased out and replaced with methods that can guide effective anti-TB therapy on the day the patient is tested. With the aid of WHO and FIND in validating and subsidizing these new technologies, this is possible in the foreseeable future.

Appendix I: Catalogue of Known Drug-Resistance SNPs for TB

The following is a comprehensive list of known high confidence mutations associated with the development of drug resistance in MTBC species. Mutations are annotated as either nucleotide changes (lower case) or amino acid changes (upper case) along with the gene locus at which the mutation may occur.

Gene	Drug	Mutation (Wildtype:Site:Mutation)	Mutation Type (Nucleotide or Amino Acid)
<i>rrs</i>	Amikacin	a514c	Nucleotide
		a514t	Nucleotide
		c517t	Nucleotide
		a1338c	Nucleotide
		a1401*	Nucleotide
		a1401g	Nucleotide
		c1402*	Nucleotide
		c1402t	Nucleotide
		g1484*	Nucleotide
		g1484t	Nucleotide
	Capreomycin	a1401*	Nucleotide
		a1401g	Nucleotide
		c1402*	Nucleotide
		c1402t	Nucleotide
		g1484*	Nucleotide
		g1484t	Nucleotide
	Kanamycin	a514c	Nucleotide
		c517t	Nucleotide
		a1401*	Nucleotide
		a1401g	Nucleotide
		c1402*	Nucleotide
		c1402t	Nucleotide
		g1484*	Nucleotide
		g1484t	Nucleotide
	Streptomycin	c462t	Nucleotide
		c492t	Nucleotide
		c513t	Nucleotide
		a514c	Nucleotide
		a514t	Nucleotide
		c517t	Nucleotide
		c905a	Nucleotide
		c905g	Nucleotide
a906g		Nucleotide	

		a907c	Nucleotide
		a907t	Nucleotide
		a908g	Nucleotide
		t1239c	Nucleotide
		a1325c	Nucleotide
<i>rv0678</i>	Bedaquiline	S63R	Amino Acid
	Clofazamine	S63R	Amino Acid
<i>gyrA</i>	Ciprofloxacin	A74S	Amino Acid
		S91*	Amino Acid
		S91P	Amino Acid
		D94*	Amino Acid
		D94A	Amino Acid
		D94G	Amino Acid
		D94H	Amino Acid
		D94N	Amino Acid
	Moxifloxacin	A90*	Amino Acid
		A90V	Amino Acid
		S91*	Amino Acid
		S91P	Amino Acid
		D94*	Amino Acid
		D94A	Amino Acid
		D94G	Amino Acid
		D94H	Amino Acid
		D94N	Amino Acid
		D94Y	Amino Acid
		A90V	Amino Acid
		D89N	Amino Acid
		G88A	Amino Acid
	G88C	Amino Acid	
	Ofloxacin	A90*	Amino Acid
		A90V	Amino Acid
		S91*	Amino Acid
		S91P	Amino Acid
		D94*	Amino Acid
		D94A	Amino Acid
		D94G	Amino Acid
		D94H	Amino Acid
		D94N	Amino Acid
		D94Y	Amino Acid
		G89N	Amino Acid
G88A		Amino Acid	
G88C	Amino Acid		
Quinolones	H70R	Amino Acid	

		A74S	Amino Acid
		H85*	Amino Acid
		P86*	Amino Acid
		H87*	Amino Acid
		G88*	Amino Acid
		D89*	Amino Acid
		A90*	Amino Acid
		A90V	Amino Acid
		S91*	Amino Acid
		S91P	Amino Acid
		I92*	Amino Acid
		Y93*	Amino Acid
		D94*	Amino Acid
		D94A	Amino Acid
		D94G	Amino Acid
		D94H	Amino Acid
		D94N	Amino Acid
		L96*	Amino Acid
V97*	Amino Acid		
<i>gidB</i>	Capreomycin	Y195H	Amino Acid
	Streptomycin	I11N	Amino Acid
		A19P	Amino Acid
		L26F	Amino Acid
		G30D	Amino Acid
		G34V	Amino Acid
		V41I	Amino Acid
		R47W	Amino Acid
		H48N	Amino Acid
		H48Q	Amino Acid
		C52F	Amino Acid
		R64W	Amino Acid
		V65G	Amino Acid
		G69D	Amino Acid
		S70N	Amino Acid
		G73A	Amino Acid
		P75L	Amino Acid
		P75R	Amino Acid
		L79S	Amino Acid
		L79W	Amino Acid
A80P	Amino Acid		
R83P	Amino Acid		
D85A	Amino Acid		
V88A	Amino Acid		

		L91P	Amino Acid
		E92D	Amino Acid
		P93L	Amino Acid
		G117V	Amino Acid
		R118L	Amino Acid
		R118S	Amino Acid
		Q125.	Amino Acid
		A134E	Amino Acid
		S136.	Amino Acid
		R137P	Amino Acid
		R137W	Amino Acid
		A138T	Amino Acid
		A138V	Amino Acid
		S149R	Amino Acid
		I162S	Amino Acid
		E173.	Amino Acid
		A200E	Amino Acid
		V203L	Amino Acid
		A205E	Amino Acid
<i>tlyA</i>	Capreomycin	c-83t	Nucleotide
		N236K	Amino Acid
<i>embB</i>	Ethambutol	N296H	Amino Acid
		S297A	Amino Acid
		M306*	Amino Acid
		A313V	Amino Acid
		Y319C	Amino Acid
		Y319S	Amino Acid
		D328G	Amino Acid
		D328V	Amino Acid
		D328Y	Amino Acid
		Y334H	Amino Acid
		S347I	Amino Acid
		D354A	Amino Acid
		A356V	Amino Acid
		V377G	Amino Acid
		E378A	Amino Acid
		P397T	Amino Acid
		E405D	Amino Acid
		G406A	Amino Acid
		G406C	Amino Acid
		G406D	Amino Acid
		G406S	Amino Acid
		Q497K	Amino Acid

		Q497P	Amino Acid
		Q497R	Amino Acid
		E504D	Amino Acid
		A659T	Amino Acid
		Q853P	Amino Acid
		H1002R	Amino Acid
		D1024N	Amino Acid
		N1033K	Amino Acid
		T1082A	Amino Acid
<i>ethA</i>	Ethionamide	M1R	Amino Acid
		G43C	Amino Acid
		T61M	Amino Acid
		T232A	Amino Acid
		I338S	Amino Acid
		T342K	Amino Acid
		A381P	Amino Acid
<i>fabG1</i>	Ethionamide	g-17t	Nucleotide
	Isoniazid	g-17t	Nucleotide
		a-16*	Nucleotide
		c-15*	Nucleotide
		t-8*	Nucleotide
		G609A	Amino Acid
<i>inhA</i>	Ethionamide	c-15t	Nucleotide
		I21T	Amino Acid
		S49A	Amino Acid
		S94A	Amino Acid
		I194T	Amino Acid
	Isoniazid	c-15t	Nucleotide
		I21T	Amino Acid
		I21V	Amino Acid
		S94A	Amino Acid
		I194T	Amino Acid
<i>katG</i>	Isoniazid	Y155C	Amino Acid
		Y155S	Amino Acid
		L159P	Amino Acid
		T180K	Amino Acid
		G182R	Amino Acid
		W191G	Amino Acid
		W191R	Amino Acid
		P232R	Amino Acid
		P241P	Amino Acid
		M257I	Amino Acid
		T275A	Amino Acid

		Q295P	Amino Acid
		G297V	Amino Acid
		G299C	Amino Acid
		W300C	Amino Acid
		W300S	Amino Acid
		S302R	Amino Acid
		D311G	Amino Acid
		S315*	Amino Acid
		S315I	Amino Acid
		S315N	Amino Acid
		S315T	Amino Acid
		W321.	Amino Acid
		W328L	Amino Acid
		I335V	Amino Acid
		L378P	Amino Acid
		A379V	Amino Acid
		D419H	Amino Acid
		A424G	Amino Acid
<i>eis</i>	Kanamycin	g-10a	Nucleotide
		c-12t	Nucleotide
		c-14t	Nucleotide
		g-37t	Nucleotide
<i>rplC</i>	Linezolid	C154R	Amino Acid
<i>pncA</i>	Pyrazinamide	t-12c	Nucleotide
		a-11g	Nucleotide
		t-7c	Nucleotide
		M1T	Amino Acid
		A3E	Amino Acid
		L4S	Amino Acid
		L4W	Amino Acid
		I5S	Amino Acid
		I6L	Amino Acid
		I6T	Amino Acid
		V7F	Amino Acid
		V7G	Amino Acid
		V7L	Amino Acid
		D8A	Amino Acid
		D8G	Amino Acid
		D8N	Amino Acid
		D8E	Amino Acid
		V9A	Amino Acid
		Q10.	Amino Acid
		Q10P	Amino Acid

		Q10R	Amino Acid
		D12A	Amino Acid
		D12N	Amino Acid
		C14.	Amino Acid
		C14G	Amino Acid
		C14R	Amino Acid
		C14Y	Amino Acid
		G17D	Amino Acid
		L19P	Amino Acid
		V21G	Amino Acid
		G24D	Amino Acid
		L27P	Amino Acid
		I31S	Amino Acid
		S32I	Amino Acid
		Y34.	Amino Acid
		Y34D	Amino Acid
		L35R	Amino Acid
		V44G	Amino Acid
		A46E	Amino Acid
		A46V	Amino Acid
		T47A	Amino Acid
		T47P	Amino Acid
		K48E	Amino Acid
		K48T	Amino Acid
		D49A	Amino Acid
		D49G	Amino Acid
		D49N	Amino Acid
		H51Q	Amino Acid
		H51R	Amino Acid
		H51Y	Amino Acid
		P54L	Amino Acid
		P54Q	Amino Acid
		P54S	Amino Acid
		H57D	Amino Acid
		H57R	Amino Acid
		H57P	Amino Acid
		H57Y	Amino Acid
		F58L	Amino Acid
		F58S	Amino Acid
		S59P	Amino Acid
		T61P	Amino Acid
		P62L	Amino Acid
		P62Q	Amino Acid

	P62T	Amino Acid
	P62R	Amino Acid
	D63A	Amino Acid
	D63G	Amino Acid
	Y64D	Amino Acid
	S66P	Amino Acid
	S67P	Amino Acid
	W68.	Amino Acid
	W68C	Amino Acid
	W68G	Amino Acid
	W68R	Amino Acid
	P69L	Amino Acid
	H71Q	Amino Acid
	H71R	Amino Acid
	H71Y	Amino Acid
	H71D	Amino Acid
	C72R	Amino Acid
	C72Y	Amino Acid
	T76I	Amino Acid
	T76P	Amino Acid
	G78C	Amino Acid
	C78D	Amino Acid
	F81V	Amino Acid
	H82D	Amino Acid
	H82R	Amino Acid
	L85P	Amino Acid
	L85R	Amino Acid
	T87M	Amino Acid
	I90S	Amino Acid
	F94L	Amino Acid
	F94S	Amino Acid
	K96E	Amino Acid
	K96N	Amino Acid
	K96Q	Amino Acid
	K96T	Amino Acid
	K96R	Amino Acid
	G97C	Amino Acid
	G97D	Amino Acid
	G97R	Amino Acid
	G97S	Amino Acid
	Y99.	Amino Acid
	A102V	Amino Acid
	Y103*	Amino Acid

	Y103.	Amino Acid
	Y103H	Amino Acid
	S104G	Amino Acid
	S104R	Amino Acid
	G108R	Amino Acid
	T114P	Amino Acid
	L116P	Amino Acid
	L116R	Amino Acid
	L120P	Amino Acid
	R123P	Amino Acid
	V125G	Amino Acid
	V125F	Amino Acid
	V128G	Amino Acid
	V130G	Amino Acid
	G132A	Amino Acid
	G132D	Amino Acid
	G132S	Amino Acid
	I133T	Amino Acid
	A134V	Amino Acid
	T135P	Amino Acid
	T135N	Amino Acid
	D136G	Amino Acid
	D136N	Amino Acid
	H137P	Amino Acid
	H137R	Amino Acid
	C138R	Amino Acid
	C138S	Amino Acid
	C138Y	Amino Acid
	V139A	Amino Acid
	V139G	Amino Acid
	V139L	Amino Acid
	C139M	Amino Acid
	Q141.	Amino Acid
	T142A	Amino Acid
	T142M	Amino Acid
	T142K	Amino Acid
	A146T	Amino Acid
	A146V	Amino Acid
	A148Insertion	Amino Acid
	L151S	Amino Acid
	R154G	Amino Acid
	V155A	Amino Acid
	V155G	Amino Acid

		V155L	Amino Acid
		L159V	Amino Acid
		L159P	Amino Acid
		T160P	Amino Acid
		A161P	Amino Acid
		G162D	Amino Acid
		T168P	Amino Acid
		A171V	Amino Acid
		A171E	Amino Acid
		L172P	Amino Acid
		L172R	Amino Acid
		M175R	Amino Acid
		M175T	Amino Acid
		M175V	Amino Acid
		M175I	Amino Acid
		V180F	Amino Acid
		V180G	Amino Acid
		V170F	Amino Acid
		A286V	Amino Acid
		V359A	Amino Acid
		T400A	Amino Acid
		F424L	Amino Acid
		F424S	Amino Acid
		F424V	Amino Acid
		F425*	Amino Acid
		G426*	Amino Acid
		T427*	Amino Acid
		S428*	Amino Acid
		Q429*	Amino Acid
		L430*	Amino Acid
		S431*	Amino Acid
		Q432*	Amino Acid
		F433*	Amino Acid
		M434*	Amino Acid
		D435*	Amino Acid
		Q436*	Amino Acid
		N437*	Amino Acid
		N438*	Amino Acid
		P439*	Amino Acid
		L440*	Amino Acid
		S441*	Amino Acid
		G442*	Amino Acid
		L443*	Amino Acid
<i>rpoB</i>	Rifampicin		

		T444*	Amino Acid
		H445*	Amino Acid
		K446*	Amino Acid
		R447*	Amino Acid
		R448*	Amino Acid
		L449*	Amino Acid
		S450*	Amino Acid
		A451*	Amino Acid
		L452*	Amino Acid
		P454H	Amino Acid
		P454L	Amino Acid
		E460G	Amino Acid
		I480T	Amino Acid
		I480V	Amino Acid
		I491F	Amino Acid
		S493L	Amino Acid
		T676P	Amino Acid
		E761D	Amino Acid
		G981D	Amino Acid
<i>rpsL</i>	Streptomycin	K43*	Amino Acid
		K43R	Amino Acid
		K43T	Amino Acid
		K88*	Amino Acid
		K88Q	Amino Acid
		K88R	Amino Acid
		T40I	Amino Acid

Appendix II – Gene Maps With Primer Sites and Known SNPs

The following are annotated FastA maps of each gene targeted by the assay. Maps are annotated with the locations of the final assay primers, nested primers, known resistance SNPs, and any extragenic buffer included for the design of amplicons.

WHOLE GENE COVERAGE INCLUDES 300bp BRACKETING KNOWN GENE

Red = Non-Gene Extension Region

Green = Primer

Pink = Nested Primer

Yellow = Known Resistance SNP

>NC_000962.3:c2289600-2288300 Mycobacterium tuberculosis H37Rv,
pncA Pyrazinamide Resistance Gene (**TOTAL GENE COVERAGE**)

```
AATGCACTTCGCTTTTCATCGCTTACGTCCCTTGCCGGCGGTTTCCTTGCCCTGCGGTGGCGACGCACGATG
TGGCTGCATGTTCCGGCGGTGATATGGGGGATCGGCATCGCCGCTAAGCGGGTCGACTGCCCGCTGACCT
GGGTGGAGCGCTGGGCTCGCACCAAGGCCGCGATGACACCTCTGTCACCGGACGGATTTGTCTGCTCACTA
CATCACCGGCGTGATCTATCCCGCCGGTTGGGTGGCCGCCGCTCAGCTGGTCATGTTGCGCATCGTCGCG
GCGTCATGGACCCATATCTGTGGCTGCCGCGTCGGTAGGCAAACCTGCCCGGGCAGTCGCCCGAACGTAT
GGTGGACGTATGCGGGCGTTGATCATCGTCGACGTGCAGAACGACTTCTGCGAGGGTGGCTCGCTGGC
TACCGGTGGCGCCGCGCTGGCCGCGCCATCAGCGACTACCTGGCCGAAGCGGCGGACTACCATCAGT
CGTGCAACCAAGGACTTCCACATCGACCCGGTGACCACTTCTCCGGCAACACCGGACTATTCCTCGTCC
TGGCCACCGCATTGCGTCAGCGGTACTCCCGGCGGGACTTCCATCCCAGTCTGGACACGTCGGCAATCG
AGGCGGTGTTCTACAAGGGTGCCTACACCGGAGCGTACAGCGGCTTGAAGGAGTCGACGAGAACGGCAC
GCCACTGCTGAATTGGCTGCGGCAACGCGCGTTCGATGAGGTCGATGTGGTCGGTATTGCCACCGATCAT
TGTGTGCCAGACGGCCGAGGACGCGGTACGCAATGGCTTGCCACCAGGGTGTGGTGACCTGACAG
CGGGTGTGTCGGCCGATAACCACCGTCGCCGCGCTGGAGGAGATGCGCACCGCCAGCGTCGAGTTGGTTT
CAGCTCCTGATGGCACCGCCGAACCGGGATGAACTGTTGGCGGCGGTGGAGCGCTCGCCGCAAGCGGCCG
CCGCGCACGACCGCGCCGGCTGGGTGGGTGTTTACCGGTGACGCGCGGGTCGAAGACCCGGTGGGTT
GCAGCCGAGGTGGGGCATGAGGCCATCGGCCGCTTCTACGACACCTTCATCGGGCCGCGGGATATCAC
TTCCATCGCGATCTGGAATATCGTCTCCGGCACGGTGGTGCTGCGCGATCTCGAACTCGAGGTCGCGATG
ACTCGGCTGTGACGGTGTTCATTCCCGCCTTCTACGCTATGACCTACGACCGGTTACCGGCGAGTGGCA
GATTGCCGCACTGCGGGCGTACTGGGAGTTGCCGGCGATGA
```

>NC_000962.3:4246514-4249810 Mycobacterium tuberculosis H37Rv,
embB Ethambutol Resistance Gene (SNP at 306bp)

ATGACACAGTGC GCGAGCAGACGCAAAAAGCACCCCAAATCGGGCGATTTTGGGGGCTTTTGC GTCTGCTC
GCGGGACGCGCTGGGTGGCCACCATCGCCGGGCTGATTGGCTTTTGTGTTGTCGGTGGCGACGCCGCTGCT
GCCCGTTCGTGCAGACCACCGCGATGCTCGACTGGCCACAGCGGGGGCAACTGGGCAGCGTGACCGCCCCG
CTGATCTCGCTGACGCCGGTCGACTTTACCGCCACCGTGCCGTGCGACGTGGTGC GCGCCATGCCACCCG
CGGGCGGGGTGGTGTGGGCACCGCAACCAAGCAAGGCAAGGACGCCAATTTGCAGGCGTTGTTTCGTCTGT
CGT**C**AGCGCCAGCGCGTGGACGTACCGACCGCAACGTGGTGAT**C**TTGT**C**CGTG**C**CGCGAGCAGGTG
ACGTCCCCCGCAGTGTCAACGCATCGAGGTCACTGTACCCACGCCGGCACCTTCGCCAACTTCGTGCGGGC
TCAAGG**A**CCCGTCGGGCGCGCCGCTGCGCAGCGCTTCCCCGACCCCAACCTGCGCCCGAGATTGTGCGG
GG**T**GTTCACCGACCTGACCGGGCCCGCGCCCGCCGGGCTGGCGGTCTCGGGGACCATCGACACCCGGTTC
TCCACCCGGCC**G**ACCACGCTGAAACTGCTGGCGATCATCGGGGCGATCGTGCCAC**C**CGTCTGCGACTGA
TCGCGTTGTGGCGCCTGGACCAGTTGGACGGGCGGGG**CTCAATTGCCAGCTCCTCG**TCAGGCCGTTCCG
GCCTGCATCGTCGCCGGGCGGCATGCGCCGGCTGATTCGGGCAAGCTGGCGCACCTTCACCCTGACCGAC
GCCGTGGTGATATTGGCTTCTGCTCTGGCATGTTCATCGGCGCAATTCGTGCGACGACGGCTACATCC
TGGGCATGGCCGAGTCGCCGACCACGCCGGCTACATGTCCAATAATTTCCGCTGGTTCGGCAGCCCGGA
GGATCCCTTCGGCTGGTATTACAACCTGCTGGCGCTGATGACCATGTCAGCGACGCCAGTCTGTGGATG
CGCCTGCCAGACCTGGCCGCCGGGCTAGTGTGCTGGCTGCTGCTGTGCGGTGAGGTGCTGCCCGCCTCG
GGCCGGCGGTGGAGGCCAGCAAACCCGCTACTGGGCGGCGGCCATGGTCTTGCTGACCGCGTGGATGCC
GTTCAACAACGGCCTGCGGCCGGAGGGCATCATCGCGCTCGGCTCG**CTGGTCACTATGTGCTGA**TCGAG
CGGTCCATGCGGTACAGCCGGCTCACACCGGCGGCGCTGGCCGTCG**TTACCGCCGCATTACACT**GGGTG
TGCAGCCACCGGCTGATCGCGGTGGCCGCGCTGGTGGCCGGCGGCCGATGCTGCGGATCTTGGT
GCGCCGTATCGCCTGGTCGGCACGTTGCCGTTGGTGTGCGCGATGCTGGCCGCCGGCACCGTTCATCCTG
ACCGTGGTGTTCGCCGACCAGACCCTGTCAACGGTGTGGAAAGCCACCAGGGTTCGCGCCAAAATCGGGC
CGAGCCAGGCGTGGTATAACCGAGAACCTGCGTTACTACTACCTCATCCTGCCACCCTGACAGGTTCCGT
GTGCGCGCGCTTCGGCTTTTGTATCACCGCGCTGATGCCTGTTACCGCGGTGTTTCATCATGTTGCGCGC
AAGCGAATTC**C**CAGCGTGGCCCGCGGACCGCGGTGGCGGCTGATGGGCGTCACTTCGGCACCATGTT**C**
TCCTGATGTTACGCCCCACCAAGTGGGTGCACCACTTCGGGCTGTTCCGCCCGTAGGGGCGGCGATGGC
CGCGCTGACGACGGTGTGGTATCCCCATCGGTGCTGCGCTGGTTCGCGCAACCGGATGGCGTTCCCTGGCG
GCGTTATTCTTCTGCTGGCGTTGTGTTGGGCCACCACCAACGGCTGGTGGTATGTCTCCAGCTACGGTG
TGCCGTTCAACAGCGCGATGCCGAAGATCGACGGGATCACAGTCAGCACAATCTTTTTTCGCCCTGTTTGC
GATCGCCGCCGGCTATGCGGCCTGGCTGCACTTCGCGCCCCGCGGCGCCGGCGAAGGGCGGCTGATCCGC
GCGCTGACGACAGCCCCGGTACCGATCGTGGCCGGTTTCATGGCGCGGTGTTTCGTGCGCTCCATGGTGG
CCGGGATCGTGCACAGTACCCGACCTACTCCAACGGCTGGTCCAACGTGCGGGCGTTTGTGCGCGGCTG
CGGACTGGCCGACGACGTACTCGTCGAGCCTGATACCAATGCGGGTTTCATGAAGCCGCTGGACGGCGAT
TCGGGTTCTTGGGGCCCCCTTGGGCCCGCTGGGTGGAGTCAACCCGGTTCGGCTTCACGCCAACGGCGTAC
CGGAACACACGGTGGCCGAGGCGATCGTGATGAAACCCAACAGCCCGGACCGACTACGACTGGGATGC
GCCGACCAAGCTGACGAGTCTTGGCATCAATGGTTCACGGTGCCGCTGCCCTATGGGCTCGATCCCGCC
CGGGTACCGTTGGCAGGCACCTACACCACCGGCGCACAGCAACAGAGCACACTCGTCTCGGCGTGGTATC
TCCTGCCTAAGCCGGACGACGGGCATCCGCTGGTTCGTGGTGACCGCCGCGGGCAAGATCGCCGGCAACAG
CGTGTGACCGGTACACCCCCGGGCGACTGTGGTGCTCGAATACGCCATGCCGGGACCCGGAGCGCTG
GTACCCCGCCGGGCGGATGGTGCCCGACGACCTATACGGAGAGCAGCCCAAGGCGTGGCGCAACCTGCGCT
TCGCCCCGAGCAAAGATGCCCGCCGATGCCGTGCGGGTCCGGGTGGTGGCCGAGGATCTGTGCTGACACC
GGAGACTGGATCGCGGTGACCCCGCCGGGTACCGGACTACCGGACTGCGCTCACTGCAGGAATATGTGGGCTCG
ACGCAGCCGGTGTGCTGGACTGGGCGGTCGGTTTGGCTTCCCGTGCCAGCAGCCGATGCTGCACGCCA
ATGGCATCGCCGAAATCCCGAAGTTCCGCATCACACCGGACTACTCGGCTAAGAAGCTGGACACCGACAC
GTGGGAAGACGGCACTAACGGCGGCTGCTCGGGATCACCGACCTGTTGCTGCGGGCCACGTCATGGCC
ACCTACCTGTCCCGGACTGGGCCCGGATGGGGTTCCTGCGCAAGTTCGACACCCCTGGTCGATGCC
CTCCCGCCAGCTCGAGTTGGGCACCGCGACCCGACCGGCTGTGGTACCAGGGCAAGATCCGAATTGG
TCCATAG

>NC_000962.3:759807-763325 Mycobacterium tuberculosis H37Rv,
rpoB Rifampicin Resistance Gene (SNPs at 508-534bp)

TTGGCAGATTCCC GCCAGAGCAAAACAGCCGCTAGTCCTAGTCCGAGTCGCCCCGAAAGTTCTC GAATA
ACTCCGTACCCGGAGCGCAAACCGGGTCTCCTTCGCTAAGCTGCGCGAACC ACTTGAGGTTCCGGGACT
CCTTGACGTCCAGACCGATTTCGTTTCGAGTGGCTGATCGGTTTCGCCGCGCTGGCGCGAATCCGCCGCCGAG
CGGGGTGATGTCAACCCAGTGGGTGGCCTGGAAGAGGTGCTCTACGAGCTGTCTCCGATCGAGGACTTCT
CCGGGTGCATGTGCTTGTGCTTCTCTGACCCTCGTTTCGACGATGTCAAGGCACCCGTCGACGAGTGCAA
AGACAAGGACATGACGTACGCGGCTCCACTGTTTCGTCACCGCCGAGTTCATCAACAACAACACCGGTGAG
ATCAAGAGTCAGACGGTGTTCATGGGTGACTTCCCGATGATGACCGAGAAGGGCAGTTCATCATCAACG
GGACCGAGCGTGTGGTG GTCAGCCAGCTGGTTCGGTTCGCCCGGGTGTACTTCGACGAGACCATTGACAA
GTCCACCGACAAGACGCTGCACAGCGTCAAGGTGATCCCAGCCGCGCGCGTGGCTCGAGTTTGACGTC
GACAAGCGCGACACCGTCGGCGTGC GCATCGACCGCAAACGCCGCAACCGGTACCCGTGCTGCTCAAGG
CGCTGGGCTGGACCAGCGAGCAGATTGTC GAGCGGTTTCGGGTTCTCCGAGATCATGCGATCGACGCTGGA
GAAGGACAACACCGTCGGCACCGACGAGGCGCTGTTGGACA TCTACCGCAAGCTGCGTC CGGGCGAGCCC
CCGACCAAAGAGTCAGCGCAGACGCTGTTGGA AAACTGTTCTTCAAGGAGAAGCGCTACGACCTGGCCC
GCGTCGGTGCCTATAAGGTCAACAAGAAGCTCGGGCTGCATGTCGGCGAGCCCATCACGTCGTCGACGCT
GACCGAAGAAGACGTCGTGGCCACCATCGAATATCTGGTCCGCTTGCACGAGGGTTCAGACCACGATGACC
GTTCCGGGCGGGCTCGAGGTGCCGGTGGAAACCGACGACATCGACCACTTCGGCAACCGCCGCTGCGTA
CGGTTCGGCGAGCTGATCCAAAACAGATCCGGGTTCGGCATGTCGCGGATGGAGCGGTTGGTCCGGGAGCG
GATGACCACCCAGGACGTGGAGGCGATCACACCGCAGACGTTGATCAACATCCGGCCGTTGGTCCGCCGCG
ATCAAGGAGTTCTTCGGCACCCAGCCAGCTGAGCCAATTCATGGACCAGAACAACCCGCTGTCCGGGTTGA
CCCACAAGCGCCGACTGTCCGGCGCTGGGGCCCGGGCTCTGTACGTCGAGCGTGCCGGGCTGGAGGTCCG
CGACGTGCACCCGTCGCACTACGGCCGGATGTGCCGATCGAAAACCCCTGAGGGGCCCAACATCGGTCTG
ATCGGCTCGCTGTCCGGTGTACGCGCGGGTCAACCCGTTTCGGGTTTCATCGAAAACCGGTACCCGCAAGGTGG
TCGACGGCGT GGTAGCGACGAGATCGTGTACCTGACCGCCGACGAGGAGGACCGCCACGTGGTGGCACA
GGCAAATTCGCCGATCGATCGGACGGTTCGCTTCGTCGAGCCGCGCTGCTGGTCCGCCCAAGGCGGGC
CCACCGCGATGATTCCCTTCTGAGGACGACGACGCAACCCGTCCTCATGGGGCAACATGCAGCG
CCAGGCGGTGCCGCTGGTCCGTAGCGAGGCCCCGCTGGTGGGCACCGGGATGGAGCTGCGCGCGGGCATC
GACGCCGGCGACGTCGTCGTCGCCGAAGAAAGCGGCGTCATCGAGGAGGTGTCGGCCGACTACATCACTG
TGATGCACGACAACGGCACCCGGCTACCTACCGGATGCGCAAAGTTTGCCCGTCCAACACGGCACCTTG
CGCCAACAGTGCCCCATCGTGGCGACCGAGTCGAGGCCGGTTCAGGTGATCGCCGACGGTCCCTGTACT
GACGACGGCGAGATGGCGCTGGGCAAGAACTGCTGGTGGCCATCATGCCGTGGGAGGGCCACAACCTACG
AGGACCGGATCATCTGTCCAACCGCTGGTTCGAAGAGGACGTGCTCACCTCGATCCACATCGAGGAGCA
TGAGATCGATGCTCGCGACACCAAGCTGGGTGCGGAGGAGATCACCCGCGACATCCCGAACATCTCCGAC
GAGGTGCTCGCCGACCTGGATGAGCGGGGCATCGTGC GCATCGGTGCCGAGGTTTCGCGACGGGGACATCC
TGGTCCGCAAGGTACCCCCGAAGGGTGAGACCGAGCTGACGCCGAGGAGCGGCTGCTGCGTGCCATCTT
CGGTGAGAAGGCCCGCGAGGTGCGCGACACTTCGCTGAAGGTGCCGCACGGCGAATCCGGCAAGGTGATC
GGCATTCCGGGTGTTTTCCCGCGAGGACGAGGACGAGTTGCCGGCCGGTGTCAACGAGCTGGTGCGTGTGT
ATGTGGCTCAGAAACGCAAGATCTCCGACGGTGACAAGCTGGCCGGCCGGCACGGCAACAAGGGCGTGAT
CGGCAAGATCCTGCCGGTTGAGGACATGCCGTTCTTGGCGACGGCACCCCGGTGGACATTAATTTTGAAC
ACCCACGGCGTGCCGCGACGGATGAACATCGGCCAGATTTTGAGACCCACCTGGGTTGGTGTGCCACA
GCGGCTGGAAGGTTCGACGCCGCCAAGGGGGTTCCGGACTGGGCCGCCAGGCTGCCCGACGAACTGCTCGA
GGCGCAGGAACGCCATTGTGTGTCGACGCGGTTTCGACCGCGCCAGGAGGCCAGCTGCAGGGCCTG
TTGTGCTGCACGCTGCCAACC CGCAGCGGTGACGTGCTGGTTCGACCGCGCCAGGCAAGGCCATGCTCTTCG
ACGGGCGCAGCGGCGAGCCGTTCCCGTACCCGGTACCGGTTGGCTACATGTACATCATGAAGCTGCACCA
CCTGGTGGACGACAAGATCCACGCCCGCTCCACCGGGCCGTA CTGATGATCACCCAGCAGCCGCTGGGC
GGTAAGGCGCAGTTCCGGTGGCCAGCGGTTTCGGGGAGATGGAGTGTGGGCCATGCAGGCCTACGGTGTG
CCTACACCCTGCAGGAGCTGTTGACCATCAAGTCCGATGACACCGTCGGCCGCTCAAGGTGTACGAGGC
GATCGTCAAGGGTGAACAACATCCCGGAGCCGGGCATCCCGAGTCGTTCAAGGTGCTGCTCAAAGAACTG
CAGTCGCTGTGCCTCAACGTCGAGGTGCTATCGAGTGACGGTGC GGCGATCGAACTGCGCGAAGGTGAGG
ACGAGGACCTGGAGCGGGCCGCGGCCAACCTGGGAATCAATCTGTCCCGCAACGAATCCGCAAGTGTCTGA
GGATCTTGCGTAA

>NC_000962.3:1673100-1674500 Mycobacterium tuberculosis H37Rv,
fabG1 Isoniazid & Ethionamide Resistance Gene (**TOTAL GENE COVERAGE, SNP
at 15**)

ACCTTCAAATCGGTGGCCTGTATCAGGGCGTTCGACGGCCGCGACGGCGGGGTCCAATGGAAATCGACTGG
TCAGGTTCGAGCGCCGTTTCGCTCCGGTGTGGTTCACGCGCATGCCCTCGATGACGCAGATCTCGTCGGGGCTC
GATGCGCTCTTCCCAGACTTGCAGCCCCGGGGCACGGCGGGGTTGGTGTTCGATGATCGCGGGCGGGAAGA
TCCGCGTTCGATCCACTTGGCGCCATGGAAGGCAGAAGCCGAGTAGCCGGCCAGCACGCCGCGGGCGGCGCG
AGCGCAGCCACAGCGCTTTTGCACGCAATTGCGCGGTCAGTTCCACACCCTGCGGCACGTACACGTCTTT
ATGTAGCGCGACATACCTGCTGCGCAATTCGTAGGGCGTCAATACACCCGACGCCAGGGCCTCGCTGCC
AGAAAGGGATCCGTCAATGGTCGAAGTGTGCTGAGTCAACCCGACAAACGTACGAGCGTAACCCAGTGC
GAAAGTTCCCGCCGGAAATCGCAGCCACGTTACGCTCGTGGACATAACCGATTTCCGGCCCGGCGCGGCGA
GACGATAGGTTGTCCGGGTGACTGCCACAGCCACTGAAGGGGCCAAACCCCATTCGTATCCCGTTCAGT
CCTGGTTACCGGAGGAAACCGGGGGATCGGGCTGGCGATCGCACAGCGGCTGGCTGCCGACGGCCACAAG
GTGGCCGTCACCCACCGTGGATCCGGAGCGCCAAAGGGGCTGTTTGGCGTCGAATGTGACGTCACCGACA
GCGACGCCGTCGATCGCGCCTTACGGCGGTAGAAGAGCACCAGGGTCCGGTTCGAGGTGCTGGTGTCCAA
CGCCGGCCTATCCGCGGACGCATTCTCATGCGGATGACCGAGGAAAAGTTCGAGAAGGTCATCAACGCC
AACCTCACCGGGGCGTTCCGGGTGGCTCAACGGGCATCGCGCAGCATGCAGCGCAACAAATTCGGTCGAA
TGATATTCATAGGTTCCGGTCTCCGGCAGCTGGGGCATCGGCAACCAGGCCAACTACGCAGCCTCCAAGGC
CGGAGTGATT

>NC_000962.3:c2156111-2153889 Mycobacterium tuberculosis H37Rv,
katG Isionazid Resistance Gene (SNP at 315bp)

GTGCCCCGAGCAACACCCACCCATTACAGAAACCACCACCGGAGCCGCTAGCAACGGCTGTCCCGTTCGTGG
GTCATATGAAATACCCCGTCGAGGGCGGCGGAAACCAGGACTGGTGGCCCAACCGGCTCAATCTGAAGGT
ACTGCACCAAAACCCGGCCGTCGCTGACCCGATGGGTGCGGCGTTCGACTATGCCCGGAGGTTCGCGACC
ATCGACGTTGACGCCCTGACGCGGGACATCGAGGAAGTGATGACCACCTCGCAGCCGTGGTGGCCCCGCC
ACTACGGCCACTACGGGCCGCTGTTTATCCGGATGGCGTGGCACGCTGCCGGCACCTACCGCATCCACGA
CGGCCGCGGCGGCGCCGGGGCGGCATGCAGCGGTTCGCGCCCTTAACAGCTGGCCCCGACAACGCCAGC
TTGGACAAGGCGCGCCGGCTGCTGTGGCCGGTCAAGAAGAAGTACGGCAAGAAGCTCTCATGGGCGGACC
TGATTGTTTTTCGCGGCAACTGCGCGCTGGAATCGATGGGCTTCAAGACGTTCCGGTTCGGCTTCGGCCG
GGTCGACCAGTGGGAGCCCGATGAGGTCTATTGGGGCAAGGAAGCCACCTGGCTCGGCGATGAGCGTTAC
AGCGGTAAGCGGGATCTGGAGAACCCGCTGGCCGCGGTGCAGATGGGGCTGATCTACGTGAACCCGGAGG
GGCCGAACGGCAACCCGGACCCCATGGCCGCGGCGGTGCACATTCGCGAGACGTTTCGGCGCATGGCCAT
GAACGACGTCGAAACAGCGGCGCTGATCGTCGGCGGTACACTTTCGGTAAGACCCATGGCGCCGGCCCCG
GCCGATCTGGTTCGGCCCCGAACCCGAGGCTGCTCCGCTGGAGCAGATGGGCTTGGGCTGGAAGAGCTCGT
ATGGCACCGGAACCGGTAAGGACCGCATCACCAGCGGCATCGAGGTTCGTATGGACGAACACCCCGACGAA
ATGGGACAACAGTTTTCTCGAGATCCTGTACGGCTACGAGTGGGAGCTGACGAAGAGCCCTGCTGGCGCT
TGGCAATACACCGCAAGGACGGCGCCGGTGCCGGCACCATCCCGGACCCGTTTCGGCGGGCCAGGGCGCT
CCCCGACGATGCTGGCCACTGACCTCTCGCTGCGGGTGGATCCGATCTATGAGCGGATCACGCGTCGCTG
GCTGGAACACCCCGAGGAATTGGCCGACGAGTTCGCCAAGGCCTGGTACAAGCTGATCCACCGAGACATG
GGTCCCGTTGCGAGATACTTGGGCCGCTGGTCCCCAAGCAGACCCTGCTGTGGCAGGATCCGGTCCCTG
CGGTACAGCCACGACCTCGTCGGCGAAGCCGAGATTGCCAGCCTTAAGAGCCAGATCCGGGCATCGGGATT
GACTGTCTCACAGCTAGTTTTGACCCGATGGGCGGCGGCGTTCGTCGTTCCGTGGTAGCGACAAGCGCGGC
GGCGCCAACGGTGGTTCGCATCCGCTGCAGCCACAAGTCGGGTGGGAGGTCAACGACCCCGACGGGGATC
TGGCAAGGTCATTCGCACCCTGGAAGAGATCCAGGAGTCATCAACTCCGCGGCGCCGGGGAACATCAA
AGTGTCCCTTCGCGGACCTCGTCGTGCTCGGTGGCTGTGCCGCATAGAGAAAGCAGCAAAGGCGGCTGGC
CACAACATCACGGTGCCTTCACCCCGGGCCGCACGGATGCGTCGAGGAACAACCCGACGTGGAATCCT
TTGCCGTGCTGGAGCCCAAGGCAGATGGCTTCCGAAACTACCTCGGAAAGGGCAACCCGTTGCCGGCCGA
GTACATGCTGCTCGACAAGGCGAACCTGCTTACGCTCAGTGCCCTGAGATGACGGTGTGGTAGGTGGC
CTGCGCGTCTCGGCGCAAACTACAAGCGCTTACCCTGGGCGTGTTCACCGAGGCCCTCCGAGTCACTGA
CCAACGACTTCTTCGTGAACCTGCTCGACATGGGTATCACCTGGGAGCCCTCGCCAGCAGATGACGGGAC
CTACCAGGGCAAGGATGGCAGTGGCAAGGTGAAGTGGACCGGCAGCCGCTGGACCTGGTCTTCGGGTCC
AACTCGGAGTTGCGGGCGCTTGTTCGAGGTCTATGGCGCCGATGACGCGCAGCCGAAGTTCGTGCAGGACT
TCGTGCTGCCTGGGACAAGGTGATGAACCTCGACAGGTTCGACGTGCGCTGA

>NC_000962.3:1673900-1675300 Mycobacterium tuberculosis H37Rv,
inhA Isionazid & Ethionamide Resistance Gene **(TOTAL GENE COVERAGE)**

```
CAGCCTCCAAGGCCGGAGTGATTGGCATGGCCCCGCTCGATCGCCCCGCGAGCTGTGGAAGGCAAACGTGAC
CGCGAATGTGGTGGCCCCGGGCTACATCGACACCGATATGACCCGCGCGCTGGATGAGCGGATTCAGCAG
GGGGCGCTGCAATTTATCCCAGCGAAGCGGGTCGGCACCCCCGCCGAGGTGCGCCGGGTGGTTCAGCTTCG
TGGCTTCCGAGGATGCGAGCTATATCTCCGGTTCGGTTCATCCCGGTTCGACGGCGGCATGGGTATGGGCCA
CTGACACAACAAGGACGCACATGACAGGACTGCTGGACGGCAAACGGATTCTGGTTAGCGGAATCATC
ACCGACTCGTCGATCGCGTTTACATCGCACGGGTAGCCCAGGAGCAGGGCGCCCAGCTGGTGCTCACCG
GGTTCGACCCGGCTGCGGCTGATTCAGCGCATACCGACCGGCTGCCGGCAAAGGCCCGCTGCTCGAACT
CGACGTGCAAAACGAGGAGCACCTGGCCAGCTTGGCCGGCCGGGTGACCGAGGCATCGGGGCGGGCAAC
AAGCTCGACGGGGTGGTGCATTTCGATTGGGTTTCATGCCCGACAGCCGGATGGGCATCAACCCGTTCTTCG
ACGCGCCCTACGCGGATGTGTCCAAGGGCATCCACATCTCGGCGTATTCGTATGCTTCGATGGCCAAGGC
GCTGCTGCCGATCATGAACCCCGGAGGTTCCATCGTCGGCATGGACTTCGACCCGAGCCGGGCGATGCCG
GCCTACAACCTGGATGACGGTCGCCAAGAGCGCGTTGGAGTCGGTCAACAGGTTTCGTGGCGCGGAGGCCG
GCAAGTACGGTGTGCGTTTCGAATCTCGTTGCCCGAGGCCCTATCCGGACGCTGGCGATGAGTGCGATCGT
CGGCGGTGCGCTCGGCGAGGAGGCCGGCGCCAGATCCAGCTGCTCGAGGAGGGCTGGGATCAGCGCGCT
CCGATCGGCTGGAACATGAAGGATGCGACGCCGGTCGCCAAGACGGTGTGCGCGCTGCTGTCTGACTGGC
TGCCGGCGACACGGGTGACATCATCTACGCCGACGGCGGCGCGCACACCCAATTGCTCTAGAACGCATG
CAATTTGATGCCGTCTCTGCTGCTGCTCGTTTCGGCGGACCGGAAGGGCCCGAGCAGGTGCGGCCGTTCTGG
AGAACGTTACCCGGGGCCGCGGTGTGCCTGCCGAACGGTTGGACGCGGTGGCCGAGCACTACCTGCATTT
CGGTGGGGTATCACCGATCAATGGCATTAAATCGCACACTGATCGCGGAGCTGGAGGCCGAGCAAGAAGT
CCGGTGTACTTCGGTAACCGCAACTGGGAGCCGTATGTAGAAGATGCCGTTACGGCCATGCGCGACAACG
G
```

>NC_000962.3:c2713000-2714124 Mycobacterium tuberculosis H37Rv,
eis Kanamycin Resistance Gene (SNP at 12-37bp, EXTENDED TO ALLOW)

TCGTGATGGCATTCACTGGAATTTTGAAGCCCACCAGGCGGTGCGCGAACTGATGCTCAAGGCACCTGGCC
GAAGCCGGGGTGC CGAACGAGAAATCGCGCGGCTGAGACATGCCCCGCGCCGGCGACGATGCAGAGCGAA
GCGATGAGGTGGGGGCACCTCCCCTTGC GGGGGAGAGCGGCGCCGGTGACCGTTGTGGTGGTGACCGAT
ACGTCGTGTGCACTGCCGGCCGACCTGCGCGAACAGTGGTGCATCCGCCAGGTCCCCTGCATATCTTGC
TTGACGGCCTCGACCTGCGCGACGGTGTGGACGAAATCCCCGATGACATCCACAAGCGCCACGCCACCAC
CGCTGGGGCCACCCCGTTGAGCTGTCCGCCCTACCAACGGGCGTTGGCGGACAGTGGCGGGCAGCGG
GTAGTGGCGGTGCACATTTCGTGCGGCGCTGTCCGGTACCTTTCGAGCCGCCGAGCTGACCGCGGCGAAC
TAGGTCCCCTCGTTAGGGTGCATCGACTCGAGTCCGGCCGCGATGGGCGTTCGTCGGCACTGGCGGC
CGGGCGGGCAGCCCGCAGGCGATGAGTGGATACGGTTCGCGCGCAGCGGCTGCGGGCGTAAAGCCGG
ATTCACGCGTTCGTGCTGTAGCGCGGTTGGACAATCTGCGCCGACGCGGGCGCATCAGTGGGGCCAAGG
CATGGTTGGGCACCGCGCTGGCGCTCAAGCCGCTGCTGTGAGTGCACGACGAAAACTTGTTCGTGGTCCA
ACGGGTTGCACTGTGAGCAACGCGACGGCGGTGATGATCGACCGGGTTTGCCAGCTTGTGCGGCGACCGC
CCCCCGCTCTCGCGGTGCATCACGTGCGCGACCCGGCAGCTGCGAACGACGTGGCGGGCGGCGCTGGCGG
AGCGGCTGCCGGCGTGTGAGCCGGCCATGGTGAACCGCATGGGACCGGTACTTGTCTGACAGTCCGGTGC
CGGAGCCGTGCGGGTATGCGTGCAGCTGGGAGCGTTCGCCCGCAGCGTAACGTACAGGGCAAATTCGTGCG
TGATTCTGCGAGTGGCGTACGCTGGCGGGGCTACCCG**ATCGCGTGATCCTTTGCCA**GACACTGTGCTGC
GTAATATTCAGTGCAGTGGCCCGCGCATATGCCACAGTCCGAT**TCTGGTACTGTGACCCTGT**GTAGCCCG
ACCGAGGACGACTGGCCGGGGATGTTCTACTGGCCGCGGCCAGTT
TCACCGATTTTCATCGGCCCTGAATCAGCGACCGCTGGCGGACCCTGGTGCCACCGACGGAGCGGTGGT
GGTCCGCGATGGTGCCGGCCCCGGTTCTGAGGTGGTTCGGGATGGCGCTGTACATGGATCTGCGGTTGACG
GTGCCTGGTGAAGTGGTGTCTCCGACCGCCG**GTCTCAGTTTCGTTCGCGGT**GGCGCCGACGCATCGCCGGC
GCGGCTTGTGCGCGGATGTGCGCCGAACTGCACCGCCGCATAGCCGATTCGGCTATCCGGTTCGCGGC
ACTGCATGCTAGCGAGGGCGGCATCTACGGCCGGTTCGGCTACGGGCCCGCTACCACCTTGATGAGCTG
ACGGTGCACCGACGCTTCGCGCGCTTTCACGCCGACGCACCGGGCGGCGGCTAGGTGGCAGCAGCGTCC
GGTTGGTCAGACCCACCGAGCATCGCGGGCAGTTTGAGGCGATCTACGAGCGATGGCGCCAGCAGGTGCC
GGGCGGGCTGCTACGCCCGCAGGTGCTCTGGGACGAGCTGCTGGCAGAATGCAAAGCCGCGCCCGGTGGA
GACCGTGAATCGTTTCGCTTACTGCATCCCGACGGGTACGCGCTGTACCGGGTGGATCGCACCGATCTCA
AGCTAGCGCGCGTACGCGAACTCAGGGCGGTAACCGCAGATGCGCATTTGTGCGTTGTGGCGGGCCCTGAT
TGGCCTCGACTCCATGGAGCGAATCAGCATCATCACCCATCCACAGGACCCGTTACCCACCTGCTCACC
GATACCCGACTGGCCCGCACTACCTGGCGCCAGGACGGCCTGTGGTTGCGCATCATGAACGTACCGGCCG
CACTCGAGGGCGGTGGTTACGCTCACGAAGTTGGCGAGTTTTCACGGTCTTCGAGGTATCCGATGGCGG
CCGTTTCGCGCTCAAGATCGGTGACGGCCGTGCGCGGTGTACCCCGACCGATGCGGCAGCCGAGATCGAA
ATGGATCGGGACGTAAGTGGGACGCTTTACCTTGGAGCGCACCGCGCTTCGACGTTAGCCGCCGTAACC
GGTTGCGCACCAAAGATTCCCAGCTGCTTCGTGCACTCGAC**GCGGCGTTTGCCAGTGATGTTCCCGTCCA**
GACCGGTTCGAGTTCTGAAGGCCGTGCTAGGCCGGCGCTAGGCTGACGGGCTTTTCGGCGTGGTCAAGC
ACCCGCGTGTGCGCGCCGGCTTCGGTCCGCACACGCCATGGATGGGGATCGGCCCGCGCGGCTCAGCACT
CGCGGATCGCGTTGCCGAGTACACTCTCGATCGCGGTGAGCCGAGTCCGGATGGACGTCGACGCCCGGTG
CTGGTTGTTTCGGGGATGTTGGCGCGGTTTGTCCCATCTTGATCCATCGCCAAAGCGGCTTGTCCACAGCC
TCGGATTGATCCACAGCAGGGCAGCGCGACCGCGTTCGTG

>NC_000962.3:1471846-1474000 Mycobacterium tuberculosis H37Rv,
rrs Amikacin Resistance Gene (SNP at 1401bp, EXTENDED TO ALLOW, Partial
overlap with RRL)

TTTTGTTTGGAGAGTTTGTATCCTGGCTCAGGACGAACGCTGGCGGCGTGCTTAACACATGCAAGTCGAAC
GGAAAGGTCTCTTCGGAGATACTCGAGTGGCGAACGGGTGAGTAACACGTGGGTGATCTGCCCTGCACTT
CGGGATAAGCCTGGGAAACTGGGTCTAATACCGGATAGGACCACGGGATGCATGTCTTGTGGTGGAAAGC
GCTTTAGCGGTGTGGGATGAGCCCGCGCCTATCAGCTTGTGGTGGGGTGACGGCTACCAAGGCGACG
ACGGGTAGCCGGCCTGAGAGGGTGTCCGGCCACACTGGGACTGAGATACGGCCAGACTCCTACGGGAGG
CAGCAGTGGGGAATATTGCACAATGGGCGCAAGCCTGATGCAGCGACGCCGCTGGGGGATGACGGCCTT
CGGGTTGTAAACCTCTTTCACCATCGACGAAGTCCGGGTCTCTCGGATTGACGGTAGGTGGAGAAGAA
GCACCGGCCAACTACGTGCCAGCAGCCGCGTAATACGTAGGGTGCAGCGCTTGTCCGGAATTACTGGGC
GTAAAGAGCTCGTAGGTGGTTTGTTCGCGTTGTTTCGTGAAATCTCACGGCTTAACTGTGAGCGTGCGGCG
ATACGGGCAGACTAGAGTACTGCAGGGGAGACTGGAATTCCTGGTGTAGCGGTGGAATGCGCAGATATCA
GGAGGAACACCGGTGGCGAAGGCGGGTCTCTGGGCAGTAACTGACGCTGAGGAGCGAAAAGCGTGGGGAGC
GAACAGGATTAGATACCCTGGTAGTCCACGCCGTAACGGTGGGTACTAGGTGTGGGTTCCTTCCTTGG
GATCCGTGCCGTAGCTAACGCATTAAGTACCCCGCCTGGGGAGTACGGCCGCAAGGCTAAAACCTCAAAGG
AATTGACGGGGCCCCGACAAAGCGGCGGAGCATGTGGATTAATTCGATGCAACGCGAAGAACCTTACCTG
GGTTTGCATGCACAGGACCGCTCTAGAGATAGGCGTTCCCTTGTGGCTGTGTGCAGGTGGTGCATGGC
TGTCGTCAGCTCGTGTGCTGAGATGTTGGGTTAAGTCCCAGCAACGAGCGCAACCCCTGTCTCATGTTGCC
AGCACGTAATGGTGGGGACTCGTGTAGAGACTGCCGGGGTCAACTCGGAGGAAGGTGGGGATGACGTCAAG
TCATCATGCCCTTATGTCCAGGGCTTCACACATGCTACAATGGCCGGTACAAAGGGCTGCGATGCCCGG
AGGTAAAGCGAATCCTTAAAAGCCGGTCTCAGTTCCGGATCGGGGTCTGCAACTCGACCCCGTGAAGTCGG
AGTCGCTAGTAAATCGCAGATCAGCAACGCTGCGGTGAATACGTTCCCGGGCCTTGTACACACCGCCCGTC
ACGTGATGAAAGTCGGTAACACCCGAAGCCAGTGGCCTAACCTCGGGAGGGAGCTGTGCAAGGTGGGAT
CGGCGATTGGGACGAAGTCGTAACAAGGTAGCCGTACCGGAAGGTGCGGCTGGATCACCTCCTTTCTAAG
GAGCACCACGAAAACGCCCCAACTGGTGGGGCGTAGGCCGTGAGGGGTTCTTGTCTGTAGTGGGCGAGAG
CCGGGTGCATGACAACAAGTTGGCCACCAACACACTGTTGGTCTCTGAGGCAACACTCGGACTTGTTC
AGGTGTTGTCCACCGCCTTGGTGGTGGGGTGTGGTGTGAGAACTGGATAGTGGTTGCGAGCATCAAT
GGATACGCTGCCGGCTAGCGGTGGCGTGTCTTTGTGCAATATTCTTTGGTTTTTGTGTGTGTTGTAAGT
GTCTAAGGGCGCATGGTGGATGCCTTGGCATCGAGAGCCGATGAAGGACGTGGGAGGCTGCGATATGCCT
CGGGGAGCTGTCAACCGAGCGTGGATCCGAGGATTTCCGAAATGGGGAAAACCCAGCAGAGTGTGTCGTG
CTACCCGCATCTGAATATATAGGGTGGCGGAGGGAACCGGGGAAGTGAACATCTCAGTACCCGTAGGA
GGAGAAAACAATTGTGATTCCGCAAGTAGTGGCGAGCGAACCGGAACAGGCTAAACCGCACGCATGGGT
AACCGGGTAGGGGTTGTGTGTGCGGGGTTGTGGGAGGATATGTCTCAGCGCTACC

>NC_000962.3:1917640-1919046 Mycobacterium tuberculosis H37Rv,
tlyA Capreomycin Resistance Gene (TOTAL GENE COVERAGE)

```
GCCGATCTTCACCAGCGGCCACTGCGCATCGAGGCCGGCGACGAGCGGGCCCGTGCGGCCCTTGCAACGCT
GGTCGTTGATGCCGACGGATCATCCGGTGACTAGCGTAGGAACGCAATGACCATCGATCCTGACCAGATC
CGTGCCGAAATCGACGCCCTACTTGCTTCGCTGCCCGACCCCGCGACGCCGAGAACGGACCGTCTCTGG
CCGAACTCGAAGGCATCGCACGTCGCTTTCCGAGGCGCACGAGGTGTTGTTGGCCGCCCTGGAGTCGGC
GGAGAAGGGTTGAGTGCGGCGTGGCACGACGTGCCCGGTTGACGCGAGCTAGTCCGGCGGGGCTGGC
GCGATCACGTCACAGGCCGCGGAGTTGATCGGCGCCGGCAAGGTGCGCATCGACGGGCTGCCGGCGGTC
AAGCCGGCCACCGCCGTGTCCGACACCACCGCGCTGACCGTGGTGACCGACAGTGAACGCGCCTGGGTAT
CGCGCGGAGCGCACAAACTAGTCGGTGCCTGGAGGCGTTCGCGATCGCGGTGGCGGGCCGCGCTGTCT
GGACGCGGGCGCATCGACCGGTGGGTTCACCGAAGTACTGCTGGACCGTGGTGCCGCCACGTGGTGGCC
GCCGATGTCCGATACGGCCAGCTGGCGTGGTTCGCTGCGCAACGATCCTCGGGTGGTGGTCCTCGAGCGGA
CCAACGCACGTGGCCTCACACCGGAGGCGATCGGCGGTTCGCGTTCGACCTGGTAGTGGCCGACCTGTCGTT
CATCTCGTTGGCTACCGTGTGGCCGCGCTGGTTGGATGCGCTTCGCGCGACGCCGATATCGTTCCACTG
GTGAAGCCGAGTTTGAGGTGGGAAAGGTCAGGTGCGCCCCGGTGGGGTGGTCCATGACCCGAGTTGC
GTGCGCGGTTCGGTGTCTCGCGGTTCGCGCGGCGGGCACAGGAGCTGGGCTGGCACAGCGTCGGCGTCAAGGC
CAGCCCGCTGCCGGGCCCATCGGGCAATGTCGAGTACTTCTGTGGTTGCGCACGCAGACCACCGGGCA
TTGTTCGGCCAAGGGATTGGAGGATGCGGTGCACCGTTCGCGATTAGCGAGGGCCCGTAGTGACCGCTCATCG
CAGTGTTCTGCTGGTTCGTCACACCGGGCGGACGAAGCCACCGAGACCGCACGGCGCGTAGAAAAAGTA
TTGGGCGACAATAAAATTGCGCTTCGCGTGTCTCGGCCGAAGCAGTCGACCGAGGGTTCGTTGCATCTGG
CTCCCAGACATGCGGGCCATGGGCGTTCGAGATCGAGGTGGTTGACCGGACAGCACGCAGCCGACGG
CTGCGAACTGGTGTGGTTTTGGGCGGCGATGGCACCTTTTTGCGGGCAGCCGAGCTGGCCCGCAACGCC
AGCATTC
```

>NC_000962.3:7302-9818 Mycobacterium tuberculosis H37Rv,
gyrA Fluoroquinolones Resistance Gene (SNP at 74bp)

ACGGTCTGCTGGAGGCGGGGCTGAAGGCCGGGAAGAAGATCAACAAGGAAGACGGCATTTCAGCGGTACAA
GGGTCTAGGTGAAATGGACGCTAAGGAGTTGTGGGAGACCACCATGGATCCCTCGGTTTCGTGTGTTGCGT
CAAGTGACGCTGGACGACGCCGCCGCCGACGAGTTGTTCTCCATCCTGATGGGCGAGGACGTCGACG
CGCGGGCGAGCTTTATCACCCGCAACGCCAAGGATGTTTCGGTTCTTGGATGTCTAACGCAACCCTGCGTT
CGATTGCAAACGAGGAATAGATGACAGACACGACGTTGCCGCCTGACGACTCGCTCGACCGGATCGAACC
GGTTGACATCGAGCAGGAGATGCAGCGCAGCTACATCGACTATCGATGAGCGTGATCGTCGGCCGCGCG
CTGCCCGAGGTGCGCGACGGGCTCAAGCCCGTGCATCGCCGGGTGCTCTATGCAATGTTTCGATTCCGGCT
TCCGCCCGGACCGCAGCCAGCCAGTCCGCGCCGGTTCGGTTCGCCGAGACCATGGGCAACTACCACCCGCA
CGGCGACGCGTCGATCTACGACAGCCTGGTGCGCATGGCCCAGCCCTGGTCGCTGCGCTACCCGCTGGTG
GACGGCCAGGGCAACTTCGGCTCGCCAGGCAATGACCCACCGCGCGGATGAGGTACACCGAAGCCCGGC
TGACCCCGTTGGCGATGGAGATGCTGAGGGAAAATCGACGAGGAGACAGTCGATTTTCATCCCTAACACGA
CGGCCGGGTGCAAGAGCCGACGGTGCTACCCAGCCGGTTCCCAACCTGCTGGCCAACGGGTCAGGCGGC
ATCGCGGTTCGGCATGGCAACCAATATCCCGCCGACAACCTGCGTGAGCTGGCCGACGCGGTGTTCTGGG
CGCTGGAGAATCACGACGCCGACGAAGAGGAGACCCTGGCCGCGGTCATGGGGCGGGTTAAAGGCCCGGA
CTTCCCGACCGCCGGACTGATCGTCGGATCCAGGGCACCCTGATGCTTACAAAACCTGGCCGCGCTCC
ATTTCGAATGCGCGGAGTTGTTGAGGTAGAAGAGGATTCGCCGCGTTCGTACCTCGCTGGTATCACCGAGT
TGCCGTATCAGGTCAACCACGACAACCTTCATCACTTCGATCGCCGAACAGGTCGAGACGGCAAGCTGGC
CGGCATTTCCAACATTGAGGACCAGTCTAGCGATCGGGTCGGTTTACGCATCGTCATCGAGATCAAGCGC
GATGCGGTGGCCAAGGTGGTGATCAATAACCTTTTACAAGCACACCCAGCTGCAGACCAGCTTTGGCCCA
ACATGCTAGCGATCGTCGACGGGGTGC CGCGCACGCTGCGGCTGGACCAGCTGATCCGCTATTACGTTGA
CCACCAACTCGACGTCATTGTGCGGCGCACCACTACCGGCTGCGCAAGGCAAACGAGCGAGCCACATT
CTGCGCGGCCTGGTTAAAGCGCTCGACGCGCTGGACGAGGTCATTCGACTGATCCGGGCGTCGGAGACCG
TCGATATCGCCCGGGCCGGACTGATCGAGCTGCTCGACATCGACGAGATCCAGGCCAGGCAATCCTGGA
CATGCAGTTGCGCGCCTGGCCGACTGGAACGCCAGCGCATCATCGACGACCTGGCCAAAATCGAGGCC
GATGATCGCCGATCTGGAAGACATCCTGGCAAAACCCGAGCGGCAGCGTGGGATCGTGCAGCAGCAACTCG
CCGAAATCGTGGACAGGCACGGCGACGACCGGCTACCCGGATCATCGCGGCGACGGAGACGTCAGCGA
CGAGGATTTGATCGCCCGCGAGGACGTCGTTGTCACTATCACCGAAACGGGATACGCCAAGCGCACCAAG
ACCGATCTGTATCGCAGCCAGAAACCGCGCGCAAGGGCGTGCAGGGTGCGGGGTTGAAGCAGGACGACA
TCGTGCGCACTTCTTCGTGTGCTCCACCCACGATTTGATCCTGTCTTACCACCCAGGGACGGGTTTA
TCGGGCCAAGGCCTACGACTTGCCCGAGGCTCCCGGACGGCGCGGGCAGCACGTGGCCAACCTGTTA
GCCTTCCAGCCCGAGGAACGCATCGCCAGGTCATCCAGATTCGCGGCTACACCGACGCCCCGTACCTGG
TGCTGGCCACTCGCAACGGGCTGGTGA AAAAGTCCAAGCTGACCGACTTCGACTCCAATCGCTCGGGCGG
AATCGTGGCGGTCAACCTGCGCGACAACGACGAGCTGGTGGTGGTGGTGTGTTTCGGCCGGCGACGAC
CTGCTGCTGGTCTCGGCCAACGGGCAGTCCATCAGGTTCTCGGCGACCGACGAGGCGCTGCGGCCAATGG
GTCGTGCCACCTCGGGTGTGCAGGGCATGCGGTTCAATATCGACGACCGGCTGCTGTCGCTGAACGTCGT
GCGTGAAGGCACCTATCTGCTGGTGGCGACGTCAGGGGGCTATGCGAAACGTACCGCGATCGAGGAATAC
CCGGTACAGGGCCGCGGGGTAAGGTGTGCTGACGGTCATGTACGACCGCCGGCGCGGACGGTTGGTTG
GGGCGTTGATTGTGACGACGACAGCGAGCTGTATGCCGTCCTTCCGGCGGTGGCGTGATCCGCACCGC
GGCACGCCAGGTTTCGCAAGGCGGGACGGCAGACCAAGGGTGTTCGGTTGATGAATCTGGGCGAGGGCGAC
ACACTGTTGGCCATCGCGCGCAACGCCAAGAAAAGTGGCGACGATAATGCCGTGGACGCCAACGGCGCAG
ACCAGACGGGCAATTAA

>NC_000962.3:c4408500-4407200 Mycobacterium tuberculosis H37Rv,
gidB Streptomycin Resistance Gene (TOTAL GENE COVERAGE)

ACGAGGTGGCGCGGCGAGTGGCCGAAACCGGTGACCGCGAGGAACTCGTTCCAATGACGCGCTTCGAACG
GAAGATCGTCCACGATGCGGTTGCAGCGGTGCCAGGTGTGCACAGCGAAAGCGAAGGCGTGGAGCCAGAA
CGCCGAGTGGTGTGCTCCGCGACTAGCTCGCGAGCCAGCGGCTCCGACCGACGCCGAGTAAGCGATGC
GTGGCCGAGCGGCTGGGCCAGCGTCTCGAGAGCGGAGAATGTTTCACGTGAAACA **TGACACAGACCTCAC**
GAGCCGGCGGAGTGCCTAATGTCTCCGATCGAGCCCGCGGCTCTGCGATCTTCGGACCGCGGCTTGGCC
TTGCTCGGCGGTACGCCGAAGCGTTGGCGGGACCCGGTGTGGAGCGGGGGCTGGTGGGACCCCGGAAGT
CGGTAGGCTATGGGACCGGCATCTACTGAACTGCGCCGTGATCGGTGAGCTCCTCGAACGCGGTGACCGG
GTCGTGGATATCGGTAGCGGAGCCGGGTTGCCGGGCGTGCCATTGGCGATAGCGCGGCCGACCTCCAGG
TAGTTCTCCTAGAACCGCTACTGCGCCGCACCGAGTTTCTTCGAGAGATGGTGACAGATCTGGG **CGTGGC**
CGTTGAGATCGTGCGGGGGCGCGCCGAGGAGTCCCTGGGTGCAGGACCAATTGGGCGGCAGCGACGCTGCG
GTGTACGGGCGGTG **GCCGCGTTGGACAAGTTG**ACGAAATGGAGCATGCCGTTGATACGGCCGAACGGGC
GAATGCTCGCCATCAAAGGCGAGCGGGCTCACGACGAAGTACGGGAGCACCGGCGTGTGATGATCGCATC
GGGCGCGTTGATGTGAGGGTGGTGACATGTGGCGGAACTATTTGCGTCCGCCCGCGACCGTGGTGTTC
GCACGACGTGGAAAGCAGATCGCCCCGAGGGTCGGCACGGATGGCGAGTGGAGGGACGGCGTGA **GTGCTCC**
GTGGGGCCCCGGTGGCCGCTGGACCGTCCGCGCTCGTAAGGTGCGGGCCAGGCTTCAACTATCGAACCATTC
CAGCGGGAAATGACACCACCGACACCGACGCCTGAGGCCGCGACAATCCGACGATGAATGTTTCACGTG
AAACATCGACAGAATTCGACACCCCCATCGGCGCTGCAGCAGAACGTGCGATGCGGGTCTTCGACACCAC
CCACGAGCCGCTGCAGCGGCCGGGTGACGCCGGGTGCTCAC **CATCGCGAATCAGAAGGGC**GGGGTCCGGT
AAGACGACCACCGCCGTCAATATCGCTGCCGCGCTTGCTGT

>NC_000962.3:781000-782300 Mycobacterium tuberculosis H37Rv,
rpsL Streptomycin Resistance Gene (TOTAL GENE COVERAGE)

```
GCCCACCACCACCCGGGTTCGGTACTCGGCCTTACCCGGATGCCGCTGGGCGGTGACGATCCCGAATACA  
CCGCTGCGACTAGGGGCGCAGCCGCGCCCGTCATCGCCGTGCTGTCCCTCGTACGGCCTCGACGGTGAGCA  
GGCTTTCTACGCGGCGCTCGAGTTTTGGTCGGCACTGCATGGGTTTTGTGTTGCTGGAAAATGACCGGCGTC  
ATGGACGACATCGATAACCGATGCGGTGTTACCCGACATGGTGTGCGGCTGGCGGCGGGCATGGAAAAGGC  
GCACCACACACGGTGGTACCGCGTCAACGTAGCGCCCTGCTTCGGCCGCAACGCCCGCTTTGACCTGCCA  
GACTGCGCGCGGGTATTGTGGTTGCTCGTGCCTGGCGGCTTACGCTTGATGTAGGGGCGTGGATGCCGGG  
CCAATTCCGATGTCGCGGATGCCTCGGATGAGACGAATCGAGTTTGAGGCAAGCTATGCGACACACCCGG  
CCGCGGGTAACCGTGGCGGGGCATGGCCGACAAACAGAACGTGAAAGCGCCCAAGATAGAAAAGCCGGTAG  
ATGCCAACCATCCAGCAGCTGGTCCGCAAGGGTCGTCGGGACAAGATCAGTAAGGTCAAGACCGCGGCTC  
TGAAGGGCAGCCCGCAGCGTTCGTGGTGTATGCACCCGCGTGTACACCACCACTCCGAAGAAGCCGAACTC  
GGCGCTTCGGAAGGTTGCCCGCGTGAAGTTGACGAGTCAGGTCGAGGTCACGGCGTACATTTCCCGGCGAG  
GGCCACAACCTGCAGGAGCACTCGATGGTGTGCTGGTGC GCGGCGGCCGGGTGAAGGACCTGCCTGGTGTGC  
GCTACAAGATCATCCGCGGTTTCGCTGGATAACGAGGGTGTCAAGAACCGCAAAACAGGCACGCAGCCGTTA  
CGGCGCTAAGAAGGAGAAGGGCTGATGCCACGCAAGGGGCGCGCCCAAGCGTCCGTTGGTCAACGACC  
CGGTCTACGGATCGCAGTTGGTCACCCAGTTGGTGAACAAGGTTCTGTTGAAGGGGAAAAAATCGCTGGC  
CGAGCGCATTGTTTTATGGTGCCTTGAGCAAGCTCGCGACAAGACCGSCACCGATCCGGTGATCACCCCTC  
AAGCGGGCTCTCGACAATGTCAAACCCGCCCTGGAGGTGCGCAGCCGTCGCGTCGGCGGCGCGACCTATC  
AGGTGCCTGTGAGGTGCGCCCCGACCGGTGACACGCTGGCGCTGCGCTGGCTCGTTCGGCTACTCGCG  
GCAACGCCGTGAGAAGACGATGATCGAGCGCCTGGCAAATGGAGATCCTGGATGCCAGCAATGGCCTTGG  
GGCCTCCGTCAAGCGGCGTGAGGACACCCACAAGATGGCCGAGGCGAACCAGACCTTTGCGCATTATCGC  
TGGTGAGAAGCGCCGGTTAGCCAGCCAGGGCGCAAACCGACAGTGATAGACAGCTAACTAGCAACCGAAA  
GAGTGGGAAGACTTCTGTGGCACAGAAGGACGTGCTGACCGACCTGAGTAGGGTCCGCAACTTCGGCATC  
ATGGCGCACATCGATGCCGGCAAGACCACAACCACCGAGCGCATCCTGTACTACACCGGTATCAACTACA  
AGATTGGTGAGGTGCACGACGGCGCAGCCACCATGGACTGGATGGAACAGGAACAGGAGCGCGGCATCAC  
CATCACCTCTGCGGCCACGACCAGTTCTGGAAAGACAACCAGCTCAATATCATCGACACGCCAGGGCAT  
GTGGATTTACCGTTCGAGGTGGAGCGCAATCTGCGCGTGTGACGCGCGGTCGCGGTTTTTCGACGGCA  
AAGAGGGTGTGCAACCGCAGTCCGAACAGGTGTGGCGGCAGGCCGACAAATACGATGTCCCCGAATCTG  
CTTCGTCAACAAGATGGACAAGATCGGTGCGGACTTCTACTTCTCGGTTTCGCACGATGGGGGAGCGGCTT  
GGGGCCAACGCCGTGCCATTTCAGCTTCCCGTCCGGTGC GGAG
```

>NC_000962.3:c4327800-4326004 Mycobacterium tuberculosis H37Rv,
ethA Ethionamide Resistance Gene (SNP at 11bp and 110bp, EXTENDED TO
ALLOW)

GTCCGCTTGATTGACCACCCGGTCCAGCAGGGTCAGCAGCACCCGCTTCCTTGGATGGGAAATAGAAGTAG
AACGTCGGCCTCGAGATACCGGCCCTTGGCCAGATCGTCGACCGAGATATCGGCCAGCGGACGGTCCCT
CGAGAAGGTTCTCGGCGGTGGCGAGGATCGCCAGTTCACGATCGTCGCCGGACGGCCGCGGGTGCGCCG
GCCCCTAGGCAGCGAAGCCTGACTGGCCGCGGAGGTGGTCACCCTGGCAGCTTACTACGTGTCGATAGTC
TCGACATCTCGTTGACGGCCTCGACATTACGTTGATAGCGTGGATCGATGACCCGAGCACTCGACGTTGT
CATCGTGGGCGCTGGAATCTCCGGTGTACGCGCGCCCTGGCACCTGCAGGACCGTTGCCCGACCAAGAGC
TACGCCATCCTGGAAAAGCGGGAATCCATGGGCGGCACCTGGGATTTGTTCCGTTATCCCGGAATTCGCT
CCGACTCCGACATGTACACGCTAGGTTTCCGATTCCGTCCCTGGACCGGACGGCAGGCGATCGCCGACGG
CAAGCCCATCCTCGAGTACGTCAAGAGCACCGCGGCCATGTATGGAATCGACAGGCATATCCGGTTCAC
CACAAGGTGATCAGTGCCGATTGGTTCGACCGCGGAAAAACCGCTGGACCGTTCACATCCAAAGCCACGGCA
CGCTCAGCGCCCTCACCTGCGAATTCCTCTTCTGTGCAGCGGCTACTACAACCTACGACGAGGGCTACTC
GCCGAGATTCGCCGGCTCGGAGGATTTTCGTCGGGCCGATCATCCATCCGCAGCACTGGCCCCGAGGACCTC
GACTACGACGCTAAGAACATCGTCGTGATCGGCAGTGGCGCAACGGCGGTCACGCTCGTCCGGCGCTGG
CGGACTCGGGCGCCAAGCACGTACGATGCTGCAGCGCTCACCCACCTACATCGTGTGCAGCCAGACCG
GGACGGCATCGCCGAGAAGCTCAACCGCTGGCTGCCGGAGACCATGGCCTACACCGCGGTACGGTGAAG
AACGTGCTGCGCCAGGCGGCCGTGTACAGCGCCTGCCAGAAGTGGCCACGGCGCATGCGGAAGATGTTCC
TGAGCCTGATCCAGCGCCAGCTACCCGAGGGGTACGACGTGCGAAAGCACTTCGGCCCGCACTACAACCC
CTGGGACCAGCGATTGTGCTTGGTGCCCAACGGCGACCTGTTCCGGGCCATTCGTACAGGGGAGGTCGAG
GTGGTGACCGACACCATTGAACGGTTCACCGGACCGGAATCCGGCTGAACTCAGGTCGCGAACTGCCGG
CTGACATCATCATTACCGCAACGGGGTTGAACCTGCAGCTTTTTGGTGGGGCGACGGCGACTATCGACGG
ACAACAAGTGGACATCACACGACGATGGCCTACAAGGGCATGATGCTTTCGGCATCCCCAACATGGCC
TACACGGTTGGCTACACCAATGCCTCCTGGACGCTGAAGGCCGACCTGGTGTGCGAGTTTGTCTGTGCT
TGTTGAATTACATGGACGACAACGGTTTTGACACCGTGGTCGTCGAGCGACCGGGCTCAGATGTCGAAGA
GCGGCCCTTCATGGAGTTCACCCAGGTTACGTGCTGCGCTCGCTGGACGAGCTGCCAAGCAGGGTTTCG
CGTACACCGTGGCGCCTGAATCAGAACTACCTACGTGACATCCGGCTCATCCGGCGCGGCAAGATCGACG
ACGAGGGTCTGCGGTTCCGCAAAAAGGCCTGCCCCGGTGGGGTTTTAG

>NC_000962.3:778690-779800 Mycobacterium tuberculosis H37Rv,
rv0678 Bedaquiline & Clofazimine Resistance Gene (TOTAL GENE COVERAGE)

AGGTCAGGGCATCCACGCCGGTTGCGGTCCGCTCGTCCTTCACTTCGCCATCGACGGTGATTTCGGCAGGT
GATGGAAGTGCCGTTCGCCTTGCGCGAGGATGTTGGGGGCCGCGGACGGCGCCGTGGTCTTCAAGGTGAGC
GACCACGGCAGGGCTGCGCCGTGATCCGCTGTGGCTTGGCGTCGAGGTCCAGGTAGTTGATGTTGACGT
AACTACCGGAGCCGAAACTTCGTACTCCACCACCTTGGGGTCGAACGGCTCCGGGTCATCGGCGAAGAC
CTTCGGCGTCAACCAAGATGCCTT **CGGAACCAAAGAAAGTGCGG**ATCCGCTGCACCGTGAAGCCGGCGATG
GCGACCACAACCAGGATGAGCAGCGGTATCCAGGCACGCTTGAGAGTTCCAATCATCGCCCTCCGCCTCT
GCCGCATGAAGTTCACGCCGGTCTGGTGACGCATACCGAACGTCACAGATTCAGAGTACAGTGAACCTT
GTGAGCGTCAACGACGGGGTCGATCAGATGGGCGCCGAGCCCGACATCATGGAATTCGTCGAACAGATGG
GCGGCTATTTTCGAGTCCAGGAGTTTGACTCGGTTGGCGGGTCGATTGTTGGGCTGGCTGCTGGTGTGTGA
TCCCGAGCGGCAGTCCCTCGGAGGAACTGGCGACGGCGCTGGCGGCCAGCAGCGGGGGATCAGCACCAAT
GCCCCGATGCTGATCCAATTTGGGTTTCATTGAGCGGCTCGCGGTCGCCGGGGATCGGCGCACCTATTTCC
GGTTGCGGCCCAACGCTTTCGCGGCTGGCGAGCGTGAACGCATCCGGGCAATGGCCGAACTGCAGGACCT
GGCTGACGTGGGGCTGAGGGCGCTGGGCGACCCCCGCCGAGCGAAGCCGACGGCTGCGGGAGATGCGG
GATCTGTTGGCATATATGGAGAACGTCGTCTCCGACGCCCTGGGGCGATACAGCCAGCGAACCGGAGAGG
ACGACTGATGAGCAACCTCGCAATCTGACCGAGGTGGCGAGCAAGACGGCGATTGGCCTGTGGTCACTCC
TTGTTGATGCGGTTGCCCGCGCCGAGGTTATCGATTGTGGGGTCACCGTTTTTTGTAGCTGACCGTGTGT
CCAGCCCAACAACAACGAGGCGCTCGTCGATCCTGTGCAAGGCGATCTTGTGTTTCGCACCACCACCGGT
CACCGTTTTTCGAGGTGCCGTTGACGGTCAGCGTGTGTCCGAGCCGCCACGTTACAGTGACTTGCCGTCA
GCGCAGTCAAGGGTGGCGGTAGTCCCGATGGAT **CCGTAGGTCAGCATGTCACC**GATCTGGATCGAAGCGG
TTGTGGATTCTCCGGTCGTACGGTCCGGCGCCGCGGTCCGGCCGCTCGTCGCTGTCGTGGTGGTGGCGGT
C

>NC_000962.3:1473658-1476795 Mycobacterium tuberculosis H37Rv,
rrl Linezolid Resistance Gene (SNP at 2058bp)

TTGTAAGTGTCTAAGGGCGCATGGTGGATGCCTTGGCATCGAGAGCCGATGAAGGACGTGGGAGGCTGCG
ATATGCCTCGGGGAGCTGTCAACCGAGCGTGGATCCGAGGATTTCCGAATGGGGAAAACCCAGCACGAGTG
ATGTGCGTGTACCCGCATCTGAATATATAGGGTTCGGGAGGGAAACCGGGGAAAGTGAACATCTCAGTAC
CCGTAGGAGGAGAAAACAATTGTGATTCCGCAAGTAGTGGCGAGCGAACCGGGAACAGGCTAAACCGCAC
GCATGGGTAACCGGGTAGGGGTTGTGTGTGCGGGGTTGTGGGAGGATATGTCTCAGCGCTACCCGGCTGA
GAGGCAGTCAGAAAGTGTGCGTGGTTAGCGGAAGTGGCCTGGGATGGTCTGCCGTAGACGGTGAGAGCCCC
GTACCGGAAAACCCCGCACCTGCCTAGTATCAATTCGAGTAGCAGCGGGCCCGTGAATCCGCTGTGA
ATCCGCGGGACCACCCGGTAAGCCTAAATACTCCTCGATGACCGATAGCGGATTAGTACCGTGAGGGAA
TGGTGAAGAGTACCCCGGGAGGGGAGTGAAGAGTACCTGAAACCGTGTGCCATAAATCCGTCAGAGCCT
CCTTTTCTCTCCGGAGGAGGGTGGTGTGATGGCGTGCCTTTTGAAGAATGAGCCTGCCGAGTCAGGGACATG
TCGCAAGGTTAACCCGTGTGGGGTAGCCGAGCGAAAAGCGAGTCTGAATAGGGCGACCCACACGCGCATA
CGCGCGTGTGAATAGTGGCGTGTCTGGACCCGAAAGCGGAGTGTACTACCCATGGCCAGGGTGAAGCGCG
GGTAAGACCGCGTGGAGGCCCGAACCCACTTAGGTTGAAGACTGAGGGGATGAGCTGTGGGTAGGGGTGA
AAGGCCAATCAAACCTCCGTGATAGCTGGTTCTCCCGAAAATGCATTTAGGTGCAGCGTTGCGTGGTTTAC
CGCGGAGGTAGAGCTACTGGATGGCCGATGGGCCCTACTAGGTTACTGACGTCAGCCAACTCCGAATGC
CGTGGTGTAAAGCGTGGCAGTGGACCGCGGGGGATAAGCTCCGTACGTCGAAAGGGAAACAGCCAGAT
CGCCGGCTAAGGCCCCCAAGCGTGTGCTAAGTGGGAAAGGATGTGCACTCGCAAAGACAACCAGGAGGTT
GGCTTAGAAGCAGCCACCCTTGAAGAGTGCCTAATAGCTCACTGGTCAAGTGATTGTGCGCCGATAATG
TAGCGGGGCTCAAGCACACCCGCCGAAGCCGCGGCACATCCACCTTGTGGTGGGTGTGGGTAGGGGAGCGT
CCCTCATTACGCGAAGCCACCGGGTACCCGGTGGTGGAGGGTGGGGGAGTGAGAATGCAGGCATGAGTAG
CGACAAGGCAAGTGAGAACCTTGCCCGCCGAAAGACCAAGGGTTCTGGGCCAGGCCAGTCCGCCCAGGG
TGAGTCGGGACCTAAGGCGAGGCCGACAGGCGTAGTGCATGGACAACGGGTTGATATTCGCGTACCCGTG
TGTGGGCGCCCGTGCAGCAATCAGCGGTAACCAACCCAAAACCGGATCGATCACTCCCTTCGGGGGTG
TGGATTCTGGGGCTGCGTGGAACTTCGCTGGTAGTGTCAAGCGAAGGGGTGACGCGAGGAAGGTAGCC
GTACCAGTCAAGTGGTAAACACTGGGGCAAGCCGGTAGGGAGAGCGATAGGCAAATCCGTGCTACTAATC
CTGAGAGGTGACGCATAGCCGGTTGAGGCGAATTCCGGTGTCTCTGCTGCCAAGAAAAGCCTCTAGCGA
GCACACACACGGCCCGTACCCCAAACCGACACAGGTGGTTCAGGTAGAGCATAACCAAGGCGTACGAGATAA
CTATGGTTAAGGAACTCGGCAAAATGCCCCCGTAACTTCGGGAGAAGGGGGACCGGAATATCGTGAACAC
CCTTGCGGTGGGAGCGGGATCCGGTTCGAGAAAACAGTGGAGGAGCGACTGTTTACTAAA AACACAGGTC
GTGCGAA GTCGCAAGACGATGTATACG GACTGACGCTGCCCGGTGCTGGAAGGTTAAGAGGACCCGTTA
ACCCGCAAGGGTGAAGCGGAGAATTTAAGCCCCAGTAAACGGCGGTGGTAACTATAACCATCCTAAGGTA
GCGAAATTCCTTGTGCGGTAAGTTCCGACCTGCACGAATGGCGTAACGACTTCTCAACTGTCTCAACCAT
AGACTCGGCGAAATTCGACTACGAGTAAAGATGCTCGTTACGCGCGGACAGGACGAAAAGACCCCGGGACC
TTCACTACAACCTTGGTATTGATGTTCCGGTACGGTTTGTGTAGGATAGGTGGGAGACTGTGAAACCTCGAC
GCCAGTTGGGGCGGAGTCGTTGTTGAAATACCCTCTGATCGTATTGGGCATCTAACCTCGAACCCGTGAA
TCGGGTTTAGGGACAGTGCCTGGCGGGTAGTTTAACTGGGGCGGTTGCCCTCTAAAATGTAACGGAGG CG
CCCAAAGGTTCCCTCA ACCTGGACGGCAATCAGGTGGCGAGTGTAAAATGCACAAGGGAGCTTGACTGCGA
GACTTACAAGTCAAGCAGGGACGAAAAGTCCG GATTAGTGATCCGGCACCCCGAGTGGAAAGGGGTGTGCG
TCAACGGATAAAAGGTACCCCGGGGATAACAGGCTGATCTTCCCAAGAGTCCATATCGACGGGATGGTT
TGGCACCTCGATGTGCGGCTCGTCGCATCCTGGGGCTGGAGCAGGTCCAAGGGTTGGGCTGTTCCGCCAT
TAAAGCGGCACGCGAGCTGGGTTTAGAACGTCGTGAGACAGTTCGGTCTCTATCCGCCGCGCGTCAGA
AACTTGAGGAAACCTGTCCCTAGTACGAGAGGACCGGGACGGAACCTCTGGTGCACCAGTTGTCCCG
CCAGGGGCACCGCTGGATA GCCACGTTCCGGTTCAGGATA ACCGCTGAAAGCATCTAAGCGGGAAACCTTCT
CCAAGATCAGGTTTCTCACCCACTTGGTGGGATAAAGGCCCCCGCAGAACACGGGTTCAATAGGTTCAGAC
CTGGAAGCTCAGTAATGGGTGTAGGGAACTGGTGTCTAACCGGCCGAAAACCTTACAACA

>NC_000962.3:800500-801800 Mycobacterium tuberculosis H37Rv,
rplC Linezolid Resistance Gene (TOTAL GENE COVERAGE)

```
AGATCCGCATCAGGCTGAAGGCCTACGACCATGAGGCCATTGACGCTTCGGCGCGCAAGATCGTCGAAAC
CGTCGTCCGCACCCGGTGCCAGCGTCGTAGGGCCGGTG CCGCTACCGACTGAGAAGAA CGTGTATTGCGTC
ATCCGCTCACCGCATAAGTACAAGGACTCGCGGGAGCACTTCGAGATGCGCACACACAAGCGGTTGATCG
ACATCATCGATCCCACGCCGAAGACCGTTGACGCGCTCATGCGCATCGACCTTCCGGCCAGCGTCGACGT
CAACATCCAGTAGGAGATTGGACAGAGCA ATGGCACGAAAGGGCATTCTCGGTACCAAGCTGGGTATGAC
GCAGGTATTTCGACGAAAGCAACAGAGTAGTACCGGTGACCGTGGTCAAGGCCGGGCCAACGTGGTAACC
CGCATCCGCACGCCCCGAACGCGACGGTTATAGCGCGGTGCAGCTGGCCTATGGCGAG ATCAGCCCACGCA
AGGTCAACAAGCCGCTGACAGGTCAGTACACCGCCCGCGCTCAACCCACGCCGATACCTGGCGGAGCT
GCGGCTGGACGACTCGGATG CCGCGACCGAGTACCAGGTTGGGCAAGAGTTGACCGCGGAGATCTTCGCC
GATGGCAGCTACGTTCGATGTGACGGGTACCTCCAAGGGCAAAGGTTTCGCCGGCACCATGAAGCGGCACG
GCTTCCGCGGTGAGGGGCCAGTACCGGTGCCAGGCGGTGCACCGCCGTCGGGGCTCCATCGGGCGGATG
TGCCACGCCGGCGCGGGTGTTC AAGGGCACCCGGATGGCCGGGCGGATGGGCAATGACCGGGTGACCGTT
CTTAACCTTTTGGTGCATAAGGTCGATGCCGAGAACGGCGTGCTGCTGATCAAGGGTGCGGTTCCCTGGCC
GCACCGGTGGACTGGTCATGGTCCGCAGTGCATCAAACGAGGTGAGAAGTGA TGGCTGCGCAAGAGCAG
AAGACTC AAAATCGACGTCAAGACGCC GCGGGCAAGGTCGACGGCGCTATCGAGCTGCCGGCCGAGC
TGTTTCGACGTCCCGGCCAACATCGCGCTGATGCACCAGGTGGTCACCGCCAGCGGGCGGCGGCACGCCA
GGGTACCCACTCGACGAAGACGCGCGGCGAGGTCAGTGGCGGTGGCCGCAAGCCCTACCGGCAGAAGGGG
ACCGGTTCGTGCCCGGCAGGGCTCGACGCGGGCGCCGAGTTCAACCGCGGTGGCGTGGTACACGGTCCCA
AGCCGCGCGACTACAGCCAGCGCACACCCAAGAAGATGATC
```

>NC_000962.3:528608-530230 Mycobacterium tuberculosis H37Rv, complete genome

Hsp65 Gene (Partial Gene Coverage)

ATGGCCAAGACAATTGCGTACGACGAAGAGGCCCGTCGCGGCCTCGAGCGGGGCTTGAACGCCCTCGCCG
ATGCGGTAAAGGTGACATTGGGCCCAAGGGCCGCAACGTCGTCCTGGAAAAGAAGTGGGGTGCCCCAC
GATCACCAACGATGGTGTGTCCATCGCCAAGGAGATCGAGCTGGAGGATCCGTACGAGAAGATCGGCCGC
GAGCTGGTCAAAGAGGTAGCCAAGAAGACCGATGACGTCGCCGGTGACGGCACCACGACGGCCACCGTGC
TGGCCCAGGCGTTGGTTCGCGAGGGCCTGCGCAACGTCGCGGCCGGCGCCAACCCGCTCGGTCTCAAACG
CGGCATCGAAAAGGCCGTGGAGAAGGTACCCGAGACCCTGCTCAAGGGCGCCAAGGAGGTTCGAGACCAAG
GAGCAGATTGCGGCCACCGCAGCGATTTCCGGCGGGTGACCAGTCCATCGGTGACCTGATCGCCGAGGCGA
TGGACAAGGTGGGCAACGAGGGCGTCATCACCGTCGAGGAGTCCAACACCTTTGGGCTGCAGCTCGAGCT
CACCGAGGGTATGCGGTTTCGACAAGGGCTACATCTCGGGTACTTCGTGACCGACCCGGAGCGTCAGGAG
GCGGTCCTGGAGGACCCCTACATCCTGCTGGTCAGCTCCAAGGTGTCCACTGTCAAGGATCTGCTGCCGC
TGCTCGAGAAGGTTCATCGGAGCCGGTAAGCCGCTGCTGATCATCGCCGAGGACGTCGAGGGCGAGGCGCT
GTCCACCCTGGTTCGTCACAAGATCCGCGGCACCTTCAAGTCGGTGGCGGTCAAGGCTCCCGGCTTCGGC
GACCGCCGCAAGGCGATGCTGCAGGATATGGCCATTCTCACCGGTGGTCAGGTGATCAGCGAAGAGGTTCG
GCCTGACGCTGGAGAACGCCGACCTGTGCTGCTAGGCAAGGCCCGCAAGGTTCGTGGTCACCAAGGACGA
GACCACCATCGTCGAGGGCGCCGGTGACACCGACGCCATCGCCGGACGAGTGGCCCAGATCCGCCAGGAG
ATCGAGAACAGCGACTCCGACTACGACCGTGAGAAGCTGCAGGAGCGGCTGGCCAAGCTGGCCGGTGGTG
TCGCGGTGATCAAGGCCGGTGCCGCCACCGAGGTTCGAACTCAAGGAGCGCAAGCACCGCATCGAGGATGC
GGTTCGCAATGCCAAGGCCCGCTCGAGGAGGGCATCGTCGCCGGTGGGGGTGTGACGCTGTTGCAAGCG
GCCCCGACCCTGGACGAGCTGAAGCTCGAAGGCGACGAGGCGACCGGCGCAACATCGTGAAGGTGGCGC
TGGAGGCCCCGCTGAAGCAGATCGCCTTCAACTCCGGGCTGGAGCCGGGCGTGGTGGCCGAGAAGGTGCG
CAACCTGCCGGCTGGCCACGGACTGAACGCTCAGACCGGTGTCTACGAGGATCTGCTCGCTGCCGGCGTT
GCTGACCCGGTCAAGGTGACCCGTTCCGGCGCTGCAGAATGCGGCGTCCATCGCGGGGCTGTTCCCTGACCA
CCGAGGCCGTCGTTGCCGACAAGCCGAAAAGGAGAAGGCTTCCGTTCCCGGTGGCGGCGACATGGGTGG
CATGGATTTCTGA

Appendix III – External Control Sequences

The following are FastA sequences of the external controls designed for inclusion in the assay. Each sequence is made of the concatenated gene targets within one of the multiplex groups to observe the success or failure of amplification and sequencing of every targeted locus throughout assessment.

>FIND_CONTROL_A

```
ATGAGGAAGGGCTTGCGTGCTCGGAGACTAACGTGACAATACCGGGCCCGCAGGCGGACTAGATGCTGTT
GAGTCATTGTTTCGAGGCCGAAATATTCATTAAGTACGACGTCGGTAAACAGCGACAACCCGCCGTCGTATA
TATTCGGACTGTCGGGTACCTTTCGAGCCGCCGAGCGGAGCGGCCACAGGCTCCGCATTAGACAATGAC
CGCGGCGGAACTAGGTCCCGCCGTTAGGGTGATCGACTCGAGGTCGGCCGCGATGGGCGTCGGTTTCGCG
GCACTGGCGGGCCGGGCGGGCAGCCGCCGAGGCGATGAGCTGGATACGGTTCGCGCGCGCAGCGGCTGC
GGCGGTAAGCCGGATTACGCGTTCGTCGCTGTAGCGCGTTGGACAATCTGCGCCGAGCGGGCGCATC
AGTGGGGCCAAGGCATGGTTGGGCACCGCGCTGGCGCTCAAGCCGCTGCTGTCAATCGACGACGAAAA
CTTGTCTGGTCCAACGGGTTTCGCACTGTGAGCAACGCGACGCGGCGGTGATGATCGACCGGGTTTGCCAGCT
TGTCGGCGACCGCCCCGCCGCTCTCGCGGTGCATCACGTCGCCGACCCGGCAGCTGCGAACGACGTGGCG
GCGGCGCTGGCGGAGCGGCTGCCGGCGTGTGAGCCGGCCATGGTGACCGCCATGGGACCGGTAATTGCT
CTGCACGTCGGTGCCGGAGCCGTCGGGGTATGCGTCGACGTGGGAGCGTCGCCGCCAGCGTAACGTCAC
GGCGAAATTCGTCGCTGATTCTCGCAGTGGCGTCACGCTGGCGGGGCTACCCGCATCGCGTGATCCTTTCG
CAGACACTGTCGTCGTAATATTCACGTGCACGTGGCCGCGGCATATGCCACAGTCGGATTCTGGTGACTGT
GACCCTGTGTAGCCCGACCGAGGACGACTGGCCGGGGATGTTCTACTGGCCGCGGCCAGTTTCACCGAT
TTCATCGGCCCTGAATCAGCGACCGCCTGGCGGACCCTGGTGCCACCGACGGAGCGGTGGTGGTCCGCG
ATGGTGCCGGCCCGGGTTCTGACAAGAGAACAGAAACCGCGCTAGACTGGCAGGTGGTTCGGGATGGCGC
TGACATGGAGATCGGGTATGGCCTCTGGGCATGGTTCGGTACACCAGGACTACCGGATACTATCGACTGG
GCACACCGTAGCTGGAGACATAACACCTATGACACTGCTCAGAACGCACATTTGCGGAGCCGTTGGTGGTG
GCCAACACAACGCCAGCAGGAAGAATAACGCCGCCAGGAACGCCATCCGGTTGCGCGACCAGCGCAGC
ACCGATGGGGATACCAACACCGTCGTCAGCGCGGCCATCGCCGCCCTACGGCGGCGAACAGCCCGAAGT
GGTGCACCCACTTGGTGGGCGTGAACATCAGGAAGAACATGGTGCCGAAGATGACGCCCATCAGCCGCCA
CGCCGGTCCGCGGGCCACGCTGGGAATTCGCTTGCGCCGAACATGATGAACACCGCGGTGAACAGGCAT
AGCGCGGTGATCAAAAAGCCGAAGCGCCGCGACAGCGAACCGTTCGACGGTGGGCGAGGATGAGGTAGTA
GTAACGCAGGTTCTCGGTATACCACGCTGGCTCGGCCGATTTTGGCGCGAACCTGGTGGCTTCCAACA
CCGTTGACAGGGTCTGGTTCGGCGAACACCAGGTCAGGATGACGGTGCCGGCGGCCAGCATCGGCGACA
CCAACGGCAACGTGCCGACCAGGCGATGACGGCGCACCAAGATCCGCAGCATCGGGCGGCCGCCGGCCA
CCAGCGCGGCCACCGCGATCAGGCCGGTGGGCTGCACACCCAGTGTGAATGCGGCGGTAACGACGGCCA
GCGCCCGCGGTGTGAGCCGGCTGTACCGCATGGACCGCTCGATCAGCACATAGGTGACCAGCGAGCCGA
GCGCGATGATGCCCTCCGGCCGAGGCCGTTGTTGAACGGCATCCACGCGGTGAGCAAGACCATGGCCGC
CGCCAGTAGGCGGGTTTGTGGCCTCCACCGCCGGCCGAGGCGGGGCGAGCACCTCACGCGACAGCAGC
AGCCAGCACACTAGCCCGCGGCCAGGTCTGGCAGGCGCATCCACAGACTGGCGTCGCTGACATGGGTCA
TCAGCGCCAGCAGGTTGTAATACCAGCCGAAGGGATCCTCCGGGCTGCCGAACCAGCGGAAATAGTTGGA
CATGTAGCCGCGTGGTTCGGCGACTCGGGCCATGCCAGGATGTAGCCGTCGTCGACGAATTCGCGCCG
ATGACATGCCAGGTTCTTCTGTAATATTAACCTCGTTCAACAGCAGGAAGCCGAATATCACACGGCGGC
CTTGTGGTCTGTGTTATCGTCGACTCGATCCTTGCTGAAATAGGTTTAGCACCTCCCTCTGGGCGAGTAAC
TGACGCTGAGGAGCATATCCTCCTACTCCGGCTAAGATCTGTCCGAAAGCGTGGGGAGCGAACAGGATTA
GATACCCTGGTAGTCCACGCCGTAACGGTGGGTAAGGTGTGGGTTTCTTCTTGGGATCCGTGCCGT
AGCTAACGCATTAAGTACCCCGCCTGGGGAGTACGGCCGCAAGGCTAAAACCTCAAAGGAATTGACGGGG
GCCCGCACAAAGCGGCGGAGCATGTGGATTAATTCGATGCAACGCGAAGAACCTTACCTGGGTTTGACATG
CACAGGACGCGTCTAGAGATAGGCGTCCCTTGTGGCCTGTGTGCAGGTGGTGCATGGCTGTCGTCAGCTC
```

GTGTCGTGAGATGTTGGGTTAAGTCCCGCAACGAGCGCAACCCTTGTCTCATGTTGCCAGCACGTAATGGT
GGGACTCGTGAGAGACTGCCGGGTCAACTCGGAGGAAGGTGGGGATGACGTCAAGTCATCATGCCCC
TTATGTCCAGGGCTTCACACATGCTACAATGGCCGTACAAAGGGCTGCGATGCCGCGAGGTTAAGCGAA
TCCTTAAAGCCGGTCTCAGTTCGGATCGGGGTCTGCAACTCGACCCCGTGAAGTCGGAGTCGCTAGTAAT
CGCAGATCAGCAACGCTGCGGTGAATACGTTCCCGGGCCTTGTACACACCGCCCGTCACGTCATGAAAGTC
GGTAACACCCGAAGCCAGTGGCCTAACCTCGGGAGGGAGCTGTCGAAGGTGGGATCGGCGATTGGGAC
GAAGTCGTAACAAGGTAGCCGTACCGGAAGGTGCGGCTGGATCACCTCCTTTCTAAGGAGCACACGAAA
ACGCCCCAACTGGTGGGGCGTAGGCCGTGAGGGGTTCTTGTCTGTAGTGGGCGAGAGCCGGGTGCATGA
CAACAAAGTTGGCCACCAACCAATTCGATACTGGTTTGAGGGCCAAACAACACTGTTGGGTCTGAGGCA
ACACTCTGGAAGAGCGCAGGGGGCCGCGAAAGGAATCACACGGCACGTAATGCTATGATGTTACCAATCA
GTCGTCTCTCCGGTTCGCTGGCAGGCCTTGGCGTCTGCTACTGATGGTAAGGTGTATCGCCCCAGGGCGT
CGGAGACGACGTTCTCCATATATGCCAACAGATCCCGCATCTCCCGCAGCCGTCGGCTTCGCTGCGGGCGG
GCGTCCAGCGCCCTCAGCCCCAGTCCAGGTCCTGCAGTTCGGCCATTGCCCGGATGCGTTCACG
CTCGCCAGCCGCGAAAGCGTTGGGCCGCAACCGGAAATAGGTGCGCCGATCCCCGGCGACCCGAGCCG
CTCAATGAACCCAAATTGGATCAGCATCCGGGCATTGGTGCTGATCCCCCGCTGCTGGCCGCCAGCGCCG
TCGCCAGTTCCTCCGAGGACTGCCGCTCGGGATCACACACCAGCAGCCAGCCCAACAATCGACCCGCCAAC
CGAGTCAAACCTCTGACTCGAAATAGCCGCCATCTGTTGACGAATTCATGATGTCGGGCTCGGCGCC
CATCTGATCGACCCCGTTCGTTGACGCTACAAGTTTCACTGTACTCTGAAATCTGTGACGTTTCGGTATGCGT
CACCAGACCCGGCGTGAATTCATGCGGCAGAGGGCGGAGGGCGATGATTGGAATCTCAAGCGTGCCTGG
ATACCGCTGCTCATCCTGGTTGTGGTCGCCATCGCCGGCTTACGGTGCAGCGGATCCGCACCTTCTTTGGT
TCCGAAGGCATCTTGGTGACGCCGAAGGTCTTCGCCGATGACCCGGAGCCGTTGACCCCAAGGTGGTGG
AGTACGAAGTTTCCGGCTCCGGTAGTTACGTCAACATCAACTACCTGGACCTCGACGCCAAGCCACAGCGG
ATCGACGGCGCAGCCCTGCCGTGGTCGCTCACCTGAAGACCACGGCGCCGTCCGCGGCCCCCAACATCCT
CGCGCAAGGCGCAGCCACTTCCATCACCTGCCGAATCAAGTCTTACATTATGTCCTAAGCGGTAGACCCCG
TCGATGGCGAAGTGAAGGACGAGCGACACCAATAACTGTGCGGCATGTTGGAGCCTGGTACCACGAAA
CAGGTGGCATTCTGCTTTTGCACGCAATTGCGCGGTGAGTTAAGGGTGGTTCGGTATTGGTACGGAGGCT
CCACACCCTGCGGCACGTACACGTCTTATGTAGCGCGACATACTGCTGCGCAATTCGTAGGGCGTCAAT
ACACCCGAGCCAGGGCCTCGCTGCCAGAAAGGGATCCGTGATGGTGAAGTGTGCTGAGTCACACCGA
CAAACGTCACGAGCGTAACCCAGTGCGAAAGTTCCCGCCGAAATCGCAGCCACGTTACGCTCGTGGAC
ATACCGATTTCCGCCCCGCGGGCGAGACGATAGTTGTCGGGGTACTGCCACAGCCACTGAAGGGG
CCAAACCCCATTCGTATCCCGTTAGTCCGTTACCGGAGGAAACCGGGGGATCGGGCTGGCGATCGC
ACAGCGGCTGGCTGCCGACGGCCACAAGGTGGCCGTACCCACCGTGGATCCGGAGCGCCAAAGGGGCT
GTTTGGCGTCGAATGTGACGTCACCGACAGCGACCGGTCGATCGCGCCTTACGGCGGTAGAAGAGCAC
CAGGGTCCGGTTCGAGGTGCTGGTGTCCAACGCCGGCCTATCCGCGGACGCATTCTCATGCGGATGACCG
AGGAAAAGTTCGAGAAGGTCATCAACGCCAACCTACCGGGGCGTTCCGGGTGGCTCAACGGGCATCGCG
CAGCATGCAGCGCAACAAATTCGGTGAATGATATTATAGTTTCGGTCTCCGGCAGCTGGGGCATCGGC
AACCAGGCCAACTACGCAGCCTCAAGGCCGAGTGATTGGCATGGCCCGCTCGATCGCCGCGAGCTGT
CGAAGGCAAACGTGACCGGAATGTGGTGGCCCCGGGCTACATCGACACCGATATGACCCGCGCGCTGGA
TGAGCGGATTCAGCAGGGGGCGCTGCAATTTATCCAGCGAAGCGGGTCCGGACCCCGCGAGGTGCC
GGGGTGGTTCAGCTTCTGGCTTCCGAGGATGCGAGCTATATCTCCGGTTCGGTTCATCCCGGTCGACGGCG
GCATGGGTATGGGCCACTGACACAAAGTTAGAGGTGACTCCACCGAAGTATTCAACACAAGGACGCACAT
GACAGGACTGCTACACATGACCTCCCCAAGACTTAACTCAGAAACGGGCTGACGTCTTATGCGCAGTCG
TCCAGCTGAACACTAGTATGGGCTCTGTACTACCTGGGCAACACGGTGTACTCGAGCTCGATTACGC
GAGAAGAAGTTCTACAATCT

>FIND_CONTROL_B

GAATTCGTCATCATATAGCGGAAGACCACACGGTGGGTTCCGTTGACTTAAGGCTACCACTACAGCGAATC
TCCAACGTATAACCAGCGTACATCTTTTCGAGATAGTGCAGCGCATGAGCAAACCTGAGAGAGCTGCGTCGC
CCGGCGTGTGACAGACACGACGTTGCCGCTGACGTACACGTAGAGCATAGATTAGCGCTCAAGGACTCG
CTCGACCGGATCGAACCGTTGACATCGAGCAGGAGATGCAGCGCAGCTACATCGACTATGCGATGAGCG
TGATCGTCGGCCGCGCGCTGCCGGAGGTGCGCGACGGGCTCAAGCCCGTGCATCGCCGGGTGCTCTATGC
AATGTTGATTCCGGCTTCGCCCGGACCGCAGCCACGCCAAGTCGGCCCGGTCGGTTGCCGAGACCATG
GGCAACTACCACCCGCACGGCGACGCGTCTACGACAGCCTGGTGGCATGGCCAGCCCTGGTCCG
TGCGCTACCCGCTGGTGGACGGCCAGGGCAACTTCGGCTCGCCAGGCAATGACCCACCGGCGGCGATGAG
GTACACCGAAGCCCGGCTGACCCCGTTGGCGATGGAGATGCTGAGGGAAATCGACGAGGAGACAGTCGA
TTTCATCCCTAACTACGACGGCCGGGTGCAAGAGCCGACGGTGTACCCAGCCGGTTCGCCAACCTGCTGG
CCAACGGGTCAGGCGGCATCGCGTCCGCATGGCAACCAATATCCCGCCGACAACCTGCGTGAGCTGGC
CGACGCGGTGTTCTGGGCGCTGGAGAATCACGACGCCGACGAAGAGGAGACCCTGGCCGCGGTGATGGG
GCGGGTTAAAGGCCCGGACTTCCCGACCGCCGACTGATCGTCGGATCCAGGGCACCGCTGATGCCTAC
AAAACCTGGCCGCGGCTCCATTGCAATGCGCGGAGTTGTTGAGGTAGAAGAGGATTCCGCGGGTGTACCT
CGCTGGTGTACCCGAGTTGCCGTATCAGGTCAACCACGACAACCTCATCACTTCGATCGCCGAACAGGTC
CGAGACGGCAAGCTGGCCGCAATTCGAACATTGAGGACCAGTCTAGCGATCGGGTCGGTTTACGCATCG
TCATCGAGATCAAGCGCGATGCGGTGGCCAAGGTGGTGTATCAATAACCTTTACAAGCACACCCAGCTGCA
GACCATAGCTATGGATAATTCTAGGAATGTTACGGGCTTTGGCGCCAACATGCTAGCGATCGCCACTAAG
GTTCACTGAAGCTAACGTCTTGCAAAGCAGCTCAAAAATATAACCTATTACACGATCTCGTCGCTAACCA
CGCCGTGTTGTTGTGAGCCATTAATAGTACCGTATGGACCACCTTGCGGTACGGCGTTCGATGAACCCG
AACGGGTTGACCCGCGCGTACACCGACAGCGAGCCGATCAGACCGATGTTGGGCCCTCAGGGGTTTCGA
TCGGGCACATCCGGCCGTAGTGCAGCGGGTGCACGTGCGGACCTCCAGCCCGGCACGCTCACGTGACAG
ACCGCCGGGCCCCAGCGCCGACAGTCGGCGCTTGTGGGTCAACCCCGACAGCGGGTTGTTCTGGTCCATG
AATTGGCTCAGCTGGCTGGTGCCGAAGAACTCCTTGATCGCGGCGACCCGGCCGGATGTTGATCAACG
TCTGCGGTGTGATCGCCTCACGTCTGGGTGGTTCATCCGCTCCCGGACCACCCGCTCCATCCGCGACATGC
CGACCCGGATCTGGTTTTGGATCAGCTCGCCGACCGTACGCAGGCGGCGGTTGCCGAAGTGGTGCATGTC
GTCGGTTTTACCCGGCACCTCGACGCCGCCGGAACGGTTCATCGTGGTCTGACCCTCGTGAAGCGGACCA
GATATTCGATGGTGGCCACGACGTCTTCTCGGTGACGTCGACGACGTGATGGGCTCGCCGACATGCAGC
CCGAGCTTCTGTTGACCTTATAGCGACCGACGCGGGCCAGGTCGTAGCGCTTCTCCTGAAGAACAAGTT
TTCCAACAGCGTCTGCGCTGACTCTTTGGTGGGGGCTCGCCCGGACGCAGCTTGGGTTAGATGTCCAACA
GCGCCTCGTGGTGGCGACGGTGTGCTTCTCCAGCGTCGATCGCATGATCTCGGAGAACCCGAACCCG
TCGACAATCTGCTCGCTGGTCCAGCCAGCGCCTGAGCAGCACGGTGACCGGTTGCCGGCGTTTGGGTC
GATGCGCACGCCGACGGTGTGCGCTTGTGACGTCAAACCTGAGCCACGCGCCGCGGCTCGGGATCACC
TTGACGCTGTGCAGCGTCTTGTGCGTGGACTTGTCAATGGTCTCGTCGAAGTACACCCCGGGCGACCCGAC
CAGCTGGCTGACCCTGCCGCTTCAAATCATGGCCGGTACCAACCACACGCTCGGTCCCGTTGATGATGA
GATATTGGCTTTCTCCTCTTGAAGTTCTGCCTCACCTACCCAGTTCGCCATGCATATTTGGATCCATGACC
GAGCACCTCGACGTAGTGATCCCATGGAATCGCGCGCCCTGTCATGTCATCGTGGGCGCTGGAATCTCCGG
TGTCAGCGCGCCTGGCACCTGCAGGACCGTTGCCGACCAAGAGCTACGCCATCCTGGAAAAGCGGGAA
TCCATGGGCGGCACCTGGGATTTGTTCCGTTATCCCGGAATTCGCTCCGACTCCGACATGTACACGCTAGGT
TTCCGATTCCGTCCCTGGACCGGACGGCAGGCGATCGCCGACGGCAAGCCCATCCTCGAGTACGTCAAGA
GCACCGCGGCCATGTATGGAATCGACAGGCATATCCGGTTCCACCACAAGGTGATCAGTGGCGATTGGTC
GACCGCGGAAAACCGCTGGACCGTTCACATCCAAAGCCACGGCACGCTCAGCGCCCTCACCTGCGAATTCC
TCTTTCTGTGACGCGGCTACTACAACTACGACGAGGGCTACTCGCCGAGATTCGCCGCTCGGAGGATTC
GTCGGGCCGATCATCCATCCGACGACTGGCCGAGGACCTCGACTACGACGCTAAGAATCGTGTGAT
CGGCAGTGGCGCAACGGCGGTACGCTCGTGGCGGCTGGCGGACTCGGGCGCAAGCACGTACGAT
GCTGCAGCGCTACCCACCTACATCGTGTGCGAGCCAGACCGGGACGGCATCGCCGAGAAGCTCAACCGC

TGGCTGCCGGAGACCATGGCCTACACCGCGGTACGGTGGAAAGACGTGCTGCGCCAGGCGGCCGTGTAC
AGGCCTGCCAGAAGTGGCCACGGCGCATGCGGAAGATGTTCTGAGCCTGATCCAGCGCCAGCTACCCG
AGGGGTACGACGTGCGAAAGCACTTCGGCCCGCACTACAACCCCTGGGACCAGCGATTGTGCTTGGTGCC
CAACGGCGACCTGTTCCGGGCCATTTCGTACGGGAAGGTCGAGGTGGTGACCGACACCATTGAACGGTTC
ACCGCGACCGGAATCCGGCTGAACTCAGGTCGCGAACTGCCGGCTGACATCATCATTACCGCAACGGGGT
TGAACCTGCAGCTTTTTGGTGGGGCGACGGCGACTATCGACGGACAACAAGTGGACATCACCACGACGAT
GGCCTACAAGGGCATGATGCTTTCCGGCATCCCAACATGGCCTACACGATCCTGAGGTCGTTAACGCTAG
CTTGGTTGGTTGGCTACACCAATGCCTCCTGGACTAATCGTACCTACGGAACTTTTCTACCCCTCCGCCAG
CGTATAGATCACGAAGTAAGCCTCGAGTGGGTACCTGGCGTGCCGCCGAAGTGCTGATTATAGTTGCTGC
TCTTATCGCCCCGTGGGCGGTGACCACCTGGTGCATCAGCGCGATGTTGGCCGGGACGTGCAACAGCTCG
GCCGGCAGCTCGATAGCGCCGTGACCTTGCCCGCCGGCGTCTTGACGTGATTTTGAGTGTCTTCTGCTCT
TGCGCAGCCATCACTTCTCACCTCGTTTGATCGCACTGCGGACCATGACCAGTCCACCGGTGCGGCCAGGA
ACCGCACCTTGATCAGCAGCACGCCGTTCTCGGCATCGACCTTATGCACAAAAGGTTAAGAACGGTAC
CCGGTCATTGCCCATCCGCCCGGCCATCCGGGTGCCCTTGAACACCCGCGCCGGCGTGGCACATCCGCCGA
TGAGCCCGGACGGCGGTGCACCGCCTGGGCACCGTGACTGGCGCCCTGACCGCGGAAGCCGTGCCGCTT
CATGGTGCCGGCGAAACCTTTGCCCTTGAGGTACCCGTACATCGACGTAGCTGCCATCGGCGAAGATCT
CCGCGGTCAACTCTTGCCCAACCTGGTACTCGGTGCGGCATCCGAGTCGTCCAGCCGACGCTCCGCCAGG
TATCGGCGTGGGTTGACGCCGGCGCGGTGTACTGACCTGTGACGGCTTGTGACCTTGCCTGGGCTGA
TCTCGCCATAGGCCAGCTGCACGGCGCTATAACCGTCGCGTTCGGGCGTGC GGATGCGGGTTACCACGTT
GGGCCCGCCTTGACCACGGTACCGGTACTACTCTGTTGCTTTCTGTCGAATACCTGCGTCATACCCAGCTT
GGTACCGAGAATGCCCTTTCGTGCCATTGCTCTGTCCAATCTCCTACTGGATGTTGACGTGACGCTGGCCG
GAAGGTCGATGCGCATGAGCGCTAACGGTCTTCGGCGTGGGATCGATGATGTCGATCAACCGCTTGTG
TGTGCGCATCTGGAAGCGAGGGTATCCGACCATATGCAACCCGAAGTGCTCCCGCGAGTCTTGTACTACC
ATGTCGTGTCTGACTATGAGTAAGTTAGCACAATTACCTCTCCAGATGAAGGACGGTCTGTGGCCGGTCAA
GAAGAAGTACGGCGATATCATGTGTGGAGTTCCACGCTCGAAAGAAGCTCTCATGGGCGGACCTGATT
GTTTTCGCCGCAACTGCGCGCTGGAATCGATGGGCTTCAAGACGTTCCGGTTCGGCTTCGGCCGGGTCG
ACCAGTGGGAGCCCGATGAGGTCTATTGGGGCAAGGAAGCCACCTGGCTCGGCGATGAGCGTTACAGCG
GTAAGCGGGATCTGGAGAACCCGCTGGCCGCGGTGCAGATGGGGCTGATCTACGTGAACCCGGAGGGGC
CGAACGGCAACCCGACCCCATGGCCGCGGGTGCACATTCGCGAGACGTTTCGGCGCATGGCCATGAA
CGACGTGAAACAGCGGCGCTGATCGTCGGCGGTACACTTTCGGTAAGACCCATGGCGCCGGCCCGGCC
GATCTGGTCGGCCCCGAACCCGAGGCTGCTCCGCTGGAGCAGATGGGCTTGGGCTGGAAGAGCTCGTATG
GCACCGAACCGGTAAGGACGCGATCACCAGCGCATCGAGGTCGTATGGACGAACACCCCGACGAAAT
GGGACAACAGTTTTCTCGAGATCCTGTACGGCTACGAGTGGGAGCTGACGAAGAGCCCTGCTGGCGCTTG
GCAATACACCGCAAGGACGGCGCCGGTGC CGGCACCATCCCGGACCGTTTCGGCGGGCCAGGGCGCTCC
CCGACGATGCTGGCCACTGACCTCTCGCTGCGGGTGGATCCGATCTATGAGCGGATCACGCGTCGCTGGCT
GGAACACCCCGAGGAATTGGCCGACGAGTTCGCAAGGCCTGGTACAAGCTGATCCACCGAGACATGGGT
CCCGTTGCGAGATACCTTGGGCCGCTGGTCCCAAGCAGACCCTGCTGTGGCAGGATCCGGTCCCTGCGGT
CAGCCACGACCTCGTCGGCGAAGCCGAGATTCAATTTAAAGCGCCTTCTGGTGCACGATTGGCCAGCCTTA
AGAGCCAGATCCGGGCAGTCAGCAACGCACAAGCGATGCGAGGGCTGATCATTATGACCTTTAGACATC
GGTTCATAAATCCAAGTGGATCTAAGTAACCATTGACCGCCACATACTAGCATGCGTAGCTGCCATAACC
CTGATACTCCTGCTGGCTGCATC

>FIND_CONTROL_C

AAGAAAGTACTCTGTATAATTTAGTGAAGAGCGATCAAGCACAGTAAAGTGTGTCGAGAGTTACCCGATC
GATAGCAAGTAGATCGCGGTGTCTCGGCAATGTCAAAGTTTATTCTCTAGCAGTGGCCATCTCGTCTATCCA
CGGATGGATGACACAGACCTCACGAGCCGGCGGAGTCGCACGTGCATTGGTGGGCGGCCGTGCAATGCG
TAATGTCTCCGATCGAGCCCGCGCGTCTGCGATCTTCGACCGCGGCTTGGCCTTGTCTCGGCGGTACGCC
GAAGCGTTGGCGGGACCCGGTGTGGAGCGGGGGTGGTGGGACCCCGGAAGTCGGTAGGCTATGGGA
CCGGCATCTACTGAACTGCGCCGTGATCGGTGAGCTCCTCGAACCGGTTGACCGGGTCTGGGATATCGGT
AGCGGAGCCGGGTTGCCGGCGTGCCATTGGCGATAGCGCGGCCGACCTCCAGGTAGTTCTCTAGAAC
CGTACTGCGCCGACCGAGTTTCTTCGAGAGATGGTGACAGATCTGGGCGTGGCCGTTGAGATCGTGCG
GGGGCGCGCCGAGGAGTCTGGGTGCAGGACCAATTGGGCGGCAGCGACGCTGCGGTGTACGGGCGG
TGGCCGCGTTGGACAAGTTGACGAAATGGAGCATGCCGTTGATACGGCCGAACGGGCGAATGCTCGCCAT
CAAAGGCGAGCGGGCTCACGACGAAGTACGGGAGACCGGCGTGTGATGATCGCATCGGGCGCGGTTGA
TGTCAGGGTGGTGACATGTGGCGCAACTATTTGCGTCCGCCCGGACCGTGGTGTTCGCACGACGTGGA
AAGCAGATCGCCGAGGGTCGGCACGGATGGCGAGTGGAGGGACGGCGTGAGTGCTCCGTGGGGCCG
GTGGCCGCTGGACCGTCCGCGCTCGTAAGGTGCGGCCAGGCTTCAACTATCGAACCATCCAGCGGGAAA
TGACACCACCGACACCGACGCCTGAGGCCGCGACAATCCGACGATGAATGTTTCACGTGAAACATCGACA
GAATTCGACACCCCATCGGCGCTGCAGCAGAACGTGCGATGCGGGTCTGCACACCACCCACGAGCCGC
TGCAGCGGCCGGTTCGACGCCGGCGACTTCAGTCACTTATTATTGCAATTCAGTGCTCACCATCGGAAT
CAGAAGGGCTACTGATTCATCCATTCTTATCTTTACACAGTTTGGCTAGGATTAATTCAGGTGGCAGGC
GTAGATGATGTACCCGTGGTGCCTGGCGCCGATGAGCTAACCGTTCGTAATGGGCAGCCAGTCAGAC
AGCAGCGCGCACACCGTCTTGGCGACCGGCGTGCATCCTTCATGTTCCAGCCGATCGGAGCGCGTATC
CCAGCCCTCCTCGAGCAGTGGATCTGGGCGCCGGCCTCCTCGCCGAGCGCACCGCCGACGATCGACTCA
TCGCCAGCGTCCGGATAGGGCTGCGGCAACGAGATTCGAACGCACACCGTACTTGCCGGCCTCGCGCGC
CACGAACCTGTTGACCGACTCCAACGCGCTCTTGGCGACCGTCATCCAGTTGTAGGCCGGCATCGCCGGC
TCGGGTGCAAGTCCATGCCGACGATGGAACCTCCGGGGTTCATGATCGGCAGCAGCGCCTTGGCCATCGA
AGCATAACGAATACGCCGAGATGTGGATGCCCTTGACACATCCGCGTAGGGCGCGTGAAGAACGGGTTG
ATGCCCATCCCGGTCTGCGGCATGAACCAATCGAATGCACCACCCGTCGAGCTTGTGCCCGCCCGAT
CGCCTCGGTACCCGGCCGGCCAAGCTGGCCAGGTGCTCCTCGTTTTGCACGTGAGTTCGAGCAGCGGG
GCCTTTGCCGGCAGCCGGTCCGTGATGCGCTGAATCAGCCGACCGGTCGAACCCGGTGAAGCACCAGCT
GGGCGCCCTGCTCCTGGGCTACCCGTGCGATGTGAAACGCGATCGACGAGTCGGTGTGATTCCGCTAAC
CAGAATCCGTTTGCCGTCCAGCAGTCTGTGATGTGCGTCTTGTGTTGTGTCAGTGGCCATACCCATGCC
GCCGTGACCGGGATGACCGCACCGGAGATATAGCTCGCATCCTCGGAAGCCAGGAAGCTGACCACCCG
GCGACCTCGGCGGGGTGCCGACCCCTTATCTCTGATCATCCCTTCTTATATCGCTTCGCTGGGATAAAT
TGCAGCGCCCGCTTGTGTAGGGTCGCGAAGCAATATACAGGTCAATTGCTCCATTGATTCTTACGTACGCG
GTCCGTGCGAAGTCGCAAGACGATCATTTCCCTATAGAGTCTTAAACGTTACAGGTATACGGACTGACGCC
TGCCCGGTGCTGGAAGGTTAAGAGGACCCGTTAACCCGCAAGGGTGAAGCGGAGAATTAAGCCCCAGTA
AACGGCGGTGGTAATACTATAACCATCCTAAGGTAGCGAAATTCCTTGTGCGGGTAAGTTCGACCTGCACGAA
TGCGGTAACGACTTCTCAACTGTCTCAACCATAGACTCGGCGAAATTGCACTACGAGTAAAGATGCTCGTT
ACGCGCGGCAGGACGAAAAGACCCCGGGACCTTCACTACAATTGGTATTGATGTTCCGTACGGTTTGTGT
AGGATAGGTGGGAGACTGTGAAACCTCGACGCCAGTTGGGGCGGAGTCGTTGTTGAAATACCACTCTGAT
CGTATTGGGCATCTAACCTCGAACCTGAATCGGGTTTGGGACAGTGCCTGGCGGGTAGTTTAACTGGG
GCGGTTGCCCTCTAAAATGTAACGGAGGCGCCAAAGGTTCCCTCAACCTGGACGGCAATCAGGTGGCGA
GTGTAATGCACAAGGGAGCTTGACTGCGAGACTTACAAGTCAAGCAGGGACGAAAGTCGGGATTAGTG
ATCCGGCACCCCGAGTGGAAAGGGTGTGCGTCAACGGATAAAAGGTACCCCGGGGATAACAGGCTGATC
TTCCCAAGAGTCCATATCGACGGGATGGTTTGGCACCTCGATGTGCGGCTCGTGCATCCTGGGGCTGGAG
CAGGTCCAAGGGTTGGGCTGTTGCCCCATTAAAGCGGCACGCGAGCTGGGTTTAGAACGTCGTGAGACA
GTTCCGGTCTCTATCCGCCGCGCGCTCAGAACTTGAGGAAACCTGTCCCTAGTACGAGAGGACCGGGAC

GGACGAACCTCTGGTGCACCAAGTTGTCCCGCCAGGGGCACCGCTGGATAGCCACGTTCCGGTCAGGATAAC
CGTGAAAGCATCTAAGCGGGAAACCTTCTCCAAGATCAGGTTTCTCACCCACTTGGTGGGATGACTTTCA
CCACTGCCTCTTGACCCAAGACAAGGCCCGCCGAGAACACGGGTTAGTTCGGCGACGAGCCTTCTGTCT
CCACGCCGGTTTCCCGCTACAACCGTTCTAGTTGACGTCCAGATCGCGATGGAACGTGATATCCAACTCAC
TGTTAAGCTTTGCCAACTGCAGCGCGGCCGATGAAGGTGTCGTAGAAGCGGCCGATGGCCTCATGCCCC
ACCTGCGGTGCGAACCACCGGGTCTTCGACCCGCGCGTCACCGGTGAACAACCCGACCCAGCCGGCGC
GGTCGTGCGCGGCCGCGCTTTCGCGGAGCGCTCCACCGCCCAACAGTTCATCCCGTTTCGGCGGTGC
CATCAGGAGCTGCAAACCAACTCGACGCTGGCGGTGCGCATCTCCTCCAGCGCGGCGACGGTGGTATCGG
CCGACACACCCGCTGTCAGGTCCACCAGCACCTGGTGGCCAAGCCATTGCGTACCGCGTCTCGGCCGTC
TGCGGCACACAATGATCGGTGGCAATACCGACCACATCGACCTCATCGACGCCGCTTGCCGCAGCCAATT
CAGCAGTGGCGTGCCGTTCTCGTCGACTCTTCGAAGCCGCTGTACGCTCCGGTGTAGGCACCCTTGAGA
ACACCGCCTCGATTGCCGACGTGTCCAGACTGGGATGGAAGTCCGCGCCGGAGTACCGCTGACGCAATG
CGGTGGCCACGACGAGGAATAGTCCGGTGTGCCGGAGAAGTGGTCAACCGGGTCGATGTGGAAGTCCTT
GGTTGCCACGACGTGATGGTAGTCCGCCGCTTCGGCCAGGTAGTTCGCTGATGGCGCGGGCCAGCGCGGC
GCCACCGTTACCGCCAGCGAGCCACCCTCGCAGAAGTCTGTTTCGACGTGACGATGATCAACGCCCGCA
TACGTCCACCATACGTTTCGGGCGACTGCCCGGCGAGTTTGCTACCGACGCGGCAGCCACAGATATAGGG
TCCATGACGCCGCGACGATCGCGAACATGACCAGCTGAGCGGCGGCCACCCAACCGCGGGATAGATCAC
GCCGGTATGTAGTTCACAGCCTAGTGGCCTGGATGTTTCGTAGTGTAGCGACAAATCCGTCCGGTGTAGCTT
AAGTCTGGCCTACGATGTCTTTGGTGTCTCAATCCCGAGGACCTAATACGCGCAGCGGGCGGGTATTGTGG
TTGCTCGTGCGGGACCCGGGAGCTTAATTAGTAGTTCGGCTCTGGCGGCTTACGCTTGATGTAGGGCGTG
GATGCCGGGCCAATTCGATGTCCGCGATGCCTCGGATGAGACGAATCGAGTTTGAGGCAAGCTATGCGA
CACACCCGGCCGCGGGTAACCGTGGCGGGCATGGCCGACAAACAGAACGTGAAAGCGCCCAAGATAGA
AAGCCGGTAGATGCCAACCATCCAGCAGCTGGTCCGCAAGGGTCGTGCGGACAAGATCAGTAAGGTCAAG
ACCGCGGCTCTGAAGGGCAGCCCGCAGCGTCTGGTGTATGCACCCGCGTGTACACCACCACTCCGAAGA
AGCCGAACTCGGCGCTTCGAAGGTTGCCCGGTGAAGTTGACGAGTCAGGTCGAGGTCACGGCGTACAT
TCCCGGCGAGGGCCACAACCTGCAGGAGCACTCGATGGTGTGGTGCGCGGCGGCCGGGTGAAGGACCT
GCCTGGTGTGCGCTACAAGATCATCCGCGGTTTCGCTGGATACGCAGGGTGTCAAGAACCGCAAACAGGCA
CGCAGCCGTTACGGCGCTAAGAAGGAGAAGGGCTGATGCCACGCAAGGGGCCCGCGCCCAAGCGTCCGT
TGGTCAACGACCCGGTCTACGGATCGCAGTTGGTCAACCGAGTTGGTGAACAAGTTCTGTTGAAGGGGAA
AAAATCGCTGGCCGAGCGCATTGTTTATGGTGCCTTGAGCAAGCTCGCGACAAGACCGGCACCGATCCG
GTGATCACCTCAAGCGGGCTCTCGACAATGTCAAACCCGCCCTGGAGGTGCGCAGCCGTCGCGTGGCG
GCGCGACCTATCAGGTGCCTGTGAGGTGCGCCCCACCGGTCGACCACGCTGGCGTGCCTGGCTCGT
CGGCTACTCGCGGCAACGCCGTGAGAAGACGATGATCGAGCGCCTGGCAAATGGAGATCCTGGATGCCA
GCAATGGCCTTGGGGCCTCCGTCAAGCGGCGTGAGGACACCCACAAGATGGCCGAGGCGAACCGAGCCTT
TGCGCATACTTGTAGGGCAGTACGAGTTCAGCCTTATCGCTGGTGAGAAGCGCCGGTTAACAGGCAAT
CTGCACTCTACTCGAATAAACTAGGCGCGTCCCTTGCGGTGTCTCCTATTTGGTCTCGGTGGCTTCGTCGCG
CCCGGTACATGTACACCCGCTTCCCGCTGAGTGTGTGGACGACCAGCAGAACACTGCGATGAGCGGTCA
CTACGGGCCCTCGCTAATCGCACGGTGCACCGCATCCTCCAATCCCTTGGCCGACAATGCCCGGTTCGGTCT
GCGTGCGAACACAGGAAGTACTCGACATTGCCCGATGGGCCCGGCAGCGGGCTGGCCTTGACGCCGAC
GCTGTGCCAGCCAGCTCCTGTGCCCGCCGCGGACCGCGAGCACCGACCGCGCACGCAACTGCGGGTCA
TGGAACACCCACCGGGGCCGACCTGACCTTTCCACCTCAAACCTGCGGCTTACCAGTGGAACGATATC
GGCGTCGCGGAAGCGCATCCAACCAGCGCGGGCAACACGGTAGCCAACGAGATGAACGACAGGTGCGC
CACTACCAGGTGACGCGACCGCCGATCGCCTCCGGTGTGAGGCCACGTGCGTTGGTCCGCTCGAGGACC
ACCACCCGAGGATCGTTGCGCAGCGACCACGCCAGCTGGCCGTATCCGACATCGGCGGCCACCACGTGGG
CGGCACCACGGTCCAGCAGTACTTCGGTGAACCCACCGGTGATGCGCCCGCTCCAGACAGCGCCGGCC
CGCCACCGGATCGCGAACGCTCCAGCGCACCGACTAGTTTGTGCGCTCCGCGCGATACCCAGGCGCGTT
CACTGTCCGTACCCACGGTACGCGCGGTGGTGTGCGACACGGCGGTGGCCGGCTTGACCGCCGGCAGCCC
GTCGATGCGCACCTTGCCGGCGCCGATCAACTCCGCGGCCCTGTTGACGTGATCGCGCCAGGCCCGCCGG

ACTAGCTCGGCGTCAACGCGGGCACGTCGTGCCACGCCGCACTCAACCCTTCTCCGCCGACTCCAGGGCGG
CCAACAACACCTCGTGCGCCTCGGAAAGACGACGTGCGATGCCTTCGAGTTCGGCCAGAGACGGTCCGTTT
TCGGCGTCGGCGGGTTCGGGCAGCGAAGCAAGTAGGGCGTCGATTTGGCACGGATCTGGTCAGGATCG
ATGGTCATTGCGTTCCTACGCTAGTGACAATACGAAGATCTTAATCCGGAATAGACACCGGATGATCGCTG
CGCATCAACGCATCTCTCGGACAATACATATCAATGTCGTATACGTCCAGTGCCGGCGAGTGGGAACGTCG
ATGGGTGCGCCGCGGATCCGTACACGCGTCCGTGAATCCTATGTATAACGGCTCGTGATGTGATAGGCAC
ACCGTTGGTCCACCAGA

Appendix IV – Total Phenotypic Resistance Calls for FIND Samples

The following is a table of complete resistance calls for 16 anti-tuberculous medications following performance of the DST assay on 392 blinded samples provided by FIND. This table, in conjunction with the table in Appendix V were provided to FIND for validation and assessment of the DST method.

Sample	Ethambutol	Isoniazid	Pyrazinamide	Rifampicin	Streptomycin	Amikacin	Bedaquiline	Capreomycin
A405	Resistant	Resistant	Resistant	Resistant	Resistant	Susceptible	Susceptible	Susceptible
A798	Resistant	Resistant	Resistant	Resistant	Resistant	Susceptible	Susceptible	Susceptible
A614	Resistant	Resistant	Resistant	Resistant	Resistant	Susceptible	Susceptible	Susceptible
A656	Resistant	Resistant	Resistant	Resistant	Resistant	Susceptible	Susceptible	Susceptible
A762	Resistant	Resistant	Resistant	Resistant	Resistant	Susceptible	Susceptible	Susceptible
A659	Resistant	Resistant	Resistant	Resistant	Resistant	Susceptible	Susceptible	Susceptible
A675	Resistant	Resistant	Susceptible	Resistant	Resistant	Susceptible	Susceptible	Susceptible
A202	Resistant	Resistant	Susceptible	Resistant	Resistant	Susceptible	Susceptible	Susceptible
A431	Resistant	Resistant	Susceptible	Resistant	Resistant	Susceptible	Susceptible	Susceptible
A521	Resistant	Resistant	Resistant	Resistant	Resistant	Resistant	Susceptible	Resistant
A320	Resistant	Resistant	Resistant	Resistant	Resistant	Resistant	Susceptible	Resistant
A284	Resistant	Resistant	Resistant	Resistant	Resistant	Resistant	Susceptible	Resistant
A872	Resistant	Resistant	Susceptible	Resistant	Resistant	Susceptible	Susceptible	Susceptible
A565	Resistant	Resistant	Susceptible	Resistant	Resistant	Susceptible	Susceptible	Susceptible
A648	Resistant	Resistant	Susceptible	Resistant	Resistant	Susceptible	Susceptible	Susceptible
A053	Resistant	Resistant	Resistant	Resistant	Resistant	Resistant	Susceptible	Resistant
A581	Resistant	Resistant	Resistant	Resistant	Resistant	Resistant	Susceptible	Resistant
A199	Resistant	Resistant	Resistant	Resistant	Resistant	Resistant	Susceptible	Resistant
A045	Resistant	Resistant	Resistant	Resistant	Resistant	Susceptible	Susceptible	Susceptible
A783	Resistant	Resistant	Resistant	Resistant	Resistant	Susceptible	Susceptible	Susceptible
A847	Resistant	Resistant	Resistant	Resistant	Resistant	Susceptible	Susceptible	Susceptible
A316	Resistant	Resistant	Resistant	Resistant	Resistant	Resistant	Susceptible	Resistant
A750	Resistant	Resistant	Resistant	Resistant	Resistant	Resistant	Susceptible	Resistant
A205	Resistant	Resistant	Resistant	Resistant	Resistant	Resistant	Susceptible	Resistant
A267	Resistant	Resistant	Not Detected	Resistant	Resistant	Susceptible	Susceptible	Susceptible
A743	Resistant	Resistant	Not Detected	Resistant	Resistant	Susceptible	Susceptible	Susceptible
A152	Resistant	Resistant	Not Detected	Resistant	Resistant	Susceptible	Susceptible	Susceptible
A246	Resistant	Resistant	Susceptible	Resistant	Resistant	Susceptible	Susceptible	Susceptible
A921	Resistant	Resistant	Susceptible	Resistant	Resistant	Susceptible	Susceptible	Susceptible
A726	Resistant	Resistant	Susceptible	Resistant	Resistant	Susceptible	Susceptible	Susceptible
A554	Resistant	Resistant	Resistant	Resistant	Resistant	Susceptible	Susceptible	Susceptible
A371	Resistant	Resistant	Resistant	Resistant	Resistant	Susceptible	Susceptible	Susceptible
A056	Resistant	Resistant	Resistant	Resistant	Resistant	Susceptible	Susceptible	Susceptible
A107	Resistant	Resistant	Susceptible	Resistant	Susceptible	Susceptible	Susceptible	Susceptible

C203	Resistant	Susceptible	Resistant	Resistant	Susceptible	Resistant	Resistant	Resistant
C543	Resistant	Susceptible	Resistant	Resistant	Susceptible	Resistant	Resistant	Resistant
C097	Resistant	Susceptible	Resistant	Resistant	Susceptible	Resistant	Resistant	Resistant
C796	Resistant	Susceptible	Resistant	Resistant	Susceptible	Resistant	Resistant	Resistant

Appendix V – Example Genotypic Resistance Calling for SNPs

The following is an example section of table used for manual observation of SNP loci and resistance calling. This section focuses on 9 high confidence SNP loci in the *embB* gene associated with resistance to ethambutol. Recording of SNPs in this manner was performed for all covered SNP loci and all 392 blinded FIND samples.

Colour key									
	≥80% of bases resistant at SNP position								
	51% to 79% bases resistant at SNP position								
	20% to 50% bases resistant at SNP position								
	Gene deletion or target dropout								
	wild type								
		Ethambutol							
Sample	embB 378	embB 306	embB 354	embB 497	embB 406	embB 297	embB 296	embB 405	embB 397
A405									
A798									
A614									
A656									
A762									
A659									
A675									
A202									
A431									
A521									
A320									
A284									
A872									
A565									
A648									
A053									
A581									
A199									
A045									
A783									
A847									
A316									
A750									
A205									
A267									
A743									

A152									
A246									
A921									
A726									
A554									
A371									
A056									
A107									
A418									
A167									
A537									
A519									
A187									
A062									
A818									
A217									
A605									
A273									
A298									
A119									
A877									
A827									
A759									
A701									
A524									
A067									
A971									
A886									
A998									
A128									
A809									
A310									
A240									
A430									
A661									
A274									
A929									
A249									
A490									
A922									
A410									
A139									
A349									
A197									

A670									
A832									
A594		Red							
A312		Red							
A820		Red							
A082									
A391									
A362									
A277					Red				
A423					Red				
A582					Red				
A908		Red							
A222		Red							
A174		Red							
A305		Red							
A844		Red							
A458		Red							
A807									
A242									
A563									
A394					Yellow				
A871					Red				
A338					Red				
A596									
A512									
A980									
A505		Green							
A662		Green							
A399		Green							
A299									
A057									
A992									
A125				Red					
A984				Red					
A471				Red					
A272								Red	
A474								Red	
A558								Red	
A528		Red							
A555		Red							
A440		Red							
A547		Red							
A808		Red							
A439		Red							

A104									
A244									
A459									
A191									
A940									
A768									
A276									
A791									
A539									
A730									
A894									
A870									
A727									
A172									
A496									
A891									
A071									
A852									
A830									
A690									
A928									
A422									
A347									
A785									
A034									
A156									
A988									
A213									
A700									
A453									
A510									
A134									
A158									
A861									
A879									
A271									
A723									
A245									
A479									
A845									
A991									
A421									
A186									
A556									

A890									
A229									
A337									
A383									
A515									
A001									
A007									
A035									
A234									
A446									
A286									
A838									
A570									
A754									
A022									
A342									
A223									
A883									
A412									
A972									
A983									
A257									
A215									
A428									
A742									
A967									
A396									
A606									
A777									
A066									
A193									
A171									
A553									
A073									
A164									
A335									
A261									
A046									
A196									
A962									
A332									
A860									
A684									
A642									

A198									
A502									
A911									
A769									
A375									
A901									
A252									
A918									
A824									
A379									
A309									
A117									
A678									
A348									
A664									
A842									
A432									
A953									
A741									
A293									
A513									
A433									
A179									
A253									
A774									
A030									
A270									
A781									
A087									
A905									
A720									
A880									
A414									
A275									
A718									
A764									
A674									
A532									
A993									
A385									
A708									
A483									
A463									
A511									

A258									
A749									
A623									
A520									
A916									
A878									
A254									
A122									
A665									
A562									
A924									
A452									
A368									
A334									
A518									
A608									
A473									
A814									
A869									
A401									
A794									
A343									
A447									
A544									
A443									
A468									
A522									
A797									
A340									
A455									
A397									
A333									
A420									
A686									
A114									
A029									
A477									
A597									
A729									
A966									
A243									
A265									
A945									
A937									

A297									
A710									
A355									
A417									
A444									
A486									
A226									
A841									
A835									
A816									
A036									
A218									
A663									
A123									
A822									
A456									
A111									
A975									
A262									
A361									
A793									
A247									
B829									
B564									
B739									
B771									
B899									
B177									
B858									
B888									
B084									
B694									
B583									
B679									
B682									
B772									
B687									
B839									
B740									
B184									
B311									
B416									
B351									
B944									

B572									
B698									
B671									
B567									
B370									
B590									
B579									
B573									
C345									
C589									
C685									
C817									
C150									
C137									
C149									
C773									
C497									
C560									
C958									
C834									
C504									
C364									
C859									
C357									
C210									
C568									
C705									
C737									
C404									
C955									
C141									
C765									
C366									
C192									
C534									
C982									
C088									
C864									
C268									
C231									
C542									
C514									
C744									
C220									

C913									
C752									
C147									
C040									
C232									
C695									
C873									
C549									
C548									
C026									
C203									
C543									
C097									
C796									

Appendix VI – Example of Detailed Clinical Validation Sequencing Analysis

The following is an example of in depth analysis of detected mutant SNPs compared to wild type genome found during analysis. This example specifically covers mutations detected within the *embB* gene for all 392 blinded FIND samples. This type of table was used for resistance calling but was not supplied in the final summarized report for ease of interpretation.

Sample	Ethambutol Resistance SNP	Ethambutol Mutation	Ethambutol Wild Type Count (#)	Ethambutol Mutant Count (#)
A405	embB M306V	ATG -> GTG	9	365
A798	embB M306V	ATG -> GTG	24	471
A614	embB M306V	ATG -> GTG	5	369
A656	embB M306I	ATG -> ATA	61	793
A762	embB M306I	ATG -> ATA	61	866
A659	embB M306I	ATG -> ATA	57	749
A675	embB N296H	AAT -> CAT	31	1086
A202	embB N296H	AAT -> CAT	17	1043
A431	embB N296H	AAT -> CAT	21	1192
A521	embB G406D	GGC -> GAC	83	1847
A320	embB G406D	GGC -> GAC	106	1791
A284	embB G406D	GGC -> GAC	77	1762
A872	embB Q497R	CAG -> CGG	44	2275
A565	embB Q497R	CAG -> CGG	15	1265
A648	embB Q497R	CAG -> CGG	29	1702
A053	embB M306V	ATG -> GTG	18	1421
A581	embB M306V	ATG -> GTG	12	1382
A199	embB M306V	ATG -> GTG	19	1115
A045	embB M306V	ATG -> GTG	21	1272
A783	embB M306V	ATG -> GTG	49	1419
A847	embB M306V	ATG -> GTG	23	1556
A316	embB Y334H	TAC -> CAC	56	1466
A750	embB Y334H	TAC -> CAC	60	1232
A205	embB Y334H	TAC -> CAC	39	533
A267	embB M306V	ATG -> GTG	14	758
A743	embB M306V	ATG -> GTG	13	976
A152	embB M306V	ATG -> GTG	13	951
A246	embB M306I	ATG -> ATC	11	327
A921	embB M306I	ATG -> ATC	37	1256
A726	embB M306I	ATG -> ATC	35	1103
A554	embB Q497R	CAG -> CGG	41	993
A371	embB Q497R	CAG -> CGG	31	865
A056	embB Q497R	CAG -> CGG	24	617

A107	embB M306V	ATG -> GTG	21	862
A418	embB M306V	ATG -> GTG	19	1112
A167	embB M306V	ATG -> GTG	10	804
A537	embB M306V	ATG -> GTG	9	998
A519	embB M306V	ATG -> GTG	13	1517
A187	embB M306V	ATG -> GTG	17	1073
A062	embB Q497R	CAG -> CGG	17	929
A818	embB Q497R	CAG -> CGG	17	608
A217	embB Q497R	CAG -> CGG	24	719
A605	embB G406S	GGC -> AGC	54	868
A273	embB G406S	GGC -> AGC	38	664
A298	embB G406S	GGC -> AGC	41	492
A119	embB M306V	ATG -> GTG	16	765
A877	embB M306V	ATG -> GTG	9	665
A827	embB M306V	ATG -> GTG	6	974
A759				
A701				
A524				
A067				
A971				
A886				
A998	embB M306I	ATG -> ATA	31	419
A128	embB M306I	ATG -> ATA	85	1011
A809	embB M306I	ATG -> ATA	33	389
A310	embB M306V	ATG -> GTG	9	649
A240	embB M306V	ATG -> GTG	7	461
A430	embB M306V	ATG -> GTG	8	521
A661	embB M306V	ATG -> GTG	13	645
A274	embB M306V	ATG -> GTG	10	677
A929	embB M306V	ATG -> GTG	16	717
A249	embB S297A	TCG -> GCG	13	471
A490	embB S297A	TCG -> GCG	13	701
A922	embB S297A	TCG -> GCG	19	706
A410	embB M306I	ATG -> ATA	35	488
A139	embB M206I	ATG -> ATA	11	143
A349	embB M306I	ATG -> ATA	44	685
A197				
A670				
A832				
A594	embB M306V	ATG -> GTG	16	630
A312	embB M306V	ATG -> GTG	11	632
A820	embB M306V	ATG -> GTG	8	537
A082				
A391				

A362				
A277	embB G406S	GGC -> AGC	88	354
A423	embB G406S	GGC -> AGC	117	430
A582	embB G406S	GGC -> AGC	135	561
A908	embB M306V	ATG -> GTG	53	1379
A222	embB M306V	ATG -> GTG	5	425
A174	embB M306V	ATG -> GTG	18	483
A305	embB M306V	ATG -> GTG	27	528
A844	embB M306V	ATG -> GTG	26	731
A458	embB M306V	ATG -> GTG	33	549
A807	embB D354A	GAC -> GCC	40	753
A242	embB D354A	GAC -> GCC	57	2043
A563	embB D354A	GAC -> GCC	18	747
A394	embB G406A	GGC -> GCC	118	406
A871	embB G406A	GGC -> GCC	151	807
A338	embB G406A	GGC -> GCC	70	336
A596				
A512				
A980				
A505	embB M306V	ATG -> GTG	617	489
A662	embB M306V	ATG -> GTG	590	480
A399	embB M306V	ATG -> GTG	995	768
A299	embB Y334H	TAC -> CAC	41	447
A057	embB Y334H	TAC -> CAC	105	1962
A992	embB Y334H	TAC -> CAC	83	1031
A125	embB Q497R	CAG -> CGG	46	1013
A984	embB Q497R	CAG -> CGG	60	2074
A471	embB Q497R	CAG -> CGG	42	1371
A272	embB E405D	GAG -> GAT	68	1112
A474	embB E405D	GAG -> GAT	81	1279
A558	embB E405D	GAG -> GAT	59	930
A528	embB M306V	ATG -> GTG	48	1170
A555	embB M306V	ATG -> GTG	22	1021
A440	embB M306V	ATG -> GTG	34	881
A547	embB M306V	ATG -> GTG	103	2475
A808	embB M306V	ATG -> GTG	63	1594
A439	embB M306V	ATG -> GTG	23	677
A104	embB N296H	AAT -> CAT	24	950
A244	embB N296H	AAT -> CAT	32	938
A459	embB N296H	AAT -> CAT	28	1068
A191	embB M306V	ATG -> GTG	29	1184
A940	embB M306V	ATG -> GTG	19	577
A768	embB M306V	ATG -> GTG	22	1132
A276	embB M306V	ATG -> GTG	33	1355

A791	embB M306V	ATG -> GTG	24	1000
A539	embB M306V	ATG -> GTG	49	1541
A730	embB M306I	ATG -> ATA	54	477
A894	embB M306I	ATG -> ATA	60	825
A870	embB M306I	ATG -> ATA	100	749
A727	embB M306I	ATG -> ATC	37	591
A172	embB M306I	ATG -> ATC	50	1326
A496	embB M306I	ATG -> ATC	60	889
A891	embB M306V	ATG -> GTG	34	1009
A071	embB M306V	ATG -> GTG	29	777
A852	embB M306V	ATG -> GTG	25	1024
A830				
A690				
A928				
A422	embB M306I	ATG -> ATC	56	1180
A347	embB M306I	ATG -> ATC	63	1136
A785	embB M306I	ATG -> ATC	57	961
A034	embB M306I	ATG -> ATA	76	969
A156	embB M306I	ATG -> ATA	79	783
A988	embB M306I	ATG -> ATA	74	895
A213	embB M306I	ATG -> ATC	26	532
A700	embB M306I	ATG -> ATC	29	590
A453	embB M306I	ATG -> ATC	88	1945
A510	embB M306V	ATG -> GTG	34	1130
A134	embB M306V	ATG -> GTG	21	529
A158	embB M306V	ATG -> GTG	37	871
A861	embB M306I	ATG -> ATA	86	676
A879	embB M306I	ATG -> ATA	93	716
A271	embB M306I	ATG -> ATA	83	524
A723	embB M306I	ATG -> ATA	62	786
A245	embB M306I	ATG -> ATA	105	729
A479	embB M306I	ATG -> ATA	61	682
A845	embB M306I	ATG -> ATC	43	725
A991	embB M306I	ATG -> ATC	33	506
A421	embB M306I	ATG -> ATC	15	300
A186	embB M306I	ATG -> ATA	52	737
A556	embB M306I	ATG -> ATA	68	660
A890	embB M306I	ATG -> ATA	59	634
A229	embB M306V	ATG -> GTG	32	1232
A337	embB M306V	ATG -> GTG	21	1104
A383	embB M306V	ATG -> GTG	21	1100
A515	embB M306I	ATG -> ATC	31	944
A001	embB M306I	ATG -> ATC	28	959
A007	embB M306I	ATG -> ATC	40	1009

A035	embB M306I	ATG -> ATC	39	1182
A234	embB M306I	ATG -> ATC	22	960
A446	embB M306I	ATG -> ATC	46	967
A286				
A838				
A570				
A754	embB M306I	ATG -> ATA	46	353
A022	embB M306I	ATG -> ATA	54	766
A342	embB M306I	ATG -> ATA	40	385
A223	embB M306I	ATG -> ATA	46	559
A883	embB M306I	ATG -> ATA	49	572
A412	embB M306I	ATG -> ATA	48	594
A972	embB G406D	GGC -> GAC	64	236
A983	embB G406D	GGC -> GAC	145	662
A257	embB G406D	GGC -> GAC	134	661
A215	embB M306V	ATG -> GTG	17	845
A428	embB M306V	ATG -> GTG	22	746
A742	embB M306V	ATG -> GTG	20	879
A967	embB M306I	ATG -> ATA	14	170
A396	embB M306I	ATG -> ATA	58	619
A606	embB M306I	ATG -> ATA	30	523
A777	embB M306I	ATG -> ATA	54	657
A066	embB M306I	ATG -> ATA	76	573
A193	embB M306I	ATG -> ATA	38	511
A171	embB M306I	ATG -> ATT	22	761
A553	embB M306I	ATG -> ATT	28	827
A073	embB M306I	ATG -> ATT	32	1258
A164	embB M306I	ATG -> ATA	51	535
A335	embB M306I	ATG -> ATA	70	788
A261	embB M306I	ATG -> ATA	42	531
A046	embB Q497R	CAG -> CGG	12	942
A196	embB Q497R	CAG -> CGG	12	721
A962	embB Q497R	CAG -> CGG	22	1045
A332	embB M306V	ATG -> GTG	19	1089
A860	embB M306V	ATG -> GTG	31	917
A684	embB M306V	ATG -> GTG	25	891
A642	embB E405D	GAG -> GAC	48	796
A198	embB E405D	GAG -> GAC	41	710
A502	embB E405D	GAG -> GAC	28	357
A911	embB M306I	ATG -> ATC	43	1032
A769	embB M306I	ATG -> ATC	34	1068
A375	embB M306I	ATG -> ATC	23	941
A901	embB M306V, embB Q497P	ATG -> GTG, CAG -> CCG	9, 7	745, 485
A252	embB M306V, embB Q497P	ATG -> GTG, CAG -> CCG	32, 15	1140, 776

A918	embB M306V, embB Q497P	ATG -> GTG, CAG -> CCG	24, 19	1004, 685
A824	embB M306I	ATG -> ATA	19	230
A379	embB M306I	ATG -> ATA	54	574
A309	embB M306I	ATG -> ATA	60	641
A117				
A678				
A348				
A664	embB M306V	ATG -> GTG	25	861
A842	embB M306V	ATG -> GTG	23	909
A432	embB M306V	ATG -> GTG	17	811
A953				
A741				
A293				
A513				
A433				
A179				
A253				
A774				
A030				
A270	embB S297A	TCG -> GCG	16	848
A781	embB S297A	TCG -> GCG	14	885
A087	embB S297A	TCG -> GCG	24	805
A905				
A720				
A880				
A414	embB E378A, embB M306V	GAG -> GCG, ATG -> GTG	14, 32	620, 711
A275	embB E378A, embB M306V	GAG -> GCG, ATG -> GTG	22, 24	566, 660
A718	embB E378A, embB M306V	GAG -> GCG, ATG -> GTG	17, 26	214, 255
A764	embB D354A, embB M306I	GAC -> GCC, ATG -> ATA	26, 39	429, 233
A674	embB D354A, embB M306I	GAC -> GCC, ATG -> ATA	19, 31	256, 146
A532	embB D354A, embB M306I	GAC -> GCC, ATG -> ATA	80, 107	1034, 505
A993	embB E378A, embB G406D	GAG -> GCG, GGC -> GAC	12, 73	327, 304
A385	embB E378A, embB G406D	GAG -> GCG, GGC -> GAC	28, 65	143, 126
A708	embB E378A, embB G406D	GAG -> GCG, GGC -> GAC	23, 115	379, 303
A483	embB M306V	ATG -> GTG	22	555
A463	embB M306V	ATG -> GTG	39	688
A511	embB M306V	ATG -> GTG	21	665
A258	embB M306I	ATG -> ATA	31	219
A749	embB M306I	ATG -> ATA	47	296
A623	embB M306I	ATG -> ATA	59	360

A520	embB Q497R	CAG -> CGG	18	784
A916	embB Q497R	CAG -> CGG	41	986
A878	embB Q497R	CAG -> CGG	33	771
A254	embB M306I	ATG -> ATA	68	761
A122	embB M306I	ATG -> ATA	76	632
A665	embB M306I	ATG -> ATA	54	320
A562	embB G406S	GGC -> AGC	148	509
A924	embB G406S	GGC -> AGC	123	344
A452	embB G406S	GGC -> AGC	147	437
A368				
A334				
A518				
A608	embB M306I	ATG -> ATC	60	1082
A473	embB M306I	ATG -> ATC	44	896
A814	embB M306I	ATG -> ATC	40	674
A869	embB M306I	ATG -> ATA	69	686
A401	embB M306I	ATG -> ATA	53	442
A794	embB M306I	ATG -> ATA	92	651
A343	embB M306V	ATG -> GTG	40	964
A447	embB M306V	ATG -> GTG	27	780
A544	embB M306V	ATG -> GTG	32	580
A443	embB M306V	ATG -> GTG	47	907
A468	embB M306V	ATG -> GTG	28	829
A522	embB M306V	ATG -> GTG	23	523
A797	embB M306V	ATG -> GTG	29	639
A340	embB M306V	ATG -> GTG	40	997
A455	embB M306V	ATG -> GTG	20	455
A397	embB M306V	ATG -> GTG	26	928
A333	embB M306V	ATG -> GTG	21	623
A420	embB M306V	ATG -> GTG	27	717
A686	embB M306V	ATG -> GTG	32	1199
A114	embB M306V	ATG -> GTG	21	578
A029	embB M306V	ATG -> GTG	35	978
A477	embB M306V	ATG -> GTG	54	1000
A597	embB M306V	ATG -> GTG	36	830
A729	embB M306V	ATG -> GTG	56	535
A966				
A243				
A265				
A945	embB M306V	ATG -> GTG	36	816
A937	embB M306V	ATG -> GTG	31	850
A297	embB M306V	ATG -> GTG	33	963
A710	embB G406A	GGC -> GCC	155	575
A355	embB G406A	GGC -> GCC	174	878

A417	embB G406A	GGC -> GCC	174	660
A444	embB G406A	GGC -> GCC	152	718
A486	embB G406A	GGC -> GCC	42	169
A226	embB G406A	GGC -> GCC	90	425
A841	embB M306I	ATG -> ATA	49	606
A835	embB M306I	ATG -> ATA	130	463
A816	embB M306I	ATG -> ATA	32	523
A036	embB M306V	ATG -> GTG	41	954
A218	embB M306V	ATG -> GTG	19	610
A663	embB M306V	ATG -> GTG	29	1091
A123	embB M306V	ATG -> GTG	32	839
A822	embB M306V	ATG -> GTG	29	1176
A456	embB M306V	ATG -> GTG	37	878
A111	embB M306V	ATG -> GTG	31	630
A975	embB M306V	ATG -> GTG	39	903
A262				
A361	embB M306I	ATG -> ATA	45	662
A793	embB M306I	ATG -> ATA	45	720
A247	embB M306I	ATG -> ATA	54	664
B829	embB Y334H	TAC -> CAC	337	814
B564	embB Y334H	TAC -> CAC	253	700
B739	embB Y334H	TAC -> CAC	77	226
B771	embB Y334H	TAC -> CAC	474	321
B899	embB Y334H	TAC -> CAC	562	415
B177	embB Y334H	TAC -> CAC	614	416
B858	embB Y334H	TAC -> CAC	702	244
B888	embB Y334H	TAC -> CAC	617	226
B084	embB Y334H	TAC -> CAC	782	284
B694				
B583				
B679				
B682				
B772				
B687				
B839	embB Y334H	TAC -> CAC	358	746
B740	embB Y334H	TAC -> CAC	273	600
B184	embB Y334H	TAC -> CAC	315	640
B311	embB Y334H	TAC -> CAC	601	375
B416	embB Y334H	TAC -> CAC	275	165
B351	embB Y334H	TAC -> CAC	630	371
B944	embB Y334H	TAC -> CAC	497	129
B572	embB Y334H	TAC -> CAC	1047	291
B698	embB Y334H	TAC -> CAC	2830	914
B671				

B567				
B370				
B590				
B579				
B573				
C345				
C589				
C685				
C817				
C150				
C137				
C149				
C773				
C497				
C560				
C958				
C834				
C504				
C364				
C859				
C357				
C210				
C568				
C705				
C737				
C404				
C955				
C141				
C765				
C366				
C192	embB M306I	ATG -> ATC	31	915
C534	embB M306I	ATG -> ATC	39	1029
C982	embB M306I	ATG -> ATC	44	1361
C088	embB M306I	ATG -> ATC	13	725
C864	embB M306I	ATG -> ATC	22	418
C268	embB M306I	ATG -> ATC	31	639
C231	embB M306I	ATG -> ATC	5	154
C542	embB M306I	ATG -> ATC	30	668
C514	embB M306I	ATG -> ATC	37	653
C744	embB M306I	ATG -> ATC	48	1101
C220	embB M306I	ATG -> ATC	70	1280
C913	embB M306I	ATG -> ATC	90	1783
C752	embB M306I	ATG -> ATC	66	1315
C147	embB M306I	ATG -> ATC	94	1451

C040	embB M306I	ATG -> ATC	61	1127
C232	embB M306I	ATG -> ATC	2467	2730
C695	embB M306I	ATG -> ATC	582	587
C873	embB M306I	ATG -> ATC	486	505
C549	embB M306I	ATG -> ATC	405	430
C548	embB M306I	ATG -> ATC	551	499
C026	embB M306I	ATG -> ATC	51	888
C203	embB M306I	ATG -> ATC	44	1163
C543	embB M306I	ATG -> ATC	75	1158
C097	embB M306I	ATG -> ATC	66	1788
C796	embB M306I	ATG -> ATC	81	1455

References

1. Coscolla M, Gagneux S. Seminars in Immunology Consequences of genomic diversity in *Mycobacterium tuberculosis*. *Semin. Immunol.* 2014;26(6):431–444. Available at: <http://dx.doi.org/10.1016/j.smim.2014.09.012>.
2. Jagielski T, Minias A, Ingen J Van, Rastogi N, Brzostek A. Methodological and Clinical Aspects of the Molecular Epidemiology of *Mycobacterium tuberculosis* and Other *Mycobacteria*. *Clin. Microbiol. Rev.* 2016;29(2):239–290.
3. Mcnerney R, Clark TG, Campino S, et al. Removing the bottleneck in whole genome sequencing of *Mycobacterium tuberculosis* for rapid drug resistance analysis : a call to action. *Int. J. Infect. Dis.* 2017;56:130–135. Available at: <http://dx.doi.org/10.1016/j.ijid.2016.11.422>.
4. Fu L, Fu-Liu C. Is *Mycobacterium tuberculosis* a closer relative to Gram-positive or Gram-negative bacterial pathogens? *Tuberculosis.* 2002;82(2–3):85–90.
5. Deurenberg RH, Bathoorn E, Chlebowicz MA, et al. Application of next generation sequencing in clinical microbiology and infection prevention. *J. Biotechnol.* 2017;243:16–24. Available at: <http://dx.doi.org/10.1016/j.jbiotec.2016.12.022>.
6. Walker TM, Kohl TA, Omar S V, et al. Whole-genome sequencing for prediction of *Mycobacterium tuberculosis* drug susceptibility and resistance : a retrospective cohort study. *Lancet Infect. Dis.* 2015;15:1193–1202.
7. Votintseva AA, Pankhurst LJ, Anson LW, et al. *Mycobacterial* DNA Extraction for Whole-Genome Sequencing from Early Positive Liquid (MGIT) Cultures. *J. Clin. Microbiol.* 2015;53(4):1137–1143.
8. Bradley P, Gordon NC, Walker TM, et al. Rapid antibiotic-resistance predictions from genome sequence data for *Staphylococcus aureus* and *Mycobacterium tuberculosis*. *Nat. Commun.* 2015;6:1–14. Available at: <http://dx.doi.org/10.1038/ncomms10063>.
9. Pankhurst LJ, Elias O, Votintseva AA, et al. Rapid , comprehensive , and affordable *mycobacterial* diagnosis with whole-genome sequencing : a prospective study. *Lancet Respir.* 4(1):49–58. Available at: [http://dx.doi.org/10.1016/S2213-2600\(15\)00466-X](http://dx.doi.org/10.1016/S2213-2600(15)00466-X).
10. Kim S, Jonghe J De, Kulesa AB, et al. preparation for accurate microbial genomics. *Nat. Commun.* 2017;8:1–10. Available at: <http://dx.doi.org/10.1038/ncomms13919>.
11. Gagneux S. Ecology and evolution of *Mycobacterium tuberculosis*. *Nat. Publ. Gr.* 2018;16(4):202–213. Available at: <http://dx.doi.org/10.1038/nrmicro.2018.8>.

12. Ip K-U, Chang J-R, Liu T-H, Dou H-Y, Lee G-B. An Integrated Microfluidic System for Identification of Live Mycobacterium Tuberculosis by Real-Time Polymerase Chain Reaction. *MEMS*. 2018;(January):1124–1127.
13. Wlodarska M, Johnston JC, Gardy JL. A Microbiological Revolution Meets an Ancient Disease : Improving the Management of Tuberculosis with Genomics. 2015;28(2):523–539.
14. Haas CT, Roe JK, Pollara G, Mehta M, Noursadeghi M. Diagnostic ‘ omics ’ for active tuberculosis. *BMC Med*. 2016. Available at: <http://dx.doi.org/10.1186/s12916-016-0583-9>.
15. Doughty EL, Sergeant MJ, Adetifa I, Antonio M, Pallen MJ. Culture-independent detection and characterisation of Mycobacterium tuberculosis and M . africanum in sputum samples using shotgun metagenomics on a benchtop sequencer. *PeerJ*. 2014;2:1–18.
16. Brown AC, Bryant JM, Einer-jensen K, et al. Rapid Whole-Genome Sequencing of Mycobacterium tuberculosis Isolates Directly from Clinical Samples. *J. Clin. Microbiol*. 2015;53(7):2230–2237.
17. Tsalik EL, Bonomo RA, Fowler VG. New Molecular Diagnostic Approaches to Bacterial Infections and Antibacterial Resistance. *Annu. Rev. Med*. 2018;69:379–394.
18. Satta G, Atzeni A, Mchugh TD. Mycobacterium tuberculosis and whole genome sequencing : a practical guide and online tools available for the clinical microbiologist. *Clin. Microbiol. Infect*. 2017;23(2):69–72. Available at: <http://dx.doi.org/10.1016/j.cmi.2016.09.005>.
19. Costa P, Botelho A, Couto I, Viveiros M, Inácio J. Standing of nucleic acid testing strategies in veterinary diagnosis laboratories to uncover Mycobacterium tuberculosis complex members. *Front. Mol. Biosci*. 2014;1(October):1–11.
20. Srivasta S, Rijn SP van, Wessels AMA, Alffenaar J-WC, Gumbo T. Susceptibility testing of antibiotics that degrade faster than the doubling time of slow-growing mycobacteria: Ertapenem sterilizing effects versus Mycobacterium tuberculosis. *Antimicrob. Agents Chemother*. 2016;(April).
21. Delogu G, Sali M, Fadda G. The biology of Mycobacterium tuberculosis infection. *Mediterr. J. Hematol. Infect. Dis*. 2013;5(1).
22. Cudahy P, Shenoi S. Diagnostics for pulmonary tuberculosis. *Postgraduate Med. J*. 2016;92(April):187–193.
23. Carr JH. Microbiology in Pictures - Tuberculosis. 2021. Available at:

https://www.microbiologyinpictures.com/bacteria_photos/mycobacterium_tuberculosis_photos/MYTU20.html [Accessed March 5, 2021].

24. N'Dira Sanoussi C, Affolabi D, Rigouts L, Anagonou S, Jong B de. Genotypic characterization directly applied to sputum improves the detection of *Mycobacterium africanum* West African 1, under-represented in positive cultures. *PLoS Negl. Trop. Dis.* 2017;1–13.
25. Couto RDM, Ranzani OT, Waldman EA. Zoonotic Tuberculosis in Humans : Control , Surveillance , and the One Health Approach. *Epidemiol. Rev.* 2020;41(14):130–144.
26. Parsons SDC, Drewe JA, Pittius NCG Van, Warren RM, Helden PD Van. Novel Cause of Tuberculosis in Meerkats, South Afric. *Emerg. Infect. Dis.* 2013;19(12).
27. Ingen J Van, Rahim Z, Mulder A, et al. Characterization of *Mycobacterium orygis* as M tuberculosis Complex Subspecies. *Emerg. Infect. Dis.* 2012;18(4):653–655.
28. Rue-albrecht K, Magee DA, Killick KE, et al. Comparative functional genomics and the bovine macrophage response to strains of the *Mycobacterium* genus. *Front. Immunol.* 2014;5(November):1–14.
29. Guthrie JL, Gardy JL. A brief primer on genomic epidemiology : lessons learned from *Mycobacterium tuberculosis*. *Ann. N. Y. Acad. Sci.* 2016:59–78.
30. Chatterjee A, Nilgiriwala K, Saranath D, Rodrigues C, Mistry N. Whole genome sequencing of clinical strains of *Mycobacterium tuberculosis* from Mumbai , India : A potential tool for determining drug-resistance and strain lineage. *Tuberculosis.* 2017;107:63–72. Available at: <https://doi.org/10.1016/j.tube.2017.08.002>.
31. World Health Organization. *WHO consolidated guidelines on drug-resistant tuberculosis treatment. Annexes 3-9.* 2019.
32. Hoffman C, Churchyard G. Chapter 29 - Pulmonary tuberculosis in adults. In: Schaaf HS, Zumla A, Donald P, eds. *Tuberculosis: A Comprehensive Clinical Reference.*; 2009:332–341.
33. World Health Organization. *Global Tuberculosis Report.* 2019.
34. World Health Organization. *Global Tuberculosis Report.* 2021.
35. World Health Organization. *Latent TB Infection : Updated and consolidated guidelines for programmatic management.* 2018.
36. Mack U, Migliori GB, Sester M, et al. LTBI: latent tuberculosis infection or lasting immune

- responses to M. tuberculosis? A TBNET consensus statement. *Eur. Respir. J.* 2009;33:956–973.
37. Gupta S, Kakkar V. Biosensors and Bioelectronics Recent technological advancements in tuberculosis diagnostics – A review. *Biosens. Bioelectron.* 2018;115(May):14–29. Available at: <https://doi.org/10.1016/j.bios.2018.05.017>.
38. Tiberi S, Carvalho ACC, Sulis G, et al. The cursed duet today : Tuberculosis and HIV-coinfection. *Presse Med.* 2017;46(2):e23–e39. Available at: <http://dx.doi.org/10.1016/j.lpm.2017.01.017>.
39. Pinto C, Carvalho A. The HIV/TB coinfection severity in the presence of TB multi-drug resistant strains. *Ecol. Complex.* 2017;32(A):1–20.
40. Bruchfeld J, Correia-Neves M, Kallenius G. Tuberculosis and HIV Coinfection. *Perspect. Med.* 2015.
41. Dheda K, Gumbo T, Maartens G, et al. The epidemiology , pathogenesis , transmission , diagnosis , and management of multidrug-resistant , extensively drug-resistant , and incurable tuberculosis. *Lancet Respir. Med. Comm.* 2017.
42. Burynski N, Buynevich I, Loginov R, Gaponyako S, Demidova E. Clinical and Morphological Features of HIV-Associated Tuberculosis. *Eur. Respir. J.* 2015;46.
43. Nelson LJ, Wells CD. Global epidemiology of childhood tuberculosis. 2004;8(5):636–647.
44. Onyango DO, Yuen CM, Masini E, Borgdorff MW. Epidemiology of Pediatric Tuberculosis in Kenya and Risk Factors for Mortality during Treatment: A National Retrospective Cohort Study. *J. Pediatr.* 2018;201:115–121. Available at: <https://doi.org/10.1016/j.jpeds.2018.05.017>.
45. Dean AS, Cox H, Zignol M. Epidemiology of Drug-Resistant Tuberculosis. In: Gagneux S, ed. *Strain Variation in the Mycobacterium tuberculosis Complex: Its Role in Biology, Epidemiology, and Control.* Springer International Publishing AG; 2017:209–220.
46. Tougousova OS, Bjune G, Caugant DA. Epidemic of tuberculosis in the former Soviet Union : Social and biological reasons. *Tuberculosis.* 2006;86:1–10.
47. Falzon D, Infuso A, Ait-Belghiti F. In the European Union , TB patients from former Soviet countries have a high risk of multidrug resistance. *Int. J. Tuberculous Lung Dis.* 2006;10(9):954–958.
48. Nimmo C, Doyle R, Burgess C, et al. International Journal of Infectious Diseases Rapid identification of a Mycobacterium tuberculosis full genetic drug resistance profile through whole genome sequencing directly from sputum. *Int. J. Infect. Dis.* 2017;62:44–46. Available at:

<http://dx.doi.org/10.1016/j.ijid.2017.07.007>.

49. Faksri K, Hao J, Chaiprasert A, Teo Y, Ong RT. Infection , Genetics and Evolution Bioinformatics tools and databases for whole genome sequence analysis of Mycobacterium tuberculosis. *MEEGID*. 2016;45:359–368. Available at: <http://dx.doi.org/10.1016/j.meegid.2016.09.013>.

50. Epomedicine. Drug Resistant TB Management Summary. *Epomedicine*. 2016. Available at: <https://epomedicine.com/medical-students/mdr-xdr-tb/> [Accessed March 10, 2021].

51. Gandy M, Zumla A eds. *The Return of the White Plague: Global Poverty and the “new” Tuberculosis*. Verso; 2003.

52. Gardy JL. Towards genomic prediction of drug resistance in tuberculosis. *Lancet Infect. Dis*. 2015;15(10):1124–1125. Available at: [http://dx.doi.org/10.1016/S1473-3099\(15\)00088-2](http://dx.doi.org/10.1016/S1473-3099(15)00088-2).

53. Papaventsis D, Casali N, Kontsevaya I, et al. Whole genome sequencing of Mycobacterium tuberculosis for detection of drug resistance : a systematic review. *Clin. Microbiol. Infect*. 2017;23(2):61–68. Available at: <http://dx.doi.org/10.1016/j.cmi.2016.09.008>.

54. Linger Y, Knickerbocker C, Sipes D, et al. Genotyping Multidrug-Resistant Mycobacterium tuberculosis from Primary Sputum and Decontaminated Sediment with an Integrated Microfluidic Amplification Microarray Test. *J. Clin. Microbiol*. 2018;56(3):1–11.

55. World Health Organization. WHO announces updated definitions of extensively drug-resistant tuberculosis. *Dep. News*. 2021. Available at: <https://www.who.int/news/item/27-01-2021-who-announces-updated-definitions-of-extensively-drug-resistant-tuberculosis> [Accessed January 31, 2022].

56. Borrell S, Trauner A. Strain Diversity and the Evolution of Antibiotic Resistance. In: Gagneux S, ed. *Strain Variation in the Mycobacterium tuberculosis Complex: Its Role in Biology, Epidemiology, and Control*. Springer International Publishing AG; 2017:263–279.

57. Quan TP, Bawa Z, Foster D, et al. Evaluation of Whole-Genome Sequencing for Mycobacterial Species Identification and Drug Susceptibility Testing in a Clinical Setting : a Large-Scale Prospective Assessment of Performance against Line Probe Assays and Phenotyping. *J. Chromatogr. B Anal. Technol. Biomed. Life Sci*. 2018;56(2):1–14.

58. Pio A, Chaulet P, World Health Organization. *Tuberculosis Handbook*. World Health Organization; 1998.

59. Glynn JR, Whiteley J, Bifani PJ, Kremer K, Soolingen D van. Worldwide Occurrence of Beijing/W

- Strains of Mycobacterium tuberculosis: A Systematic Review. *Emerg. Infect. Dis.* 2002;8(8).
60. Crofton J, Mitchison DA. Streptomycin resistance in pulmonary tuberculosis. *Br. Med. J.* 1948.
61. World Health Organization. Treatment strategies for MDR-TB and XDR-TB. In: *Companion Handbook to the WHO Guidelines for the Programmatic Management of Drug-Resistant Tuberculosis.*; 2014.
62. World Health Organization. *Treatment of drug-susceptible tuberculosis: rapid communication.* 2021.
63. Pontali E, Raviglione MC, Migliori GB, Committee GTNCT. Regimens to treat multidrug-resistant tuberculosis: past, present and future perspectives. *Tuberculosis.* 2019;28.
64. Deun A Van, Maug AKJ, Alim MAH, et al. Short, highly effective, and inexpensive standardized treatment of multidrug-resistant tuberculosis. *Am. J. Respir. Crit. Care Med.* 2010;182:684–692.
65. Heldal E, Deun A Van, Chiang C-Y, Rieder HL. Shorter regimens for multidrug-resistant tuberculosis should also be applicable in Europe. *Eur. Respir. J.* 2017;49.
66. Balabanova Y, Fiebig L, Ignatyeva O, et al. Multidrug-resistant TB in Eastern region of the EU: is the shorter regimen an exception or a rule? *Thorax.* 2017;72(9):850–852.
67. Dalcolmo M, Gayoso R, Sotgiu G, et al. Resistance profile of drugs composing the “shorter” regimen for multidrug-resistant tuberculosis in Brazil, 2000-2015. *Eur. Respir. J.* 2017;49(4).
68. Sotgiu G, Tiberi S, Centis R, et al. Applicability of the shorter “Bangladesh regimen” in high multidrug-resistant tuberculosis settings. *Int. J. Infect. Dis.* 2017;56(March):190–193.
69. TCG TCG for the M-A of IPD in M-T-2017. Treatment correlates of successful outcomes in pulmonary multidrug-resistant tuberculosis: an individual patient data meta-analysis. *Lancet.* 2018;392:821–834.
70. World Health Organization. *WHO consolidated guidelines on drug-resistant tuberculosis treatment.* 2019.
71. Conradie F, Diacon AH, Ngubane N, et al. Treatment of Highly Drug-Resistant Pulmonary Tuberculosis. *N. Engl. J. Med.* 2020;382(10):893–902.
72. Alliance T. Nix-TB. 2022. Available at: <https://www.tballiance.org/portfolio/trial/5089> [Accessed January 28, 2022].
73. Alliance T. SimpliciTB. 2022. Available at: <https://www.tballiance.org/portfolio/trial/11937>

[Accessed February 1, 2022].

74. Gupta A, Juneja S, Mulder C, Sahu S. Projected use of pretomanid, bedaquiline and linezolid in all-oral regimens for multi-drug resistant tuberculosis from 2021-2025. *Lancet*. 2021;Preprint.
75. Taheri MS, Karimi M, Haghghatkah H, et al. Central Nervous System Tuberculosis: An Imaging-Focused Review of a Reemerging Disease. *Radiol. Res. Pract.* 2015;8.
76. Jeon D. Infection Source and Epidemiology of Nontuberculous Mycobacterial Lung Disease. 2019;3536:94–101.
77. Lipman M, Cleverley J, Fardon T, et al. Current and future management of non- -tuberculous mycobacterial pulmonary disease (NTM- PD) in the UK. *BMJ Open Respir. Res.* 2020;1–8.
78. Prevots DR, Marras TK. Epidemiology of Human Pulmonary Infection with Non-Tuberculous Mycobacteria: A Review. *Clin Chest Med.* 2015;36(1):13–34.
79. Dewan S, Chugh T Das. Nocardiosis : A Neglected Disease. *Med. Princ. Pract.* 2020;29:514–523.
80. Kunkel D. *Nocardia Asteroides*. 2020:1.
81. Embden JDA Van, Cave MD, Crawford JT, et al. Strain identification of *Mycobacterium tuberculosis* by DNA fingerprinting: Recommendations for a standardized methodology. *J. Clin. Microbiol.* 1993;31(2).
82. Shi J, Zheng D, Zhu Y, et al. Role of MIRU-VNTR and spoligotyping in assessing the genetic diversity of *Mycobacterium tuberculosis* in Henan Province, China. *BMC Infect. Dis.* 2018:1–12.
83. Nikolayevskyy V, Trovato A, Broda A, et al. MIRU-VNTR Genotyping of *Mycobacterium tuberculosis* Using QIAxcel Technology: A Multicentre Evaluation Study. *PLoS One*. 2016.
84. Jonsson J, Hoffner S, Berggren I, Bruchfeld J, Ghebremichael S. Comparison between RFLP and MIRU-VNTR Genotyping of *Mycobacterium tuberculosis* Strains Isolated in Stockholm 2009 to 2011. *PLoS One*. 2014;9(4).
85. Kamerbeek J, Schouls LEO, Kolk A, et al. Simultaneous Detection and Strain Differentiation of *Mycobacterium tuberculosis* for Diagnosis and Epidemiology. *J. Clin. Microbiol.* 1997;35(4):907–914.
86. Gori A, Bandera A, Marchetti G, et al. Spoligotyping and *Mycobacterium tuberculosis*. *Emerg. Infect. Dis.* 2005;11(8).
87. Doyle RM, Burgess C, Williams R, et al. Direct Whole-Genome Sequencing of Sputum

Accurately Identifies Drug-Resistant Mycobacterium tuberculosis Faster than MGIT Culture Sequencing. *J. Clin. Microbiol.* 2018;56(8).

88. Satta G, Lipman M, Smith GP, et al. Mycobacterium tuberculosis and whole-genome sequencing: how close are we to unleashing its full potential ? *Clin. Microbiol. Infect.* 2018;24(6):604–609. Available at: <https://doi.org/10.1016/j.cmi.2017.10.030>.

89. Witney AA, Cosgrove CA, Arnold A, et al. Clinical use of whole genome sequencing for Mycobacterium tuberculosis. *BMC Med.* 2016;14(46). Available at: <http://dx.doi.org/10.1186/s12916-016-0598-2>.

90. Coll F, McNerney R, Preston M, et al. Rapid determination of anti-tuberculosis drug resistance from whole-genome sequences. *Genome Med.* 2015;7(51).

91. Phelan JE, O'Sullivan D, Machado D, et al. Integrating informatics tools and portable sequencing technology for rapid detection of resistance to anti-tuberculous drugs. *Genome Med.* 2019;11(41).

92. Talbot EA, Williams DL, Frothingham R. PCR Identification of Mycobacterium bovis BCG. *J. Clin. Microbiol.* 1997;35(3):566–569.

93. Allahyartorkaman M, Mirsaeidi M, Hamzehloo G, et al. Low diagnostic accuracy of Xpert MTB / RIF assay for extrapulmonary tuberculosis : A multicenter surveillance. *Sci. Rep.* 2019;9:1–6. Available at: <http://dx.doi.org/10.1038/s41598-019-55112-y>.

94. Fisher M, Dolby T, Surtie S, et al. Improved method for collection of sputum for tuberculosis testing to ensure adequate sample volumes for molecular diagnostic testing. *J. Microbiol. Methods.* 2017;135:35–40. Available at: <http://dx.doi.org/10.1016/j.mimet.2017.01.011>.

95. Zumla A, Al-Tawfiq JA, Enne VI, et al. Rapid point of care diagnostic tests for viral and bacterial respiratory tract infections-needs, advances, and future prospects. *Lancet Infect. Dis.* 2014;14(11):1123–1135.

96. Neshani A, Kakhi RK, Sankian M, et al. Modified genome comparison method: a new approach for identification of specific targets in molecular diagnostic tests using Mycobacterium tuberculosis complex as an example. *BMC Infect. Dis.* 2018;18:517.

97. Schürch AC, Soolingen D Van. Infection , Genetics and Evolution DNA fingerprinting of Mycobacterium tuberculosis : From phage typing to whole-genome sequencing. 2012;12:602–609.

98. Zhang Z, Wang Y, Pang Y, Liu C. Comparison of difference drug susceptibility test methods to detect rifampin heteroresistance in *Mycobacterium tuberculosis*. *Antimicrob. Agents Chemother.* 2014;58(9):5632–5635.
99. Wiegand I, Hilpert K, Hancock RE. Agar and broth dilution methods to determine the minimal inhibitory concentration (MIC) of antimicrobial substances. *Nat. Protoc.* 2008;3(2):163–175.
100. EUCAST. *Reference protocol for MIC determination of anti-tuberculous agents against isolates of the Mycobacterium tuberculosis complex in Middlebrook 7H9 broth.* 2019.
101. Hodille E, Maisson A, Charlet L, et al. Evaluation of XpertMTB/RIF Ultra performance for pulmonary tuberculosis diagnosis on smear-negative respiratory samples in a French centre. *Eur. J. Clin. Microbiol. Infect. Dis.* 2019;38(3):601–605.
102. Rasheed W, Rao N, Adel H, Baig M, Adil S. Diagnostic Accuracy of Xpert MTB/RIF in Sputum SMear-Negative Pulmonary Tuberculosis. *Cureus.* 2019;11(8):e5391.
103. Tomasicchio M, Theron G, Pietersen E, et al. The diagnostic accuracy of the MTBDRplus and MTBDRsl assays for drug-resistant TB detection when performed on sputum and culture isolates. *Sci. Rep.* 2016;6.
104. Lee RS, Pai M. Real-Time Sequencing of *Mycobacterium tuberculosis*: Are We There Yet? *J. Clin. Microbiol.* 2017;55(5):1249–1254.
105. Weinstein RA, Singh K. Laboratory-Acquired Infections. *Clin. Infect. Dis.* 2009;49(1):142–147.
106. Colijn C, Cohen T. Whole-Genome sequencing of *Mycobacterium tuberculosis* for rapid diagnostics and beyond. *Lancet Respir.* 2015;4:6–8.
107. Barnard M, Gey van Pittius N, Helden P van, et al. The Diagnostic Performance of the GenoType MTBDRplus Version 2 Line Probe Assay is Equivalent to that of the Xpert MTB/RIF Assay. *J. Clin. Microbiol.* 2012;50(11):3712–3716.
108. Cole S, Brosch R, Parkhill J, et al. Deciphering the biology of *Mycobacterium tuberculosis* from the complete genome sequence. *Nature.* 1998;393(June):537–544.
109. Walker TM, Lalor MK, Broda A, et al. Assessment of *Mycobacterium tuberculosis* transmission in Oxfordshire, UK, 2007–12, with whole pathogen genome sequences: an observational study. *Lancet Infect. Dis.* 2014;2(4):285–292.
110. Crisan A, Mckee G, Munzner T, Gardy JL. Evidence-based design and evaluation of a whole genome sequencing clinical report for the reference microbiology laboratory. *PeerJ.* 2018:1–25.

111. Charalampous T, Kay GL, Richardson H, et al. Nanopore metagenomics enables rapid clinical diagnosis of bacterial lower respiratory infection. *Nat Biotech.* 2019;37(July). Available at: <http://dx.doi.org/10.1038/s41587-019-0156-5>.
112. Charalampous T. Development and application of clinical metagenomics for the diagnosis and characterisation of lower respiratory infections. 2020.
113. Charalampous T, Richardson H, Kay GL, et al. Rapid Diagnosis of Lower Respiratory Infection Using Nanopore-Based Clinical Metagenomics. 2018:1–40.
114. Rehm HL. Disease-targeted sequencing: a cornerstone in the clinic. *Nat. Rev. Genet.* 2013;14(April):295–300.
115. Grada A, Weinbrecht K. Next-Generation Sequencing: Methodology and Application. *J. Invest. Dermatol.* 2013;133.
116. Genoscreen. *Deplex[®] Myc- TB*. 2020.
117. Kayomo MK, Mbula VN, Aloni M, et al. Targeted next-generation sequencing of sputum for diagnosis of drug-resistant TB: results of a national survey in Democratic Republic of the Congo. *Sci. Rep.* 2020;July.
118. Tagliani E, Hassan MO, Waberi Y, et al. Culture and Next-generation sequencing-based drug susceptibility testing unveil high levels of drug-resistant-TB in Djibouti: results from the first national survey. *Sci. Rep.* 2017;7.
119. Makhado NA, Matabane E, Faccin M, et al. Outbreak of multidrug-resistant tuberculosis in South Africa undetected by WHO-endorsed commercial tests: an observational study. *Lancet Infect. Dis.* 2018;18(12):1350–1359.
120. Suresh A, Rodwell T, Uplekar S, Colman B. Next Generation Sequencing for Drug Resistant TB Testing in LMICs Unitaid Project Proposal. 2019;(April).
121. Mertes F, Elsharawy A, Sauer S, et al. Targeted enrichment of genomic DNA regions for next-generation sequencing. 2011;10(6):374–386.
122. George S, Xu Y, Rodger G, et al. DNA thermo-protection facilitates whole-genome sequencing of Mycobacteria direct from clinical samples. *J. Clin. Microbiol.* 2020;58(10).
123. Partnership ST. *Mycobacteriology Laboratory Manual*. First. (Stinson K, Eisenach K, Kayes S, et al., eds.); 2014.

124. World Health Organization. *Molecular Line Probe Assays for Rapid Screening of Patients at Risk of Multidrug-resistant Tuberculosis (MDR-TB)*. 2008.
125. Kolia-Diafouka P, Godreuil S, Bourdin A, et al. Optimized lysis-extraction method combined with IS6110-amplification for detection of Mycobacterium tuberculosis in paucibacillary sputum specimens. *Front. Microbiol.* 2018.
126. Pan S, Gu B, Wang H, et al. Comparison of four DNA extraction methods for detecting Mycobacterium tuberculosis by real-time PCR and its clinical application in pulmonary tuberculosis. *J. Thorac. Dis.* 2013;5(3).
127. Neves de Almeida I, Carvalho W da S, Rossetti ML, Dalla Costa ER, Spindola de Miranda S. Evaluation of six different DNA extraction methods for detection of Mycobacterium tuberculosis by means of PCR-IS6110: preliminary study. *BMC Res. Notes.* 2013;6.
128. Sundarsingh JA, Ranjitha J, Rajan A, Shankar V. Features of the biochemistry of Mycobacterium smegmatis, as a possible model for Mycobacterium tuberculosis. *J. Infect. Public Health.* 2020;13(9):1255–1264.
129. Kaser M, Ruf M-T, Hauser J, Marsollier L, Pluschke G. Optimized Method for Preparation of DNA from Pathogenic and Environmental Mycobacteria. *Appl. Environ. Microbiol.* 2009;75(2):414–418.
130. Hurley S, Splitter G, Welch R. Rapid lysis technique for mycobacterial species. *J. Clin. Microbiol.* 1987;25(11):2227–2229.
131. Kirchgesser M, Schlagenhauser R, Kirchner B, et al. The New MagNA Pure Compact Nucleic Acid Isolation Kits – Fast and Flexible Fully Automated Sample Preparation. *Biochemica.* 2003;4:12–14.
132. Schuurman T, Breda A Van, Boer R De, et al. Reduced PCR Sensitivity Due to Impaired DNA Recovery with the MagNA Pure LC Total Nucleic Acid Isolation Kit. *J. Clin. Microbiol.* 2005;43(9):4616–4622.
133. Thakur R, Sarma S, Goyal R. Comparison of DNA extraction for Mycobacterium tuberculosis in diagnosis of tuberculous meningitis by real-time polymerase chain reaction. *J. Glob. Infect. Dis.* 2011;3(4):353–356.
134. Wozniak A, Geoffroy E, Miranda C, et al. Comparison of manual and automated nucleic acid extraction methods from clinical specimens for microbial diagnosis purposes. *Diagn. Microbiol. Infect. Dis.* 2016;86(3):268–269. Available at:

<http://dx.doi.org/10.1016/j.diagmicrobio.2016.07.008>.

135. Promega. *Maxwell RSC System*.

136. Rhoads DD, Cherian SS, Roman K, et al. Comparison of Abbott ID Now, DiaSorin Simplexa, and CDC FDA Emergency Use Authorization Methods for the Detection of SARS-CoV-2 from Nasopharyngeal and Nasal Swabs from Individuals Diagnosed with COVID-19. *J. Clin. Microbiol.* 2020;58(8):9–10.

137. Miller M, Jansen M, Bisignano A, et al. Validation of a self-administrable, saliva-based RT-qPCR test detecting SARS-CoV-2. *MedRxiv*. 2020:1–18.

138. Pérez-cataluña A, Cuevas-ferrando E, Randazzo W, et al. Comparing analytical methods to detect SARS-CoV-2 in wastewater. *Sci. Total Environ.* 2020;758.

139. Trotter A. Personal Correspondance. 2021.

140. Amaro A, Duarte E, Amado A, Ferronha H, Botelho A. Comparison of three DNA extraction methods for *Mycobacterium bovis*, *Mycobacterium tuberculosis* and *Mycobacterium avium* subsp. *avium*. *J. Appl. Microbiol.* 2008;47(1).

141. Salgado M, Verdugo C, Heuer C, Castillo P, Zamorano P. A novel low-cost method for *Mycobacterium avium* subsp. *paratuberculosis* DNA extraction from an automated broth culture system for real-time PCR analysis. *J. Vet. Sci.* 2014;15:233–239.

142. World Health Organization. The Use of Next-Generation Sequencing Technologies for the Detection of Mutations Associated with Drug Resistance in *Mycobacterium tuberculosis* Complex: Technical Guide. 2018.

143. Miotto P, Tessema B, Tagliani E, et al. A standardised method for interpreting the association between mutations and phenotypic drug resistance in *Mycobacterium tuberculosis*. *Eur. Respir. J.* 2017;50. Available at: <http://dx.doi.org/10.1183/13993003.01354-2017>.

144. Zhao L, Sun Q, Liu H, et al. Analysis of embCAB Mutations Associated with Ethambutol Resistance in Multidrug-Resistant *Mycobacterium tuberculosis* Isolates from China. *Antimicrob. Agents Chemother.* 2015;59(4):2045–2050.

145. Villellas C, Coeck N, Meehan CJ, et al. Unexpected high prevalence of resistance-associated Rv0678 variants in MDR-TB patients without documented prior use of clofazimine or bedaquiline. *J. Antimicrob. Chemother.* 2017;72:684–690.

146. Andries K, Villellas C, Coeck N, et al. Acquired resistance of *Mycobacterium tuberculosis* to

bedaquiline. *PLoS One*. 2014;July.

147. Ismail NA, Omar S V, Joseph L, et al. Defining Bedaquiline Susceptibility , Resistance , Cross-Resistance and Associated Genetic Determinants : A Retrospective Cohort Study. *EBioMedicine*. 2018;28:136–142. Available at: <https://doi.org/10.1016/j.ebiom.2018.01.005>.

148. Beckert P, Hillemann D, Kohl TA, et al. rplC T460C identified as a dominant mutation in linezolid-resistant Mycobacterium tuberculosis strains. *Antimicrob. Agents Chemother*. 2012;2743–2745.

149. Wasserman S, Louw G, Ramangoela L, et al. Linezolid resistance in patients with drug-resistant TB and treatment failure in South Africa. *J. Antimicrob. Chemother*. 2019;74:2377–2384.

150. Sreevatsan S, Stockbauer KE, Pan XI, et al. Ethambutol Resistance in Mycobacterium tuberculosis : Critical Role of embB Mutations. *Antimicrob. Agents Chemother*. 1997;41(8):1677–1681.

151. Plinke C, Rusch-Gerdes S, Niemann S. Significance of mutations in embB codon 306 for prediction of ethambutol resistance in clinical Mycobacterium tuberculosis isolates. *Antimicrob. Agents Chemother*. 2006;50(5):1900–1902.

152. Locke J, Hilgers M, Shaw K. Novel ribosomal mutations in Staphylococcus aureus strains identified through selection with the oxazolidinones linezolid and torezolid. *Antimicrob. Agents Chemother*. 2009;53:5265–5274.

153. Locke J, Hilgers M, Shaw K. Mutations in ribosomal protein L3 are associated with oxazolidinone resistance in staphylococci of clinical origin. *Antimicrob. Agents Chemother*. 2009;53:5275–5278.

154. Rifat D, Li S-Y, Ioerger T, et al. Mutations in fbiD (Rv2983) as a novel determinant of resistance to pretomanid and delamanid in Mycobacterium tuberculosis. *Am. Soc. Microbiol*. 2020;(September).

155. Kadura S, King N, Nakhoul M, et al. Systematic review of mutations associated with resistance to the new and repurposed Mycobacterium tuberculosis drugs bedaquiline, clofazimine, linezolid, delamanid and pretomanid. *J. Antimicrob. Chemother*. 2020;75:2013–2043.

156. World Health Organization. *Catalogue of mutations in Mycobacterium tuberculosis complex and their association with drug resistance*. 2021.

157. Henegariu O, Heerema N, Dlouhy S, Vance G, Vogt P. Multiplex PCR: Critical Parameters and

- Step-by-Step Protocol. *Biotechniques*. 1997;23(September):504–511.
158. Satterfield B. Cooperative primers: 2.5 million-fold improvement in the reduction of nonspecific amplification. *J. Mol. Diagnostics*. 2014;16:163–173.
159. Rychlik W. Selection of primers for polymerase chain reaction. *Methods Mol. Biol.* 1993;15:31–40.
160. Hendling M, Pabinger S, Peters K, et al. Oli2Go: an automated multiplex oligonucleotide design tool. *Nucleic Acids Res.* 2018;46(W1):W252–W256.
161. Conzemius R, Hendling M, Pabinger S, Bariši I. PRIMEval : Optimization and screening of multiplex oligonucleotide assays. *Sci. Rep.* 2019:1–5.
162. Yuan J, Yi J, Zhan M, et al. The web-based multiplex PCR design software Ultiplex and the associated experimental workflow: up to 100-plex multiplicity. *BMC Genomics*. 2021;22.
163. Kaplinski L, Andreson R, Puurand T, Remm M. MultiPLX: automatic grouping and evaluation of PCR primers. *Bioinformatics*. 2005;21(8):1701–1702.
164. Blakemore R, Story E, Helb D, et al. Evaluation of the Analytical Performance of the Xpert MTB/RIF Assay. *J. Clin. Microbiol.* 2010;48(7):2495–2501.
165. Jouet A, Gaudin C, Badalato N, et al. Deep amplicon sequencing for culture-free prediction of susceptibility or resistance to 13 anti-tuberculous drugs. *Eur. Respir. J.* 2020;(June 2020). Available at: <http://dx.doi.org/10.1183/13993003.02338-2020>.
166. QIAGEN. *QIAGEN® Multiplex PCR Handbook For fast and efficient multiplex PCR without optimization*. 2010.
167. Anjum G, Du W, Klein R, et al. Pyrosequencing-based strategy for a successful SNP detection in two hypervariable regions: HV-1/HV-II of the human mitochondrial displacement loop. *Electrophoresis*. 2010;31(2):309–314.
168. Wang J, Xu Z, Niu P, et al. A Two-tube multiplex reverse transcription PCR assay for simultaneous detection of viral and bacterial pathogens of infectious diarrhea. *Biomed Res. Int.* 2014.
169. Leal A, Grieken NCT van, Palsgrove DN, et al. White blood cell and cell-free DNA analyses for detection of residual disease in gastric cancer. *Nat. Commun.* 2020.
170. Phallen J, Sausen M, Adleff V, et al. Direct detection of early-stage cancers using circulating

- tumor DNA. *Sci. Transl. Med.* 2019;9(403).
171. Forsberg KJ, Patel S, Gibson MK, et al. Bacterial phylogeny structures soil resistomes across habitats. *Nature.* 2014.
172. Alli OA, Ogbolu OD, Alaka O. Direct molecular detection of Mycobacterium tuberculosis complex from clinical samples - An adjunct to cultural method of laboratory diagnosis of tuberculosis. *North Am. J. Med. Sci.* 2011;3(6):281–288.
173. Zyl-Smit RN van, Binder A, Meldau R, et al. Comparison of Quantitative Techniques including Xpert MTB/RIF to Evaluate Mycobacterial Burden. *PLoS One.* 2011.
174. Marlowe EM, Novak-weekley SM, Cumpio J, et al. Evaluation of the Cepheid Xpert MTB / RIF Assay for Direct Detection of Mycobacterium tuberculosis Complex in Respiratory Specimens. *J. Clin. Microbiol.* 2011;49(4):1621–1623.
175. Cepheid. *MTB/RIF MTB/RIF Ultra Product Comparison.* 2019.
176. GenoType. *Geno Type MTBDR plus.* 2015.
177. Friedrich SO, Rachow A, Saathoff E, et al. Assessment of the sensitivity and specificity of Xpert MTB/RIF assay as an early sputum biomarker of response to tuberculosis treatment. *Lancet Respir.* 2013;1(6):462–470. Available at: [http://dx.doi.org/10.1016/S2213-2600\(13\)70119-X](http://dx.doi.org/10.1016/S2213-2600(13)70119-X).
178. Huyen MNT, Tiemersma EW, Lan NTN, et al. Validation of the GenoType® MTBDRplus assay for diagnosis of multidrug resistant tuberculosis in South Vietnam. *BMC Infect. Dis.* 2010;10(149).
179. Theron G, Peter J, Richardson M, et al. GenoType MTBDRsl assay for resistance to second-line anti-tuberculosis drugs. *Cochrane Database Syst. Rev.* 2016;(9).
180. World Health Organization. *IGRA TB Tests Policy Statement.* 2011.
181. Li S, Liu B, Peng M, et al. Diagnostic accuracy of Xpert MTB/RIF for tuberculosis detection in different regions with different endemic burden: A systematic review and meta-analysis. *PLoS One.* 2017;12(7).
182. Takasaki J, Manabe T, Morino E, et al. Sensitivity and specificity of QuantiFERON-TB Gold Plus compared with QuantiFERON-TB Gold In-Tube and T-SPOT.TB on active tuberculosis in Japan. *J. Infect. Chemother.* 2018;24(3):188–192.
183. Javed H, Bakula Z, Plen M, et al. Evaluation of Genotype MTBDR plus and MTBDR sl Assays for Rapid Detection of Drug Resistance in Extensively Drug-Resistant Mycobacterium tuberculosis

- Isolates in Pakistan. *Front. Microbiol.* 2018;9(September):1–10.
184. Nikolayevskyy V, Balabanova Y, Simak T, et al. Performance of the Genotype MTBDRPlus resistance pattern: Samara, Russian Federation. *BMC Clin. Pathol.* 2009;9.
185. Zhang M, Xue M, He J. Diagnostic accuracy of the new Xpert MTB / RIF Ultra for tuberculosis disease : A preliminary systematic review and. *Int. J. Infect. Dis.* 2020;90:35–45. Available at: <https://doi.org/10.1016/j.ijid.2019.09.016>.
186. Boehme CC, Nabeta P, Hillemann D, et al. Rapid molecular detection of tuberculosis and rifampin resistance. *N. Engl. J. Med.* 2010;363(11):1005–1015.
187. Chakravorty S, Simmons AM, Rowneki M, et al. The new Xpert MTB/RIF Ultra: improving detection of Mycobacterium tuberculosis and resistance to rifampin in an assay suitable for point-of-care testing. *Am. Soc. Microbiol.* 2017.
188. Ngabonziza JCS, Ssengooba W, Mutua F, et al. Diagnostic performance of smear microscopy and incremental yield of Xpert in detection of pulmonary tuberculosis in Rwanda. *BMC Infect. Dis.* 2016;16(November).
189. Diagnostics F for IN. Clinical Evaluation of tNGS for Diagnosis of DR-TB (Seq&Treat). *ClinicalTrials.gov.* 2021. Available at: <https://clinicaltrials.gov/ct2/show/NCT04239326>.
190. Nielsen CK, Kjems J, Mygind T, Snabe T, Meyer RL. Effects of Tween 80 on growth and biofilm formation in laboratory media. *Front. Microbiol.* 2016;7.
191. Melnikov A, Galinsky K, Rogov P, et al. Hybrid selection for sequencing pathogen genomes from clinical samples. *Genome Biol.* 2011;12.
192. Wylezich C, Calvelage S, Schlottau K, et al. Next-generation diagnostics: virus capture facilitates a sensitive viral diagnosis for epizootic and zoonotic pathogens including SARS-CoV-2. *Microbiome.* 2021;9.
193. Eckert SE, Chan JZ, Houniet D, et al. Enrichment by hybridisation of long DNA fragments for Nanopore sequencing. *Microb. Genomics.* 2016;2(9).
194. Horn S. Target Enrichment via DNA Hybridization Capture. In: Shapiro B, Hofreiter M, eds. *Ancient DNA.* Humana Press; 2012:177–188.
195. Takenaka S. *Developing new TB diagnostics: Needs, challenges and opportunities.* 2020.
196. Colman RE, Anderson J, Lemmer D, et al. Rapid Drug Susceptibility Testing of Drug-Resistant

- Mycobacterium tuberculosis Isolates Directly from Clinical Samples by Use of Amplicon Sequencing : a Proof-of-Concept Study. *J. Clin. Microbiol.* 2016;54(8):2058–2067.
197. Jiang Y, Luo L, Gui M, et al. Duration and determinants of delayed diagnosis with tuberculosis in Shenzhen, China: a cross-sectional study. *Risk Manag. Healthc. Policy.* 2022;2022(15):1473–1481.
198. Figueredo LJDA, Miranda SS De, Benício L, et al. Cost analysis of smear microscopy and the Xpert assay for tuberculosis diagnosis : average turnaround time. *J. Brazilian Soc. Trop. Med.* 2020;53.
199. Raoot A, Dev G. Evaluate “rifampicin resistance” as surrogate marker for rapid detection of MDR-TB using real-time PCR directly on FNAC samples of tuberculous lymphadenitis. *Br. J. Med. Med. Res.* 2015;9(5):1–8.
200. WHO/IUATLD. *Global project on anti-tuberculosis drug resistance surveillance (1999-2000)*. 2004.
201. Shah M, Chihota V, Coetzee G, Churchyard G, Dorman SE. Comparison of laboratory costs of rapid molecular tests and conventional diagnostics for detection of tuberculosis and drug-resistant tuberculosis in South Africa. *BMC Infect. Dis.* 2013;13(352).
202. Mueller D, Mwenge L, Muyoyeta M, et al. Costs and cost-effectiveness of tuberculosis cultures using solid and liquid media in a developing country. *Int. J. Tuberculous Lung Dis.* 2008;12(10):1196–1202.
203. Kaso AW, Hailu A. Costs and cost-effectiveness of Gene Xpert compared to smear microscopy for the diagnosis of pulmonary tuberculosis using real-world data from Arsi zone, Ethiopia. *PLoS One.* 2021;16(10).
204. Puri L, Oghor C, Denkinger CM, Pai M. Xpert MTB/RIF for tuberculosis testing: access and price in highly privatised health markets. *Lancet Glob. Heal.* 2016;4(2):e94–e95.
205. Silva SCA da, Vater MC, Ramalho DM de P, et al. Cost-effectiveness of Xpert MTB/RIF in the diagnosis of tuberculosis: pragmatic study. *J. Brazilian Soc. Trop. Med.* 2021;54.
206. Hardy A, Varma R, Collyns T, et al. Cost-effectiveness of the NICE guidelines for screening for latent tuberculosis infection: the QuantiFERON-TB Gold IGRA alone is more cost-effective for immigrants from high burden countries. *Thorax.* 2010;65(2).
207. Rodwell TC, Team FN. *Implementing WGS and Culture-free NGS : An Overview of Challenges*

and Solutions Implementing NGS for Diagnosis of Drug-resistant TB. 2019.

208. ONT. Nanopore DNA sequencing. 2022. Available at:

<https://nanoporetech.com/applications/dna-nanopore-sequencing> [Accessed March 27, 2022].

209. Proffitt A. Illumina announces iSeq 100, Thermo Fisher partnership. *BioIT World*. 2018.

Available at: [https://www.bio-itworld.com/news/2018/01/09/illumina-announces-iseq-100-thermo-fisher-partnership#:~:text=Now officially dubbed iSeq 100,U.S. list price of %2419%2C900.](https://www.bio-itworld.com/news/2018/01/09/illumina-announces-iseq-100-thermo-fisher-partnership#:~:text=Now%20officially%20dubbed%20iSeq%20100,U.S.%20list%20price%20of%20%2419%2C900.) [Accessed March 27, 2022].

210. Mongan AE, Tuda JSB, Runtuwene LR. Portable sequencer in the fight against infectious disease. *J. Hum. Genet.* 2020;65:35–40.

211. Gowers G-OF, Vince O, Charles J-H, et al. Entirely off-grid and solar-powered DNA sequencing of microbial communities during an ice cap traverse expedition. *Genes (Basel)*. 2019;10(11).

212. BBC. Paignton Zoo culls antelope herd after bovine TB infection. *BBC News*. 2017. Available at: <https://www.bbc.co.uk/news/uk-england-devon-41353859> [Accessed March 3, 2022].